ORGANOMETALLIC NITROSYL HYDRIDES OF TUNGSTEN

By

JEFFREY THOMAS MARTIN

B.Sc. (Hons, Eng. Chem.), Queen's University at Kingston, 1978

M.Sc., Queen's University at Kingston, 1983

A THESIS SUBMITTED IN PARTIAL FULFILLMENT OF

THE REQUIREMENTS FOR THE DEGREE OF

DOCTOR OF PHILOSOPHY

in

THE FACULTY OF GRADUATE STUDIES

(Department of Chemistry)

We accept this thesis as conforming

to the required standard

THE UNIVERSITY OF BRITISH COLUMBIA

September 1987

In presenting this thesis in partial fulfilment of the requirements for an advanced degree at the University of British Columbia, I agree that the Library shall make it freely available for reference and study. I further agree that permission for extensive copying of this thesis for scholarly purposes may be granted by the head of my department or by his or her representatives. It is understood that copying or publication of this thesis for financial gain shall not be allowed without my written permission.

Department of Chemistry

The University of British Columbia
1956 Main Mall
Vancouver, Canada
V6T 1Y3

Date 17 September, 1987

Abstract

Although hydrides of metal carbonyls are widely known, the number of hydrides in the related family of metal nitrosyls is extremely small. The preparation of a series of nitrosyl hydrides from the treatment of $[CpW(NO)I_2]_2$ ($Cp=\eta^5-C_5H_5$) with $Na[H_2Al(OCH_2CH_2OCH_3)_2]$ is described. The addition of one or two equivalents of the aluminum reagent results in the formation of $[CpW(NO)IH]_2$ or $[CpW(NO)H_2]_2$ respectively. The reaction of $[CpW(NO)IH]_2$ with a Lewis base ($L=P(OPh)_3$, $P(OMe)_3$, PPh_3 or PMe_3) gives the monometallic $CpW(NO)IHL$, while $[CpW(NO)H_2]_2$ reacts with $P(OPh)_3$ or $P(OMe)_3$ to yield $[CpW(NO)HL]_2$ which undergoes further reaction to give $CpW(NO)H_2L$. Proton NMR spectroscopy shows that all bimetallic species contain bridging hydride ligands and are therefore best formulated as $[CpW(NO)I]_2(\mu\text{-}H)_2$, $[CpW(NO)H]_2(\mu\text{-}H)_2$ and $[CpW(NO)L]_2(\mu\text{-}H)_2$.

The ^1H NMR spectrum of $[CpW(NO)H]_2(\mu\text{-}H)_2$ shows that there is no hydride ligand exchange on the NMR time scale and that $^1J_{H(terminal)W} \approx {}^1J_{H(bridging)W} > {}^2J_{HW}$. From this finding, it is possible to develop new criteria for assessing the static or fluxional nature of hydride ligands for several families of organotungsten hydrides (Cp_2W, $CpW(CO)_3$, $W(CO)_5$ and $CpW(NO)_x$ (x=1 or 2)). Within each family, the magnitude of $^1J_{HW}$ strongly reflects the type of metal hydride bonding, i.e.

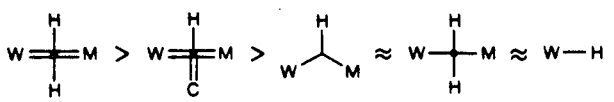

and suggests that bridge bonding involves all the atoms in the bridge and therefore the "fused" notation is introduced.

Treatment of $CpW(NO)(CH_2SiMe_3)_2$ with low pressures of H_2 (60-80 psig) in the presence of Lewis bases ($L=P(OPh)_3$, $PMePh_2$) gives the unusually stable alkyl hydride compounds $CpW(NO)(H)(CH_2SiMe_3)L$. This chemistry is then extended to the Cp* ($Cp^*=\eta^5-C_5Me_5$) analogues, including the preparation of the appropriate starting materials. Upon thermolysis of $Cp^*W(NO)(H)(CH_2SiMe_3)(PMe_3)$ in C_6H_6, the intermolecular C-H activation product $Cp^*W(NO)(H)(C_6H_5)(PMe_3)$ is cleanly formed. However, intermolecular activation of CH_4, C_6H_{12} or $n-C_6H_{14}$ does not occur under similar experimental conditions.

Hydrogenolysis of $Cp^*W(NO)(CH_2SiMe_3)_2$ at high pressures (≈920 psig) with no Lewis base present results in the formation of isolable $[Cp^*W(NO)H]_2(\mu-H)_2$ and $[Cp^*W(NO)H](\mu-H)_2[Cp^*W(NO)(CH_2SiMe_3)]$. The latter is a new example of the rare class of dinuclear alkyl hydride complexes. Proton NMR spin tickling experiments on this compound allow the complete assignment of all couplings in the spectrum and show that $^1J_{H(terminal)W}$, $^1J_{H(bridging)W}$ and $^2J_{HW}$ have the same sign.

Table of Contents

List of Tables

List of Figures

List of Schemes

List of Abbreviations

Cp - η^5-cyclopentadienyl

Cp* - η^5-pentamethylcyclopentadienyl

CP - centroid of a Cp or Cp* ring

Me - CH_3, methyl

Et - CH_2CH_3, ethyl

Ph - C_6H_5, phenyl

Et_2O - $(CH_3CH_2)_2O$, diethyl ether

THF - C_4H_8O, tetrahydrofuran

TMS - Me_4Si, tetramethylsilane

C_6D_6 - benzene-d_6

$CDCl_3$ - chloroform-d_1

CD_2Cl_2 - dichloromethane-d_2

CD_3NO_2 - nitromethane-d_3

$(CD_3)_2CO$ - acetone-d_6

IR - infrared

NMR - nuclear magnetic resonance

MS - mass spectrum

P^+ - molecular ion (in the mass spectrum)

GC-MS - gas chromatography-mass spectrum

EI - electron impact

CV - cyclic voltammogram

SCE - standard calomel electrode

$^1H\{^{31}P\}$ - phosphorus-31 decoupled proton

$^{31}P\{^1H\}$ - proton decoupled phosphorus-31

$^{13}C\{^{1}H\}$ - proton decoupled carbon-13

NOE - nuclear Overhauser effect

psig - pounds per square inch gauge (14.7 psig = 1 atm above atmospheric pressure)

m/z - mass-to-charge ratio in the mass spectrum

dppm - bis(diphenylphosphino)methane

dppe - bis(diphenylphosphino)ethane

Acknowledgements

I would first like to thank the boss, Professor Peter Legzdins, for providing much useful advice and lots of encouragement during the last five years.

I also want to thank all the denizens of 325/319, both past and present, for their friendship and occasional abuse. In particular, my thanks go to George Richter-Addo and Luis Sánchez, not only for their technical help, but also for discussions too numerous to mention. My thanks also go to Julius Balatoni for some T_1 measurements and to Neil Dryden for some computing assistance. I would also like to express my appreciation to Richard Jones, Tony Willis and Fred Einstein at Simon Fraser for solving the X-ray structures.

This work was aided enormously by the excellent technical staff in the department and I would particularly like to thank Steve and Steve in the glass shop, Marietta and Liane in the NMR lab and Peter Borda in the microanalysis lab. My thanks also goes to numerous other members of the department for a lot of useful advice and many profitable discussions.

I would like to acknowledge also the financial support of the H.R. MacMillan Foundation for the receipt of a Family Fellowship.

The support, encouragement and enthusiasm of my family has made all this possible and I want to express my deepest thanks to them for putting up with me all this time. Finally, vill jag

också tacka Anna-Tora för hennes kärlek och tålamod under dessa fem långa år.

"If the Lord Almighty had consulted me before embarking upon Creation, I would have recommended something simpler"

Alfonso X
(the Wise, King of Castille)
1226-1284

Chapter 1

Introduction

A. Historical Background

The first organometallic (or organometallic-like) transition-metal hydride complexes identified were $H_2Fe(CO)_4$[1] and $HCo(CO)_4$[2] by Hieber's group in 1931 and 1935 respectively. These remained the only such hydride complexes known until the mid-1950's when the foundations of modern organometallic chemistry were being laid and Cp_2ReH[3] and $CpM(CO)_3H$ (M=Cr,Mo,W)[4] were isolated. Although the true nature of the metal-H link was not properly understood then, it was recognized that there was a direct metal-H interaction and this caused an explosion of interest in these types of compounds, with many more being prepared in the succeeding years.

This explosion of interest was further fuelled because it was realized from early on that transition-metal hydride compounds were important in a number of highly desirable, catalytic reactions. Even in the 1940's, $HCo(CO)_4$ was recognized as a key element in the newly developed hydroformylation (C_n olefin → C_{n+1} aldehyde)[5] and alcohol homologation reactions (C_n alcohol → C_{n+1} alcohol).[6] In the early 1960's, $ClRh(PPh_3)_3$ via a hydride intermediate was discovered to be a rapid and efficient homogeneous catalyst for olefin hydrogenation under exceptionally mild conditions.[7] Still today, much of the

interest in this general class of compounds stems from their utility in catalytic systems.

The first two hydrides were identified as having H atoms in the molecule since H_2 was produced upon their hydrolysis. Early electron-diffraction measurements suggested a tetrahedral arrangement of C atoms about the metal-centre and the formulations $Co(CO)_3(COH)$ and $Fe(CO)_2(COH)_2$ were suggested.[8] Later, Hieber had chemical evidence for a direct M-H link and so it was suggested that the H atom(s) was buried in the orbitals of the metal.[9] This explanation was used for a number of years to explain the results of numerous IR, NMR, broad-line NMR and electron diffraction experiments carried out over the period 1939-59. In particular, it was used to explain the unusual high-field chemical shifts that the hydride H's exhibited in their high-resolution NMR spectra that greatly aided Wilkinson and Birmingham in their initial studies on Cp_2ReH and its relatives.[3]

However, the presently accepted nature of hydride ligands, that they occupy normal coordination positions with normal covalent bonds, was recognized in the early sixties when X-ray diffraction studies on such compounds as trans-$HPtBr(PEt_3)_2$[10] and $HRh(CO)(PPh_3)_3$[11] were done. The first neutron diffraction study confirmed this nature, as ReH_9^{2-} was found to be a tricapped trigonal prism with Re-H distances of 1.68Å.[12]

B. Structure and Bonding

The most common type of hydride complexes are those containing simple, two electron covalent bonds between the metal and terminal hydride ligands. These complexes may have anywhere from one to nine hydride ligands (e.g. $HCo(CO)_4$, $H_2Fe(CO)_4$, ReH_9^{2-}). Also common are hydrides that bridge two or more metal centres. Since this thesis is only concerned with mono and dinuclear compounds, hydride bonding in higher order clusters will not be discussed here.

When one hydride bridges two atoms, its bonding is generally discussed in terms of "open" or "closed" centre bonding, after the classic bonding descriptions developed in borane chemistry.[13] The first two such molecules to be thoroughly studied were $HW_2(CO)_9(NO)$ and $HW_2(CO)_8(NO)[P(OMe)_3]$,[14] where it was found that the W-H-W linkages are distinctly bent, with the H atom displaced away from its expected position based on a strictly octahedral model:

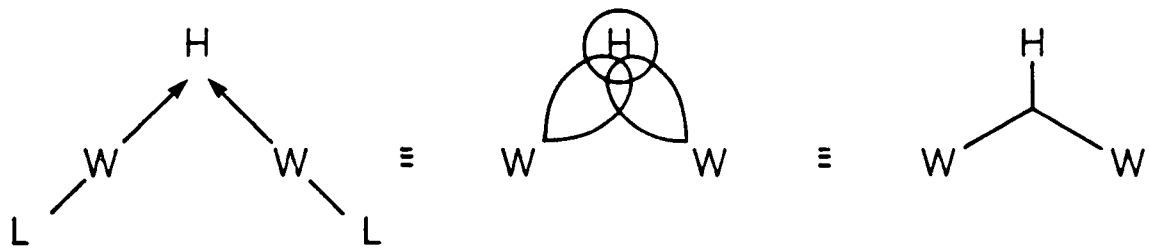

This bonding has always been described as a "closed", 3-centre, 2 electron system, with overlap of orbitals from all three atoms

involved and a direct metal-metal interaction.[15a] This is the commonly accepted bonding rationale for most unsupported M-H-M' bridge bonds in transition-metal complexes. However, some calculations suggest that there is little or no direct bonding between the metal atoms, and that the bonding takes place almost exclusively through the hydrogen bridge in an open fashion, the same as that commonly accepted for boranes (e.g. B_2H_6).[15b,c] It is apparent that this point still needs clarification.

There are also a number of compounds that have two H atoms bridging two metal centres, such as in $[H_2W_2(CO)_8]^{2-}$.[15] In these cases, the H atoms are almost always found inside the positions expected based on an octahedral model. Although there is unquestionably a direct metal-metal interaction (e.g. W-W = 3.0162 Å in $[H_2W_2(CO)_8]^{2-}$) there is considerable debate as to

what the best description of the bonding is in these complexes and this will be dealt with in more detail in chapter 3.

Earlier transition-metal and actinide hydrides also exhibit $M(\mu\text{-}H)_2M$ systems, but these differ somewhat in character. In $[Cp^*ThH]_2(\mu\text{-}H)_2$[16] and $[\eta^5\text{-}C_5H_4Me)_2ZrH]_2(\mu\text{-}H)_2$,[17] the metal-

metal separations are 4.007 and 3.4599 Å, respectively, indicating no direct metal-metal bonding 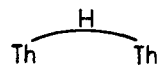 . This therefore seems to be analogous to the open centre bonding used to describe the B-H-B bridging system.

There are a few examples of three or four hydride ligands bridging two metal centres. These include $\{(\mu\text{-H})_3Fe_2[(Ph_2PCH_2)_3CMe]_2\}^{+}$[18] and $H_4(\mu\text{-H})_4Re_2(PEt_2Ph)_4$.[19] The latter is an example of a complex that contains both bridging and terminal hydride ligands--as is common with compounds of this type, it is highly fluxional and all eight H atoms are equivalent on the NMR time scale (see chapter 3).

More recently, two new types of hydrogens bonded directly to transition metals have been recognized. The first of these, dubbed "agostic", is observed as an H atom bridging a metal and a carbon of an alkyl group, usually itself bonded to the metal.[20]

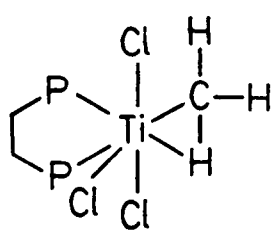

1

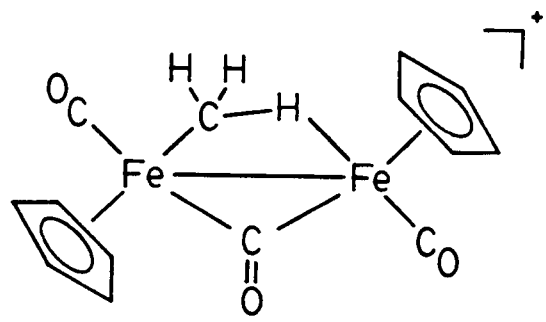

2

This may be described as an arrested elimination (e.g. α-elimination in 1) or oxidative addition (e.g. 2) reaction. This type of interaction is generally the result of an electron deficient metal centre attempting to relieve this deficiency by accepting some electron density from the C-H bond. It is usually identified by the observation of unusual chemical shifts and/or one-bond carbon-H coupling constants for the alkyl H's involved in the interaction.

The second, new type of "hydride" is the interesting situation of dihydrogen bonded in a dihapto fashion to the metal.

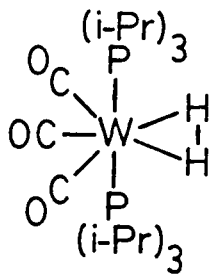

(ref. 21)

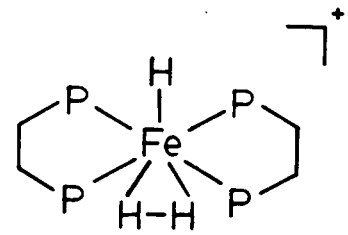

(ref. 22)

This may be described as an arrested oxidative addition of H_2 to the metal centre. It is interesting to note that both classical hydride and η^2-H_2 ligands may be present on the same metal.[22] The compounds are generally identified by the large magnitude of the H-D J coupling observed in the ^1H NMR spectrum of the HD (vs. H_2) analogue,[21] or by the observation of very short T_1

relaxation times for the coordinated η^2-H_2,[23] as well as by the usual diffraction techniques.

C. Characterization of Metal Hydrides

There are essentially three techniques used to characterize and identify transition metal hydrides: IR and NMR spectroscopy, and diffraction methods.

Terminal metal hydrides usually exhibit IR stretching frequencies (ν_{MH}) in the region 1650-2250 cm^{-1}.[24] These bands are generally quite weak in intensity making them difficult to identify, particularly in carbonyl, cyano and nitrosyl complexes where they are often degenerate with the ν_{CO}, ν_{CN} and ν_{NO} bands. Comparisons of the spectra of the compounds with those of their deuterio analogue are frequently done, as the ν_{MH}/ν_{MD} ratio is usually the expected 1.4. Even so, it is not always possible to find these bands. Hydride ligands bridging two metal centres generally exhibit IR frequencies at much lower energies, typically 1000-1700 cm^{-1}.[25] They are usually even weaker in intensity than the terminal M-H bands, and very broad, and are therefore often impossible to detect in routine IR spectra. Raman and low-temperature (4K) IR studies can sometimes be used to find these bands.

Not surprisingly, ^{1}H NMR spectroscopy is an extremely useful tool in detecting the presence of hydride ligands. Usually, particularly for the later transition metals, hydride ligands

exhibit characteristic high-field chemical shifts, with resonances generally in the region δ = -5 to -50 ppm.[26] Earlier transition metal, and lanthanide and actinide hydrides commonly exhibit hydride resonances in the more usual "organic" region of the spectrum and are consequently more difficult to identify.[27] The observation of spin-spin couplings of the hydride ligand to other NMR active nuclei in the molecule is often an extremely useful way of determining structure and/or number of hydride hydrogens. This may take the form of coupling directly to an NMR active metal centre (e.g. ^{89}Y, ^{183}W, ^{103}Rh, ^{195}Pt) or to nuclei of other ligands, particularly ^{31}P in phosphine or phosphine-like ligands.

Of course, the most definitive ways of establishing the structures of compounds (in the solid state) are single-crystal diffraction techniques. As mentioned earlier, it was through the use of these techniques that the true nature of the hydride ligand was discovered. Unfortunately, since X-ray diffraction depends upon electron density and hydrogen atoms have few electrons associated with them, it is often difficult to find hydride hydrogens, particularly when they are close to heavy metal centres such as W or Pt. Frequently, therefore, the location of a hydride hydrogen is inferred from the observation of a "hole" in the coordination sphere of the metal. For example, the first single-crystal X-ray structure of a hydride complex was done on trans-$HPtBr(PEt_3)_2$ and the Br and PEt_3

ligands were found to form a T-shape about the metal. The hydride was assumed to occupy the fourth position in a normal square-planar compound.[10] This situation is complicated by the fact that the hydride ligand is not very stereochemically demanding and so it is not always possible to find an obvious "hole" where the hydride may be located.[15] Under the best conditions, the hydride ligand may be found by X-ray diffraction such as for $HRh(CO)(PPh_3)_3$.[11] Neutron diffraction remains the most definitive way to fully solve a hydride compound's structure, since the neutron scattering factors for most elements are of the same order of magnitude and so hydrides are not "swamped out" by heavier atoms. This allowed the proper identification of ReH_9^{2-} in the now-classic case.[12] Neutron diffraction is, however, very expensive to do and demands crystals 100 to 1000 times larger than those needed for X-ray diffraction and consequently the number of hydride compounds that have been analyzed using this technique is smaller than might be desired.[15] X-ray and neutron studies have been successfully combined on occasion to yield very useful results--for example in the solution of the structure of $H_2Os_3(CO)_{10}$.[28] The two techniques generally give slightly different bond lengths for the metal-H distance. This is because in a metal-H link, the electron density is skewed toward the heavy atom and so X-ray data tend to give unreasonably short M-H distances. Neutron diffraction, on the other hand, depends on the properties of the

atomic nuclei and so M-H interatomic distances from this technique are much more reliable.

D. Preparation

Metal hydride complexes can be made in a number of different ways but the preparations may generally be divided into five categories.[29]

1. Oxidative Addition

a) oxidative addition of H_2

$$\text{trans}[IrCl(CO)(PPh_3)_2] \xrightarrow[PhMe]{H_2} H_2IrCl(CO)(PPh_3)_2 \qquad (30)$$

b) hydrogenolysis of alkyl groups

$$2\ (\eta^5\text{-}C_5H_4Me)_2ZrMe_2 \xrightarrow[PhH]{H_2} [(\eta^5\text{-}C_5H_4Me)_2ZrH]_2(\mu\text{-}H)_2 \quad +4\ CH_4 \qquad (31)$$

c) oxidative addition of HX (X = halide, carbyl)

$$IrCl(CO)(PEt_2Ph)_2 \xrightarrow[EtOH]{HCl(aq)} HIrCl_2(CO)(PEt_2Ph)_2 \qquad (32)$$

$$Cp^*(PMe_3)IrH_2 \xrightarrow[h\nu,-H_2]{C_6H_{12}} Cp^*(PMe_3)Ir(H)(C_6H_{11}) \qquad (33)$$

2. Reduction of Metal Halides (metathesis)

$$ReCl_3(PEt_2Ph)_3 \xrightarrow[THF]{LiAlH_4} ReH_5(PEt_2Ph)_3 \qquad (34)$$

3. Hydride Transfer

a) base catalyzed reductions using alcohols

$$IrCl_3(PEt_2Ph)_3 \xrightarrow[EtOH]{OH^-} HIrCl_2(PEt_2Ph)_3 \qquad (35)$$

b) hydride abstraction from solvents

$$RhCl_3 + 2\ PPh(t\text{-}Bu)_2 \xrightarrow[Na/Hg]{THF,\ N_2} H\text{-}Rh(PPh(t\text{-}Bu)_2)_2\text{-}N{\equiv}N \qquad (36)$$

4. Protonation of Complex Metal Anions

$$1/2\ Co_2(CO)_6[PMePh_2]_2 \xrightarrow[THF]{Na/Hg} Na[Co(CO)_3(PMePh_2)] \xrightarrow{H_3PO_4} HCo(CO)_3(PMePh_2) \qquad (6)$$

5. Protonation of Neutral Complexes

$$(\eta^4\text{-}C_7H_8)(CO)_3Fe \xrightarrow[liq\ SO_2]{HSO_3F} [(\eta^4\text{-}C_7H_8)(CO)_3Fe(H)]^+ \qquad (37)$$

Methods #1, 2 and 4 are the most common but the choice of method is primarily governed by the availability of appropriate starting materials. Hydride complexes can also result from more indirect routes, such as decomposition of existing compounds (e.g. β-elimination of metal alkyl complexes).

E. Nitrosyl Hydrides

Although hydrides of metal carbonyls are widely known and examples exist for almost every transition metal, the number of hydrides of the related family of metal nitrosyls is extremely small. When work began on the project described in this thesis, only a handful of nitrosyl hydride complexes had been identified. The first of this class of compound prepared was $HMn(NO)_2(PPh_3)_2$ in 1962.[38] The next report did not appear until 1972 when $CpRe(CO)(NO)H$ was communicated by Graham and Sweet.[39] Since that time, other than work done in our laboratory, only $HW_2(CO)_8(NO)L$ (L=CO, $P(OMe)_3$),[14] $HRe(NO)_2(PPh_3)_2$,[40] $H_2Re(NO)(PPh_3)_3$,[41] $HM_3(CO)_{10}(NO)$ (M=Ru, Os),[42] $HFe(CO)_2(PPh_3)_2(NO)$[43] and $HW(CO)_2[P(O\text{-}i\text{-}Pr)_3]_2(NO)$[44] have been described (as well as a few phosphine substitution products of these compounds).

Hydride preparation in our laboratory started in 1979 when $CpW(NO)_2H$ was synthesized from $CpW(NO)_2Cl$ and $Na[H_2Al(OCH_2CH_2OCH_3)_2]$.[45] This compound is particularly interesting in that it acts as a mild source of H^-, as opposed to

the related carbonyl analogue $CpW(CO)_3H$, which is a moderately strong acid (H^+).[4] Molecular orbital calculations have attributed this to the three-legged piano-stool structure of $CpW(NO)_2H$, as compared to the four-legged configuration of the carbonyl hydride.[46] In addition, partial hydride abstraction by Ph_3C^+ of $CpW(NO)_2H$ leads to the formation of the dinuclear hydride $[CpW(NO)_2](\mu\text{-}H)^+$ (and analogues).[47] Because of the chemistry observed for $CpW(NO)_2H$, it was of interest to prepare other nitrosyl hydrides and investigate their properties.

F. Scope of the Present Work

The work described in this thesis is a direct continuation of the work started by J.C. Oxley.[48]

Chapter 2 describes the preparation of a series of nitrosyl hydrides derived from $[CpW(NO)I_2]_2$[49] and in particular the properties of three dimeric compounds. As a result of characterizing the compounds described in chapter 2 and the associated survey of the literature, some interesting and significant NMR properties of tungsten hydrides were discovered--these are discussed in chapter 3. While the work described in chapters 2 and 3 was in progress, the novel, stable 16 electron compounds $CpM(NO)R_2$ (M=Mo, W; R=bulky alkyl) were prepared in our laboratory[50] by the reaction

$$[CpM(NO)I_2]_2 \xrightarrow[2.\ H_2O]{1.\ RMgX} 2\ CpM(NO)R_2$$

These compounds were found to undergo unique reactivity with S_8,[51] O_2[52] and NO.[53] Because the yields of the interesting compounds described in chapter 2 were too low to allow much derivative chemistry to be done, it was decided to try and obtain nitrosyl hydrides from the hydrogenation of $CpW(NO)(CH_2SiMe_3)_2$. This work is detailed in chapter 4, along with its extension to the Cp* analogues.

G. References and Notes

1. Hieber, W.; Leutert, F. Z. Anorg. Allg. Chem. 1932, **204**, 145-164.

2. Hieber, W. Z. Elektrochem. 1934, **40**, 158-159.

3. Wilkinson, G.; Birmingham, J.M. J. Am. Chem. Soc. 1955, **77**, 3421-3422.

4. Fisher, E.O.; Hafner, W.; Stahl, H.O. Z. Anorg. Allg. Chem. 1955, **282**, 47-62.

5. Parshall, G.W. "Homogeneous Catalysis", Wiley-Interscience: Toronto, 1980 and references therein.

6. Martin, J.T.; Baird, M.C. Organometallics 1983, **2**, 1073-1078.

7. Osborn, J.A.; Jardine, F.H.; Young, J.F.; Wilkinson, G. J. Chem. Soc. A 1966, 1711-1732.

8. Ewens, R.V.G.; Lister, M.W. Trans. Faraday Soc. 1939, **35**, 681-691.

9. Hieber, W. Die Chemie 1942, **55**, 7-11, 24-28.

10. Owsten, P.G.; Partridge, J.M.; Rowe, J.M. Acta Crystallogr. 1960, **13**, 246-252.

11. LaPlaca, S.J.; Ibers, J.A. J. Am. Chem. Soc. 1963, **85**, 3501-3502.

12. Abrahams, S.C.; Ginsberg, A.P.; Knox, K. Inorg. Chem. 1964, **3**, 558-567.

13. Huheey, J.E.; "Inorganic Chemistry", Harper & Row: San Francisco, 1972, p 535 and references therein.

14. a) Olsen, J.P.; Koetzle, T.F.; Kirtley, S.W.; Andrews, M.; Tipton, D.L.; Bau, R. J. Am. Chem. Soc. 1974, **96**, 6621-6627.

b) Love, R.A.; Chin, H.B.; Koetzle, T.F.; Kirtley, S.W.; Whittlesey, B.R.; Bau, R. J. Am. Chem. Soc. 1976, **98**, 4491-4498.

15. a) Teller, R.G.; Bau, R. "Crystallograhic Studies of Transition Metal Hydride Complexes", in: Struct. Bonding (Berlin) 1981, **44**, 1-82 and references therein.

b) Jeżowska-Trzebiatowska, B; Nissen-Sobocińska, B. J. Organometal. Chem. 1987, **322**, 331-350.

c) Sherwood, D.E.Jr.; Hall, M.B. Organometallics 1982, **1**, 1519-1524.

16. Broach, R.W.; Schultz, A.J.; Williams, J.M.; Brown, G.M.; Manriquez, J.M.; Fagan, P.J.; Marks, T.J. Science (Washington, D.C.) 1979, **203**, 172-174.

17. Jones, S.B.; Petersen, J.L. Inorg. Chem. 1981, **20**, 2889-2894.

18. Dapporto, P.; Midollini, S.; Sacconi, L. Inorg. Chem. 1975, **14**, 1643-1650.

19. Bau, R.; Carroll, W.E.; Teller, R.G.; Koetzle, T.F. J. Am. Chem. Soc. 1977, **99**, 3872-3874.

20. Brookhart, M.; Green, M.L.H. J. Organometal. Chem. 1983, **250**, 395-408 and references therein.

21. Kubas, G.J.; Ryan, R.R.; Swanson, B.J.; Vergamini, P.J.; Wasserman, H.J. J. Am. Chem. Soc. 1984, 106, 451-452.

22. Morris, R.H.; Sawyer, J.F.; Shiralian, M.; Zubkowski, J.D. J. Am. Chem. Soc. 1985, 107, 5581-5582.

23. Crabtree, R.H.; Lavin, M.; Bonneviot, L. J. Am. Chem. Soc. 1986, 108, 4032-4037.

24. Adams, D.M. "Metal Ligand and Related Vibrations", Edward Arnold: London, 1967, pp 1-25 and references therein.

25. Cooper, C.B.; Shriver, D.F.; Onaka, S. Adv. Chem. Ser. 1978, 167, 232-247.

26. Moore, D.S.; Robinson, S.D. Chem. Soc. Rev. 1983, 12, 415-452.

27. Manriquez, J.M.; Fagan, P.J.; Marks, T.J. J. Am. Chem. Soc. 1978, 100, 3938-3941 and references therein.

28. Orpen, A.G.; Rivera, A.V.; Bryan, E.G.; Pippard, D.; Sheldrick, G.M.; Rouse, K.D. J. Chem. Soc., Chem. Commun. 1978, 723-724.

29. Green, M.L.H.; Jones, D.J. Adv. Inorg. Chem. Radiochem. 1965, 7, 115-183.

30. Vaska, L.; Rhodes, R.E. J. Am. Chem. Soc. 1965, 87, 4970-4971.

31. Couturier, S.; Tainturier, G.; Gautheron, B. J. Organometal. Chem. 1980, 195, 291-306.

32. Chatt, J.; Johnson, N.P.; Shaw, B.L. J. Chem. Soc. (A) 1967, 604-607.

33. Janowicz, A.H.; Bergman, R.G. J. Am. Chem. Soc. 1983, **105**, 3929-3939.

34. Chatt, J.; Coffey, R.S. J. Chem. Soc. (A) 1969, 1963-1972.

35. Vaska, L.; DiLuzio, J.W. J. Am. Chem. Soc. 1962, **84**, 4989-4990.

36. Yoshida, T.; Okano, T.; Thorn, D.L.; Tulip, T.H.; Otsuka, S.; Ibers, J.A. J. Organometal. Chem. 1979, **181**, 183-201.

37. Falkowski, D.R.; Hunt, D.F.; Lillya, C.P.; Rausch, M.D. J. Am. Chem. Soc. 1967, **89**, 6387-6389.

38. Hieber, W.; Teryler, H. Z. Anorg. Allg. Chem. 1962, **318**, 136-154.

39. Sweet, J.R.; Graham, W.A.G. Organometallics 1982, **7**, 982-986 and references therein.

40. La Monica, G.; Freni, M.; Cenini, S. J. Organometal. Chem. 1974, **71**, 57-64.

41. Giusto, D.; Ciani, G.; Manassero, M. J. Organometal. Chem. 1976, **105**, 91-95.

42. Johnson, B.F.G.; Raithby, P.R.; Zuccaro, C J. Chem. Soc., Dalton Trans. 1980, 99-104.

43. Roustan, J.-L.A.; Forgues, A.; Merour, J.Y.; Venayuk, N.D.; Morrow, B.A. Can. J. Chem. 1983, **61**, 1339-1346.

44. Kundel, P.; Berke, H. J. Organometal. Chem. 1986, **314**, C31-C33.

45. Legzdins, P.; Martin, D.T. Inorg. Chem. 1979, **18**, 1250-1254.

46. Bursten, B.E.; Gatter, M.G. J. Am. Chem. Soc. 1984, 106, 2554-2558.

47. Hames, B.W.; Legzdins, P. Organometallics 1982, 1, 116-124.

48. Oxley, J.C. Ph.D. Dissertation, The University of British Columbia, 1983.

49. Legzdins, P.; Martin, D.T.; Nurse, C.R. Inorg. Chem. 1980, 19, 1560-1564.

50. Legzdins, P.; Rettig, S.J.; Sánchez, L.; Bursten, B.E.; Gatter, M.G. J. Am. Chem. Soc. 1985, 107, 1411-1413.

51. Legzdins, P.; Sánchez, L. J. Am. Chem. Soc. 1985, 107, 5525-5526.

52. Legzdins, P.; Rettig, S.J. Sánchez, L. Organometallics 1985, 4, 1470-1471.

53. Evans, S.V.; Legzdins, P.; Rettig, S.J.; Sánchez, L.; Trotter, J. personal communication.

Chapter 2

New Organometallic Hydrido Nitrosyl Complexes of Tungsten

Very few organometallic nitrosyl hydride complexes are known. As discussed in the previous chapter, when work in this area was started in our laboratory, only CpRe(CO)(NO)H was known and the unusual properties of $CpW(NO)_2H$ subsequently found spurred our interest in the topic. In 1980, $[CpW(NO)I_2]_2$[1] was prepared in our laboratory and it was hoped that hydride complexes could be made from it by halide/hydride metathesis (preparation method #2 - chapter 1). This work was started by J.C. Oxley,[2] who prepared the series of compounds CpW(NO)IHL (L=$P(OPh)_3$, $P(OMe)_3$, PPh_3) and $CpW(NO)H_2[P(OPh)_3]$, as well as the compounds $[CpW(NO)IH]_2$, $[CpW(NO)H_2]_2$ and $[CpW(NO)H\{P(OPh)_3\}]_2$. However, these three dimeric species were not correctly characterized and the work described in this chapter mainly involved the synthesis and complete characterization of these three complexes, as well as a full description of the properties of the CpW(NO)XX'L (X=I or H; L=$P(OPh)_3$, $P(OMe)_3$, PPh_3 and/or PMe_3) series of compounds.

Experimental Section

All manipulations were performed so as to maintain all chemicals under an atmosphere of prepurified dinitrogen either on the bench using conventional Schlenk techniques[3] or in a Vacuum

Atmospheres Corp. Dri-Lab Model HE-43-2 drybox. All chemicals used were of reagent grade or comparable purity. All reagents were either purchased from commercial suppliers or prepared according to published procedures, and their purity was checked by elemental analyses and/or other suitable methods. Melting points were taken in capillaries under nitrogen using a Gallenkamp Melting Point apparatus and are uncorrected. Hexanes and benzene were dried with CaH_2, toluene, diethyl ether and THF were dried with Na/benzophenone ketyl and CH_2Cl_2 was dried with P_2O_5. All solvents were distilled off their respective drying agents and purged with N_2 just prior to use. Unless otherwise specified, the reactions described below were done at ambient temperatures.

Infrared spectra were recorded on a Nicolet 5DX FT-IR instrument. Proton magnetic resonance spectra were obtained on a Bruker WP-80, WH-400, HXS-270, Nicolet-Oxford H-270 or Varian XL-300 spectrometer with reference to the residual proton signal of the deuteriated solvent employed,[4] and are reported in ppm downfield from Me_4Si. ^{31}P NMR spectra were recorded at 121.4-MHz on a Varian XL-300, 40.5-MHz on a Varian XL-100, or at 32.38-MHz on a Bruker WP-80 spectrometer using ^2H as the internal lock. The observed resonances were referenced to external $P(OMe)_3$ which was considered to have a chemical shift of +141 ppm downfield from 85% H_3PO_4.[5] Mrs. M.T. Austria, Ms. M.A. Heldman, Ms. L.K. Darge and Dr. S.O. Chan assisted in obtaining the NMR data.

Electron impact mass spectra were recorded at 70 eV on an Atlas CH4B or a Kratos MS50 spectrometer using the direct-insertion method with the assistance of Mr. M.A. Lapawa, Mr. J.W. Nip and Dr. G.K. Eigendorf. The GC-MS samples were run on a Varian Vista 6000 gas chromatograph interfaced with a Nermag R10-10 quadrupole mass spectrometer or a Carlo Erba GC interfaced with a Kratos MS-80 RFA spectrometer using the conditions specified below with the assistance of Ms. C. Moxham. Gas chromatographic analyses were carried out on a Perkin Elmer Sigma 4B instrument using a 30' x 1/8" 23% SP-1700 on 80/100 Chromosorb P AW column at 70°C with 25 mL/min He carrier gas. Elemental analyses were performed by Mr. P. Borda.

Preparation of $CpW(NO)I_2L$ (L = $P(OMe)_3$ or PMe_3).

These compounds were prepared by treating $[CpW(NO)I_2]_2$ in CH_2Cl_2 with 2 equivalents of L in the manner described previously[1] for L=$P(OPh)_3$ or PPh_3. Both complexes were isolated as brown crystals in yields of 87%. The analytical, IR and NMR data for these and the other compounds synthesized in this work, as well as related species from preliminary work[2] are collected in Tables 2-I and 2-II.

Preparation of $[CpW(NO)IH]_2$.

A vigourously stirred mixture of $[CpW(NO)I_2]_2$[1] (3.00 g, 2.82 mmol), CH_2Cl_2 (25 mL) and benzene (150 mL) was heated gently

to solubilize the organometallic starting material. Once a clear, yellow-brown solution was obtained, the mixture was cooled to room temperature with a water bath. Then, before precipitation of $[CpW(NO)I_2]_2$ could occur, 0.85 mL (2.9 mmol) of a 3.4 M solution of $Na[H_2Al(OCH_2CH_2OCH_3)_2]$ in toluene[6] was rapidly added dropwise. The reaction mixture immediately turned an intense, dark green colour with the simultaneous formation of a large amount of very fine, brown, intractable precipitate. The mixture was then filtered as rapidly as possible through a 3 x 4 cm column of Celite supported on a medium porosity glass frit, which was subsequently washed with 2 x 15 mL portions of benzene. The filtrate was concentrated under vacuum to 10-15 mL which induced the formation of very intensely coloured dark green microcrystals. This material was collected by filtration, washed with benzene (3 x 5 mL) and dried under vacuum (0.005 mm Hg) to give 0.80 g (35% yield) of analytically pure $[CpW(NO)IH]_2$.

Preparation of $CpW(NO)IH(PMe_3)$.

Addition of neat PMe_3 (0.40 mL, 0.30 g, 4.0 mmol) to the dark green filtrate containing $[CpW(NO)IH]_2$ (described above) caused an immediate colour change to orange and the precipitation of a brown intractable solid. The supernatant solution was filter cannulated away from the precipitate and its volume decreased to 50 mL under reduced pressure. Hexanes (60 mL) were added, and the resulting solution was further concentrated to 40

mL and let stand overnight. This resulted in the formation of a light brown, microcyrstalline precipitate which was collected by filtration and washed with hexanes (5 x 10 mL) to obtain 0.98 g (36% yield based on $[CpW(NO)I_2]_2$) of a solid which analyzed as $CpW(NO)IH(PMe_3)$ (see results and discussion).

Preparation of $[CpW(NO)H_2]_2$.

The stirred dark green filtrate containing $[CpW(NO)IH]_2$ (generated as above) was treated dropwise with a 3.4 M toluene solution of $Na[H_2Al(OCH_2CH_2OCH_3)_2]$ until the green colour just disappeared (~0.7 mL, ≈ 2.4 mmol). The final reaction mixture consisted of a large amount of the usual fine, brown precipitate and a dark red-brown solution. The mixture was then filtered as rapidly as possible through a 3 x 4 cm column of Celite supported on a medium porosity glass frit and the column washed with benzene (2 x 15 mL). The resulting red-brown filtrate was then concentrated under vacuum to ~10 mL, let stand for several hours, and the resulting orange powder collected by filtration. It was then washed with benzene (3 x 5 mL) and dried under vacuum (0.005 mm Hg) to give 0.16 g (10% yield based on original $[CpW(NO)I_2]_2$) of analytically pure $[CpW(NO)H_2]_2$. This powder could be converted to small, well-formed crystals of $[CpW(NO)H_2]_2$ in very low yield in the following manner. The powder was stirred with toluene (50 mL) and warmed slightly (~50°C) to promote solubilization. The orange solution was then filter cannulated

into another flask and volume reduced under vacuum until precipitation started to occur (~15 mL). The solution was then filter cannulated into a long, narrow Schlenk tube, ensuring that no precipitate came over and the solution was completely clear. The Schlenk tube was then stored at -25°C overnight, inducing formation of the crystals. The mother liquor was then cannulated off and the crystals washed with 3 x 10 mL of diethyl ether, and dried under vacuum (0.005 mm Hg) to yield ~20 mg of crystalline $[CpW(NO)H_2]_2$.

Preparation of $[CpW(NO)H\{P(OPh)_3\}]_2$ and $CpW(NO)H_2[P(OPh)_3]$.

A mixture of $[CpW(NO)H_2]_2$ (0.10 g, 0.18 mmol) and benzene (30 mL) was stirred and warmed with a water bath (~50°C) until a clear, orange solution resulted (~10 min). To this was added neat $P(OPh)_3$ (93 µL, 0.35 mmol) and the solution stirred for 6 h as it turned a very intense purple colour. The solvent was then removed under vacuum and the purple, oily residue taken up in 15 mL benzene, filtered, and 25 mL of hexanes were added to precipitate the product. The very intensely coloured, purple, microcrystalline material was collected by filtration, washed with hexanes and dried under vacuum to give 0.086 g (41% yield) of $[CpW(NO)H\{P(OPh)_3\}]_2$.

A small amount of the purple crystals was dissolved in CH_2Cl_2 (10 mL) and the resulting solution was stirred for 3 h whereupon it became orange. Addition of hexanes to this solution

induced the precipitation of a small amount of analytically pure $CpW(NO)H_2P(OPh)_3$ as an orange powder, which was collected by filtration as above.

Preparation of $[CpW(NO)Br_2]_2$.

A solution of $CpW(CO)_2(NO)$ (5.00 g, 15.0 mmol) in 40 mL CH_2Cl_2 was stirred and cooled to -40^oC whereupon a solution of Br_2 (0.77 mL, 15.0 mmol) in 10 mL CH_2Cl_2 was slowly added dropwise. The mixture immediately turned dark red-brown and vigorous gas evolution occurred while a dark brown precipitate began to form. After stirring for ~5 min, the cold bath was removed and the reaction mixture gradually allowed to warm to near room temperature. The solvent was removed under vacuum until ~20 mL remained, giving a deep green solution above a dark brown precipitate. An IR spectrum of the solution showed bands at 2099(s), 2010(s), 1927(s), 1693(s) and 1655 cm^{-1}. Hexanes (25 mL) were added and the volume of the solution further decreased under vacuum until ~10 mL of a very pale green solution was left over a dark brown precipitate. This precipitate was then filtered, washed with 3 x 20 mL hexanes and dried in vacuum (0.005 mm Hg) overnight to give 5.20 g (79.2% yield) of dark brown microcrystalline $[CpW(NO)Br_2]_2$.

Preparation of $CpW(NO)BrH[P(OPh)_3]$.

To a dark green solution of $[CpW(NO)Br_2]_2$ (1.00 g, 1.14 mmol) in 10 mL CH_2Cl_2 and 50 mL benzene was added rapidly dropwise 0.34 mL (1.1 mmol) of a 3.4 M solution of $Na[H_2Al(OCH_2CH_2OCH_3)_2]$ in toluene. The solution instantly turned orange and a large amount of brown precipitate formed. The mixture was rapidly filtered through a 3 x 4 cm column of Celite supported on a medium porosity glass frit which was then washed with 2 x 15 mL portions of benzene. Triphenylphosphite ($P(OPh)_3$, 0.60 mL, 2.28 mmol) was then added to the filtrate and no significant colour change was observed. The volume of the solution was reduced to ~10 mL under vacuum and chromatographed on Florisil (2 x 10 cm) using benzene as eluent to give only one orange band. This band was collected, the solvent removed under vacuum, and the resulting oil recrystallized from CH_2Cl_2/hexanes to give 0.20 g (13% yield) of large, red-brown crystals of $CpW(NO)BrH[P(OPh)_3]$.

Table 2-I. Analytical and Infrared Data for the Complexes

complex	mp, °C (dec)	analytical data: C calcd	C found	H calcd	H found	N calcd	N found	other	other calcd	other found	IR data (CH_2Cl_2): ν_{NO}, cm^{-1}	ν_{WH}, cm^{-1}
$CpW(NO)I_2[P(OPh)_3]$ [1]											1663	
$CpW(NO)I_2[P(OMe)_3]$	178	14.63	14.58	2.15	2.18	2.13	2.12	I	38.64	38.49	1653	
$CpW(NO)I_2(PPh_3)$ [1]											1646	
$CpW(NO)I_2(PMe_3)$	160	15.78	15.70	2.32	2.28	2.30	2.28	I	41.69	41.55	1638	
$CpW(NO)IH[P(OPh)_3]$	112	38.52	38.46	2.95	3.10	1.95	1.89				1643	1883
$CpW(NO)IH[P(OMe)_3]$	103	18.08	17.96	2.82	2.84	2.64	2.65				1629	1923
$CpW(NO)IH(PPh_3)$ [2]											1615	?[a]
$CpW(NO)IH(PMe_3)$	101	19.90	19.80	3.13	3.24	2.90	2.85				1613 (isomer A)	1931
		19.90	19.86	3.13	3.00	2.90	2.85	I	26.28	26.40	1609 (A + B)	1929, 1898
$[CpW(NO)I_2]_2$ [1]											1655	
$[CpW(NO)IH]_2$	174	14.74	14.75	1.47	1.50	3.44	3.49				1646	n.o.
$[CpW(NO)H_2]_2$	130	21.37	21.44	2.51	2.46	4.99	4.93	O	5.69	6.00	1599	1906
$[CpW(NO)H[P(OPh)_3]]_2$	85	46.80	46.64	3.59	3.63	2.37	2.36				1578	n.o.
$CpW(NO)H_2[P(OPh)_3]$ [2]											1607	1863
$[CpW(NO)Br_2]_2$		13.69	13.57	1.15	1.16	3.19	3.15	Br	36.42	36.28	1655	
$CpW(NO)BrH[P(OPh)_3]$	102	41.22	41.40	3.16	3.29	2.09	2.05	Br	11.96	12.11	1636	1869

a The ν_{WH} for $CpW(NO)IH(PPh_3)$ cannot be unequivocally assigned as there are several bands in the appropriate spectral regions.

Table 2-II. NMR Data for the Complexes

Complex	nucleus	solv	isomer	assg't	δ(J, Hz)
$CpW(NO)I_2[P(OPh)_3]$	^1H	$CDCl_3$		Cp	5.90 (d, 5, $^3J_{HP}$ = 3)
				$P(O\underline{Ph})_3$	7.2 (br, 15)
		C_6D_6		Cp	5.43 (d, 5, $^3J_{HP}$ = 3)
				$P(O\underline{Ph})_3$	7.1 (br, 15)
$CpW(NO)I_2[P(OMe)_3]$	^1H	$CDCl_3$		Cp	5.98 (d, 5, $^3J_{HP}$ = 2)
				$P(O\underline{Me})_3$	3.83 (d, 9, $^3J_{HP}$ = 11)
		C_6D_6		Cp	5.43 (d, 5, $^3J_{HP}$ = 3)
				$P(O\underline{Me})_3$	3.45 (d, 9, $^3J_{HP}$ = 11)
$CpW(NO)I_2(PPh_3)$	^1H	$CDCl_3$		Cp	5.91 (d, 5, $^3J_{HP}$ = 1.2)
				$P\underline{Ph}_3$	7.5 (br, 15)
		C_6D_6		Cp	5.26 (d, 5, $^3J_{HP}$ = 2)
				$P\underline{Ph}_3$	7.1 (br, 15)
$CpW(NO)I_2(PMe_3)$[a]	^1H	$CDCl_3$	A	Cp	5.94 (d, 5, $^3J_{HP}$ = 2.8)
				$P\underline{Me}_3$	1.90 (d, 9, $^3J_{HP}$ = 10.2)
		C_6D_6	A	Cp	5.06 (d, 5, $^3J_{HP}$ = 2.8)
				$P\underline{Me}_3$	1.08 (d, 9, $^3J_{HP}$ = 10.2)
			B	Cp	5.20 (s, 5)
				$P\underline{Me}_3$	1.54 (d, 9, $^3J_{HP}$ = 10)

Table 2-II (Cont'd)

$CpW(NO)(H)[P(OPh)_3]$	^1H	$CDCl_3$	Cp	5.25 (s, 5)
			$P(O\underline{Ph})_3$	7.2 (br, 15)
			W-$\underline{H}$	-2.04 (d, 1, $^2J_{HP}$ = 112, $^1J_{HW}$ = 54)
		C_6D_6	Cp	4.85 (s, 5)
			$P(O\underline{Ph})_3$	7.1 (br, 15)
			W-$\underline{H}$	-2.06 (d, 1, $^2J_{HP}$ = 112, $^1J_{HW}$ = 54)
	$^{31}P\{^1H\}$	C_6D_6		115.5 (s, $^1J_{PW}$ = 363)
$CpW(NO)(H)[P(OMe)_3]$	^1H	$CDCl_3$	Cp	5.81 (s, 5)
			$P(O\underline{Me})_3$	3.73 (d, 9, $^3J_{HP}$ = 12)
			W-$\underline{H}$	-1.44 (d, 1, $^2J_{HP}$ = 101, $^1J_{HW}$ = 57)
		C_6D_6	Cp	5.12 (s, 5)
			$P(O\underline{Me})_3$	3.36 (d, 9, $^3J_{HP}$ = 12)
			W-$\underline{H}$	-1.41 (d, 1, $^2J_{HP}$ = 101, $^1J_{HW}$ = 57)
	$^{31}P\{^1H\}$	C_6D_6		131 (s)
$CpW(NO)(H)(PPh_3)$	^1H	$CDCl_3$	Cp	5.63 (s, 5)
			$P\underline{Ph}_3$	7.4 (br, 15)
			W-$\underline{H}$	0.31 (d, 1, $^2J_{HP}$ = 85, $^1J_{HW}$ = 58)
		C_6D_6	Cp	5.10 (s, 5)
			$P\underline{Ph}_3$	7.4 (br, 15)
			W-$\underline{H}$	0.10 (d, 1, $^2J_{HP}$ = 85, $^1J_{HW}$ = 58)
	$^{31}P\{^1H\}$	C_6D_6		14.1 (s)

Table 2-II (Cont'd)

$CpW(NO)IH(PMe_3)$	^1H	$CDCl_3$	A	Cp	5.60 (d, 5, $^3J_{HP}$ < 1)
				PMe_3	1.87 (d, 9, $^3J_{HP}$ = 9.5)
				W-H	-0.65 (d, 1, $^2J_{HP}$ = 84, $^1J_{HW}$ = 66)
			B	Cp	5.73 (dd, 5, $^3J_{HP}$, $^3J_{HW}$ = 1.5, < 1)
				PMe_3	1.80 (d, 9, $^3J_{HP}$ = 9.7)
				W-H	NO[b]
		C_6D_6	A	Cp	5.11 (s, 5)
				PMe_3	1.39 (d, 9, $^3J_{HP}$ = 9)
				W-H	-1.13 (d, 1, $^2J_{HP}$ = 84, $^1J_{HW}$ = 66)
			B	Cp	4.80 (d, 5, J = 1.8)
				PMe_3	1.20 (d, 9, $^3J_{HP}$ = 9.5)
				W-H	NO[b]
$CpW(NO)H_2[P(OPh)_3]$	^1H	$CDCl_3$		Cp	5.10 (s, 5)
				$P(OPh)_3$	7.3 (br, 15)
				W-H	-1.82 9d, 2, $^2J_{HP}$ = 86, $^1J_{HW}$ = 88)
		C_6D_6		Cp	4.69 (s, 5)
				$P(OPh)_3$	7.2 (br, 15)
				W-H	-1.58 (d, 2, $^2J_{HP}$ = 87, $^1J_{HW}$ = 87)
	$^{31}P\{^1H\}$	C_6D_6			137 (s)
$CpW(NO)H_2[P(OMe)_3]$	^1H	C_6D_6		Cp	5.17 (s, 5)
				$P(OMe)_3$	3.47 (d, 9, $^3J_{HP}$ = 12)
				W-H	-1.74 (d, 2, $^2J_{HP}$ = 81, $^1J_{HW}$ = 87)

Table 2-II (Cont'd)

$[CpW(NO)I_2]_2$	^1H	$CDCl_3$		Cp	6.30 (s, $^2J_{HW}$ = 1.8)
		C_6D_6[e]		Cp	5.00 (s)
$[CpW(NO)I]_2(\mu\text{-}H)_2$[c]	^1H	$CDCl_3$		Cp	6.21 (s, 10)
				W-<u>H</u>-W	-1.21 (s, 2, $^1J_{HH'}$ = 3.7, $^1J_{HW}$ = 88.3, $^1J_{H'W}$ = 70.8)
		C_6D_6		Cp	5.31 (s, 10)
				W-<u>H</u>	-1.21 (s, 2)[d]
$[CpW(NO)H]_2(\mu\text{-}H)_2$[c]	^1H	$CDCl_3$	A	Cp	5.95 (s, 10)
				W-<u>H</u>$_A$	6.99 (m, 2, $^3J_{H(A)H(A')}$ = 1, $^2J_{H(A)H(X)}$ = 8, $^2J_{H(A)H(X')}$ = 4.5, $^1H_{HW}$ = 95, $^2J_{HW}$ = 13)
				W-<u>H</u>$_X$-W	-2.05 (m, 2, $^1J_{H(X)H(X')}$ = 4, 1/2|$^1J_{H(X)W}$ + $^1J_{H(X')W}$| = 93)
			B	Cp	5.93 (s, 10)
				W-<u>H</u>$_A$	6.55 (dd, 2, $^2J_{H(A)H(M)}$ = 3.0, $^2J_{H(A)H(X)}$ = 8.5, $^1J_{H(A)W}$ = 99)
				W-<u>H</u>$_M$-W	1.39 (~q, 1, $^1J_{H(M)H(X)}$ = 2.5, $^1J_{H(M)W}$ = 92)
				W-<u>H</u>$_X$-W	-5.94 (td, 1, $^1J_{H(X)W}$ = 96)
		C_6D_6[e]	A	Cp	5.23 (s, 10)
				W-<u>H</u>$_A$	7.01 (m, 2)
				W-<u>H</u>$_X$-W	-1.90 (m, 2)
			B	Cp	5.26 (s, 10)

Table 2-II (Cont'd)

				W-$\underline{H}_A$	6.64 (dd, 2)
				W-$\underline{H}_M$-W	1.66 (~q, 1)
				W-$\underline{H}_X$-W	-5.99 (td, 1)
$[CpW(NO)(P(OPh)_3)]_2(\mu\text{-}H)_2$	[c]	^1H	$CDCl_3$ [f]	Cp	4.97 (s, 10)
				$P(O\underline{Ph})_3$	7.4 (br, 30)
				W-$\underline{H}$-W	1.10 (m, 2)
			C_6D_6	Cp	5.17 (d, 10, $^3J_{HP}$ = 1)
				$P(O\underline{Ph})_3$	7.0 (br, 30)
				W-$\underline{H}$-W	1.32 (t, 2, $^2J_{HP}$ = 24, $^1J_{HW}$ = 55)
		$^{31}P\{^1H\}$	C_6D_6		151 (s, $^1J_{PW}$ = 595)
$[CpW(NO(P(OMe)_3)]_2(\mu\text{-}H)_2$		^1H	C_6D_6	A Cp	5.23 (s, 10)
				$P(O\underline{Me})_3$	3.67 (d, 18, $^3J_{HP}$ = 12)
				W-$\underline{H}$-W	0.82 (t, 2, $^2J_{HP}$ = 24, $^1J_{HW}$ = 53)
				B Cp	5.60 (s, 10, $^3J_{HP}$ = 1)
				$P(O\underline{Me})_3$	3.55 (d, 18, $^3J_{HP}$ = 12)
				W-$\underline{H}$-W	0.84 (t, 2, $^2J_{HP}$ = 26, $^1J_{HW}$ = 54)
$[CpW(NO)Br_2]_2$		^1H	$CDCl_3$	Cp	6.35 (s, $^2J_{HW}$ = 1.8)
			C_6D_6 [e]	Cp	5.08 (s)

Table 2-11 (Cont'd)

$CpW(NO)BrH[P(OPh)_3]$	^1H	$CDCl_3$	Cp	5.29 (d, 5, $^3J_{HH}$ = 0.7)
			$P(O\underline{Ph})_3$	7.3 (br, 15)
			W-$\underline{H}$	0.21 (d sex, 1, $^3J_{HH}$ = 0.7, $^2J_{HP}$ = 112, $^1J_{HW}$ = 49)
		C_6D_6	Cp	4.84 (d, 5, $^3J_{HH}$ = 0.7)
			$P(O\underline{Ph})_3$	6.8-7.5 (br, 15)
			W-$\underline{H}$	0.20 (d sex, 1, $^3J_{HH}$ = 0.7, $^2J_{HP}$ = 112, $^1J_{HW}$ = 48)
	$^{31}P\{^1H\}$	C_6D_6		120.2 ($^1J_{PW}$ = 360)

a In $CDCl_3$, $CpW(NO)I_2(PMe_3)$ exists exclusively as isomer A.

b NO = not observed.

c See text for a complete discussion of the ^1H NMR spectrum of this complex.

d $[CpW(NO)I]_2(\mu\text{-}H)_2$ is not sufficiently soluble in C_6D_6 to permit resolution of the ^{183}W satellites.

e Couplings not as well resolved as in $CDCl_3$.

f Couplings not resolved in $CDCl_3$.

Results and Discussion

The interrelationships between the compounds studied in this investigation are summarized in Scheme 2-I. The preparation and characterization of each of these complexes will now be considered in turn.

A. Preparation of $[CpW(NO)IH]_2$.

As has been previously reported,[2] $[CpW(NO)IH]_2$ may be prepared as an analytically pure compound via step a in Scheme 2-I (eq. 2-1) by the treatment of $[CpW(NO)I_2]_2$ with an equimolar

$$[CpW(NO)I_2]_2 \xrightarrow[CH_2Cl_2/PhH]{Na[H_2Al(OCH_2CH_2OCH_3)_2]} [CpW(NO)IH]_2 \qquad (2\text{-}1)$$

amount of $Na[H_2Al(OCH_2CH_2OCH_3)_2]$ in a mixed solvent system of CH_2Cl_2/PhH. However, there are a number of important factors in this preparation which have not previously been detailed that must be controlled in order to obtain uncontaminated $[CpW(NO)IH]_2$. Firstly, the reaction must be done as quickly as possible since the preparation of $[CpW(NO)IH]_2$ is accompanied by the formation of some brown, insoluble byproducts which appear to catalyze the decomposition of the desired species and so this material must be rapidly filtered away. Secondly, the stoichiometry of the $Na[H_2Al(OCH_2CH_2OCH_3)_2]$ addition is important because it reacts further with $[CpW(NO)IH]_2$ (see below).

Scheme 2-I

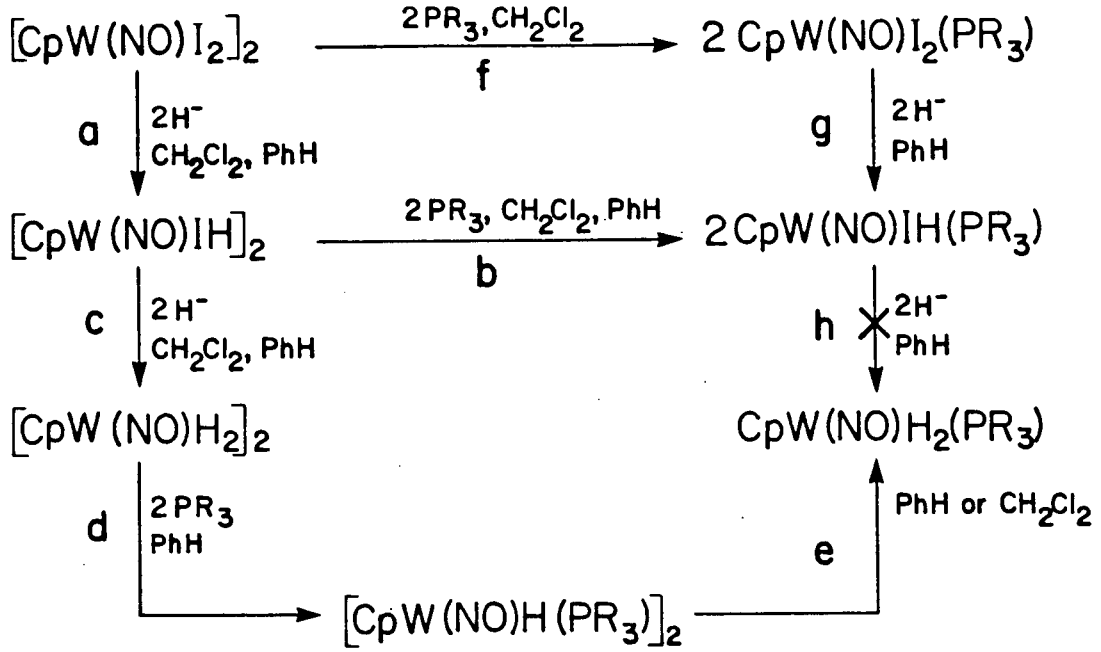

where R= Me, Ph, OMe, or OPh

Thirdly, the specified mixed solvent system is necessary. The presence of CH_2Cl_2 is needed to solubilize the $[CpW(NO)I_2]_2$ starting material, but using this exclusively as a solvent results in the final product being contaminated with NaI.[7] (NaI is insoluble in the prescribed solvent system). If benzene alone is used as the solvent, a large amount is needed to solubilize the starting material and isolated yields are generally reduced. Interestingly enough, $[CpW(NO)I_2]_2$ is sufficiently less soluble in toluene than in benzene so as to make the former solvent inappropriate for this reaction. Finally, if $[CpW(NO)IH]_2$ is obtained in an impure form, it is

prone to undergo rapid decomposition both in solution and in the solid state to a brown, intractable solid.

Pure $[CpW(NO)IH]_2$ is a deeply coloured, dark green solid which is thermally stable at room temperature in the solid state under N_2 for several months. As a solid, it is air-stable for short periods of time, although solutions are somewhat more air-sensitive. The complex is only slightly soluble in nondonor or weakly donating solvents, with the solubility increasing in the order hexanes, Et_2O (insoluble) < toluene < benzene < CH_2Cl_2. The resulting solutions are intensely green in colour and appear red to transmitted light. Donor solvents, however, appear to cleave the dimer after initital solubilization (cf. step b of Scheme 2-I) with $t_{1/2}$ ~20 min in THF (eq 2-2). In solvents in

$$[CpW(NO)IH]_2 + 2\ THF \longrightarrow 2\ CpW(NO)IH(THF) \qquad (2\text{-}2)$$

green, initial ν_{NO} = 1650 cm^{-1} → orange, final ν_{NO} = 1632 cm^{-1}

which it retains its dimeric form, $[CpW(NO)IH]_2$ is much less stable than as a solid, thereby precluding recrystallization. For example, over the course of 3 days in C_6D_6 (more quickly in $CDCl_3$) at room temperature, a green solution of $[CpW(NO)IH]_2$ slowly deposits the ubiquitous brown solid, and a sharp singlet at δ = 1.50 appears in the ^1H NMR of the colourless supernatant, along with attendant loss of all signals due to $[CpW(NO)IH]_2$. Analysis by gas chromatography and GC-MS[8] of the solvent after

distillation showed the product of this decomposition to be undeuteriated cyclopentane, C_5H_{10}, in ~60-70% yield based on available hydride H atoms. This must result from the auto-hydrogenation by the compound of its cyclopentadienyl ligands. This mode of decomposition is in marked contrast to that observed for the unstable molybdenum analogue, which apparently rapidly loses H_2 in solution and converts to the well-known $[CpMo(NO)I]_2$.[1,9] The tungsten congener of this latter complex is, as yet, unknown.

B. Spectroscopic Properties of $[CpW(NO)IH]_2$.

The dimeric nature of the complex is suggested by the observation of a parent ion (mixture of P^+, $(P+2H)^+$; m/z = 816) in the low-resolution mass spectrum. Unfortunately, overlapping of some medium and strong intensity peaks in the lower mass range makes any further unambiguous assignments extremely difficult.

Infrared spectra of $[CpW(NO)IH]_2$, either as a concentrated Nujol mull or as a CH_2Cl_2 solution, show strong absorptions attributable to terminal NO groups (eg. 1646 cm^{-1} in CH_2Cl_2), but appear to lack any bands attributable to terminal W-H linkages;[10]; absorptions attributable to W-H-W bridges are not visible either, but, as noted in chapter 1, these are expected to be extremely weak and difficult to identify.[11]

The ^1H NMR spectrum of the complex in $CDCl_3$ (see Table 2-II, Fig. 2-1) is particularly interesting. The hydride region

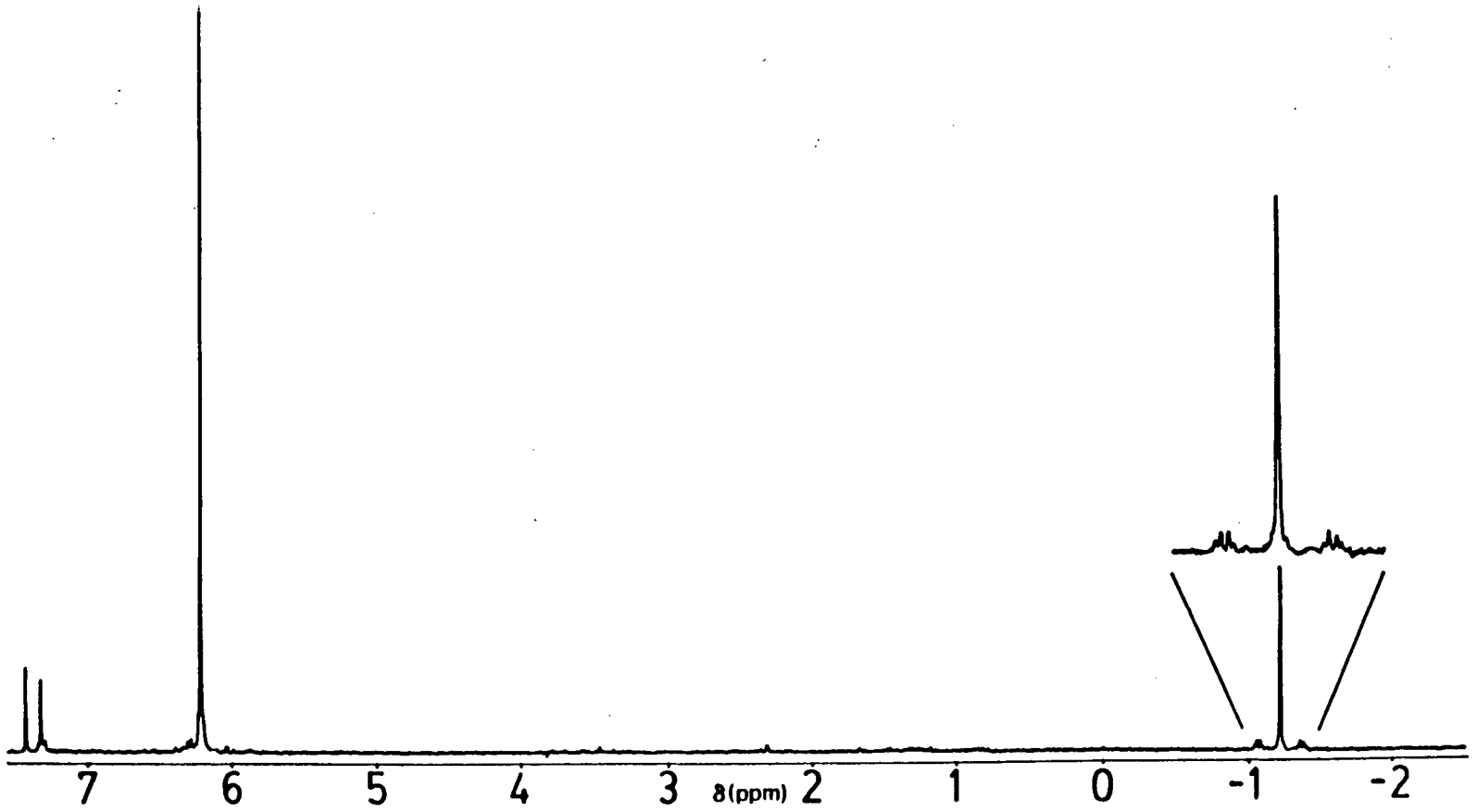

Fig. 2-1. The 270-MHz ^{1}H NMR spectrum of $[CpW(NO)I]_2(\mu\text{-}H)_2$ in $CDCl_3$.

consists of a singlet, surrounded by two AA'X quartets due to coupling to ^{183}W (I = 1/2, natural abundance = 14.4%) whose combined area integrates to ~25% of the total hydride resonance (the coupling constants given in Table 2-II were calculated from conventional algebraic equations).[12] Furthermore, if the ^{1}H NMR spectrum is recorded under our usual Fourier transform conditions of a 45° flip angle and ~2.5 s between pulses, the relative integrations of the C_5H_5:W-H resonances are ~3.5:1 instead of the expected 5:1. This was curious, as metal hydrides are known for often having lengthy relaxation times.[13] Consequently, a T_1 experiment was performed with the result that the T_1 for the C_5H_5 peak was found to be 15.3 s, while that for the hydride resonance was 2.74 s (see Fig. 2-2).[14] Reports of such a long relaxation time for cyclopentadienyl protons are rare, only one having previously appeared.[15] This phenomenon has been attributed to rapid rotation of the Cp ligand about the metal-Cp centroid axis. We have also found analogously low integrations for C_5H_5 resonances in the ^{1}H NMR spectra of most of the complexes investigated in this study when a suitable delay between pulses was not employed. T_1 values were not measured for any of the other compounds.

With the IR spectrum of the compound showing no bands attributable to terminal W-H ligands and the hydride region of the ^{1}H NMR spectrum showing ^{183}W satellites integrating to 25% of the area (see below), the possibility of $[CpW(NO)IH]_2$ containing

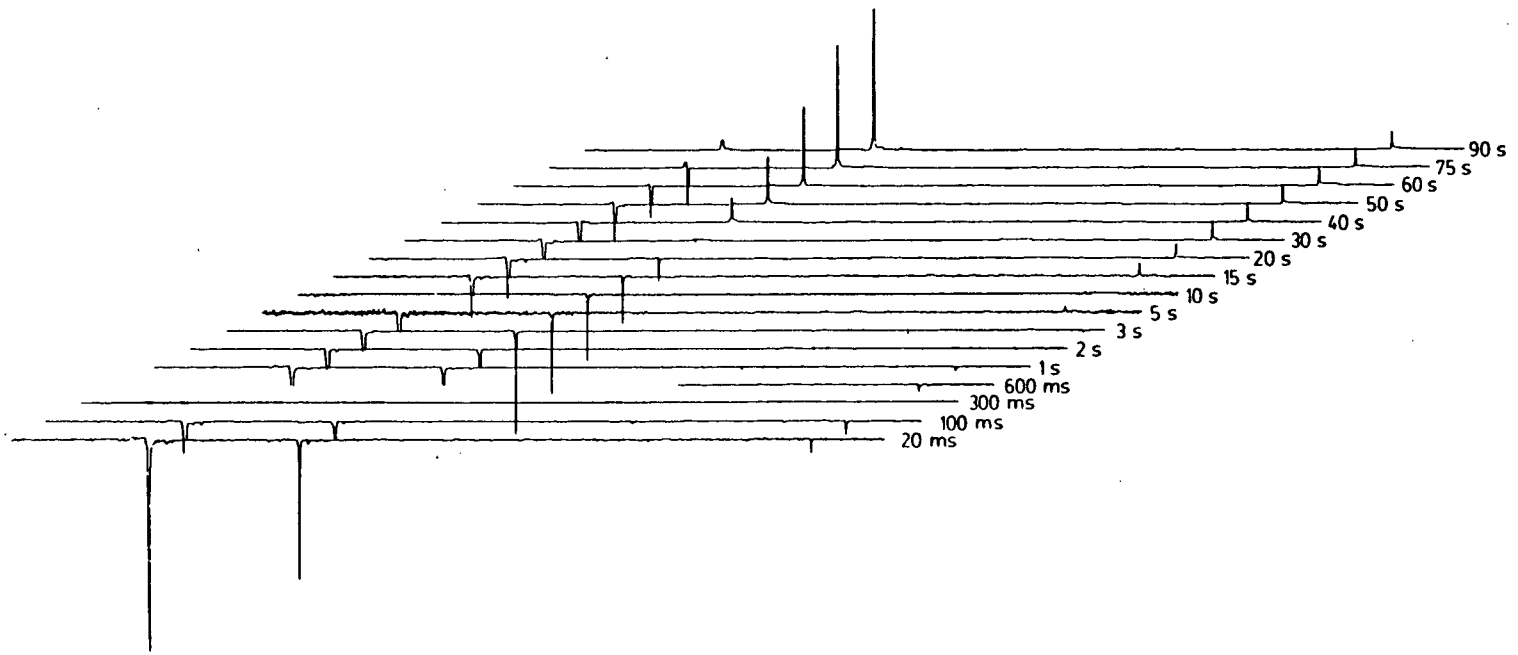

Fig. 2-2. Stacked plots of the results of the 270-MHz ^1H NMR T_1 experiment on $[CpW(NO)I]_2(\mu\text{-}H)_2$ in C_6D_6 using a $180^\circ\text{-}\tau\text{-}90^\circ$ pulse sequence. The τ for each sub-experiment is given beside each plot. T_1's : Cp = 15.3 s, $W_2(\mu\text{-}\underline{H})_2$ = 2.7 s.

bridging H ligands is suggested. However, further discussion on the structure of this compound will be deferred until the properties of several related compounds are discussed.

C. The Complexes CpW(NO)IHL (L=Phosphine or Phosphite).

The orange compounds CpW(NO)IHL (L=$P(OPh)_3$, $P(OMe)_3$ and PPh_3) have been described previously[2] and their IR and NMR data have been included in Tables 2-I and 2-II for the sake of completeness. Briefly, they are prepared in ~40% yield (based on $[CpW(NO)I_2]_2$ by addition of a stoichiometric quantity of the Lewis base to a dark green solution of $[CpW(NO)IH]_2$, followed by chromatography on Florisil and crystallization from CH_2Cl_2/hexanes (steps a and b in Scheme 2-I, eq. 2-3). The

$$[CpW(NO)IH]_2 + 2\ L \xrightarrow[CH_2Cl_2/PhH]{} 2\ CpW(NO)IHL \qquad (2\text{-}3)$$

yields of monomers are essentially quantitative from the $[CpW(NO)IH]_2$ dimer and are marked improvements on their preparations via steps f and g in Scheme 2-I.[2]

The physical and spectral properties of these three compounds, as well as isomer A of $CpW(NO)IH(PMe_3)$ (see below), suggest they are all monomers and are isostructural. They are all orange, diamagnetic compounds that are stable in air for at least several hours with no noticable decomposition occurring. They are quite soluble in polar organic solvents (e.g. CH_2Cl_2),

but only sparingly soluble in non-polar ones, to give mildly air-sensitive solutions. Their low-resolution mass spectra display peaks corresponding to P^+, $(P-I)^+$ and $(P-L)^+$, where P = monomeric parent fragment. Their IR spectra display ν_{NO}'s in the region 1643-1613 cm^{-1} (Table 2-I), suggesting terminal NO ligands. These frequencies decrease, as expected, as the electron-donating abilities of L increase[16] in the order $L=P(OPh)_3 < P(OMe)_3 < PPh_3 < PMe_3$. In addition, weak absorptions attributable to terminal W-H stretching vibrations (ν_{WH})[10] are observable at ~1900 cm^{-1} in these spectra. These latter vibrations increase in frequency with the electron donating abilities of L,[16] thereby presumably indicating a corresponding increase in the W-H bond strength. By analogy with the better known $CpM(CO)_2HL$ (M=Cr, Mo or W; L=CO or phosphine), these compounds probably possess a conventional "four-legged piano-stool" molecular structure.[17]. In our case, with four unique ligands in addition to the Cp group, there are a number of possible arrangements of these ligands in the basal plane. Because the W atom in these molecules is a chiral centre, these isomers consist of three sets of enantiomeric pairs.

The ^1H NMR spectra of these complexes in $CDCl_3$ or C_6D_6 (Table 2-II) suggest the presence of only one isomer (as well, of course, as its enantiomer) in solution. The observation of a singlet C_5H_5 resonance and (large) $^2J_{HP}$ values in the range of 84 to 112 HZ is indicative of a cis orientation[18] of the L and H

ligands (I and II) ($^{2}J_{HP}$'s of ~20 Hz would be expected for a trans configuration).[18] In addition to coupling to ^{31}P, the

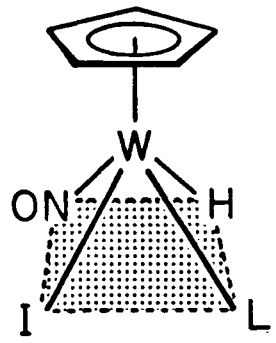

I

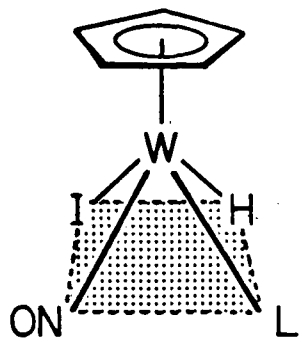

II

hydride resonances exhibit coupling to ^{183}W, with these satellites integrating to the expected 15% of the total hydride integration. Unlike the positions of the ν_{NO} and ν_{WH} frequencies in the IR spectra, no trends are evident in the positions of the cyclopentadienyl or hydride resonances in the NMR spectra with respect to the electron donating abilities or steric bulks of L.[16] This is in agreement with Darensbourg and co-workers' observations on the $[HW(CO)_4 L]^-$ system.[19] However, as summarized in Table 2-II, the values of $^{1}J_{HW}$ do increase and those of $^{2}J_{HP}$ do decrease as the electron-donating ability of L increases. This is in contrast with the carbonyl results, where the $^{2}J_{HP}$ values were observed to correlate with the steric, rather than electronic, properties of L, and no trend was observable with respect to $^{1}J_{HW}$.[19] The matter of the magnitude

of $^1J_{HW}$ in these and other complexes will be dealt with in much more detail in chapter 3. On the basis of all these data, it is not possible to determine whether the NO ligand is trans to L (structure I) or trans to H (structure II). Our preference is for structure I, with the strongly electron withdrawing NO trans to the L donor ligand, and the two, one-electron ligands mutually trans, but such an identification must await a single-crystal X-ray analysis of one of these compounds.

When L in reaction 2-3 is PMe_3, the situation is slightly more complicated than with the other L's just considered. The $CpW(NO)IH(PMe_3)$ product is formed as a mixture of two isomers (designated A and B in Tables 2-I and 2-II). One of the isomers (A) is isolable in 11% yield by using the chromatographic procedure employed for the other CpW(NO)IHL compounds. However, fractional crystallization of the reaction mixture before chromatography gives an analytically pure light brown mixture of the two isomers in 36% yield. As discussed above, the spectroscopic properties of isomer A suggest it is isostructural with the other CpW(NO)IHL compounds. Comparison of the IR spectrum (CH_2Cl_2) of the isomeric mixture with that of A alone shows both a broadening of the NO stretching band and the appearance of a new ν_{WH} at 1898 cm^{-1}. The ^1H NMR spectrum of the mixture in C_6D_6 shows that they exist in an approximate 5:1 ratio (A:B) initially. The spectrum in $CDCl_3$, which has better resolution, shows the Cp resonance for isomer B to be resolved

into a doublet of doublets, presumably due to coupling to both the P and hydride atoms. This suggests[18] that isomer B probably has the structure of the third pair of enantiomers referred to above, namely with the H and PMe_3 ligands mutually trans, i.e.

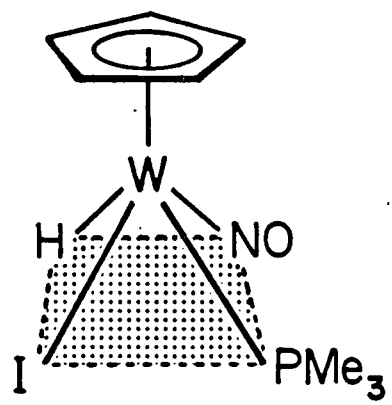

Curiously, no distinct resonance due to the hydride atom of isomer B could be found in the ^1H NMR spectrum of the mixture.

Now having the CpW(NO)IHL compounds, it is interesting to compare their properties with those of the $CpW(CO)_2HL$[18] and $CpW(NO)I_2L$[1] series. The most striking difference between the CpW(NO)IHL and $CpW(CO)_2HL$ complexes is that the latter undergo rapid cis/trans isomerization in solution under ambient conditions and the isomers cannot be isolated independently.[18] The CpW(NO)IHL compounds, on the other hand, generally exist as

only one isomer (H and L cis) and no isomerization appears to occur. In the one case where mixtures of isomers can be prepared (L=PMe_3), the isomer with H and L trans undergoes spontaneous isomerization to the other isomer in $CDCl_3$ solution over the course of one week at 20°C. Similarly, preparation of the $CpW(NO)I_2L$ complexes according to step f in Scheme 2-I (eq. 2-4) results in only one isomer when L=$P(OPh)_3$, $P(OMe)_3$ or PPh_3. Again, when L=PMe_3, two isomers (A and B in Table 2-II) are formed in the ratio of ~5:1. In this case, isomer B is even

$$[CpW(NO)I_2]_2 + 2\ L \xrightarrow{CH_2Cl_2} 2\ CpW(NO)I_2L \qquad (2\text{-}4)$$

less kinetically stable than in the case of $CpW(NO)IHL$, as it is converted into isomer A immediately upon dissolution in $CDCl_3$ and somewhat more slowly in C_6D_6.

The second difference between the carbonyl and nitrosyl complexes is that the hydride resonances in the ^1H NMR spectra of the $CpW(NO)IHL$ complexes appear at much lower field (by 6-8 ppm) than do the corresponding signals for the $CpW(CO)_2HL$ compounds. In fact, the hydride resonances for all the hydrido nitrosyl complexes investigated during this study are much less shielded than is customary for middle and late transition-metal hydrides (see chapter 1). This point will be discussed further in chapter 3.

Finally, a comparison of IR data shows another interesting

trend (Table 2-I). When one of the I atoms of $CpW(NO)I_2L$ is replaced by an H atom, the ν_{NO} diminishes by 20-25 cm^{-1}. This is probably a reflection of the lower electronegativity of the H atom versus an I atom and the correspondingly greater electron density on the metal centre of the hydride complex available for back-donation to the NO ligand. However, no trend in the chemical shifts of the ^1H NMR signals of the cyclopentadienyl ligands is evident when the replacement occurs (Table 2-II).

D. Synthesis and Properties of $[CpW(NO)H_2]_2$.

As is shown in step c of Scheme 2-I, further addition of $Na[H_2Al(OCH_2CH_2OCH_3)_2]$ to the green filtrate containing $[CpW(NO)IH]_2$ gives, after workup, low yields of orange $[CpW(NO)H_2]_2$ (eq. 2-5). Unfortunately, this addition is very

$$[CpW(NO)IH]_2 \xrightarrow[CH_2Cl_2/PhH]{Na[H_2Al(OCH_2CH_2OCH_3)_2]} [CpW(NO)H_2]_2 \qquad (2\text{-}5)$$

difficult to monitor because the quantity of $[CpW(NO)IH]_2$ contained in the filtrate is not precisely known. It has proven impossible to follow the reaction by IR spectroscopy, as the NO band of the $[CpW(NO)IH]_2$ starting material is very weak in this system and it is difficult to tell when it has just disappeared. Furthermore, the benzene solvent has a band that directly overlaps the ν_{NO} of the product. Attempts to follow the reaction

by FT-IR spectroscopy and employing computer subtraction of solvent peaks were unsuccessful because the reaction must be done rapidly for the same reasons as discussed above for the preparation of $[CpW(NO)IH]_2$. Consequently, the addition of the aluminum reagent must be monitored visually, with addition ceasing when the reaction mixture is no longer green, but rather a dark, orange-brown colour. Again, this is difficult to do because the solutions are extremely intensely coloured, but it has proven to be the only successful method. Independent experiments involving addition of the aluminum hydride to a solution made from a known amount of isolated $[CpW(NO)IH]_2$ established that the stoichiometry is 1:1, however, isolation of the product $[CpW(NO)H_2]_2$ from this procedure led to a lower overall yield (based on $[CpW(NO)I_2]_2$) than that above. Addition of excess $Na[H_2Al(OCH_2CH_2OCH_3)_2]$ results in further reaction to give, as yet, unidentified hydride-containing products (as judged by ^1H NMR spectroscopy).

The $[CpW(NO)H_2]_2$ isolated from the reaction mixture is an orange powder and may be crystallized to give small, red-orange crystals in low yield as described in the Experimental Section. The pure compound is a diamagnetic solid which persists in air for short periods of time and is remarkably thermally stable, being left unchanged when heated at 100°C overnight under N_2. Its solubility properties are very similar to those of $[CpW(NO)IH]_2$. Like the latter complex, the dihydride dimer

undergoes decomposition during 1 week in $CDCl_3$ at room temperature with the resulting formation of cyclopentane. However, C_6D_6 solutions of this compound show no evidence of decomposition even after several weeks under the same conditions.

The IR spectrum of $[CpW(NO)H_2]_2$ in CH_2Cl_2 shows a strong ν_{NO} at 1599 cm^{-1} and a much weaker, terminal ν_{WH} at 1906 cm^{-1}, the latter contrasting to the spectrum of $[CpW(NO)IH]_2$, which has no such band. The low-resolution mass spectrum (probe temperature 120°C) of $[CpW(NO)H_2]_2$ suggests the expected dimeric structure, with a highest-mass peak at m/z = 560, corresponding to $(P-2H)^+$.[2]

It is the ^1H NMR spectrum, however, particularly in $CDCl_3$, that provides the most information about the structure of the compound (Fig. 2-3). This spectrum shows that two isomers (A and B in Fig. 2-3) are present in solution, in an approximate 1.3:1 ratio, with this constant in $CDCl_3$ and C_6D_6. The assignments of the observed resonances to individual isomers were made on the basis of homonuclear decoupling experiments.[2] Exclusive of ^{183}W satellites, isomers A and B exhibit AA'XX' and A_2MX patterns, respectively, for their hydride ligands. The coupling constants for isomer B are, of course, easily calculated since it is a first-order spectrum. However, precise calculation of such constants[12] is not possible for the AA'XX' system of isomer A because the spectrum is not sufficiently well resolved.[12] Nevertheless, these numbers may be reasonably estimated by

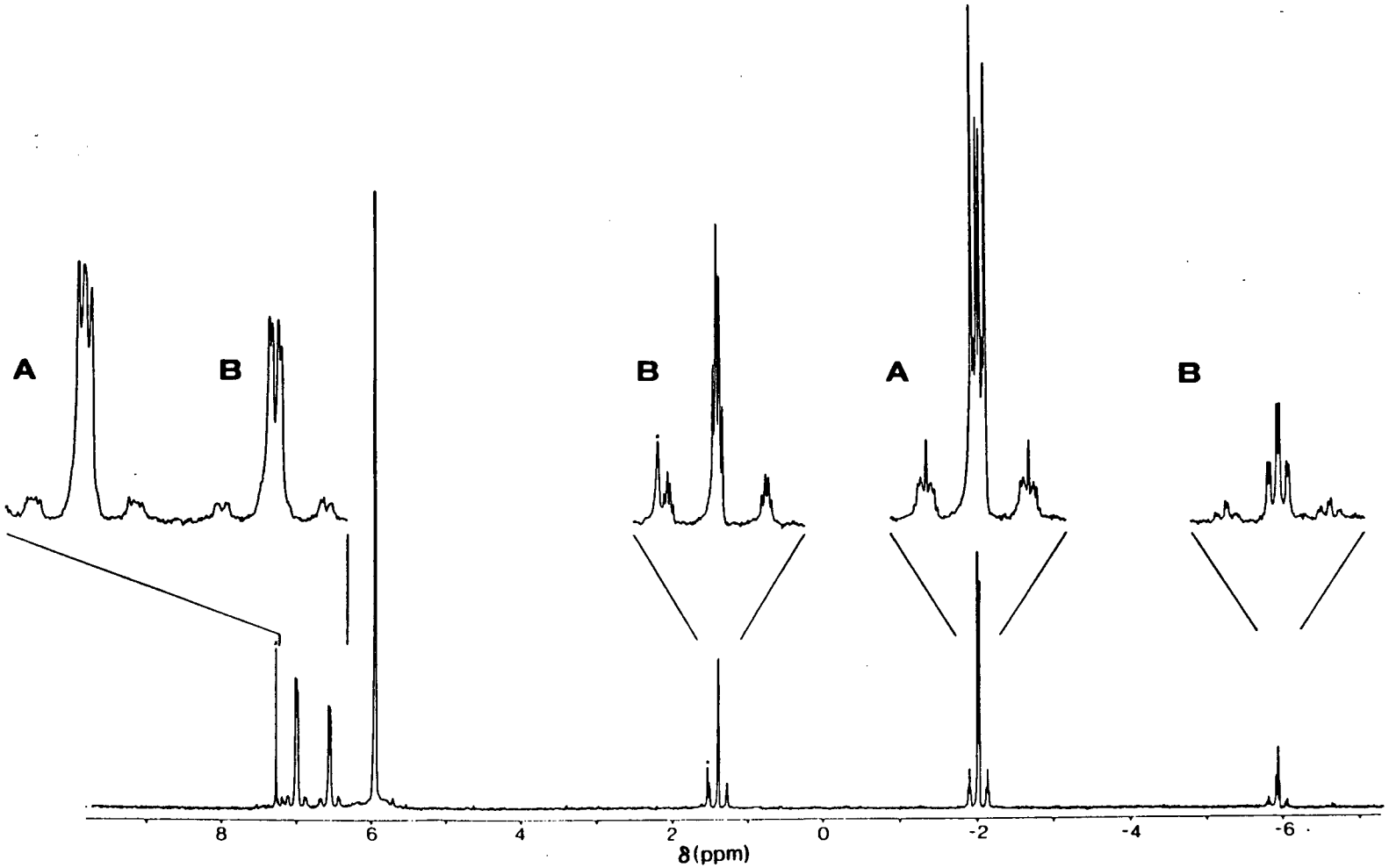

Fig. 2-3. The 400-MHz ^1H NMR spectrum of $[CpW(NO)H]_2(\mu\text{-}H)_2$ in $CDCl_3$. "A" and "B" refer to the hydride resonances assignable to isomers A and B.

iterative simulation[20] and they are included in Table 2-II. The assignment of cis and trans ^{1}H-^{1}H couplings across the metal centres (see below and Fig. 2-4) are based on related assignments discussed in chapter 4.

E. Molecular Structures of $[CpW(NO)H]_2(\mu\text{-}H)_2$ and $[CpW(NO)I]_2(\mu\text{-}H)_2$.

Numerous possible structures of $[CpW(NO)H_2]_2$ having different configurations of bridging and terminal hydride ligands can be envisaged. The ^{1}H NMR spectrum of this complex, however, clearly shows that each of the two isomers A and B have two bridging and two terminal hydride ligands. Generally speaking, in molecules of this kind, the resonances for bridging hydrides occur at higher field than those for terminal hydrides.[21] On this basis, the low field signals for each isomer (which have a relative intensity of 2) may be tentatively assigned to terminal W-H groups with the remaining signals attributable to W-H-W bridging linkages. More definitive, however, are the integrations of the ^{183}W satellites associated with each hydride signal. The two downfield signals (δ = 6.99 and 6.55) have satellites that integrate to ~16% of the total area for each signal, while the the three upfield signals (δ = 1.39, -2.05 and -5.94) have satellites integrating to ~28%. In a binuclear system, the relative proportions of isotopomers containing zero, one and two ^{183}W nuclei (14.4% natural abundance) are

73.3:24.7:2.1.[22] Therefore, the three higher field resonances are due to H atoms that show almost equal (and large) coupling to a ^{183}W nucleus when it is at either metal centre. On the other hand, the two lower field hydride peaks show coupling to a ^{183}W nucleus (with large, one-bond coupling of 90-100 Hz) when it is at only one of the two metal centres. Hence, the three upfield resonances are due to bridging hydrides and the two downfield due to terminal hydrides. Deubzer and Kaesz have found that for $Cp_2H_2W{\rightarrow}W(CO)_5$, $^2J_{HW}$ = 19.2 Hz[23] -- with this in mind, shoulders on the two downfield peaks may be attributed to two-bond, tungsten-hydrogen coupling across the H-W-^{183}W system, with $^2J_{HW}$ ≈13 and ≈15 Hz for isomers A and B, respectively. This attribution is also consistent with the absence of these shoulders on the resonances due to the bridging hydrides, for which such two-bond coupling is not possible.

On the basis of this evidence, $[CpW(NO)H_2]_2$ can therefore be more properly formulated as $[CpW(NO)H]_2(\mu\text{-}H)_2$. A large number of structures consistent with the spectroscopic evidence are still possible. After most of the work described in this chapter had been published,[27] we were fortunate to obtain a single crystal of this compound suitable for X-ray analysis. This structure will be discussed in detail in chapter 3 in a bonding context, but inspection of the structure obtained (Fig. 3-1 and 3-2) shows that its hydride ligands would exhibit an AA'XX' pattern in the ^1H NMR spectrum and the structure is therefore that of isomer A.

A drawing of this structure is shown in Fig. 2-4.[24]. The tungsten centres in this compound may be simplistically thought of as four-coordinate and chiral due to having four different substituents (H, NO, Cp and $CpW(NO)H_2$). Further examination of isomer A shows, in fact, that it is a meso structure. It is probable, therefore, that isomer B is a mixture of two enantiomers of a diastereomer of A. However, unlike at analogous chiral C centres where there is free rotation about all C-X axes (X=any substituent), there is no free rotation about the W-W axis in $[CpW(NO)H]_2(\mu\text{-}H)_2$ (see chapter 3). This means any reorientation of the $W_2(\mu\text{-}H)_2$ plane with respect to a fixed orientation of the two CpW(NO)H end units would result in a different molecule and a different hydride pattern in its ^1H NMR spectrum. Consequently, there are a number of possible structures of isomer B that can be envisaged--one of these is depicted in Fig. 2-4. This was chosen simply on the basis that it can be derived from the structure of A by the minimum number of ligand exchanges and still yield an A_2MX pattern for the ^1H NMR spectrum of the hydride ligands.

The $W_2(\mu\text{-}H)_2$ linkage of the dihydride dimer is not without precedence in the literature, having been demonstrated crystallographically by Churchill and Chang, and Bau and co-workers[25] for $[(\mu\text{-}H)_2W_2(CO)_8]^{2-}$ and having been proposed by Alt and co-workers[26] for $[CpW(CO)_2]_2(\mu\text{-}H)_2$. In the latter case, the structural proposal was based primarily on the ^1H NMR

spectrum exhibiting ^{183}W satellites which were 24% of the total hydride signal intensity. Our observations on the valence isoelectronic $[CpW(NO)H]_2(\mu\text{-}H)_2$ support this proposal.

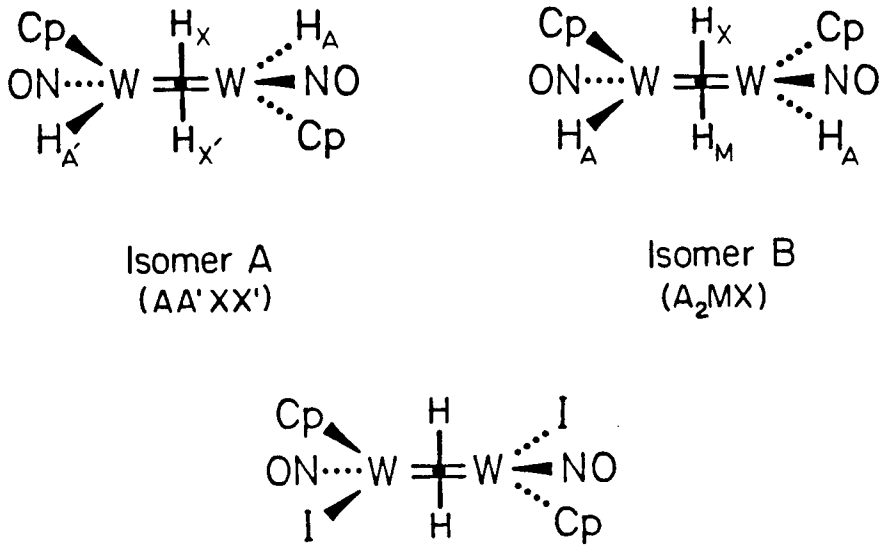

Fig. 2-4. Probable molecular structures of $[CpW(NO)H]_2(\mu\text{-}H)_2$ and $[CpW(NO)I]_2(\mu\text{-}H)_2$.[24] The structure of isomer A of $[CpW(NO)H]_2(\mu\text{-}H)_2$ has been verified by a single crystal X-ray analysis (see chapter 3).

Bearing in mind the spectral properties of $[CpW(NO)H]_2(\mu\text{-}H)_2$, we can now consider the structure of $[CpW(NO)IH]_2$. J.C. Oxley originally formulated this compound[2] as

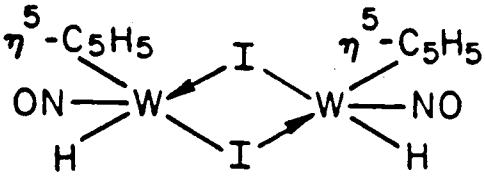

on the basis of the 18-electron rule and incomplete analysis of the ^{1}H NMR spectrum. The observation of ^{183}W satellites integrating to 25% of the total area of the hydride signal rules out this possibility as a static (non-fluxional) structure. In addition, the AA'X pattern of the ^{183}W satellites with strong ^{1}H-^{183}W coupling ($^{1}J_{HW}$ = 88.3 and $^{1}J_{H'W}$ = 70.8 Hz) leads us to reformulate this compound as $[CpW(NO)I]_2(\mu\text{-}H)_2$ (Fig. 2-4). (We have previously suggested the formulation of $[CpW(NO)]_2(\mu\text{-}H)_2(\mu\text{-}I)_2$,[27] but now believe the structure with bridging hydrides and terminal halides to be the correct one based on arguments presented in chapter 3). Such a bridging hydride formulation also accounts for the lack of absorption attributable to terminal W-H groups in its IR spectrum. Unfortunately, it has not yet proven possible to grow single crystals of $[CpW(NO)I]_2(\mu\text{-}H)_2$ suitable for X-ray analysis due to its instability in solution.

F. Reactions of $[CpW(NO)H]_2(\mu\text{-}H)_2$ with PR_3 (R=OPh or OMe).

Upon the addition of 2 equivalents of $P(OPh)_3$ to a benzene solution of $[CpW(NO)H]_2(\mu\text{-}H)_2$ at room temperature, the reaction gradually changes from orange to intense purple in colour as reaction 2-6 occurs (step d of Scheme 2-I). The organometallic

$$[CpW(NO)H_2]_2 + 2\ P(OPh)_3 \xrightarrow[PhH]{} [CpW(NO)H\{P(OPh)_3\}]_2 + H_2 \qquad (2\text{-}6)$$

product may be isolated as a purple microcrystalline solid in 41% yield, while the H_2 product was identified by GC-MS[28]. The solid may be handled in air for short periods of time and is moderately soluble in non-aliphatic organic solvents to produce intense purple, air-sensitive solutions.

The IR spectrum of $[CpW(NO)H\{P(OPh)_3\}]_2$ in CH_2Cl_2 shows a strong ν_{NO} at 1591 cm^{-1} (which is very similar to that of the dihydride dimer at 1599 cm^{-1}) but no absorption attributable to a terminal ν_{WH}. The ^1H NMR spectrum of the complex in C_6D_6 contains the expected signals due to the phosphite and cyclopentadienyl ligands and, more importantly, only one complex multiplet that may be attributed to hydride hydrogens (Fig. 2-5a). Careful integration of the spectrum, run with a sufficient delay (45° pulse angle, ~10 s delay) between pulses to allow the cyclopentadienyl peaks to relax properly, shows that the ratio of Cp to hydride hydrogens is 5:1[29]. In addition, the ^1H spectrum run with ^{31}P decoupling (Fig. 2-5b) shows $^1J_{HW}$ = 55 Hz. This fact permits the assignment of the complex multiplet shown in Fig. 2-5a as the superimposition of a 1:2:1 triplet (due to ^1H-^{31}P coupling, $^2J_{HP}$ = 24 Hz) on top of a doublet (due to ^1H-^{183}W coupling) of 1:2:1 triplets. Integration of either of the hydride signals in Figure 5 shows the ^{183}W satellites to constitute ~25% of the total signal intensity. Finally, the ^{31}P NMR spectrum, recorded with only the phosphite protons decoupled, consists of a 1:2:1 triplet with $^2J_{PH}$ = 24 Hz, in agreement with

the ^{1}H spectrum.[2] This relatively small $^{1}H-^{31}P$ coupling is of the magnitude expected for a trans H-L configuration by analogy to those observed for the $CpM(CO)_2HL$ (L=tertiary phosphine) series of compounds.[18]

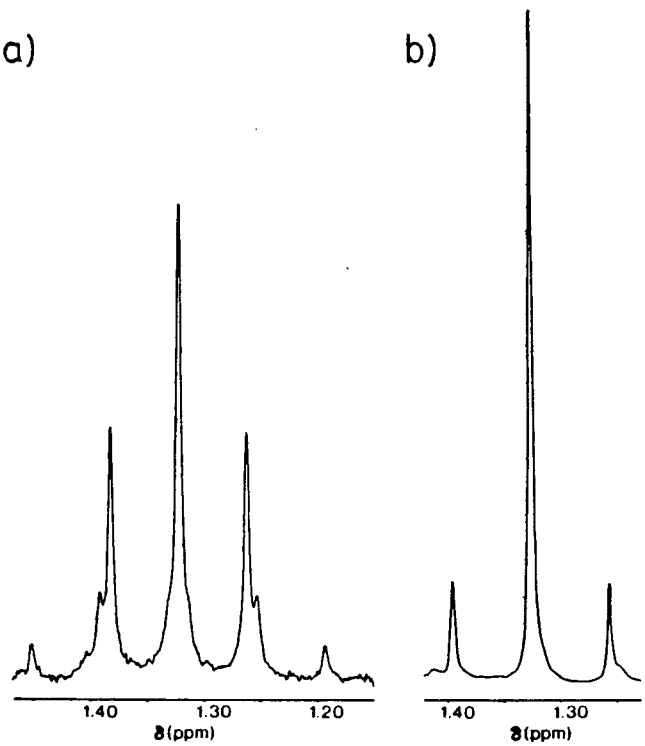

Fig. 2-5. The hydride regions of the 400-MHz a) ^{1}H, and b) $^{1}H\{^{31}P\}$ NMR spectra of $[CpW(NO)\{P(OPh)_3\}]_2(\mu\text{-}H)_2$ in C_6D_6.

Taken together, the spectroscopic properties of $[CpW(NO)H\{P(OPh)_3\}_2]$ suggest its dimeric formulation and it is therefore, perhaps, best formulated as $[CpW(NO)\{P(OPh)_3\}]_2(\mu\text{-}H)_2$ with a structure as depicted in Fig. 2-6.[24] The two phosphite

ligands are shown as being trans to each other since molecular models suggest that a cis configuration would be very unfavourable on steric grounds. The hydride ligands must be exchanging rapidly on the NMR time scale in order to maintain, on the average, something akin to a trans orientation with respect to the two phosphite ligands. This will be dealt with further in chapter 3. The $W_2(\mu\text{-}H)_2$ linkage in this system must be weaker than those in $[CpW(NO)I]_2(\mu\text{-}H)_2$ and $[CpW(NO)H]_2(\mu\text{-}H)_2$ since the low-resolution mass spectrum of $[CpW(NO)\{P(OPh)_3\}]_2(\mu\text{-}H)_2$ (probe temperature = 120°C) shows highest-mass peaks attributable only to a mixture of $[CpW(NO)H\{P(OPh)_3\}]^+$ and $[CpW(NO)\{P(OPh)_3\}]^+$ (m/z = 590, ^{184}W).[2]

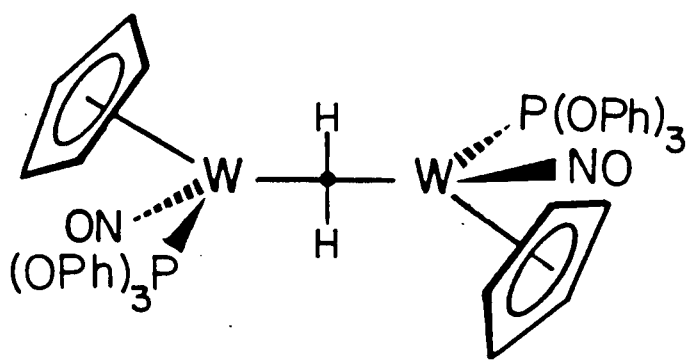

Fig.2-6. Proposed structure of $[CpW(NO)\{P(OPh)_3\}]_2(\mu\text{-}H)_2$.[24]

The weakness of this $W_2(\mu\text{-}H)_2$ interaction is reflected in the instability of the compound. As summarized in step e of Scheme 2-1, when a purple solution of $[CpW(NO)\{P(OPh)_3\}]_2(\mu\text{-}H)_2$

is stirred at room temperature (for a few days in benzene or a few hours in CH_2Cl_2) it gradually becomes orange. Addition of hexanes to the final solution induces the precipitation of a small amount of $CpW(NO)H_2[P(OPh)_3]$ as an analytically pure orange powder. This complex evidently results from a disproportionation reaction of the starting dimer (eq. 2-7), but the nature of the other organometallic products is not clear. A number of new,

$$[CpW(NO)\{P(OPh)_3\}]_2(\mu\text{-}H)_2 \xrightarrow[-\text{"}CpW(NO)[P(OPh)_3]\text{"}]{CH_2Cl_2 \text{ or } PhH} CpW(NO)H_2[P(OPh)_3] \qquad (2\text{-}7)$$

cyclopentadienyl-type resonances are observed when this reaction is followed by ^1H NMR spectroscopy. In any event, the occurrence of the individual reactions 2-6 and 2-7 (steps d and e of Scheme 2-I) clearly shows that the reaction of $[CpW(NO)H]_2(\mu\text{-}H)_2$ with Lewis base does not proceed simply in a manner analogous to that of steps b and f (eq. 2-3 and 2-4), as in eq. 2-8. Surprisingly, $CpW(NO)H_2[P(OPh)_3]$ does not appear to be accessible via step h (Scheme 2-I)--i.e. metathesis of an iodo ligand with $Na[H_2Al(OCH_2CH_2OCH_3)_2]$. Stirring of $CpW(NO)IH[P(OPh)_3]$ with the aluminum hydride reagent overnight results only in partial decomposition of the starting nitrosyl hydride and no formation of the desired product.

$$[CpW(NO)H]_2(\mu\text{-}H)_2 + 2\ L \xrightarrow[PhH]{CH_2Cl_2\ or} \not\rightarrow \quad 2\ CpW(NO)H_2L \qquad (2\text{-}8)$$

The complex $CpW(NO)H_2[P(OPh)_3]$ is an orange, diamagnetic, relatively air-stable solid which is soluble in most common, organic solvents. An IR spectrum of a CH_2Cl_2 solution of this compound (Table 2-I) has absorptions due to both terminal hydride and terminal nitrosyl ligands. Its ^1H NMR spectrum (Table 2-II) shows a Cp to hydride H atom ratio of 5:2 and has a hydride resonance pattern qualitatively very similar to those of the CpW(NO)IHL complexes (see above). This compound, therefore, likely has a conventional "four-legged piano-stool" structure with two equivalent, mutually trans, hydride ligands, i.e.

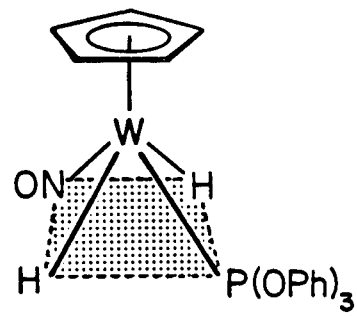

Proton NMR monitoring of the reaction of $[CpW(NO)H]_2(\mu\text{-}H)_2$ with $P(OMe)_3$ in C_6D_6 suggests that it proceeds analogously to that of $P(OPh)_3$ (eq. 2-6 and 2-7), albeit more rapidly. The only difference is that in the presence of the sterically less demanding phosphite, the purple intermediate

$[CpW(NO)\{P(OMe)_3\}]_2(\mu\text{-}H)_2$ is formed as a mixture of isomers (designated A and B in Table 2-II). The isomers show resonances consistent with their having structures analogous to that in Fig. 2-6, with the $P(OMe)_3$ ligands cis to each other in isomer A and trans in isomer B. Both isomers appear to disproportionate in solution at room temperature (the sterically crowded A more rapidly than B) to form $CpW(NO)H_2[P(OMe)_3]$ with the same trans dihydride structure as the $P(OPh)_3$ complex described above. No other hydride complexes of tungsten are detectable in the final solution. None of these $P(OMe)_3$ compounds have been isolated in a pure form.

G. Preparation and Properties of $[CpW(NO)Br_2]_2$.

The yields of all the hydride preparations discussed above are not very satisfactory. In particular, it was especially desired to raise the yield of $[CpW(NO)H]_2(\mu\text{-}H)_2$ so that its potentially interesting chemistry could be conveniently studied. It was felt that one contributing factor to the low yields of all the preparations is the low solubility of the $[CpW(NO)I_2]_2$ starting material in the reaction solvents and the consequent necessity of performing the reactions at room temperature. Therefore, the bromo analogue was prepared in the hope that it would be more soluble (on the grounds of smaller size and lower molecular weight) and the reactions could then be tried at lower temperature.

The preparation of $[CpW(NO)Br_2]_2$ by the addition of a stoichiometric amount of a Br_2/CH_2Cl_2 solution to $CpW(CO)_2(NO)$ proceeds analogously to that of $[CpW(NO)I_2]_2$[1] (Scheme 2-II).

Scheme 2-II

$CpW(CO)_2(NO)$ — ν_{CO} = 2010, 1927, ν_{NO} = 1655 cm^{-1}

↓ Br_2/CH_2Cl_2, − CO

$CpW(CO)(NO)Br_2$ — ν_{CO} = 2099, ν_{NO} = 1693 cm^{-1}

↓ − CO

$CpW(NO)Br_2$ — ν_{NO} = 1655 cm^{-1}

The IR bands described in the Experimental Section may be assigned to starting $CpW(CO)_2(NO)$, the $CpW(CO)(NO)Br_2$ intermediate and the final $CpW(NO)Br_2$ (see below). The particularly unusual feature of this reaction is that the final green reaction solution deposits a <u>brown</u>, analytically pure, microcrystalline solid, which is the $[CpW(NO)Br_2]_2$ product. This material is much more air-sensitive than its iodo analogue and, although it may be rapidly handled and weighed in air as a solid, such exposure must be brief. Solutions are sufficiently air-sensitive that complete decomposition of the complex occurs within five minutes upon exposure to air. The brown complex is considerably more soluble in most non-aliphatic, non-coordinating organic solvents than is $[CpW(NO)I_2]_2$ to yield brilliant <u>green</u>

coloured solutions reminiscent of $CpW(NO)_2Cl$.[30] In coordinating solvents, such as acetone, $[CpW(NO)Br_2]_2$ dissolves to instantly give orange solutions of what presumably is the solvated monomer, $CpW(NO)Br_2L$ (L=solvent). The IR spectrum of the bromo complex in CH_2Cl_2 shows a single ν_{NO} at 1655 cm^{-1}, 8 cm^{-1} lower than that of its iodo analogue.[1] Interestingly, the ^1H NMR spectrum of $CpW(NO)Br_2$ dissolved in $CDCl_3$ shows the expected singlet (at δ = 6.35), but this peak is sufficiently narrow that coupling of the cyclopentadienyl protons to ^{183}W can be observed ($^2J_{HW}$ = 1.8 Hz - Fig. 2-7). Reinspection of the spectrum of the iodo compound shows the same phenomenon ($CDCl_3$, δ = 6.29, $^2J_{HW}$ = 1.8 Hz). None of the other cyclopentadienyl tungsten compounds discussed in this thesis have narrow enough cyclopentadienyl resonances for this coupling to be observable. Unlike $[CpW(NO)I_2]_2$,[1] the low-resolution, electron-impact mass spectrum of $[CpW(NO)Br_2]_2$ (probe temperature = 150°C) has no peaks that can be attributed to a di-tungsten species, with the highest mass peaks (m/z = 439; ^{81}Br, ^{184}W) observed being due to the monomeric ion $[CpW(NO)Br_2]^+$ ($(P/2)^+$).

The unusual brown/green solid/solution colour characteristic of $[CpW(NO)Br_2]_2$ when compared to $[CpW(NO)I_2]_2$, which forms dark yellow-brown solutions from the brown solid, led us to speculate that the bromo compound might have a different solution structure. Therefore, qualitative UV-vis spectra of the two

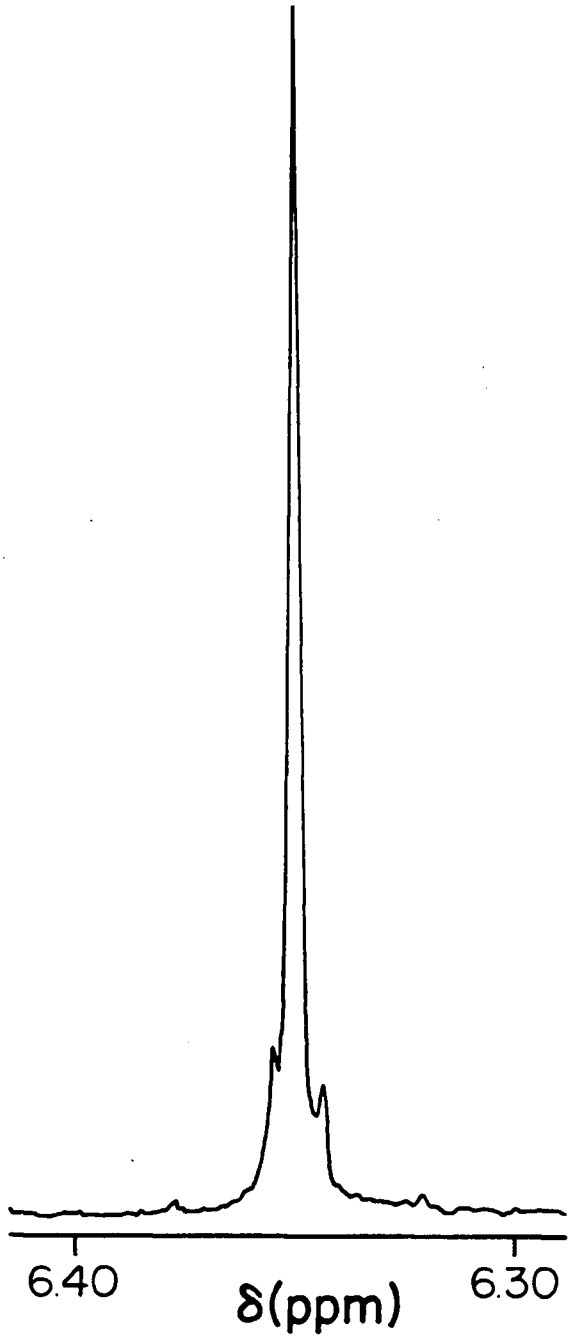

Fig. 2-7. The 80-MHz ^{1}H NMR spectrum of $CpW(NO)Br_2$ in $CDCl_3$ showing $^{2}J_{HW}$ = 1.8 Hz.

compounds were run in CH_2Cl_2 (Fig. 2-8). At concentrations appropriate for such spectra (10^{-3} to 10^{-5} M), solutions of the iodo compound are bright yellow in colour, while those of the bromo are a pale yellow-green. Although no attempt to measure extinction coefficients was made, it was clear that much less concentrated solutions of the iodo complex were needed to obtain good spectra. Inspection of these (Fig. 2-8) shows that they are qualitatively very similar, except the peaks for the iodo compound are shifted ~100 nm to lower energy. The d-d transitions may be assigned to the weak bands at 698 and 772 nm for the bromo and iodo compounds, respectively, while a number of much more intense charge-transfer bands may be seen at higher energies.[31] The spectrophotometric reason for the different colours in solution is now apparent. The colour of the bromo compound is governed by the weak d-d transition whose maximum is just within the visible region (400-700 nm), while that of the more intensely coloured iodo compound is governed by the much stronger charge-transfer band at 447 nm. This band has shifted from the ultraviolet region for the bromo complex into the visible region for the iodo as part of the above mentioned 100 nm shift. The overall similarity of the spectra suggest no radical structural difference between the two complexes in solution.

The most obvious possible structural difference between two such compounds would be a monomer/dimer differentiation. The $[CpW(NO)I_2]_2$ complex was formulated as a dimer on the basis of

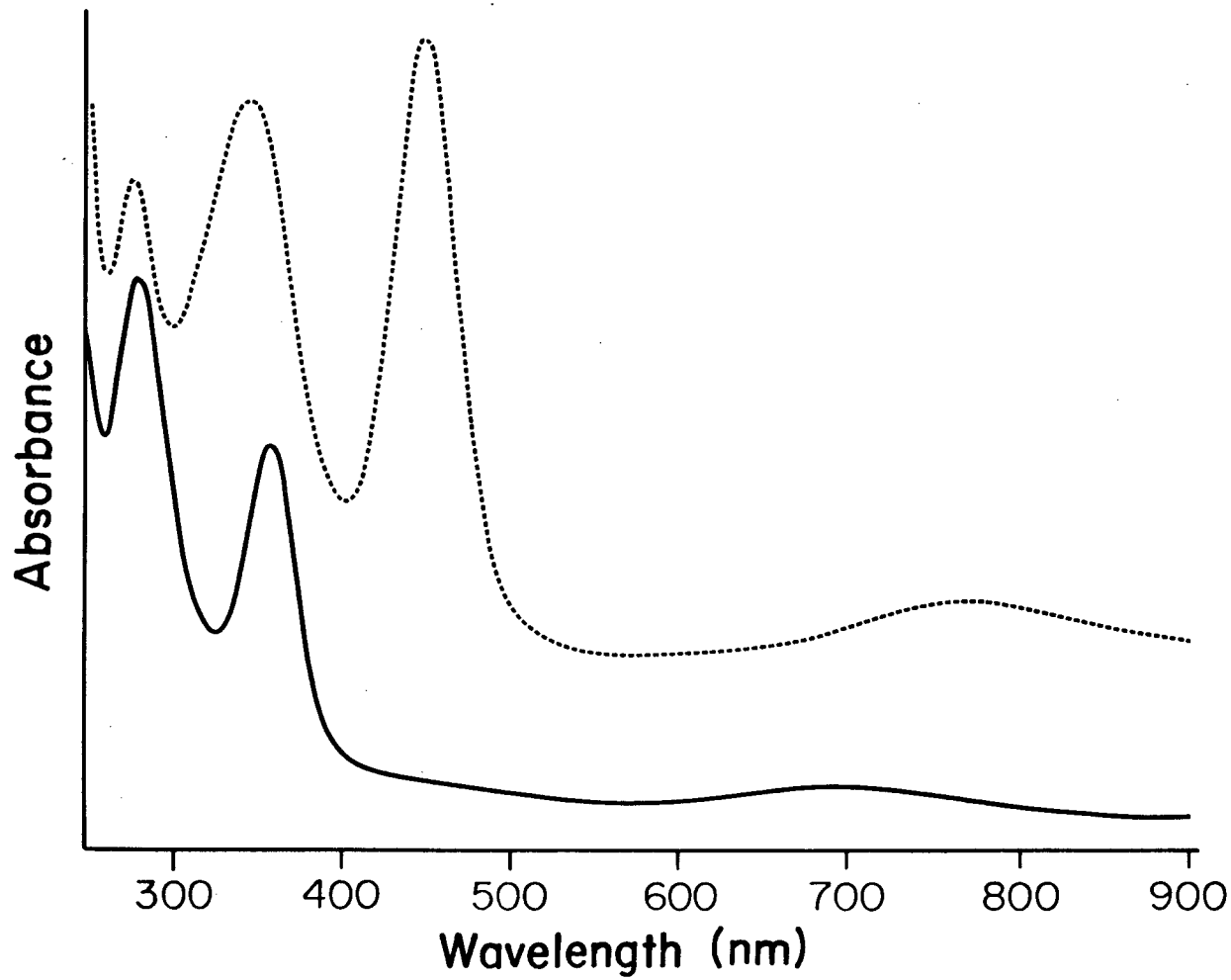

Fig. 2-8. UV-visible spectra of $CpW(NO)Br_2$ (——) and $CpW(NO)I_2$ (-------) in CH_2Cl_2.

the 18-electron rule and the observation of peaks in the mass spectrum due to di-metallic containing fragments.[1] The first compound of this type, $[CpMo(NO)I_2]_2$, was formulated as a dimer on the same basis.[32a] However, the tris-pyrazolylborate analogues are believed to be dimers when the pyrazole rings are unsubstituted (e.g. $[(HBpz_3)Mo(NO)I_2]_2$) but monomers when these rings are partially methyl substituted (e.g. $[HB(3,5\text{-}Me_2pz)_3]Mo(NO)I_2$).[32b] The latter conclusions were based on solubility properties and solution molecular weight measurements on the substituted compounds. Additionally, $Cp^*W(NO)I_2$ was recently prepared in our laboratory (see chapter 4) and shown to exist as a monomer both in the solid-state and in CH_2Cl_2 solution.[33]

It is clear from the fact that the electron-impact mass-spectrum of $[CpW(NO)Br_2]_2$ shows no di-tungsten fragments that any (presumably) halide bridges holding such a dimer together must be weaker in this compound that in its iodo analogue. However, although the bromo compound is much more soluble than the iodo, it is still not soluble enough for a solution molecular-weight determination.[34] Nevertheless, our belief is that $[CpW(NO)Br_2]_2$ exists as a brown dimer in the solid-state, but probably dissociates substantially upon dissolution to give green solutions of the monomer, $CpW(NO)Br_2$, although the evidence is not very conclusive. The similarity of the UV-vis spectra of the bromo and iodo compounds would therefore suggest that the latter,

too, forms a monomer in solution. These suggestions are supported by recent electrochemical studies which show the similarities of the cyclic voltammograms of the $CpM(NO)X_2$ species and by the preparation of a series of $[CpM(NO)X_2]^{\bullet -}$ radical anions.[35] Additionally, the observation of orange coloured solutions when $[CpW(NO)Br_2]_2$ is dissolved in coordinating solvents (e.g. acetone) is suggestive of the formation of a $CpW(NO)Br_2L$ (where L = solvent) species. This is the same colour as those observed for the $CpW(NO)X_2L$ (X=I, H, L=tertiary phosphine or phosphite) series of complexes discussed earlier.

H. Preparation and Properties of $CpW(NO)BrH[P(OPh)_3]$.

Regardless of whether $[CpW(NO)Br_2]_2$ exists as a monomer or dimer in solution, it does meet the above stated objective of greater solubility than its iodo analogue. The first step in assessing its utility as a starting material for hydride synthesis was to prepare the most easily isolated analogue to a known iodo compound. Consequently, $CpW(NO)BrH[P(OPh)_3]$ was prepared, at room temperature, in a manner exactly analogous to that of $CpW(NO)IH[P(OPh)_3]$ (steps a and b, Scheme 2-I above and ref. 2). The bromo compound is a bright, orange-red crystalline material whose air-sensitivity, solubility and mass-spectral properties are analogous to those of its iodo relative.

Its other spectroscopic properties are given in Tables 2-I and 2-II and it is informative to compare them with those of

$CpW(NO)IH[P(OPh)_3]$. For ease of comparison these data have been partially relisted in Table 2-III. Primarily, these spectral data indicate that the bromo and iodo compounds are isostructural. However, there are some interesting comparisons that can be made. Infrared spectra (CH_2Cl_2 solution) of the two

Table 2-III. Comparative Spectroscopic Data for the $CpW(NO)XH[P(OPh)_3]$ Complexes.

X		I	Br
IR(CH_2Cl_2)	ν_{NO}	1643	1636
(cm^{-1})	ν_{WH}	1883	1869
^1H NMR (C_6D_6)	δCp	4.85	4.84
(δ:ppm, J:Hz)	δW-H	-2.06	0.20
	$^1J_{HW}$	54	48
	$^1J_{HP}$	112	112
$^{31}P\{^1H\}$ NMR (C_6D_6)	δP	115.5	120.2
(δ:ppm, J:Hz)	$^1J_{PW}$	363	360

compounds show decreases in both the ν_{NO} (7 cm^{-1}) and ν_{WH} (14 cm^{-1}) vibrational frequencies upon substitution of Br for I. A decrease in ν_{NO} is usually ascribed to an increase in electron density on the metal centre, thereby permitting more back-bonding into the NO π^* orbital.[36] The observed reduction in ν_{NO} is

opposite to expectation, as substitution of I by the more electronegative Br (2.5 vs. 2.8)[37] would be anticipated to diminish the electron density on the tungsten centre available for back-bonding. The reason for the observation of the opposite trend is not clear. The decrease in ν_{WH} is more in line with expectations, as the draining of metal electron density onto the Br atom should weaken the W-H bond. The hydride regions of the ^1H NMR spectra are also interesting to compare. Substitution of I by Br shifts δ_{WH} by + 2.26 ppm. Electronegativity considerations would lead one to anticipate such a deshielding, but these arguments are usually not useful when discussing transition-metal hydrides.[38] On the other hand, the decrease in $^1J_{HW}$ is consistent with the trend observed for the CpW(NO)IHL complexes with decreasing donor ability of L discussed above.

The initial objective of turning to the bromo analogues was to improve the yields of hydride complexes. Unfortunately, a yield of only 13% was obtained in the preparation of $CpW(NO)BrH[P(OPh)_3]$--less than one-third of that obtained for the iodo compound. Likewise, numerous attempts to prepare $[CpW(NO)H]_2(\mu\text{-}H)_2$ in CH_2Cl_2/toluene at 0°C from $[CpW(NO)Br_2]_2$ only gave very low yields of poor quality material. Reaction temperatures lower than 0°C were not accessible because the dibromo compound became too insoluble at about this temperature for the reaction to be practicable. Attempts to use $[CpW(NO)Br_2]_2$ as a starting material for hydride synthesis were

therefore abandoned.

I. The Cyclic Voltammogram of $[CpW(NO)I_2]_2$.

In her preliminary work, J.C. Oxley explored a number of different routes to some of these hydride complexes.[2] As she so correctly pointed out, the low-yield step in all the routes attempted, including those described in this thesis, was always the halide/hydride metathesis. In addition to being metathesis reagents, hydride complexes such as $Na[H_2Al(OCH_2CH_2OCH_3)_2]$ can act as reducing agents. In fact, $Na[H_2Al(OCH_2CH_2OCH_3)_2]$ has been shown to work almost as well as Na amalgam as a reducing agent in the preparation of $CpMo(NO)L_2$ complexes (L=tertiary phosphine) from $[CpMo(NO)I_2]_2$[39] (eq. 2-9). Sometime after the synthetic work described in this chapter was completed, the cyclic voltammogram (CV) of $CpW(NO)I_2$ was run[35] in CH_2Cl_2 and this appears to offer some explanation for the low yields.[40] A CV

$$[CpMo(NO)I_2]_2 + 4\ L \xrightarrow[THF]{\text{Na/Hg or } Na[H_2Al(OCH_2CH_2OCH_3)_2]} 2\ CpMo(NO)L_2 \qquad (2\text{-}9)$$

is shown in Fig. 2-9 and, as can be seen, there are at least two reduction waves at relatively low potentials (-0.34 and -0.63 V vs. SCE). The ease of these reductions suggests the metathesis goes via an electron transfer mechanism, or, at the very least,

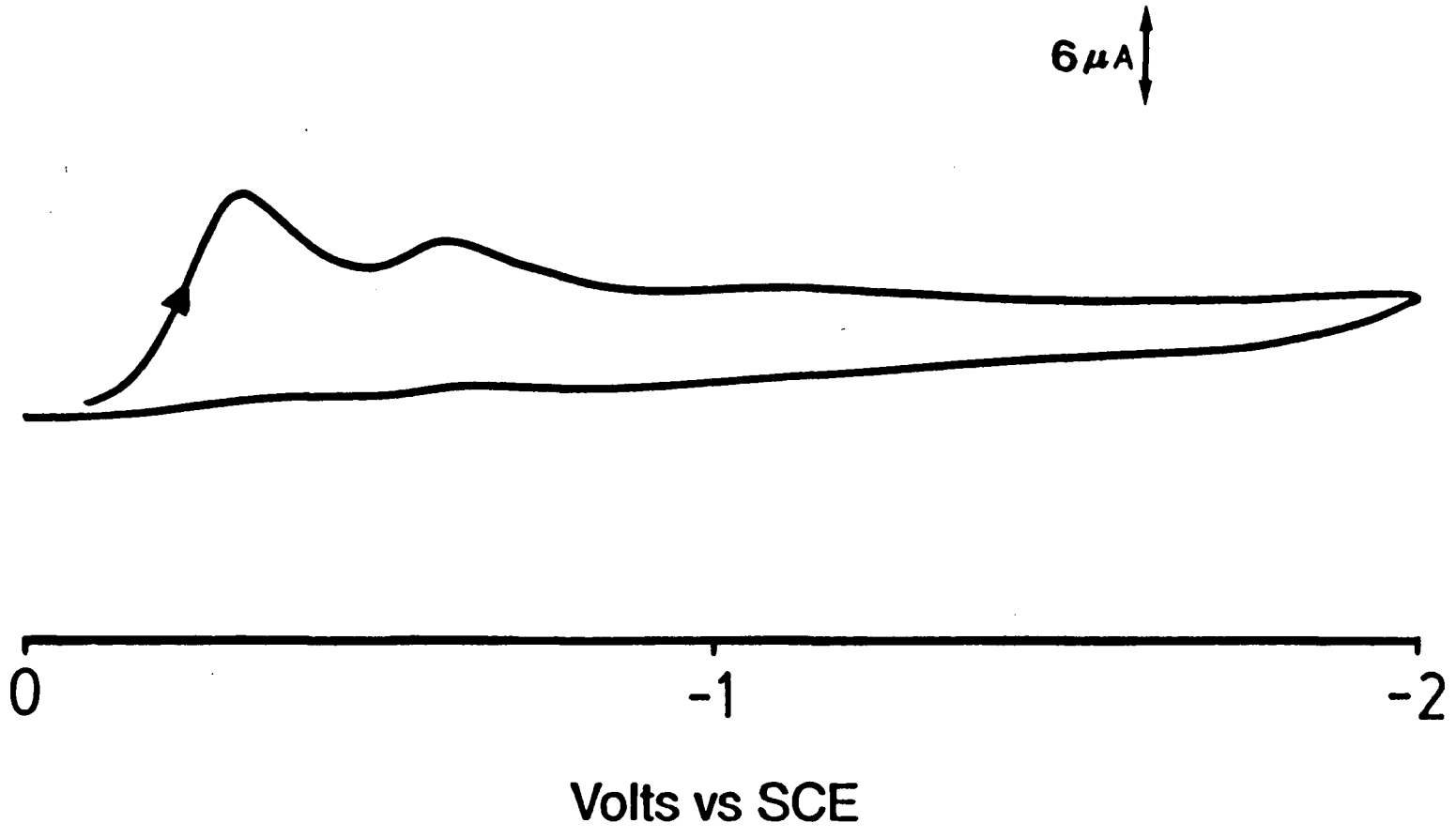

Fig. 2-9. The (reductive) cyclic voltammogram of $CpW(NO)I_2$ in CH_2Cl_2 using a Pt bead electrode and Bu_4NPF_6 as the support electrolyte. Scanrate = 0.4 Vs^{-1}.[35,41]

an electron transfer reaction is competing with metathesis. The fact that the reaction between $CpW(NO)I_2$ and $Na[H_2Al(OCH_2CH_2OCH_3)_2]$ to form $[CpW(NO)I]_2(\mu\text{-}H)_2$ is instantaneous is also consistent with an electron transfer mechanism. As Fig. 2-9 shows, the first reduction wave is completely irreversible and so electron transfer from $Na[H_2Al(OCH_2CH_2OCH_3)_2]$ to $CpW(NO)I_2$ must result in an unstable species that rapidly undergoes chemical change. The low yields for the metathesis reactions can therefore be explained by suggesting that this change removes the tungsten reagent from any pathway leading to the metathesis product, $[CpW(NO)I]_2(\mu\text{-}H)_2$. The desired product is obtained, therefore, only because the metathesis is extremely rapid and can compete with the electron transfer pathway. Further studies to clarify this issue are underway by other members of our research group.[35]

J. References and Notes

1. Legzdins, P.; Martin, D.T.; Nurse, C.R. Inorg. Chem. 1980, 19, 1560-1564.

2. Oxley, J.C. Ph.D. Dissertation, The University of British Columbia, 1983.

3. Shriver, D.F.; Drezdzon, M.A. "The Manipulation of Air-Sensitive Compounds", 2nd ed.; Wiley-Interscience: Toronto, 1986.

4. Merck Deuterated Solvents for NMR Catalogue, MSD Isotopes, Montreal, Que, Price List 47C, p 7.

5. Nixon, J.F.; Pidcock, A. Annu. Rev. Nucl. Magn. Reson. Spectrosc. 1969, 22, 345.

6. $Na[H_2Al(OCH_2CH_2OCH_3)_2]$ was purchased as a 3.4 M solution in toluene from the Aldrich Chemical Co. under the trade name Red-Al.

7. It is interesting to note that $[CpW(NO)I_2]_2$ does appear to react with $Na[H_2Al(OCH_2CH_2OCH_3)_2]$ in CH_2Cl_2 without any noticeable interference of the halogenated solvent.

8. GC-MS analysis of C_5H_{10} was done on a Nermag R10-10 spectrometer using a 30-m Carbowax capillary column at 1^oC.

9. Hames, B.W.; Legzdins, P.; Oxley, J.C. Inorg. Chem. 1980, 19, 1565-1571.

10. Adams, D.M. "Metal Ligand and Related Vibrations"; Edward Arnold Ltd.: London, 1967; pp 1-25 and references therein.

11. Cooper, C.B.; Shriver, D.F.; Onaka, S. Adv. Chem. Ser.

1978, **167**, 232-247.

12. Becker, E.D. "High Resolution NMR", 2nd ed.; Academic Press: New York, 1980; Chapter 7.

13. Jesson, J.P. in "The Hydrogen Series, Vol. 1. Transition-Metal Hydrides", Muetterties, E.L., Ed.; Marcel Dekker: New York, 1971; Chapter 4, p 79.

14. T_1 measurements were obtained with the assistance of Mr. J. Balatoni on a modified Nicolet-Oxford H-270 spectrometer using a $180^{\circ}-\tau-90^{\circ}$ pulse sequence. The absolute signal intensities were processed using standard Nicolet software.

15. Adam, M.J.; Hall, L.D. J. Organometal. Chem. 1980, **186**, 289-296.

16. Tolman, C.A. Chem. Rev. 1977, **77**, 313-348 and references therein.

17. Kubácek, P.; Hoffmann, R.; Havlas, Z. Organometallics 1982, **1**, 180-188 and references therein.

18. Kalck, P.; Poilblanc, R.J. J. Organometal. Chem. 1970, **24**, 445-452 and references therein.

19. Slater, S.G.; Luck, R.; Schumann, B.F.; Darensbourg, M. Organometallics 1982, **1**, 1662-1666.

20. Schatz, P.F. RACCOON 2.0; Moore, J.W. director; Project SERAPHIM; Eastern Michigan University: Ypsilanti, MI, 48197, 1984.

21. a) Kaesz, H.D.; Saillant, R.B. Chem. Rev. 1972, **72**, 231-281
b) Jones, S.B.; Petersen, J.L. Inorg. Chem. 1981, **20**, 2889-

2894 and references therein.

22. Since the isotopomer containing two ^{183}W nuclei is so scarce (and was never observed in our systems due to the low solubility of these complexes), the relative proportions of isotopomers having zero and one ^{183}W nucleus would be 74.8:25.2.

23. Deubzer, B.; Kaesz, H.D. J. Am. Chem. Soc. 1968, **90**, 3276-3277.

24. Reasons for depicting the $W_2(\mu\text{-}H)_2$ interaction using the "fused" representation will be discussed in chapter 3.

25. a) X-ray structure: Churchill, M.R.; Chang, S.W.-Y. Inorg. Chem. 1974, **13**, 2413-2419. b) neutron structure: Wei, C.-Y.; Marks, M.W.; Bau, R.; Kirtley, S.W.; Bisson, D.E.; Henderson, M.E.; Koetzle, T.F. Ibid 1982, **21**, 2556-2565.

26. Alt, H.G.; Mahmoud, K.A.; Rest, A.J. Angew. Chem. Int. Ed. Engl. 1983, **22**, 544-545.

27. Legzdins, P.; Martin, J.T.; Oxley, J.C. Organometallics 1985, **4**, 1263-1271.

28. GC-MS analysis for H_2 was done on a Kratos MS80 spectrometer scanning continuously at a rate of 1 scan/s using a 30 m, DB-1 capillary column with 5 μL coating at $0^{\circ}C$.

29. This is in contrast with the previously reported ratio of 5:2 and the previously assigned structure of cis-$CpW(NO)H_2[P(OPh)_3]$.[2]

30. Legzdins, P.; Malito, J.T. Inorg. Chem. 1975, **14**, 1875-1878

and references therein.

31. Cotton, F.A.; Wilkinson, G. "Advanced Inorganic Chemistry", 4th ed.; Wiley-Interscience: Toronto, 1980. pp 657-669.

32. a) King, R.B. Org. Mass. Spectrom. 1969, 2, 401-412 and references therein. b) McCleverty, J.A.; Seddon, D.; Bailey, N.A.; Walker, N.W. J. Chem. Soc., Dalton Trans. 1976, 898-908.

33. Einstein, F.W.B.; Jones, R.A.; Dryden N.H. personal communication.

34. Clark, E.P. Ind. Eng. Chem., Anal. Ed. 1941, 13, 820-821.

35. Richter-Addo, G.B. personal communication.

36. Chisholm, M.H.; Cotton, F.A.; Extine, M.W.; Kelly, R.L. Inorg. Chem. 1979, 18, 116-119 and references therein.

37. Pauling L. "The Nature of the Chemical Bond", 3rd ed.; Cornell University Press: Ithaca, New York, 1960, p 90.

38. Buckingham, A.D.; Stephens, P.J. J. Chem. Soc. 1964, 2747-2759.

39. Hunter, A.D.; Legzdins, P. Organometallics 1986, 5, 1001-1009.

40. A full analysis of the CV of $[CpW(NO)I_2]_2$ is outside the scope of this thesis.

41. Legzdins, P.; Wassink, B. Organometallics 1984, 3, 1811-1817.

CHAPTER 3

On the ^{1}H Nuclear Magnetic Resonance Spectra of Organometallic Tungsten Hydrides

In the last chapter, the syntheses and characterizations of $[CpW(NO)IH]_2$, $[CpW(NO)H_2]_2$ and $[CpW(NO)H\{P(OPh)_3\}]_2$ were discussed. During this work, one of the classic problems in bimetallic hydride chemistry was encountered--namely, determining the mode of attachment of the hydride ligands to the metal centres.[1] In trying to establish the structure of a bimetallic hydride complex, any investigator must deal with two questions: 1) Are the H atoms attached in a terminal or bridging fashion? and 2) Even if the physical properties of the complex in solution suggest the presence of a bridging H ligand, is this a truly static linkage or is it a time-averaged structure reflecting the occurrence of rapid fluxional processes such as

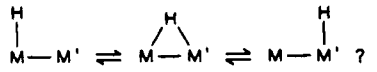

As in our case, when one of the metals involved is tungsten, the principal tool employed to attempt to answer these questions is ^{1}H NMR spectroscopy, since tungsten has a naturally occurring (14.4% abundant), spin 1/2 isotope, ^{183}W. Arguments about the nature of the W-H interaction in bimetallic compounds have involved both the chemical shifts of the hydride resonances and the magnitudes of the ^{1}H-^{183}W coupling constants observed in the solution ^{1}H NMR spectra of these species.[28] However, there has

been considerable uncertainty as to how these NMR parameters are affected by the bridging or terminal nature of the H ligands[33] as well as by the other ligands present in the complex. In this chapter, ^{1}H NMR arguments are made that eliminate much of this uncertainty.

For our di-tungsten complexes, we, too, had to answer the two questions posed above. Fortunately, our problem was simplified by the unique nature of $[CpW(NO)H_2]_2$. As discussed in chapter 2, and will be dealt with further in this chapter, this compound is more correctly represented as $[CpW(NO)H]_2(\mu\text{-}H)_2$ and has both bridging and terminal hydride ligands that are static. Moreover, the distinctive ^{1}H NMR spectral parameters of this complex have allowed us to develop criteria with which to reinterpret numerous ^{1}H NMR spectra of bimetallic organotungsten hydrides reported in the literature. In doing so, the static or fluxional characters of a number of such species have been deciphered, some of whose structures in solution have not been known with certainty for over 20 years. Furthermore, it has been found that the magnitudes of experimentally observed $^{1}H\text{-}^{183}W$ coupling constants permit reasonable estimates of the types of fluxional processes operating and, occasionally, the approximate time scales involved. Finally, and perhaps most importantly, it will be demonstrated that within certain, well-defined families of compounds the dependence of the magnitude of $^{1}J_{HW}$ on the nature of the W-H link can often be rationalized in terms of

straightforward bonding arguments.

Because of the central importance of $[CpW(NO)H]_2(\mu\text{-}H)_2$ to the overall discussion, the results of a single crystal X-ray analysis of this compound will be presented first.

Results and Discussion

A. Crystal and Molecular Structures of $[CpW(NO)H]_2(\mu\text{-}H)_2$.

The complex $[CpW(NO)H]_2(\mu\text{-}H)_2$ was prepared as described in chapter 2 and small single-crystals suitable for X-ray analysis were grown by slow evaporation under N_2 of a saturated CH_2Cl_2 solution of the compound at room temperature in a three-neck flask closed with a shut gas inlet tube and two unpunctured Suba-Seal septa[2] (CH_2Cl_2 loss occurred via absorption of the solvent vapour by the septa). Details of the data collection and refinement have been published elsewhere.[3]

The crystal structure of $[CpW(NO)H]_2(\mu\text{-}H)_2$ consists of discrete molecular units separated by normal intermolecular contact distances. Each unit, two views of which are shown in Fig. 3-1 and 3-2, consists of a centrosymmetric dimer of the form $Cp(NO)(H)W(\mu\text{-}H)_2W(H)(NO)Cp$ whose atomic coordinates and important structural parameters are given in Tables 3-I and 3-II. The W-N-O groups are essentially linear ($174(1)^{o}$), with the short W-N (1.753(11) Å) and long N-O (1.218(16) Å) bond lengths indicating the existence of considerable back-bonding from the electron-rich

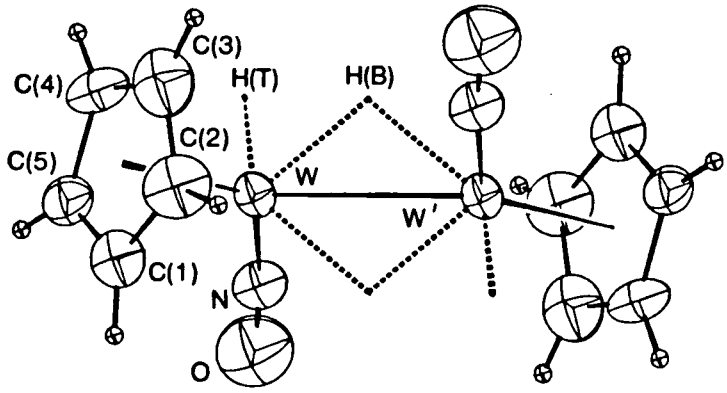

Fig. 3-1. View of the molecular structure of $[CpW(NO)H]_2(\mu\text{-}H)_2$. H(B) and H(T) are shown in observed (but unrefined) positions.

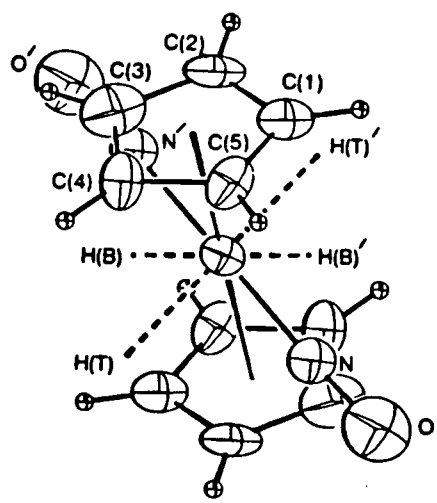

Fig. 3-2. End view of $[CpW(NO)H]_2(\mu\text{-}H)_2$ down the W-W axis.

Table 3-I. Atomic Coordinates for $[CpW(NO)H]_2(\mu\text{-}H)_2$.[a]

Atom	x	y	z
W	0.17165(5)	0.04140(6)	0.16400(8)
N	0.2563(14)	-0.1300(16)	0.0122(19)
O	0.3282(17)	-0.2363(18)	-0.0860(23)
C(1)	0.3499(17)	0.3538(19)	0.2323(26)
C(2)	0.2024(22)	0.4023(20)	0.2673(29)
C(3)	0.1876(20)	0.3124(24)	0.4711(32)
C(4)	0.3226(20)	0.2090(24)	0.5598(23)
C(5)	0.4247(16)	0.2425(21)	0.4117(23)
H(T)[b]	0.182	-0.150	0.351
H(B)[b]	-0.049	-0.022	0.168

a Crystal Data: triclinic system, $P\bar{1}$ space group, a = 8.542(1) Å, b = 6.607(2) Å, c = 5.838 Å, $\alpha = 94.64(2)^{\circ}$, $\beta = 108.06(1)^{\circ}$, $\gamma = 98.70(2)^{\circ}$.

b Hydride positions estimated from the electron-density difference maps, but not refined (see text and ref. 3).

Table 3-II. Important Interatomic Distances (Å) and Angles (deg) for $[CpW(NO)H]_2(\mu\text{-}H)_2$.[a,b]

W-W'	2.9032(9)	N-O	1.218(16)
W-N	1.753(11)	W-CP	2.019
W'-W-N	99.5(4)	W-N-O	174.3(10)
W'-W-CP	127.8	N-W-CP	126.6

a Primes indicate atoms related to those given in Table 3-I by the tranformation x,y,z → -x,-y,-z.

b CP is the centroid of C(1)-C(5):(0.2974, 0.3040, 0.3884).

metal centres to the nitrosyl ligands.[4] These structural features are consistent with the relatively low nitrosyl-stretching frequency (1599 cm^{-1} in CH_2Cl_2) observable in the IR spectrum of the compound (see chapter 2).

The most interesting part of this molecular structure is the W_2H_4 grouping. The tungsten-tungsten separation of 2.9032(8) Å is less than that of the W-W single bond (3.222(1) Å) in $[CpW(CO)_3]_2$,[5] and rather greater than the Mo≡Mo triple bond (2.448(1) Å) in the most closely related species, $[CpMo(CO)_2]_2$.[6] The molecular structure of the tungsten analogue, $[CpW(CO)_2]_2$, of this latter compound, has not yet been reported, but it is probable that its W≡W distance is similar to the Mo≡Mo bond length in the molybdenum complex due to the "lanthanide contraction."[7] In fact, the W-W bond length in the dihydride dimer resembles the 3.0162(11) Å separation found in the valence isoelectronic anion $[\{W(CO)_4\}_2(\mu\text{-}H)_2]^{2-}$,[8] thereby indicating substantial metal-metal bonding in $[CpW(NO)H]_2(\mu\text{-}H)_2$ (see below). The positions of the Cp and NO groups, and the metal-metal axis (Fig. 3-1) leave a "hole" in each tungstens coordination sphere, suggesting the presence of one terminal hydride ligand on each metal centre. Taken together with the ^1H NMR spectrum discussed in chapter 2 and the crystallographic centre of symmetry, this further implies the existence of two bridging hydride ligands between the tungsten atoms. These conclusions are given qualified support by the observation of

regions of increased electron-density in the expected places in the difference maps,[3] but none of the hydride atom positions could be successfully refined.[3] Nevertheless, reasonable positions for the bridging and terminal hydride ligands (H(B) and H(T) respectively) could be assigned and they are given in Table 3-I and Fig. 3-1 and 3-2. The plane defined by W, H(B), W' and W'(B) lies staggered between N'O' and H(T) (Fig. 3-2) as would be expected on the basis of simple steric considerations and lends credence to the assigned locations of the bridging hydride ligands. By analogy with the solid-state structure of $[\{W(CO)_4\}_2(\mu\text{-}H)_2]^{2-}$,[8] it is believed that H(B) and H'(B) are indeed equidistant from the two tungsten centres and that the bridging systems are regular.

As discussed in chapter 2, $[CpW(NO)H]_2(\mu\text{-}H)_2$ exists in solution as a mixture of two isomers, A and B (ratio ~1.3:1 at 20°C), and the solid-state structure found here is that of isomer A. Since a crystal of A was subjected to X-ray analysis, the possibility arises that in the solid-state, $[CpW(NO)H]_2(\mu\text{-}H)_2$ may exist solely as this isomer and that isomer B is formed only upon dissolution of the compound in various solvents. We believe that this is unlikely since the relative proportions of A and B are the same in $CDCl_3$ and C_6D_6. Hence, it is more likely that both A and B are formed during the initial synthesis of the complex and its is mere chance that a crystal of A was selected for X-ray analysis.

B. Bonding in the $W_2(\mu\text{-}H)_2$ Unit of $[CpW(NO)H]_2(\mu\text{-}H)_2$.

Conventionally, the bridging system in $[CpW(NO)H]_2(\mu\text{-}H)_2$ would be formulated as 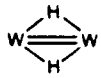 the formal W=W double bond being invoked so that each metal centre could attain the favoured 18-valence electron configuration.[9] Identical bridging systems have also been proposed for $[\{W(CO)_4\}_2(\mu\text{-}H)_2]^{2-}$[8a] and $[CpW(CO)]_2(\mu\text{-}H)_2$.[10] However, the only related system to have been subjected to detailed theoretical analysis to date is the 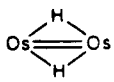 link in $(\mu\text{-}H)_2Os_3(CO)_{10}$. On the basis of Fenske-Hall molecular orbital calculations and the gas-phase ultraviolet photoelectron spectrum of $(\mu\text{-}H)_2Os_3(CO)_{10}$, Sherwood and Hall[11] concluded that the major part of the bonding in the $Os_2(\mu\text{-}H)_2$ system is composed of two three-centre, two-electron Os-H-Os bonds with an additional "t_{2g}-t_{2g}" bonding interaction between the metal centres. In addition, however, they noted significant hydrogen-hydrogen anti-bonding interactions. Because of these results and our observations discussed later in this chapter that this type of $W_2(\mu\text{-}H)_2$ system has a considerably different effect on $^1J_{HW}$ than would be expected from its representation as primarily two independent three-centre, two-electron W-H-W bridges, we believe that the planar $W_2(\mu\text{-}H)_2$ entity is best considered as a single, four-centre unit. To reflect this unity, we therefore propose the "fused" notation  to represent the bridging system in $[CpW(NO)H]_2(\mu\text{-}H)_2$. Such an interaction results in a formal tungsten-tungsten bond order somewhat greater

than one, as is reflected by the W-W separation observed in the solid-state, above. That this $W_2(\mu\text{-}H)_2$ interaction is quite strong is also suggested by the rigidity of the complex in solution (see below). Finally, this linkage is also probably aided by the presence of the NO ligands, which are known strong π-acids.[4] Like the CO groups in $(\mu\text{-}H)_2Os_3(CO)_{10}$,[11] the nitrosyl ligands can, in principle, remove W-W π^* antibonding electron density and thereby increase the net metal-metal bonding. Obviously, the confirmation of these inferences must await a theoretical analysis of the bonding in $[CpW(NO)H]_2(\mu\text{-}H)_2$.

C. The ^1H NMR Spectrum of $[CpW(NO)H]_2(\mu\text{-}H)_2$.

The assignment of the ^1H NMR spectrum of $[CpW(NO)H]_2(\mu\text{-}H)_2$ has been discussed in chapter 2 in some detail. However, thorough analysis of this spectrum yields considerably more information than mere assignment of the bridging and terminal nature of the hydride ligands. Firstly, it can be seen that observed values of the $^1J_{HW}$ and $^2J_{HW}$ coupling constants are in the range of 90-100 Hz and 13-15 Hz respectively (see Table 2-II). Secondly, and very importantly, the spectrum shows that both isomers A and B of $[CpW(NO)H]_2(\mu\text{-}H)_2$ are stereochemically rigid on the NMR time scale. This can be concluded because of observations of well-resolved ^1H-^1H coupling amongst the hydride ligands. In fact, from this, a reasonable estimate for the minimum lifetime of (e.g.) isomer B with respect to

intramolecular H(T) and H(B) exchange can be calculated to be $\tau \approx$ 90 ms, since $\Delta\nu = {}^{1}J_{HH} \approx 2.5$ Hz.[12]

Therefore, this spectrum indicates that for a given electronic environment in bimetallic complexes of this type, 1) the magnitude of the $^{1}H-^{183}W$ coupling is essentially independent of whether the hydride ligand is attached in a bridging or terminal fashion; 2) one-bond $^{1}H-^{183}W$ coupling is greater than two-bond; and 3) the resonances due to bridging hydrides appear upfield of those due to terminal hydrides.

These key results, particularly 1), coupled with the spectral parameters of appropriate monomeric tungsten hydrides, now enable us to reanalyze the ^{1}H NMR spectra of a number of bimetallic tungsten hydride complexes that have been reported in the literature over the years. First, however, we must discuss what sort of spectral patterns would be expected for given situations and how our results shed light on these patterns.

D. ^{1}H NMR Spectroscopic Criteria for Elucidating the Structures of Bimetallic Organotungsten Hydrides in Solution.

For a W_2H spin system, the ^{1}H NMR spectrum should consist of an equally spaced, five-peak pattern having an integrated intensity ratio of 0.5:12.3:74.4:12.3:0.5 regardless of whether the system involves a static, bridged W-H-W link or is undergoing rapid H-W-W $\rightleftharpoons$ W-W-H fluxionality.[13] The fundamental

difference between the two cases is that in the static situation, $J_{obsd} = {}^{1}J_{H(B)-W}$, while in the fluxional case $J_{obsd} = 1/2({}^{1}J_{H(T)-W} + {}^{2}J_{H(T)-W})$ as shown in Fig. 3-3. Analyses of heterobimetallic spin systems of the type WHM give similar conclusions, although for these systems only a three-line ^{1}H NMR pattern (intensity ratio = 7.7:85.6:7.7) due to coupling to ^{183}W would be expected. Reasonable estimates of the three ^{1}H-^{183}W coupling constants involved in all these cases are obtainable by analysis of the ^{1}H spectra of appropriate monomeric hydrido-tungsten complexes and by application of the principles derived from our analysis of the spectrum of $[CpW(NO)H]_2(\mu\text{-}H)_2$, above. Having these estimates of ${}^{1}J_{H(T)-W}$, ${}^{1}J_{H(B)-W}$ and ${}^{2}J_{H(T)-W}$ in hand (see Table 3-III), we are in a position to judge whether a particular bimetallic organotungsten hydride is static or fluxional in solution (with respect to the exchange of H ligands between metal centres) on the NMR time scale if the appearance of its ^{1}H spectrum does not resolve this question unambiguously. Furthermore, if the bimetallic complex is judged to be fluxional, the magnitude of J_{HW} observed enables us to make reasonable estimates of the types of fluxional processes involved and, on occasion, their approximate time scales.

The systems whose reported ^{1}H NMR spectra we have analyzed are grouped according to families in Tables 3-IV and 3-VII. These groupings contain most of the bimetallic tungsten hydrides and related monomeric complexes to be found in the literature to

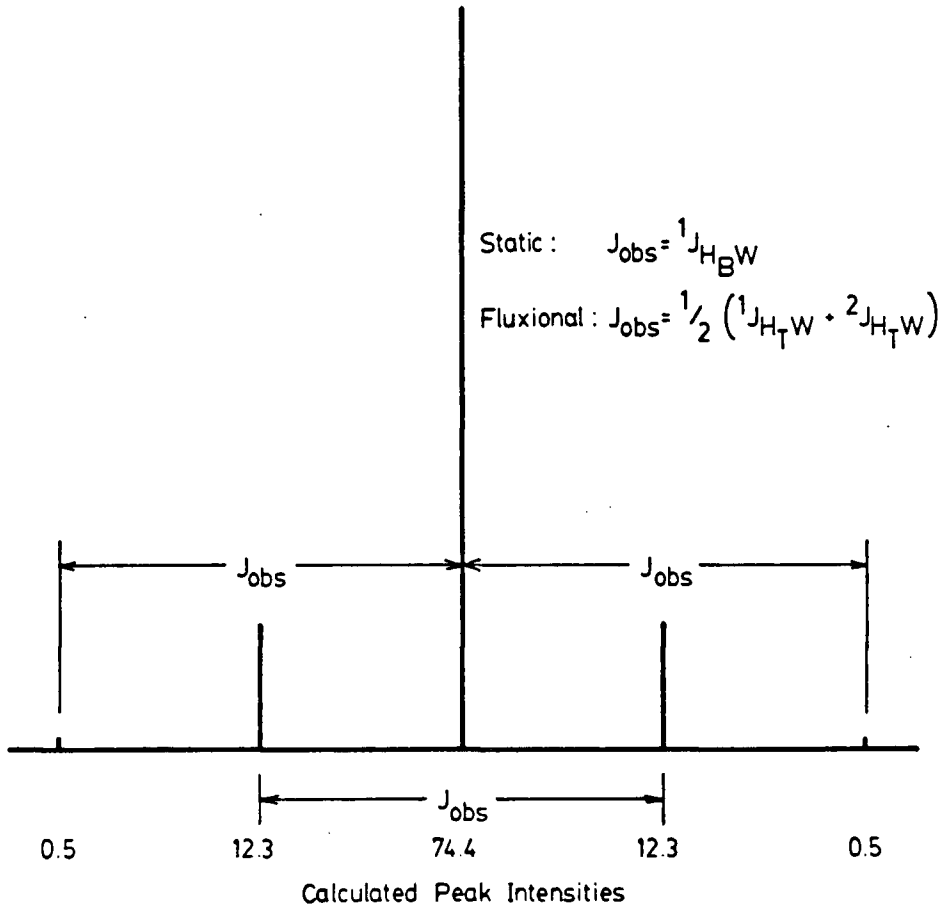

Fig. 3-3. Expected ^{1}H NMR pattern for static and fluxional W-H-W systems, the outer lines being drawn twice their actual size for clarity.

date. In addition to the chemical formula of each complex and the relevant ^{1}H NMR data, static representations of the tungsten-hydrogen bonding interactions have been included since they are central to many of the arguments presented below. These "fused" bonding representations are not, however, intended to reflect the structural dynamics of the complexes in solution, but rather what

Table 3-III. Approximate $^{1}H-^{183}W$ Coupling Constants Expected for Stereochemically Rigid Organotungsten Hydrides.

family of compds	nature of W-H linkage: conventnl reprsntn	nature of W-H linkage: fused[a] reprsntn	approximate expected $^{n}J_{^{1}H-^{183}W}$: n	approximate expected $^{n}J_{^{1}H-^{183}W}$: J (Hz)
Cp_2W	W-H	W-H	1	75
			1	65
			2	20
			1	100
			1	75
$CpW(CO)_3$	W-H	W-H	1	40
			1	80
			1	55
			1	40
$W(CO)_5$	W-H	W-H	1	55
			2	15
			1	60
			1	40
$CpW(NO)_2$	W-H	W-H	1	200
			2	20
$CpW(NO)^{b}$	W-H	W-H	1	50-90
			1	70-100
			1	55

a The rationale behind the use of the fused representation for the various W-H linkages is presented in the text.

b Because of the variety of other ligands coordinated to the CpW(NO) fragment, this family of compounds exhibits more variation in the expected $^{n}J_{HW}$ values.

the bonding would be if the compound were static. In the following discussion, all the $^{1}H-^{183}W$ coupling constants are assumed to have the same sign, although no determinations of such signs have been reported in the literature. However, spin tickling experiments on $[Cp^*W(NO)H](\mu-H)_2[Cp^*W(NO)(CH_2SiMe_3)]$ discussed in chapter 4 show that for this system, at least, $^{1}J_{H(B)-W}$, $^{1}J_{H(T)-W}$ and $^{2}J_{H(T)-W}$ all have the same sign, suggesting that the above assumption is valid.

E. Cp_2W Derivatives (Table 3-IV)

This family of compounds provides, perhaps, the most unambiguous series of organotungsten hydrides for analysis. Consideration of the ^{1}H NMR parameters in Table 3-IV for the Cp_2W derivatives which are unquestionably rigid[24] in solution on the NMR time scale leads to the approximate $^{n}J_{HW}$ values listed in Table 3-III for this family. These approximate coupling constants can be used to predict the solution molecular structures of the various fluxional species in this family.

The observed $^{1}H-^{183}W$ coupling constant of 45 Hz for the $[(CpWH)_2(\mu-H)\{\mu(\eta^5-C_5H_4-\eta^5-C_5H_4)\}]^+$ cation at ambient temperature is consistent with the system undergoing terminal-terminal hydrogen exchange

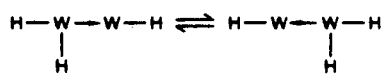

For such an exchange, J_{HW} (predicted) = $1/6\ (3 \times {}^{1}J_{HW} + 3 \times {}^{2}J_{HW}) = 1/6\ (3 \times 65 + 3 \times 20)$ Hz = 42.5 Hz, in excellent agreement with the observed value. This exchange

Table 3-IV. Tungsten Hydride ^{1}H NMR Parameters for Cp_2W Derivatives.

complex	T^a (°C)	solv	W-H interaction[b]	δ^c (ppm)	$^n J_{^1H-^{183}W}$ n	J^c (Hz)	J_{obsd} (Hz)	ref
Cp_2WH_2		C_6H_6		−12.28	1	73.2		14,15
$[Cp_2WH_3]^+$		conc HCl		H_A, −6.44	1	47.8[d]		14
				H_B, −6.08	1	NR		
$Cp_2W(H)Ph$		C_6D_6	W-H	−11.1	1	80		16
$Cp_2W(CH_3)_2$		C_6D_6	$W-CH_3$	0.24	2	6.0		17
$Cp_2WH_2{\cdot}W(CO)_5$		THF	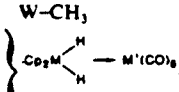	−15.2	1	63.0		15
				NR	2	19.2		
$Cp_2WH_2{\cdot}Mo(CO)_5$		THF		NR	1	65.8		15
$Cp_2MoH_2{\cdot}W(CO)_5$		THF		NR	2	19.6		15
$[(CpWH)_2(\mu\text{-}H)\{\mu(\eta^5\text{-}C_5H_4\text{-}\eta^5\text{-}C_5H_4)\}]^+$		CD_3CN	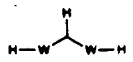	−16.0[e]			45	18
$[Cp_2W(\mu\text{-}H)_2Pt(PEt_3)(Ph)]^+$	−30	CD_2Cl_2	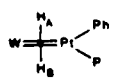	H_A, −14.1	1	99.1		19
				H_B, −17.1	1	101.1		
$[Cp_2HW(\mu\text{-}H)Pt(PEt_3)_2(Ph)]^+$	−20	CD_2Cl_2	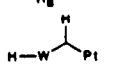	−18.7[e]			59.7	19
$[Cp_2W(\mu\text{-}H)_2Rh(PPh_3)_2]^+$		CD_2Cl_2		−18.11[e]			107	20,21
$[CpW(\mu,\sigma\text{:}1\text{-}5\text{-}\eta\text{-}C_5H_4)(\mu\text{-}H)_2IrH(PPh_3)_2]^+$		CD_2Cl_2	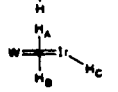	H_A, −16.41	1	92		21
				H_B, −18.28	1	~90		
				H_C, −24.55	2	NO		
$[CpW(H)(\mu,\sigma\text{:}1\text{-}5\text{-}\eta\text{-}C_5H_4)(\mu\text{-}H)IrH(dppe)(PPh_3)]^+$		CD_2Cl_2	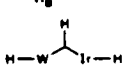	−15.88[e]			38	21
$Cp_2WH_2{\cdot}AlEt_3$		C_6H_6		−12.43	1	~72		22
$Cp_2WH_2{\cdot}ZnCl_2{\cdot}DMF$		DMF		−13.0	1	76.0		23

a Ambient temperatures unless indicated otherwise.

b The W-H bonding interactions are discussed in detail in the text.

c NO = not observed (i.e., the cited paper specifically states that no ^{1}H-^{183}W coupling was observed). NR = not reported (i.e., no mention whatsoever is made of this parameter).

d This coupling constant may be too low by a factor of 2 (cf. ref 15).

e The complex is fluxional on the NMR time scale at the indicated temperature and all hydride H's are equivalent.

probably proceeds via a symmetrically bridged W-H-W intermediate, but the intermediate does not possess a significant lifetime on the NMR time scale and is therefore undetectable. A similar exchange mechanism,

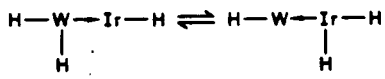

may be invoked for the $[CpWH(\mu,\sigma:1\text{-}5\text{-}\eta\text{-}C_5H_4)(\mu\text{-}H)IrH(dppe)\text{-}(PPh_3)]^+$ cation at room temperature to account for its observed J_{HW} of 38 Hz. For both these cases an approximate maximum lifetime for the exchanging species can be calculated to be $\tau \approx 5$ ms, since $\Delta\nu = \Delta J \approx (65\text{-}20) = 45$ Hz.[12] This same type of calculation can be done for all the exchanging species discussed in this chapter.

The fluxionality of the $[Cp_2HW(\mu\text{-}H)Pt(PEt_3)_2(Ph)]^+$ cation at -20^oC is clearly different from that just considered since its J_{HW} value is 59.7 Hz. This observation may be reasonably well accounted for by invoking either of the exchange mechanisms shown below, i.e.

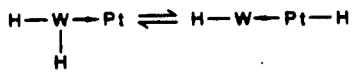

for which J_{HW} (predicted) = 1/4 (3 x $^1J_{H(T)-W}$ + $^2J_{H(T)-W}$) = 1/4 (3 x 65 + 20) Hz = 54 Hz, or

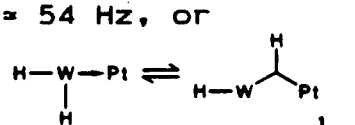

for which J_{HW} (predicted) = 1/4 (3 x $^1J_{H(T)-W}$ + $^1J_{H(B)-W}$) = 1/4 (3 x 65 + 65) Hz = 65 Hz, if it is assumed that $^1J_{H(T)-W} \approx {}^1J_{H(B)-W}$ as is true for $[CpW(NO)H]_2(\mu\text{-}H)_2$. Both these types of fluxionality are also consistent with the limited variable

temperature ^1H NMR data on this complex.[19]

The ^1H NMR spectrum of $[Cp_2W(\mu\text{-}H)_2Rh(PPh_3)_2]^+$ in CD_2Cl_2 at ambient temperature is particularly interesting in that it indicates both hydride ligands to be equivalent (rather than the expected AA'MXX' (= HH'RhPP' system) and therefore fluxional, and displays a large J_{HW} value of 107 Hz. As can be seen from Table 3-III and from a general perusal of Tables 3-IV to 3-VII, a tungsten-hydride interaction that can be written (in static form) as 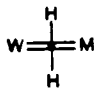 always shows a $^1H\text{-}^{183}W$ coupling constant considerably greater than that for its monomeric parent. The observation of such a large coupling for this 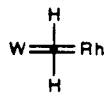 linkage immediately suggests what type of fluxionality is occurring. If this compound were undergoing

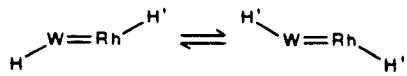

fluxionality, then J_{HW} (predicted) = 1/2 ($^1J_{H(T)-W}$ + $^2J_{H(T)-W}$) = 1/2 (100 + 20) Hz = 60 Hz--a long way from the observed value. On the other hand, if the exchange process involves the two hydride ligands maintaining direct interaction with both metal centres (e.g. by spinning about the metal-metal axis), then J_{HW} (predicted) = 1/2 ($^1J_{H(B)-W}$ + $^1J_{H(B)-W}$) = 1/2 (100 + 100) Hz = 100 Hz--very much in agreement with observation. An identical conclusion was reached by the original investigators[20,21] on the basis of variable temperature ^1H NMR studies.

The Lewis adduct complexes of Cp_2WH_2 (e.g. $Cp_2WH_2 \cdot AlEt_3$ and $Cp_2WH_2 \cdot ZnCl_2 \cdot DMF$) present a different and interesting situation.

These complexes have traditionally been assumed to involve a simple W→M donor bond[22] of the sort invoked for the $Cp_2H_2W{\rightarrow}M(CO)_5$ compounds.[15] This is because in the original report on this type of compound (on $Cp_2WH_2{\cdot}AlMe_3$), the IR spectrum (KBr disc) showed a decrease in ν_{WH} upon complexation (1912 to 1898 cm^{-1}) which was thought to be too small for the H's to have gone from terminal to bridging.[25] However, a recent, low-temperature (-166°C) X-ray crystal analysis of $Cp_2WH_2{\cdot}AlMe_3$ shows this assumption to be incorrect.[26] For this structure, all the atoms including the hydride ligands could be refined, and it showed these ligands to be truly bridging--i.e. $Cp_2W(\mu\text{-}H)_2AlMe_3$. An earlier structure of $Cp_2MoH_2{\cdot}ZnBr_2{\cdot}DMF$ showed essentially the same thing.[27] Simple electron-counting on these compounds shows that they cannot have a formally metal-metal double-bond type of structure, e.g. 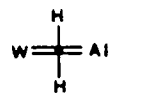 and this is reflected in the observed J_{HW} values (~75 Hz vs. 100 Hz). Rather, these compounds have a formally singly bonded 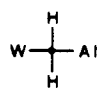 type of linkage which appears to exhibit $^1J_{HW}$ couplings essentially unchanged from those of the mononuclear precursor. More will be said about this later in the discussion.

One final point concerning the data in Table 3-IV requires discussion. This is that the chemical shifts of the individual resonances due to the hydride ligands are unreliable guides to their bridging or terminal natures. Signals due to static hydrides terminally bound to the Cp_2W moiety can be found from

δ -6 to -15 ppm, whereas those due to static, bridging hydrides range from -12 to -18 ppm. Although this agrees with the generally observed trend of bridging hydrides exhibiting signals upfield of those due to terminal H ligands,[28] it remains that the overlapping of these two regions means that the chemical shift of just a single signal cannot be employed with certainty to determine whether a hydride is bridging or terminal. In addition, in cases of fluxional molecules, the chemical shifts provide no information whatsoever about whether the fluxionality involves terminal-terminal, terminal-bridging or bridging-bridging exchange while, as we have seen, the observed J_{HW} is quite informative on this point. These same conclusions apply to the other families of organotungsten hydrides which are considered below.

F. $CpW(CO)_3$ Derivatives (Table 3-V)

Although the magnitudes of the $^1H-^{183}W$ coupling constants observed for this family are smaller than those for the Cp_2W derivatives, a similar type of analysis is possible. The model complex, $CpW(CO)_3H$, exhibits $^1J_{HW}$ of ~37 Hz, which increases to 48 Hz upon replacement of one of the CO ligands by the strongly basic PMe_3. This is presumably a manifestation of the increased s-electron density at the metal centre in this latter complex (see section I). As for the Cp_2W-containing compounds, involvement of derivatives of this family in 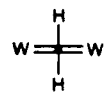

Table 3-V. Tungsten Hydride ^{1}H NMR Parameters for $CpW(CO)_3$ Derivatives.

complex	T^a (°C)	solv	W-H interaction[b]	δ^c (ppm)	$^nJ_{^1H-^{183}W}$ n	$^nJ_{^1H-^{183}W}$ J (Hz)	J_{obsd} (Hz)	ref
$CpW(CO)_3H$		C_6H_{12}	W-H	-7.33	1	37.7		29
	-70	$CDCl_3$	W-H	-7.3	1	36.7[d]		30
cis-$CpW(CO)_2(PMe_3)H$	-38	C_7D_8	W-H	-8.32	1	48.0		31
trans-$CpW(CO)_2(PMe_3)H$	-38	C_7D_8	W-H	-7.51	1	48.0		31
$CpW(PMe_3)H_5$		C_6D_6	W-H	-3.95	1	42.5		32
$CpW(PMe_3)_2(\eta^2\text{-}C_5H_8)H$		C_6D_6	W-H	-7.35	1	40		32
$[[CpW(CO)_3]_2(\mu\text{-}H)]^+$		conc H_2SO_4		-24.77	1	38.6[e]		33
$[[CpW(CO)_3](\mu\text{-}H)[CpMo(CO)_3]]^+$		conc H_2SO_4		-22.88	1	38.0[d]		33
$[CpW(CO)_2]_2(\mu\text{-}H)(\mu\text{-}OMe)$	-80	$(CD_3)_2CO$		-10.56	1	57.4		34
$[[CpW(CO)_2]_2(\mu\text{-}H)(\mu\text{-}MeCCMe)]^+$		$(CD_3)_2CO$		-18.5	1	32		35
$[CpW(CO)_2](\mu\text{-}H)(\mu\text{-}CHMe)[Pt(PMe_3)_2]$								
isomer i	-30	CD_2Cl_2		-7.77	1	53		36
isomer ii	-30	CD_2Cl_2		-8.29	1	56		
$Cp(CO)_2\overline{WCH(PMe_3)\text{–}CHCOMe}$	-20	CD_2Cl_2		2.49	2	3.2		37
				2.01	2	4.5		
$[(Ph_3PC_5H_4)W(CO)_3H]^+$		CF_3COOH	W-H	-7.15	1	36		38
$[CpW(CO)_2]_2(\mu\text{-}H)_2$	-30	$(CD_3)_2CO$		-13.24	1	83.1[e]		10
$[(\eta^5\text{-}C_5Me_5)W(CO)_2]_2(\mu\text{-}H)_2$		$(CD_3)_2CO$		-9.30	1	82.8		10
$CpW(CO)_3(SnMe_3)$		C_6H_6	$(\eta^5\text{-}C_5H_5)W$	NR	2	1.4		39
			W-Sn-CH_3	0.52	3	~0.6		

a Ambient temperatures unless indicated otherwise.

b The W-H bonding interactions are discussed in detail in the text.

c NR = not reported (i.e., the cited paper makes no mention whatsoever of this parameter).

d ^{183}W satellites were reported to constitute ~14% of the total integrated area of the resonance.

e ^{183}W satellites were reported to constitute ~24% of the total integrated area of the resonance.

interactions markedly increases $^{1}J_{HW}$, for example, to ~83 Hz for $[CpW(CO)_2]_2(\mu\text{-}H)_2$.

The complexes listed in Table 3-V that can be represented as having 3-centre, 2-electron  bridges constitute a most interesting class. These compounds fall into two categories: unsupported and supported. In the former, the two complexes which contain such an unsupported bridge, $[\{CpW(CO)_3\}(\mu\text{-}H)\{CpM(CO)_3\}]^+$ (M=W or Mo), show $^{1}H\text{-}^{183}W$ coupling constants of 38.6 and 38.0 Hz, which are similar to those observed for the monomeric species. If these systems were fluxional, then J_{HW} (predicted) = 1/2 ($^{1}J_{HW}$ + $^{2}J_{HW}$) = 1/2 (40 + 15) Hz = 27.5 Hz if it is assumed that two-bond $^{1}H\text{-}^{183}W$ coupling in these systems is similar to that found for Cp_2W derivatives. The only two-bond data available for the $CpW(CO)_3$ family involve coupling through a carbon centre ($^{2}J_{HW}$ = 4 Hz)[37]--a scan of the limited data in Tables 3-IV to 3-VII suggest that through-carbon couplings are generally less than through-metal. Nevertheless, the observation of coupling of the magnitude expected for a monomer suggests that the $[\{CpW(CO)_3\}(\mu\text{-}H)\{CpM(CO)_3\}]^+$ cations in solution are static with respect to hydride ligand exchange.

In the second category are those complexes in which the formally electron-deficient, 3-centre, 2-electron bridge is supported by some other bridging ligand. Superficially, the bridges in $[CpW(CO)_2]_2(\mu\text{-}H)(\mu\text{-}OMe)$ and $[CpW(CO)_2](\mu\text{-}H)\text{-}(\mu\text{-}CHMe)[Pt(PMe_3)_2]$ each appear to be a combination of a

separate, 3-centre, 2-electron bridge and an electron-sufficient (μ-OMe) or (μ-CHMe) bridge. However, these complexes exhibit ^{1}H-^{183}W couplings some 20 Hz greater than those for the unsupported systems. Nevertheless these values are still ~25 Hz less than those observed for the 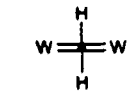 grouping in this family. To reflect these facts, we believe that these two supported, planar bridging systems are best viewed as single, four centre groupings as the fused representations 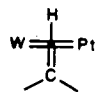 and 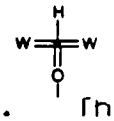 imply, rather than as, for example, 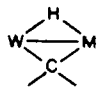 or 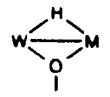 . These fused symbols also visually suggest the similarity of these linkages to the  bridge, which Sherwood and Hall have described[11] as being fundamentally the same, although the  interaction was shown to be weaker. Interestingly, this intuitively agrees with the observed trend in coupling constants. When the bridge incorporates a perpendicular acetylene to give  in $[\{CpW(CO)_2\}_2(\mu\text{-}H)(\mu\text{-}MeCCMe)]^+$, the ^{1}H-^{183}W coupling constant reverts back to that of an unsupported bridge, suggesting the removal of planarity from the supported bridge results in a W-H-W interaction that is essentially the same as an unsupported one. Since the unsupported 3-centre, 2-electron linkages appear to be static in solution, it is believed that the supported ones are non-fluxional as well.

G. $W(CO)_5$ Derivatives (Table 3-VI)

The obvious parent monomer presently known in this family is $[HW(CO)_5]^-$, and it exhibits $^1J_{HW}$ = 53.4 Hz. Surprisingly, this parameter does not change significantly upon replacement of a carbonyl ligand by a phosphine or a phosphite. Nevertheless, when these species engage in 3-centre, 2-electron 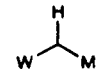 linkages, there is a decrease in the observed $^1H-^{183}W$ coupling constant to 38-45 Hz. At first glance, this would appear to be suggestive of terminal-terminal hydrogen exchange (as for the analogous Cp_2W derivatives discussed earlier). In such a situation, J_{HW} (predicted) = 1/2 ($^1J_{HW}$ + $^2J_{HW}$) = 1/2 (54 + 15) Hz = 34.5 Hz.[49] However, the static nature of $[\{W(CO)_4P(OMe)_3\}(\mu\text{-}H)\{W(CO)_5\}]^-$ is established unambiguously by the observation of two distinct $^1H-^{183}W$ coupling constants, a fact attributed to the presence of an asymmetric hydride bridge.[41] Furthermore, variable-temperature ^1H NMR studies of $[W(CO)_5](\mu\text{-}H)[AuPPh_3]$ have confirmed the absence of hydride ligand exchange in this compound.[45] By analogy, it therefore seems likely that all the related species listed in Table 3-VI are also static. This apparent contravention of the principles established for the other families may possibly be explained by the fact that the parent in this case is a monoanion, while the parents in all the other cases are neutral. The anionic nature of $[HW(CO)_5]^-$ would undoubtedly result in increased s-electron density at the metal centre over what would be expected in a

Table 3-VI. Tungsten Hydride ^1H NMR Parameters for $W(CO)_5$ Derivatives.

complex	T^a (°C)	solv	W-H interaction[b]	δ (ppm)	$^nJ_{^1H-^{183}W}$ n	$^nJ_{^1H-^{183}W}$ J (Hz)	J_{obsd} (Hz)	ref
$[HW(CO)_5]^-$		CD_3CN	W-H	−4.2	1	53.4		40
$[HW(CO)_4\{P(OMe)_3\}]^-$		CD_3CN	W-H	−4.5	1	54		41
$[HW(CO)_4(PMe_3)]^-$		CD_3CN	W-H	−3.6	1	54		41
$[\{W(CO)_5\}_2(\mu\text{-H})]^-$		THF		−12.52	1	41.9[c]		42
$[\{W(CO)_5\}(\mu\text{-H})\{Mo(CO)_5\}]^-$		THF		−12.37	1	42.3		42
$[\{W(CO)_5\}(\mu\text{-H})\{Cr(CO)_5\}]^-$		THF		−15.43	1	~40		42
$[\{W(CO)_4P(OMe)_3\}_2(\mu\text{-H})]^-$		CD_3CN		−11.9	1	45.2		43a
$[\{W(CO)_4P(OMe)_3\}(\mu\text{-H})\{Cr(CO)_5\}]^-$		CD_3CN	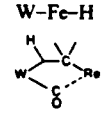	−14.4	1	38.4		41
$[\{W(CO)_4P(OMe)_3\}(\mu\text{-H})\{W(CO)_5\}]^-$		CD_3CN		−12.2	1	42, 45.6[d]		41
$[W(CO)_3(NO)\{P(OMe)_3\}](\mu\text{-H})[W(CO)_5]$		$CDCl_3$		−12.50	1	39.5		44
$[W(CO)_5](\mu\text{-H})[AuPPh_3]$		CD_2Cl_2		−2.69	1	46		45
$[W(CO)_5](\mu\text{-H})[Cp_2Ta(CO)]$		C_6D_6		−15.48	1	42.5		46
$[\{W(CO)_5\}\{Fe(CO)_4H\}]^-$		THF	W-Fe-H	−11.8	2	15.0		47
$[W(CO)_3](\mu\text{-CO})(\mu\text{-}\eta^2\text{-}CH_2C_6H_4Me\text{-}4)(\mu\text{-dppm})[Re(CO)_3]$	−20	CD_2Cl_2		−3.69	1	48		48
$[\{W(CO)_4\}_2(\mu\text{-H})_2]^{2-}$		$(CD_3)_2CO$		−4.0	1	62[e,d]		43
$W(CO)_5(PMePh_2)$		CH_2Cl_2	W-P-CH_3	2.21	3	2.1		39

a Ambient temperatures unless indicated otherwise.

b The W-H bonding interactions are discussed in the text.

c ^{183}W satellites were reported to constitute ~24% of the total integrated area of the resonance.

d Two separate $^1H-^{183}W$ coupling constants are observable due to the asymmetry of the complex.

e See text for discussion of this species.

f Redetermined value.

neutral species, and this could be the cause of the unexpectedly large value of $^1J_{HW}$. The most appropriate parent for this family could therefore be $(\eta^2\text{-}H_2)W(CO)_3(PCy_3)_2$ (Cy = cyclohexyl). Unfortunately, probably because of dipolar broadening, ^{183}W

satellites of the η^2-H_2 resonance were not observable.[50] If coupling to ^{183}W is ever observed, it is predicted that the coupling constant will be in the vicinity of 40-45 Hz (such coupling may more conceivably be observable in the (η^2-HD) analogue). Because of the well-known isolobal analogy between $AuPPh_3$ and H,[51] the above mentioned $[W(CO)_5](\mu\text{-}H)[AuPPh_3]$ (perhaps better described as $(\eta^2\text{-}HAuPPh_3)W(CO)_5$) may therefore be a suitable parent "monomer." An alternative parent is one of the recently reported $HW(CO)_x(NO)(PR_3)_{4-x}$ (x = 3 or 2) complexes, however the $^1J_{HW}$ values were not included in the report.[52]

The $[\{W(CO)_5\}\cdot\{Fe(CO)_4H\}]^-$ anion is quite an interesting species. It was originally formulated as $[\{W(CO)_5\}\text{-}(\mu\text{-}H)\{Fe(CO)_4\}]^-$[47a] but was later reformulated as having "considerable Fe-H terminal character" on the basis of its solid-state molecular structure.[47b] In solution, some bridging character was attributed to the hydride ligand because of "the distinctive highfield position of the hydride resonance (-11.8 ppm) and a definite (albeit small, 15.0 Hz) W-H coupling."[47b] As has been noted earlier, the chemical shift is not a particularly useful criterion to use in these situations. Since the observed coupling constant is of the magnitude expected for $^2J_{HW}$, we believe that direct W-H interaction in $[\{W(CO)_5\}\cdot\{Fe(CO)_4H\}]^-$ is negligible. More recently, the original investigators of the system have also adopted this view.[53]

Previous investigators have reported $^{1}J_{HW}$ values for $[\{W(CO)_4\}_2(\mu\text{-}H)_2]^{2-}$ of 32[8b] and 30.4 Hz.[43a] These numbers seemed too low for what would be expected for a 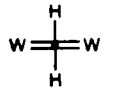 grouping (see above). Consequently, we have redetermined this coupling constant and found it to be 62 Hz, that is, twice the published value.[43b] This magnitude is more in line with the trends in $^{1}H\text{-}^{183}W$ coupling found for the other families of organotungsten hydrides (Table 3-III).

H. $CpW(NO)_x$ (x = 2 or 1) Derivatives (Table 3-VII).

This general class of compounds may be divided into dinitrosyl and mononitrosyl species. Contrary to the original report,[54a] the ^{1}H NMR spectrum of the parent dinitrosyl hydride, $CpW(NO)_2H$ (Fig. 3-4) shows a $^{1}J_{HW}$ of 200 Hz,[54b] by far the largest value yet observed for this parameter. However, the binuclear derivatives $[\{CpW(NO)_2\}(\mu\text{-}H)\{CpM(NO)_2\}]^{+}$ (M=Mo, W) exhibit couplings only slightly greater than one-half that of the parent. This immediately implies the occurrence of terminal-terminal H exchange,

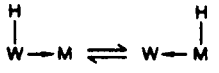

for which J_{HW} (predicted) = 1/2 ($^{1}J_{H(T)-W}$ + $^{2}J_{H(T)-W}$) = 1/2 (200 + 15) Hz = 107.5 Hz, a value not far from those observed. A reasonable estimate for the maximum lifetime of each isomer containing a terminal M-H is $\tau \approx 1.2$ ms, since $\Delta\nu = \Delta J \approx$ 185 Hz.[12]

Table 3-VII. Tungsten Hydride ^1H NMR Parameters for $CpW(NO)_x$ (x = 2 or 1) Derivatives

complex	T^a (°C)	solv	W–H interaction[b]	δ (ppm)	$^nJ_{^1H-^{183}W}$ n	J (Hz)	J_{obsd} (Hz)	ref
$CpW(NO)_2H$		C_6D_6	W–H	2.67	1	200[c,f]		54
$[\{CpW(NO)_2\}_2(\mu\text{-}H)]^+$		CD_3NO_2	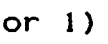	-8.33			114.2[d]	13
$[\{CpW(NO)_2\}(\mu\text{-}H)\{CpMo(NO)_2\}]^+$		CD_3NO_2		-8.92			123.6[f]	13
$CpW(NO)IH\{P(OPh)_3\}$		$CDCl_3$	W–H	-2.04	1	54		55
trans-$CpW(NO)H_2\{P(OPh)_3\}$		$CDCl_3$	H–W–H	-1.82	1	88		55
$[CpW(NO)I]_2(\mu\text{-}H)_2$		$CDCl_3$	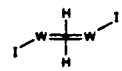	-1.21[d,g]	1 1	88.3 70.8		55
$[CpW(NO)H]_2(\mu\text{-}H)_2$								
isomer A		$CDCl_3$	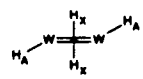	H_A, 6.99	1 2	95[f] ~13		55
				H_X, -2.05	1	93[d,g]		
isomer B		$CDCl_3$	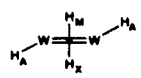	H_A, 6.55	1 2	99[f] ~15		55
				H_M, 1.39 H_X, -5.94	1 1	92[d] 96[d]		
$[CpW(NO)\{P(OPh)_3\}]_2(\mu\text{-}H)_2$		C_6D_6		1.32			55[d]	55
$Cp(NO)(Cl)W\{CHCHC(O)Me\}$	-20	CD_2Cl_2		7.64	2	8.8		56

a Ambient temperatures unless indicated otherwise.

b The W–H bonding interactions are discussed in detail in the text.

c Redetermined value.

d ^{183}W satellites were reported to constitute ~24% of the total integrated area of the resonance.

e The ^{183}W satellites form an AA'X system; see text for a discussion of this species.

f ^{183}W satellites were reported to constitute ~14% of the total integrated area of the resonance.

g $J_{obsd} = 1/2(^1J_{H(X)-W} + {}^1J_{H(X')-W})$.

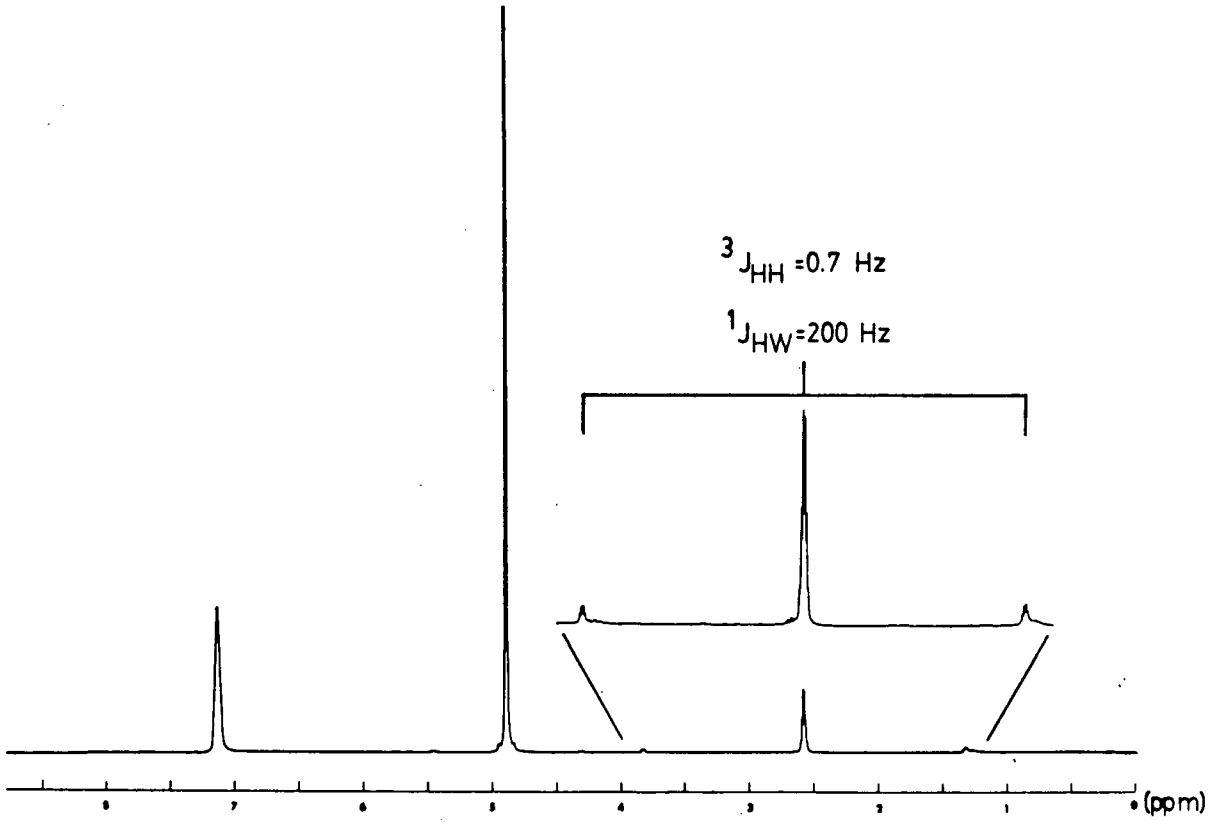

Fig. 3-4. The 80-MHz ^1H NMR spectrum of $CpW(NO)_2H$ in C_6D_6.

The monomeric mononitrosyl compounds listed in Table 3-VII display considerably smaller $^1H-^{183}W$ coupling constants. Nevertheless, these values are larger than those found for analogous $CpW(CO)_3H$ derivatives (Table 3-V). For the mononitrosyl compounds, the fact that $CpW(NO)H_2[P(OPh)_3]$ exhibits a larger coupling than does $CpW(NO)IH[P(OPh)_3]$ is again probably a manifestation of greater s-electron density at the metal centre of the former compound. This is consistent with the electronic changes expected when a terminal H ligand is formally replaced by the more electronegative I ligand. As was discussed in chapter

2, the series $CpW(NO)IH(PR_3)$ (R=OPh, OMe, Ph, Me) shows an increase in the $^1J_{HW}$ coupling as the electron donating ability of the phosphine increases (Table 2-II)--this, again, is as expected (see below).

The ^1H NMR spectrum of $[CpW(NO)IH]_2$ (Fig. 2-1) unequivocally establishes that the complex is rigid in solution on the NMR time scale and that the hydride ligands are bridging. This is because the ^{183}W satellites exhibit an AA'X pattern, with the H's inequivalent in the isotopomers with one ^{183}W nucleus, with fully resolved coupled (Table 2-II) and the satellites integrating to ~25% of the total hydride integration. In our original paper on the subject,[57] this complex was formulated as $[CpW(NO)]_2(\mu\text{-}H)_2(\mu\text{-}I)_2$. The greater understanding of $^1H\text{-}^{183}W$ coupling constants developed since then leads us to reformulate this compound as $[CpW(NO)I]_2(\mu\text{-}H)_2$, with a structure closely akin to that of $[CpW(NO)H]_2(\mu\text{-}H)_2$ (Fig. 2-4) and containing the familiar  bridging group.[58] The reasons for this are two-fold. Firstly, the $^1J_{HW}$ values exhibited by $[CpW(NO)I]_2(\mu\text{-}H)_2$ are only slightly less than those displayed by $[CpW(NO)H]_2(\mu\text{-}H)_2$, and this slight decrease is expected upon formal I for H substitution (see above). Secondly, involvement of a CpW(NO)IH moiety in a  interaction would be expected to result in increased $^1H\text{-}^{183}W$ coupling constants relative to those exhibited by related monomers, and just such an increase is observed. As mentioned in chapter 2, however, it has not yet

proven possible to grow crystals of this compound suitable for an X-ray crystallographic analysis in order to resolve this issue. As an aside, if $[CpW(NO)I]_2(\mu\text{-}H)_2$ is the correct formulation for this compound, this brings up an interesting bonding question. Assuming that the starting material for this compound, $[CpW(NO)I_2]_2$, is a monomer in solution as discussed in chapter 2, then metathesis of an I^- by an H^- in the preparation would lead to the formation of CpW(NO)IH, which must subsequently dimerize. Dimerization leads to several possible products, the most obvious of which are $[CpW(NO)H]_2(\mu\text{-}I)_2$, $[CpWIH]_2(\mu\text{-}NO)_2$ and $[CpW(NO)I]_2(\mu\text{-}H)_2$. The first two of these have electron-sufficient bridging systems, while the last, the apparent structure, has a formally electron-deficient bridge. Why that this electron-deficient system appears to be favoured over electron-sufficient systems is intriguing and it would be most interesting to see some thermodynamic data and theoretical calculation on the subject.

The work described in chapter 2 on $[CpW(NO)\{P(OPh)_3\}]_2(\mu\text{-}H)_2$, which contains a 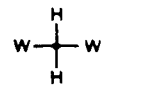 bridging system, established that, in solution, the two hydride ligands are exchanging rapidly on the NMR time scale so as to maintain, on average, a trans orientation with respect to the phosphite phosphorus atoms. If they were undergoing rapid terminal-terminal exchange, that is,

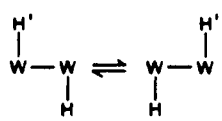

then the observed $^{1}H-^{183}W$ coupling constant of 55 Hz would imply J_{HW} (observed) = 1/2 ($^{1}J_{HW}$ + $^{2}J_{HW}$), and therefore 55 = 1/2 ($^{1}J_{HW}$ + 15) Hz, yielding a value of $^{1}J_{HW}$ = 95 Hz. This is higher than those usually found for terminal W-H linkages in this class (Tables 3-III and 3-VII) (excluding $HW(\mu-H)_2WH$ system). Consequently, the nonrigidity of $[CpW(NO)\{P(OPh)_3\}]_2(\mu-H)_2$ likely involves the two bridging hydride ligands exchanging by spinning about the metal-metal axis and maintaining direct contact with both metal centres in a manner analogous to that suggested for $[Cp_2W(\mu-H)_2Rh(PPh_3)_2]^+$ discussed above.

As noted in passing above, all the nitrosyl complexes listed in Table 3-VII exhibit $^{1}H-^{183}W$ couplings that are considerably greater than those shown by analogous carbonyl compounds (Table 3-V). This is probably a manifestation of the fact that NO ligands appear to be much stronger donors of σ electron density than are CO groups.[59] Such donation by the nitrosyls would be expected to increase the tungsten centres valence s-electron density and, consequently, $^{1}J_{HW}$ (see below). In addition, to their effect on the $^{1}H-^{183}W$ coupling constants, the NO groups also influence the chemical shifts of the resonances due to the hydride ligands. The signals range from +7 to -2 ppm for static, terminal hydrides and from +1.4 to -6 ppm for static, bridging hydrides for the complexes given in Table 3-VII. These are substantially downfield of those exhibited by most of the other organotungsten hydrides considered in this study. In terms of

the chemical shift of the hydride ligand, these nitrosyl complexes seem to be between the electron-rich later transition metal hydrides and the electron-poor early transition-metal hydrides (see chapter 1). While the general trend of bridging hydride signals being upfield of terminal hydride signals[28] also holds for the hydrido nitrosyl complexes, the fact remains that the chemical shift of a single hydride resonance is not a particularly useful indicator of the bridging or terminal nature of the H ligand.[60]

I. Justification for Using "Fused" Bonding Representations.

Although the theoretical factors that influence the magnitudes of one-bond, metal-hydrogen coupling constants have not been studied in detail,[61] more general analyses of one-bond spin-spin couplings have appeared.[62] It has been shown that this interaction is usually dominated by the Fermi contact term, which, in turn, is dominated by the polarizability of the bond (i.e. the amount of s-character in the bond) and the valence s-electron densities at the coupled nuclei. In the case of transition-metal-phosphorus coupling, it has been suggested that the polarizability factor predominates.[63] If these analyses hold true for one-bond tungsten-hydrogen couplings, then increases in the metal s bonding components and valence s-electron densities at the metal and hydrogen nuclei should be reflected in increased magnitude of $^{1}J_{HW}$. In fact, this latter

factor has been noted in several of the families of tungsten hydrido nitrosyl complexes discussed above.

Inspection of the data summarized in Table 3-III shows that the magnitudes of $^{1}J_{HW}$ depend on the nature of the tungsten-hydrogen interaction and decrease in the order

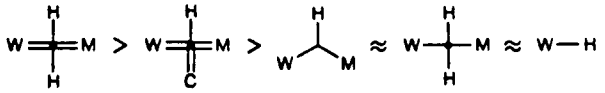

within each family of compounds. The fact that the 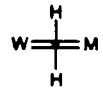 bridging systems exhibit the largest $^{1}H-^{183}W$ coupling suggests it possess the greatest s-character of all these interactions. This supposition is given indirect support by the results of the calculations on $(\mu\text{-H})_2Os_3(CO)_{10}$ which show that the analogous planar $(\mu\text{-H})_2Os_2$ bonding unit contains a substantial amount of Os 6s character.[11] Surprisingly enough, only recently have detailed molecular orbital calculations on transition-metals involved in unsupported  3-centre, 2-electron interactions appeared in the literature.[64] This discussion on the $[\{M(CO)_5\}_2(\mu\text{-H})]^-$ species suggests that the orbitals that make up the M(μ-H)M bridge contain, at most, only a very small amount of metal s-character. This appears to be reflected in the smaller couplings observed for these systems. Of course, detailed, comparative calculations are necessary to confirm these arguments.

At least as important as these points is the trend in coupling constants which indicates that 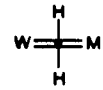 groupings do not simply involve two separate, three-centre, two-electron 

(or ) groups as is implied by their representation as 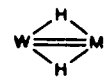 . Therefore, they are best viewed as single, four-centre units, and therefore the 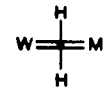 notation is suggested. [The 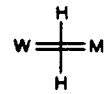 representation was considered, but rejected, since this could be viewed as involving dihydrogen as a ligand,[50,66,67] a connotation we wanted to avoid.] For similar reasons, the "fused" representations are employed throughout this thesis. One primary advantage of this notation is that each line from an atom represents one orbital contributed by that atom to the bonding interaction, just as in the familiar three-centre, three-orbital 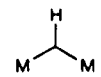 description. Consequently, 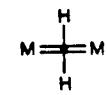 indicates a four-centre, six-orbital interaction (as the calculations on $(\mu\text{-H})_2Os_3(CO)_{10}$ show), 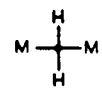 a four-centre, four-orbital interaction, and so on. The simplest way of deducing the appropriate "fused" representation for any given dinuclear situation is to use the idea of a protonated metal-metal bond.[33,68] That is, to perform a normal electron count[9] on the molecule after considering it to have lost any bridging hydrogens as protons, leaving the molecule anionic (assuming, of course, it was neutral to begin with). The bridging hydrides are then added by <u>formal</u> protonation of the resulting metal-metal bond to give the "fused" picture, as in

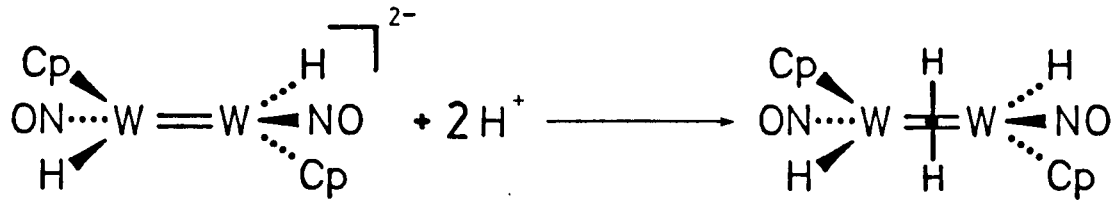

Of course, the number of electrons involved in the bonding interaction cannot be inferred directly from the notation. However, the  system is generally believed to involve two electrons,[9] and the calculations on $(\mu\text{-H})_2Os_3(CO)_{10}$ do suggest that the 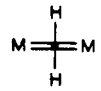 interaction does involve four electrons[11] as this counting technique implies. We therefore feel that the "fused" notation is a useful, accurate and simple representation of these electron-deficient bridging systems.

J. Summary

The unique nature of $[CpW(NO)H]_2(\mu\text{-H})_2$, along with the analysis of a large amount of data on tungsten hydrides in the literature, has allowed us to gain considerable insight into the factors that govern the magnitude of observed tungsten-hydrogen coupling constants in mono and dinuclear systems. It can now be seen that the observation of the size of these couplings can generally give an excellent idea of the type of metal-hydrogen interaction involved when such couplings are compared with others of the appropriate family. It has been shown that in a given

electronic environment, $^{1}J_{H(terminal)-W} \approx {}^{1}J_{H(bridging)-W} > {}^{2}J_{HW}$ and that estimates for these values may be obtained from the ^{1}H NMR spectra of the appropriate monomeric parent. Using these, a large number of observed couplings can be explained on the basis of static interactions or specific types of fluxional pathways involving exchange of hydrides between metal centres, and that some idea of the time scales of these fluxionalities may be obtained. Not surprisingly, it was found that compounds with 4-centre, 6-orbital interactions, 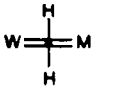 are considerably less fluxional than those with 3-centre, 3-orbital  bridging systems. Inferences regarding fluxionality drawn in this way are generally consistent with exchange mechanisms suggested on the basis of variable temperature ^{1}H NMR studies. Although bridging hydride ligands generally show chemical shifts in areas upfield of those due to terminal ones, the fact that these regions always overlap even in any one particular family means that a particular resonance cannot be used diagnostically to determine the bridging or terminal nature of a particular hydride ligand in a complex.

The magnitude of the ^{1}H-^{183}W couplings appears to be influenced primarily by the valence s-electron densities at the tungsten centre and the s-orbital component of the bonding. Within a given family of bimetallic tungsten hydrides, these couplings decrease in the order

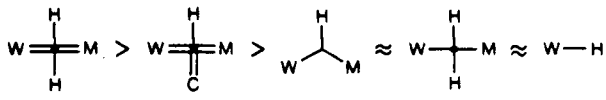

This fact suggests that the four groups that contain bridging hydride ligands are best thought of as single units held together by delocalized bonding which extends over <u>all</u> the atoms involved in the bridge. This conclusion supports various molecular orbital calculations in the literature on some of these bridging systems. To convey the unitary view, the use of these "fused" representations for the interactions is suggested. Finally, it may be noted that similar trends may exist for the coupling of hydrides to other transition-metal centres; for example, $^{1}J_{HRh}$ is greater for 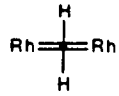 than for 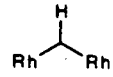 .(69)

K. References and Notes

1. Transition Metal Hydrides; Muetterties, E.L. Ed.; Marcel Dekker: New York, 1971 and references therein.

2. Suba-Seal septa are obtainable from the Aldrich Chemical Co., Inc.

3. Legzdins, P.; Martin, J.T.; Einstein, F.W.B.; Willis, A.C. J. Am. Chem. Soc. 1986, 108, 7971-7981.

4. Chisholm, M.H.; Cotton, F.A.; Extine, M.W.; Kelly, R.L. Inorg. Chem. 1979, 18, 116-119 and references therein.

5. Adams, R.D.; Collins, D.M.; Cotton, F.A. Inorg. Chem. 1974, 13, 1086-1090.

6. Klingler, R.J.; Butler, W.; Curtis, M.D. J. Am. Chem. Soc. 1975, 97, 3535-3536.

7. Chisholm, M.H.; Cotton, F.A. Acc. Chem. Res. 1978, 11, 356-362.

8. a) X-ray structure: Churchill, M.R.; Chang, S.W.-Y. Inorg. Chem. 1974, 13, 2413-2419. b) Neutron structure: Wei, C.-Y.; Marks, M.W.; Bau, R.; Kirtley, S.W.; Bisson, D.E.; Henderson, M.E.; Koetzle, T.F. Ibid 1982, 21, 2556-2565.

9. Collman, J.P.; Hegedus, L.S.; Norton, J.R.; Finke, R. G. Principles and Applications of Organotransition Metal Chemistry, University Science Books: Mill Valley, CA, 1987, chapter 2.

10. Alt, H.G.; Mahmoud, K.A.; Rest, A.J. Angew. Chem., Int. Ed. Engl. 1983, 22, 544-545.

11. Sherwood, D.E., Jr.; Hall, M.B. Inorg. Chem. 1982, 21, 3458-3464 and references therein.

12. Calculated by employing the equation $\tau = [(\sqrt{2})\pi\Delta\nu]^{-1}$, where $\Delta\nu$ is the difference in energy states of the exchanging system (e.g. J, ΔJ or $\Delta\delta$ (Hz)); see Bryant, R.G. J. Chem. Ed. 1983, **60**, 933-935.

13. Hames, B.W.; Legzdins, P. Organometallics 1982, 1, 116-124.

14. Green, M.L.H.; McCleverty, J.A.; Pratt, L.; Wilkinson, G. J. Chem. Soc. 1961, 4854-4859.

15. Deubzer, B.; Kaesz, H.D. J. Am. Chem. Soc. 1968, **90**, 3276-3277.

16. Green, M.L.H.; Knowles, P.J. J. Chem. Soc. A. 1971, 1508-1511.

17. Benfield, F.W.S.; Green, M.L.H. J. Chem. Soc., Dalton Trans. 1974, 1324-1331.

18. Green, M.L.H.; Otero, A. J. Organometal. Chem. 1980, **202**, 421-425.

19. Albinati, A.; Naegeli, R.; Togni, A.; Venanzi, L.M. Organometallics 1983, **2**, 926-928.

20. Alcock, N.W.; Howarth, O.W.; Moore, P.; Morris, G.E. J. Chem. Soc., Chem. Commun. 1979, 1160-1162.

21. Howarth, O.W.; McAteer, C.H.; Moore, P.; Morris, G.E.; Alcock, N.W. J. Chem. Soc., Dalton Trans. 1982, 541-548.

22. Storr, A.; Thomas, B.S. Can. J. Chem. 1971, **49**, 2504-2507 and references therein.

23. Aripovskii, A.V.; Bulychev, B.M.; Krividin, L.B.; Polyakova, V.B. Zhur. Neorg. Khim. 1981, **26**, 2109-2111 (Russ. J. Inorg. Chem. 1981, **26**, 1137-1138.)

24. This rigidity refers only to exchange of hydride ligands between metal centres.

25. Brunner, H.; Wailes, P.C.; Kaesz, H.D. Inorg. Nucl. Chem. Lett. 1965, 1, 125-129.

26. Bruno, J.W.; Hoffman, J.C.; Caulton, K.G. J. Am. Chem. Soc. 1984, **106**, 444-445.

27. Crotty, D.E.; Anderson, T.J.; Glick, M.D.; Oliver, J.P. Inorg. Chem. 16, 2346-2350.

28. a) Humphries, A.P.; Kaesz, H.D. Prog. Inorg. Chem. 1979, **25**, 145-222. b) Moore, D.S.; Robinson, S.D. Chem. Soc. Rev. 1983, **12**, 415-452.

29. Davison, A.; McCleverty, J.A.; Wilkinson, G. J. Chem. Soc. 1963, 1133-1138.

30. Faller, J.W.; Anderson, A.S.; Chen, C.-C. J. Chem. Soc. D 1969, 719-720.

31. a) Kalck, P.; Poilblanc, R. J. Organomet. Chem. 1969, **19**, 115-121. b) Kalck, P.; Pince, R.; Poilblanc, R.; Roussel, J. Ibid 1970, **24**, 445-452.

32. Green, M.L.H.; Parkin, G. J. Chem. Soc., Chem. Commun. 1984, 1467-1468.

33. Davison, A.; McFarlane, W.; Pratt, L.; Wilkinson, G. J. Chem. Soc. 1962, 3653-3666.

34. Alt, H.G.; Eichner, M.E. Angew. Chem., Int. Ed. Engl. 1982, **21**, 205-206.

35. Jeffery, J.C.; Laurie, J.C.V.; Moore, J.; Stone, F.G.A. J. Organomet. Chem. 1983, **258**, C37-C40.

36. Awang, M.R.; Jeffery, J.C.; Stone, F.G.A. J. Chem. Soc., Chem. Commun. 1983, 1426-1428.

37. Alt, H.G.; Thewalt, U. J. Organomet. Chem. 1984, **268**, 235-245.

38. Kotz, J.C.; Pedrotty, D.G. J. Organomet. Chem. 1970, **22**, 425-438.

39. McFarlane, H.C.E.; McFarlane, W.; Rycroft, D.S. J. Chem. Soc., Dalton Trans. 1976, 1616-1622.

40. Darensbourg, M.Y.; Slater, S. J. Am. Chem. Soc. 1981, **103**, 5914-4915.

41. Slater, S.G.; Lusk, R.; Schumann, B.F.; Darensbourg, M. Organometallics 1982, **1**, 1662-1666.

42. Hayter, R.G. J. Am. Chem. Soc. 1966, **88**, 4376-4382.

43. a) Lin, J.T.; Hagen, G.P.; Ellis, J.E. J. Am. Chem. Soc. 1983, **105**, 2296-2303. b) We have redetermined the ^{1}H NMR spectrum of $[Bu_4N][\{W(CO)_4\}_2(\mu\text{-}H)_2]$ in $(CD_3)_2CO$. The salt was prepared by a minor modification of the procedure reported by Churchill, M.R.; Chang, S.W.-Y.; Berch, M.L.; Davison, A. J. Chem. Soc., Chem. Commun. 1973, 691-692.

44. Love, R.A.; Chin, H.B.; Koetzle, T.F.; Kirtley, S.W.; Whittlesey, B.R.; Bau, R. J. Am. Chem. Soc. 1976, **98**, 4491-

4498.

45. Green, M.; Orpen, A.G.; Salter, I.D.; Stone, F.G.A. J. Chem. Soc., Dalton Trans. 1984, 2497-2503.

46. Leblanc, J.C.; Reynoud, J.F.; Moise, C. J. Organometal. Chem. 1983, **244**, C24-C26.

47. a) Arndt, L.; Delord, T.; Darensbourg, M.Y. J. Am. Chem. Soc. 1984, **106**, 456-457. b) Tooley, P.A.; Arndt, L.W.; Darensbourg, M.Y. Ibid 1985, **107**, 2422-2427.

48. Jeffery, J.C.; Orpen, A.G.; Robinson, W.T.; Stone, F.G.A.; Went, M.J. J. Chem. Soc., Chem. Commun. 1984, 396-398.

49. It is possible that the magnitude of $^{2}J_{HW}$ may be increased from its usual value (≤15 Hz) in the case of a particularly electron-rich dative bonded system: $[(OC)_3W(\mu\text{-dppm})_2Pt(H)(Cl)]$ with W←Pt-H and $^{2}J_{HW}$ = 30 Hz (CD_2Cl_2, -90°C)--see: Blagg, A.; Shaw, B.L. J. Chem. Soc., Dalton Trans. 1987, 221-226.

50. Kubas, G.L.; Ryan, R.R.; Swanson, B.J.; Vergamini, P.J.; Wasserman, H.J. J. Am. Chem. Soc. 1984, **106**, 451-452.

51. Lo Schiavo, S.; Bruno, G.; Nicolò, F.; Piraino, P.; Faraone, F. Organometallics 1985, **4**, 2091-2096 and references therein.

52. Berke, H.; Kundel, P. Z. Naturforsch. B 1986, **40**, 527-531.

53. a) Arndt, L.W.; Darensbourg, M.Y.; Fackler, J.P.; Lusk, R.J.; Marler, D.O.; Youngdahl, K.A. J. Am. Chem. Soc. 1985, **107**, 7218-7219. b) Arndt, L.W.; Darensbourg, M.Y.; Delord,

T.; Bancroft, B.T. Ibid 1986, **108**, 2617-2627. c) See also: Halpin, C.F.; Hall, M.B. Ibid 1986, **108**, 1695-1696.

54. a) Legzdins, P.; Martin, D.T. Inorg. Chem. 1979, **18**, 1250-1254. b) Redetermined 80-MHz ^{1}H NMR of $CpW(NO)_2H$ (C_6D_6): δ 4.96 (d, 5H, $C_5\underline{H}_5$, $^{3}J_{HH}$ = 0.7 Hz), 2.67 (sextet, 1H, W-$\underline{H}$, $^{1}J_{HW}$ = 200 Hz).

55. See chapter 2.

56. Alt, H.G.; Hagen, H.J.; Klein, H.-P.; Thewalt, U. Angew. Chem., Int. Ed. Engl. 1984, **23**, 809-810.

57. Legzdins, P.; Martin J.T.; Oxley, J.C. Organometallics 1985, **4**, 1263-1271.

58. A similar type of structure has also been proposed for $[Cp^*IrCl]_2(\mu\text{-}H)_2$ on the basis of infrared labelling studies--see: Gill, D.S.; Maitlis, P.M. J. Organometal. Chem. 1975, **87**, 359-364.

59. a) Hubbard, J.L. Ph.D. Dissertation, The University of Arizona, 1982. b) Hartley, F.R. Chem. Soc. Rev. 1972, **2**, 163-179.

60. A striking illustration of this fact is provided in the report of $W_2H(O\text{-}i\text{-}Pr)_4(\mu\text{-}C_4Me_4)(\mu\text{-}CPh)$, a ditungsten complex containing a static, terminal W-H group which exhibits a ^{1}H NMR resonance at δ +20.42 ppm. This is approximately 10 ppm downfield from the $W_2(\mu\text{-}H)$ signals exhibited by the high-oxidation state alkoxides of the type $[W_2(\mu\text{-}H)(O\text{-}i\text{-}Pr)_7]_2$ and $Na[W_2(\mu\text{-}H)(O\text{-}i\text{-}Pr)_8]\cdot$diglyme--see:

Chisholm, M.H.; Eichhorn, B.W.; Huffman, J.C. J. Chem. Soc., Chem. Commun. 1985, 861-863 and references therein.

61. For brief discussions, see: a) Green, M.L.H.; Jones, D.J. Adv. Inorg. Chem. Radiochem. 1965, **7**, 115-183--in particular, see pp 128-131. b) Atkins, P.W.; Green, J.C.; Green, M.L.H. J. Chem. Soc. A 1968, 2275-2280. c) Church, M.J.; Mays, M.J. J. Chem. Soc. A 1970, 1938-1941 and references therein.

62. a) Pople, J.A.; Santry, D.P. Mol. Phys. 1964, **8**, 1-18. b) Kowalewski, J. Annu. Rev. Nucl. Magn. Reson. Spectrosc. 1982, **12**, 82-176.

63. Pregosin, P.S.; Kunz, R.W. in NMR, Basic Principles and Progress; Diehl, P.; Fluck, E.; Kosfeld, R., Eds.; Springer-Verlag: New York, 1979; Vol. 16.

64. Jeżowska-Trzebiatowska, B.; Nissen-Sobocińska, B. J. Organometal. Chem. 1987, **322**, 331-350--for further discussion, see ref. 65.

65. a) $[\{M(CO)_5\}_2(\mu\text{-}H)]^-$: Albright, T.A. Tetrahedron 1982, **38**, 1339-1388--in particular, see p 1349. For the frontier molecular orbitals of the $M(CO)_5$ fragment, see b) Hay, J.P. J. Am. Chem. Soc. 1978, **100**, 2411-2417. c) Elian, M.; Hoffmann, R. Inorg. Chem. 1975, **14**, 1058-1076.

66. Morris, R.H.; Sawyer, J.F.; Shiralian, M.; Zubkowski, J.D. J. Am. Chem. Soc. 1985, **107**, 5581-5582 and references therin.

67. Crabtree, R.H.; Lavin, M.; Bonnevoit, L. J. Am. Chem. Soc. 1986, **108**, 4032-4037.

68. a) Handy, L.B.; Ruff, J.K.; Dahl, L.F. J. Am. Chem. Soc. 1970, **92**, 7312-7326. b) Churchill, M.R.; DeBoer, B.G.; Rotella, F.J. Inorg. Chem. 1976, **15**, 1843-1853.

69. Fryzuk, M.D. Organometallics 1982, **1**, 408-409.

Chapter 4

Stable Alkyl Hydride Complexes of Tungsten

The yields of the hydride preparations from the metathesis reactions of $[CpW(NO)I_2]_2$ discussed in chapter 2 were not satisfactory. In particular, the $[CpW(NO)H]_2(\mu\text{-}H)_2$ compound, which has the potential to exhibit much interesting chemistry, could only be prepared in such a low yield (~10%) and through such a tedious procedure so as to make the extensive investigation of its chemistry impractical. Consequently, another synthetic route into this area was highly desirable.

While the work described in chapters 2 and 3 was in progress, other work from our laboratory detailed the preparation of the unique compounds $CpM(NO)R_2$ (M=Mo, W and R=bulky alkyl) via reaction 4-1.[1] The compounds were isolated in reasonable

$$[CpM(NO)I_2]_2 \xrightarrow{RMgX} [CpM(NO)R_2]_2 \cdot MgX_2 \xrightarrow{H_2O} 2\ CpM(NO)R_2 \qquad (4\text{-}1)$$

yields, particularly $CpW(NO)(CH_2SiMe_3)_2$, which was obtained in greater than 70% yield. These are unusually stable, 16-electron compounds that have an available, open coordination site and have been shown to exhibit interesting reactivity with several small molecules, including O_2,[2] S_8[3] and NO.[4]

It was hoped, therefore, that hydrogenolysis of this compound (hydride preparation route #1--chapter 1) would result

in the formation of $[CpW(NO)H]_2(\mu\text{-}H)_2$ (eq. 4-2). Preliminary

$$2\ CpW(NO)(CH_2SiMe_3)_2 \xrightarrow[?]{H_2} [CpW(NO)H]_2(\mu\text{-}H)_2 + 2\ Me_4Si \qquad (4\text{-}2)$$

reactions at low H_2 pressures (<60 psig) resulted only in decomposition and the desired product was not obtained. However, when this reaction was attempted in the presence of a tertiary phosphine (or phosphite), PR_3, novel products of the form $CpW(NO)(H)(CH_2SiMe_3)(PR_3)$ were obtained. These preparations and associated chemistry of the product complexes form part of the work described in this chapter. For reasons that will become clear in the discussion, this work was extended to the Cp* analogues and a description of this system, including the preparations of the relevant starting materials, constitute the remainder of the chapter.

Experimental Section

Standard techniques employed were detailed in chapter 2. Tetramethylsilane was identified using a Carbowax 20M 12m capillary column in a Hewlett-Packard HP 5880A Level 4 gas chromatograph with helium carrier gas and an oven temperature of 50°C. Carbon-13 NMR spectra were run on a Varian XL-300 spectrometer operating at 75.429-MHz referenced to C_6D_6 at 128.00 ppm or CD_3NO_2 at 62.8 ppm[5] and are reported in ppm downfield

from TMS. $CpW(NO)(CH_2SiMe_3)_2$,[1,6] C_5Me_5H[7] and NaC_5Me_5[8] were prepared as described in the literature. The physical and spectroscopic properties of all new compounds prepared are given in Tables 4-I and 4-II. CAUTION: The glass Fisher-Porter pressure vessels must be handled with care as the manufacturer does not specify a safe operating pressure and they are not equipped with any automatic pressure relief system.

Preparation of $CpW(NO)(H)(CH_2SiMe_3)L$ ($L=P(OPh)_3$, $PMePh_2$).

$CpW(NO)(CH_2SiMe_3)$ (0.30 g, 0.66 mmol) was dissolved with stirring in hexanes (10 mL) and cannulated into a 300 mL Fisher-Porter vessel that had been evacuated and filled with H_2 three times. A stoichiometric amount of L (0.66 mmol, 0.18 mL $P(OPh)_3$ or 0.12 mL $PMePh_2$) was then added via syringe to the Fisher-Porter vessel, which was subsequently pressurized to ~80 psig H_2. The vessel was then agitated for a few moments to allow mixing of L and speed solubilization of the H_2, and left standing with no stirring.

$L=P(OPh)_3$: Over the course of the reaction, the initial dark purple solution gradually lightened to a very pale purple with a concomitant deposition of a pale yellow powdery precipitate. After 2 h total reaction time, the pressure in the vessel was relieved and the mother liquor cannulated away from the precipitate. The reaction vessel was then opened in air and the precipitate transferred into a nitrogen-filled flask. The

precipitate was washed with hexanes (3 x 10 mL) under N_2 and dried under vacuum (0.05 mm Hg, 2 h) to yield 0.29 g (65% yield) of yellow microcrystalline $CpW(NO)(H)(CH_2SiMe_3)[P(OPh)_3]$.

L=$PMePh_2$: As the reaction proceeded, the initial dark purple solution changed to a deep red-brown colour as several large, red-brown brick-shaped crystalline masses formed on the bottom of the vessel, along with some other, amorphous material. After 3 h total reaction time, the pressure was relieved and the mother liquor cannulated away from the solid material, whereupon the Fisher-Porter vessel was opened in air and the brick-shaped masses carefully and quickly transferred to a nitrogen-filled flask. This crystalline material was then taken up in Et_2O, filter cannulated to remove a small amount of dark coloured insoluble material and the filtrate slowly concentrated under vacuum to give a small amount of yellow, microcrystalline $CpW(NO)(H)(CH_2SiMe_3)(PMePh_2)$. Single crystals of this material suitable for X-ray analysis were grown in less than 1 h from CH_2Cl_2/hexanes at -25°C.

Preparation of $\overline{CpW(NO)(H)[P(OPh)_2(OC_6H_4)]}$.

This compound was prepared by combining $CpW(NO)(CH_2SiMe_3)$, $P(OPh)_3$ and H_2 as above (on one-half the scale), but letting the reaction proceed for 4 days at room temperature. This resulted in an almost colourless solution above a yellow microcrystalline crusty precipitate. The hexanes were removed under reduced

pressure (in the Fisher-Porter vessel), Et_2O was added and the vessel agitated to help break up the hard crusty residue enough to allow both the solid and solution to be poured into a nitrogen filled flask. The Et_2O was then removed under vacuum and the solid material recrystallized overnight from toluene at -25°C. The product was washed once with hexanes (10 mL) and dried overnight (0.005 mm Hg) to give yellow, microcrystalline $CpW(NO)(H)[P(OPh)_2(OC_6H_4)]$. X-ray quality single crystals of this compound were grown by slow evaporation of a C_6D_6 solution in an NMR tube capped by a septum punctured with a needle in air at room temperature.

Reactions of $CpW(NO)(CH_2SiMe_3)_2$, H_2 and L (L=$P(OPh)_3$, $PMePh_2$) in an NMR Tube.

To a small, N_2-filled Schlenk tube was added $CpW(NO)(CH_2SiMe_3)_2$ (~0.01 g, ~0.04 mmol), C_6D_6 (~2 mL) and (by syringe) an approximately stoichiometric amount of L (12 µL $P(OPh)_3$ or 9 µL $PMePh_2$). This mixture was stirred until a homogeneous solution was obtained and part of this solution cannulated into a thick-walled[9] NMR tube until ~3 cm of solution was in the tube. The solution was then freeze-pump-thaw degassed three times, following which 1 atm of H_2 was allowed into the NMR tube at -196°C and the tube flame sealed. After the mixture had reached room temperature (resulting in an H_2 pressure of ~4 atm), ^1H and ^{31}P NMR spectra were obtained over the course

of ~60 h with intermittent shaking of the NMR tube.

Equilibrium between $CpW(NO)(CH_2SiMe_3)_2$ and $PMePh_2$.

A mixture of $CpW(NO)(CH_2SiMe_3)_2$ (0.0244 g, 5.38×10^{-2} mmol), $PMePh_2$ (10 µL, ~5.4×10^{-2} mmol), and toluene-d_8 (0.90 mL) was placed in an NMR tube, freeze-pump-thaw degassed three times and the tube flame-sealed under vacuum. Proton and $^{31}P\{^1H\}$ NMR spectra were then obtained at temperatures from -85°C to 25°C.

Preparation of $Cp^*W(CO)_2(NO)$.[10,11]

This compound was prepared by the standard method used for $CpW(CO)_2(NO)$[12] in 92.7% yield using isolated, crystalline NaC_5Me_5.[8]

Preparation of $Cp^*W(NO)I_2$.[13]

To a well stirred solution of $Cp^*W(CO)_2(NO)$ (10.02 g, 24.7 mmol) in toluene (100 mL) was added I_2 (6.34 g, 24.8 mmol) in 4 portions while vigourous gas evolution occurred (CAUTION: this CO gas should be vented to the fume hood). After gas evolution had significantly subsided, a dark red-brown microcrystalline precipitate was observed beneath a dark red-brown solution. The solution was stirred under a slight dynamic vacuum while warming with a warm water bath. The initial precipitate eventually redissolved and was replaced by a brilliant-green (below room temperature) or gold (above room temperature) coloured

microcrystalline precipitate over the course of several hours as the toluene solvent was slowly reduced in volume. After ~3 h of pumping and periodic additions of toluene when the solution volume dropped below ~50 mL, the volume of solvent was reduced to ~20 mL under vacuum and the resulting precipitate collected by filtration, washed with small aliquots of Et_2O (5 mL each) until the filtrate was no longer dark brown and finally with hexanes (3 x 20 mL). The precipitate was dried under vacuum (0.005 mm Hg, 2 h) to yield 12.6 g (84.6%) of green or gold thermochromic microcrystalline $Cp^*W(NO)I_2$.

Preparation of $Cp^*W(NO)(CH_2SiMe_3)_2$.

This preparation is a slight modification of that for $CpW(NO)(CH_2SiMe_3)_2$.[1,6] To a rapidly stirring green or gold suspension of $Cp^*W(NO)I_2$ (12.6 g, 21.2 mmol) in Et_2O (150 mL) was added 43 mL of 1.0 M Me_3SiCH_2MgCl[14] (43 mmol) dropwise from a syringe. The mixture darkened to a red-brown colour as soon as the addition of the Grignard reagent had started and a dark coloured precipitate began to appear. After ~1/2 h of stirring the suspension, ~4 mL of N_2-purged deionized H_2O was added via syringe through a septum whereupon the solution turned purple and a white precipitate was deposited over the course of ~1 h. The volume of the mixture was then reduced to ~20 mL under vacuum and transferred by cannula to the top of a 15 x 4 cm Florisil column made up in 4:1 hexanes:Et_2O solvent. The residue at the bottom

of the reaction flask was then extracted with 3 x 10 mL portions of 4:1 hexanes:Et_2O and this transferred by cannula to the top of the column. The column was then slowly eluted with a 4:1 hexanes:Et_2O mixture causing the development of a broad dark purple band and a smaller, reddish yellow second band. The two bands were collected separately with the second band being eluted off the column using pure Et_2O. The volume of the solution containing the first band was reduced under vacuum to ~15 mL and storage overnight at -25°C induced the crystallization of $Cp^*W(NO)(CH_2SiMe_3)_2$. The mother liquor was then removed from this crystalline material at -25°C by cannulation and the crystals washed with 5 mL cold hexanes to give 5.62 g of product after drying (0.05 mm Hg, 2 h). Reducing the volume of the combined mother liquor and washings to ~2 mL and storage at -25°C overnight induced further crystallization. These crystals were isolated by cannula removal of the mother liquor at -25°C and washing once with ~2 mL cold hexanes and drying to give a further 1.20 g of product for a total yield of 6.82 g (61.4% yield) of dark purple, crystalline $Cp^*W(NO)(CH_2SiMe_3)_2$. The solution containing the second band was taken to dryness under vacuum and the residue recrystallized from hexanes to give a small number of colourless crystals identified by elemental analysis and IR and NMR spectroscopies as $Cp^*W(O)_2(CH_2SiMe_3)$.[15]

Preparation of $Cp^*W(NO)(H)(CH_2SiMe_3)(PMe_3)$.

$Cp^*W(NO)(CH_2SiMe_3)$ (3.00 g, 5.7 mmol) was dissolved in hexanes (15 mL) in a 100-mL 3-necked flask and then cannulated into a 300 mL Fisher-Porter vessel that had been evacuated and filled three times with H_2. The 100-mL flask was rinsed with hexanes (5 mL) and the rinsings cannulated into the Fisher-Porter vessel. PMe_3 (~3 mL, ~30 mmol) was then syringed into the vessel and 80 psig H_2 added. The contents of the pressure vessel were stirred for ~3 h as the colour changed from dark purple to red-brown and a red-brown powder precipitated. The pressure was then carefully relieved and the suspension cannulated under N_2 into a Schlenk tube, following which the Fisher-Porter vessel was washed with 2 x 10 mL hexanes and the washings added to the suspension. The solvent volume in the suspension was then reduced to ~10 mL under reduced pressure and the mother liquor discarded by cannula. Recrystallization of the resulting solid from CH_2Cl_2/hexanes gave 1.35 g of dark coloured well-formed single crystals of $Cp^*W(NO)(H)(CH_2SiMe_3)(PMe_3)$ which a further crystallization from CH_2Cl_2/hexanes lightened to bright yellow. The dark red-brown mother liquor from the first recrystallization was dried under vacuum, taken up in an approximately 6:1 hexanes:CH_2Cl_2 mixture and put on a 10 x 2 cm Alumina V column made up in hexanes. Elution first with hexanes caused the development of a small dark red-brown band which was discarded. Subsequent elution with a 6:1 hexanes:CH_2Cl_2 mixture gave a

second band which was collected and from which could be crystallized a further 0.24 g of yellow, microcrystalline $Cp^*W(NO)(H)(CH_2SiMe_3)(PMe_3)$ for a total yield of 1.59 g (54.0%).

Preparation of $Cp^*W(NO)(PMe_3)_2$.

This compound was prepared via the Na/Hg reduction of $Cp^*W(NO)I_2$ in the presence of an excess of PMe_3 by the method of Hunter and Legzdins[16] in 32% yield as a bright orange, very air-sensitive, microcrystalline solid.

Thermolysis of $Cp^*W(NO)(H)(CH_2SiMe_3)(PMe_3)$ in C_6H_6.

$Cp^*W(NO)(H)(CH_2SiMe_3)(PMe_3)$ (0.10 g) was placed in a Schlenk tube in a glove box and the tube closed with a new Suba-Seal septum. Benzene (15 mL) was then added via syringe through the septum and the Schlenk tube put in a 40°C warm water bath overnight, resulting in very little colour change. After the benzene solvent was removed under vacuum, the oily residue was recrystallized from CH_2Cl_2/hexanes to yield a small amount of red-brown microcrystalline $Cp^*W(NO)(H)(C_6H_5)(PMe_3)$.

Oxidation of $Cp^*W(NO)(H)(CH_2SiMe_3)(PMe_3)$ with $AgBF_4$.

A few crystals of $Cp^*W(NO)(H)(CH_2SiMe_3)(PMe_3)$ were dissolved in C_6D_6 (~2 mL) in a small Schlenk tube and a spatula tip full of finely divided $AgBF_4$ added. A silver mirror immediately appeared and the solution turned from orange to orange-red. The volatile

material was trap-to-trap distilled off, analyzed by GC, GC-MS and ^{1}H NMR spectroscopy and found to contain principally $(CH_3)_4Si$ as the reaction product.

Preparations of $[Cp^*W(NO)H]_2(\mu\text{-}H)_2$ and $[Cp^*W(NO)H](\mu\text{-}H)_2[Cp^*W(NO)(CH_2SiMe_3)]$.

In a glove box, $Cp^*W(NO)(CH_2SiMe_3)_2$ (2.00 g, 3.82 mmol) was loaded into a 300 mL Parr mini-reactor and hexanes (10 mL) was added. The reactor was closed in the glove box and then properly tightened up on the bench. Hydrogen (920 psig) was introduced into the reactor and the contents stirred for 20 min. The pressure was then relieved, the reactor opened in air and the contents quickly poured into a nitrogen-containing Schlenk tube. The reactor was rinsed with CH_2Cl_2 (10 mL) and the rinsings added to the other material. The resulting solution was taken to dryness under vacuum leaving a red-brown glass. Addition of ~10 mL of hexanes followed by vigourous trituration with a metal spatula gave an orange-brown microcrystalline powder beneath a dark red-brown solution. The solution was cannulated away and the powder dried under vacuum. Recrystallization of this powder from toluene-hexanes at -25^{o}C gave a small amount of analytically pure orange microcrystalline $[Cp^*W(NO)H]_2(\mu\text{-}H)_2$. Two further recrystallizations of the mother liquor from the first recrystallization allowed the isolation of a small amount of analytically pure red crystalline

$[Cp^*W(NO)H](\mu\text{-}H)_2[Cp^*W(NO)(CH_2SiMe_3)]$. Small, "half-moon" shaped single crystals of this latter compound were grown from a Celite-filtered CD_3NO_2 solution at -25^oC.

Table 4-I. Analytical, Infrared and Mass Spectral Data for the Complexes

Complex	analytical data					
	C		H		N	
	calcd	found	calcd	found	calcd	found
$CpW(NO)(H)(CH_2SiMe_3)[P(OPh)_3]$	47.87	48.00	4.76	4.84	2.07	2.12
$CpW(NO)(H)(CH_2SiMe_3)(PMePh_2)$	46.57	46.52	5.33	5.33	2.47	2.51
$CpW(NO)(H)[P(OPh)_2(OC_6H_4)]$	46.88	46.90	3.42	3.40	2.38	2.52
$Cp^*W(NO)I_2$	19.92	19.86	2.51	2.44	2.32	2.40
$Cp^*W(NO)(CH_2SiMe_3)_2$	41.30	41.03	7.12	7.30	2.68	2.67
$Cp^*W(O)_2(CH_2SiMe_3)$	38.37	38.20	5.98	5.99	0.00	0.00
$Cp^*W(NO)(H)(CH_2SiMe_3)(PMe_3)$	39.77	39.82	7.07	6.96	2.73	2.59
$Cp^*W(NO)(PMe_3)_2$	38.34	37.99	6.64	6.48	2.79	2.60
$[Cp^*W(NO)H]_2(\mu\text{-}H)_2$	34.21	33.90	4.88	4.89	3.99	4.04
$[Cp^*W(NO)H](\mu\text{-}H)_2[Cp^*W(NO)(CH_2SiMe_3)]$	36.56	36.83	5.62	5.56	3.55	3.50

Table 4-I (Cont'd)

Complex	phase	IR data $\nu_{NO}(cm^{-1})$	IR data $\nu_{WH}(cm^{-1})$	low resolution mass spectrum m/z	probe temp	assig't
$CpW(NO)(H)(CH_2SiMe_3)[P(OPh)_3]$	Nujol	1579	1837			
	CH_2Cl_2	1601	1836			
$CpW(NO)(H)(CH_2SiMe_3)(PMePh_2)$	Nujol	1553	1838	479	80	$(P-CH_2SiMe_3)^+$, $(P-Me_4Si)^+$
	CH_2Cl_2	1560	1865			
$CpW(NO)(H)[P(OPh)_2(OC_6H_4)]$	Nujol	1611	1856	589	100	$(P)^+$, $(P-H)^+$
	CH_2Cl_2	1626	1850			
$Cp^*W(NO)I_2$	Nujol	1627		952	120	$(2P-I_2)^+$
	CH_2Cl_2	1629				
$Cp^*W(NO)(CH_2SiMe_3)_2$	Nujol (solid)[a]	1549		523	120	$(P)^+$
	Nujol (soln)	1572				
	CH_2Cl_2	1543				
$Cp^*W(NO)(H)(CH_2SiMe_3)(PMe_3)$	Nujol	1547	1852		b	
	CH_2Cl_2	1545	1850			
$Cp^*W(NO)(H)(C_6H_5)(PMe_3)$	Nujol	1551	1813	425	150	$(P-C_6H_6)^+$
	CH_2Cl_2[c]	1560 or 1550	1807			
$Cp^*W(NO)(PMe_3)_2$	Nujol	1514, 1505				
	CH_2Cl_2	1498				

Table 4-I (Cont'd)

$[Cp^*W(NO)H]_2(\mu\text{-}H)_2$	Nujol	1575(s), 1533(w)	1898	700	120	$(P\text{-}2H)^+$
	CH_2Cl_2	1566(s), 1533(sh)	1902			
$[Cp^*W(NO)H](\mu\text{-}H)_2[Cp^*W(NO)(CH_2SiMe_3)]$	Nujol	1574(sh), 1559(s)	1910	787	120	$(P\text{-}H)^+$
	CH_2Cl_2	1557	1921			

a $Cp^*W(NO)CH_2SiMe_3)_2$ partially dissolves in Nujol upon mulling.

b See text for a discussion of this mass spectrum.

c The ν_{NO} is overlapped by aromatic ring vibration bands.

Table 4-II. NMR Data for the Complexes

Complex	nucleus	assg't	δ (J, Hz) [a]
$CpW(NO)(H)(CH_2SiMe_3)[P(OPh)_3]$	^1H	Cp	4.65 (s, 5)
		$P(O\underline{Ph})_3$	6.7-7.3 (m, 15)
		$Si\underline{Me}_3$	0.56 (s, 9)
		$WCH_{\underline{A}}H_B$	0.07 (ddd, 1, $^2J_{H(A)H(B)}$ = 13.2, $^3J_{H(A)H(W)}$ = 3.2, $^3J_{H(A)P}$ = 9.6, $^2J_{H(A)W}$ = 8)
		$WCH_AH_{\underline{B}}$	0.87 (ddd, 1, $^3J_{H(B)H(W)}$ = 8.3, $^3J_{H(B)P}$ = 30.8, $^2J_{H(B)W}$ = 7)
		$W\text{-}H_{\underline{W}}$	-2.49 (ddd, 1, $^2J_{H(W)P}$ = 117.1, $^1J_{H(W)W}$ = 47)
	$^{13}C\{^1H\}$	ipso PhC	152.03 (d, $^2J_{CP}$ = 8.9)
		ortho PhC	129.80 (s)
		meta PhC	122.29 (d, $^4J_{CP}$ = 4.5)
		para PhC	125.06 (s)
		Cp	96.42 (d, $^2J_{CP}$ = 2.1)
		$Si\underline{Me}_3$	3.49 (s)
		$W\underline{CH}_2Si$	-14.88 (d, $^3J_{CP}$ = 19.5, $^1J_{CW}$ = 67.5)
	$^{31}P\{^1H\}$		127.42 (s, $^1J_{PW}$ = 353)
$CpW(NO)(H)(CH_2SiMe_3)(PMePh_2)$	^1H	Cp	5.02 (s, 5)
		$PMe\underline{Ph}_2$	7-7.6 (m, 10)
		$P\underline{Me}Ph_2$	1.70 (d, 3, $^2J_{HP}$ = 8.0)

Table 4-II (Cont'd)

	$Si\underline{Me}_3$	0.37 (s, 9)
	$WCH_A\underline{H}_B$	-0.24 (ddd, 1, $^2J_{H(A)H(B)}$ = 13.5, $^3J_{H(A)H(W)}$ = 2, $^3J_{H(A)P}$ = 7.5, $^2J_{H(A)W}$ = 5)
	$WCH_A\underline{H}_B$	-0.15 (ddd, 1, $^3J_{H(B)H(W)}$ = 7.5, $^3J_{H(B)P}$ = 24.5, $^2J_{H(B)W}$ = 5.5)
	$W\text{-}\underline{H}_W$	-0.47 (ddd, 1, $^2J_{H(W)P}$ = 89.5, $^1J_{H(W)W}$ = 48.5)
$^{13}C\{^1H\}$	ipso PhC_1	139.50 (d, $^1J_{CP}$ = 45)
	ipso PhC_2	137.79 (d, $^1J_{CP}$ = 46)
	ortho PhC_1	133.36 (d, $^2J_{CP}$ = 11)
	ortho PhC_2	131.87 (d, $^2J_{CP}$ = 10)
	meta PhC_1	128.48 (d, $^3J_{CP}$ = 10)
	meta PhC_2	128.31 (d, $^3J_{CP}$ = 9)
	para PhC_1	130.14 (d, $^4J_{CP}$ = 2)
	para PhC_2	129.52 (d, $^4J_{CP}$ = 1)
	Cp	95.68 (d, $^2J_{CP}$ = 2)
	$P\underline{Me}Ph$	16.16 (d, $^1J_{CP}$ = 29)
	$Si\underline{Me}_3$	3.69 (s)
	$W\underline{C}H_2Si$	-8.97 (d, $^2J_{CP}$ = 13, $^1J_{CW}$ = 66)
$^{31}P\{^1H\}$		7.49 (s, $^1J_{PW}$ = 202)

Table 4-II (Cont'd)

$CpW(NO)(H)[P(OPh)_2(OC_6H_4)]$	^1H	$P(OPh)(OC_6\underline{H}_4)$	6.7-7.5 (m, 14)
		Cp	4.78 (d, 5, $^3J_{HP}$ = 0.6)
		W-$\underline{H}_W$	-1.85 (d, 1, $^2J_{HP}$ = 100.3, $^1J_{HW}$ = 54.7)
	$^{31}P\{^1H\}$		176 (s, $^1J_{PW}$ = 345)
$Cp^*W(NO)I_2$	^1H	$C_5\underline{Me}_5$	1.62 (s)
	$^{13}C\{^1H\}$	$\underline{C}_5Me_5$	116.92 (s)
		$C_5\underline{Me}_5$	12.36 (s)
$Cp^*W(NO)(CH_2SiMe_3)_2$	^1H	$C_5\underline{Me}_5$	1.51 (s, 15)
		$Si\underline{Me}_3$	0.36 (s, 18)
		$WCH_A\underline{H}_B$	1.54 (d, $^2J_{H(A)H(B)}$ = 10.9)[b]
		$WCH_A\underline{H}_B$	-1.48 (d, $^2J_{H(B)W}$ = 8.4)
	$^{13}C\{^1H\}$[c]	$\underline{C}_5Me_5$	110.16 (s)
		$C_5\underline{Me}_5$	9.83 (s, $^1J_{CH}$ = 128)
		$Si\underline{Me}_3$	2.83 (s, $^1J_{CH}$ = 118, $^1J_{CSi}$ = 51)
		$W\underline{C}H_2Si$	62.70 (s, $^1J_{CH}$ = 120,116, $^1J_{CW}$ = 88, $^1J_{CSi}$ = 46)

Table 4-II (Cont'd)

$Cp^*W(O)_2(CH_2SiMe_3)$	^1H	$C_5\underline{Me}_5$	1.67 (s, 15)
		$Si\underline{Me}_3$	0.38 (s, 9, $^2J_{HSi}$ = 6.4)
		$WC\underline{H}_2Si$	0.42 (s, 2, $^2J_{HW}$ = 10.7)
	$^{13}C\{^1H\}$	$\underline{C}_5Me_5$	116.50 (s)
		$C_5\underline{Me}_5$	10.36 (s)
		$Si\underline{Me}_3$	0.80 (s, $^1J_{CSi}$ = 32)
		$W\underline{C}H_2Si$	24.39 (s, $^1J_{CW}$ = 135)
$Cp^*W(NO)(H)(CH_2SiMe_3)(PMe_3)$	^1H	$C_5\underline{Me}_5$	1.77 (s, 15)
		$P\underline{Me}_3$	1.09 (d, 9, $^2J_{HP}$ = 8.3)
		$Si\underline{Me}_3$	0.48 (s, 9)
		$WCH_A\underline{H}_B$	-0.97 (ddd, 1, $^2J_{H(A)H(B)}$ = 13.4, $^3J_{H(A)H(W)}$ = 5.9, $^3J_{H(A)P}$ = 16.7, $^2J_{H(A)W}$ = 7.8)
		$WCH_A\underline{H}_B$	-0.68 (ddd, 1, $^3J_{H(B)H(W)}$ = 6.7, $^3J_{H(B)P}$ = 24.9, $^2J_{H(B)W}$ = 8.1)
		$W\text{-}\underline{H}_W$	-1.25 (ddd, 1, $^2J_{H(W)P}$ = 87.9, $^1J_{H(W)W}$ = 56.6)
	$^{13}C\{^1H\}$	$\underline{C}_5Me_5$	105.02 (d, $^2J_{CP}$ = 2)
		$C_5\underline{Me}_5$	10.79 (s)
		$P\underline{Me}_3$	18.90 (d, $^1J_{CP}$ = 31)
		$Si\underline{Me}_3$	4.02 (s, $^1J_{CSi}$ = 49)

		$W\underline{CH_2}Si$	-5.73 (d, $^2J_{CP}$ = 14, $^1J_{CW}$ = 40)
	$^{31}P\{^1H\}$		-28.74 (s, $^1J_{PW}$ = 195)
$Cp^*W(NO)(H)(C_6H_5)(PMe_3)$	^1H	$C_5\underline{Me_5}$	1.62 (s, 15)
		$P\underline{Me_3}$	1.15 (d, 9, $^2J_{HP}$ = 9.3)
		$C_6\underline{H_5}$	7.1-8.0 (m, 5)
		$W\text{-}\underline{H}_W$	5.15 (d, 1, $^2J_{HP}$ = 97.0, $^1J_{HW}$ = 79)
	$^{31}P\{^1H\}$		-3.14 (s, $^1J_{PW}$ = 201)
$Cp^*W(NO)(PMe_3)_2$	^1H	$C_5\underline{Me_5}$	1.91 (s, 15)
		$P\underline{Me_3}$	1.34 (m^d, 9, $^2J_{HP}$ = 7.55, $^4J_{HP'}$ = 0.05, $^2J_{PP'}$ = -9.6, |N| = 7.6 Hz)
	$^{31}P\{^1H\}$		-22.56 (s, $^1J_{PW}$ = 454)
$OPMe_3$[e]	^1H		0.88 (d, $^2J_{HP}$ = 12.8)
	$^{13}C\{^1H\}$		17.85 (d, $^1J_{CP}$ = 68.6)
	$^{31}P\{^1H\}$		33.52 (s)
$[Cp^*W(NO)H]_2(\mu\text{-}H)_2$[f]	^1H	isomer A:	
		$C_5\underline{Me_5}$	2.03 (s, 15)
		$W\text{-}\underline{H}_A$	7.75 (m, 2)
		$W\text{-}\underline{H}_X\text{-}W$	-0.05 (m, 2)

Table 4-II (Cont'd)

		isomer B:	
		$C_5\underline{Me}_5$	2.03 (s, 15)
		W-$\underline{H}_A$	7.41 (m, 2)
		W-$\underline{H}_M$-W	4.56 (m, 1)
		W-$\underline{H}_X$-W	g
	^1H in CD_2Cl_2	isomer A:	
		$C_5\underline{Me}_5$	2.22 (s, 15)
		W-$\underline{H}_A$	7.44 (m, 2, $^2J_{H(A)H(X)}$ = 5.5, $^2J_{H(A)H(X')}$ = 8.0, $^3J_{H(A)H(A')}$ = 1.0, $^1J_{H(X)W}$ = 92, $^2J_{H(X)W}$ = 15)
		W-$\underline{H}_X$-W	-0.33 (m, 2, $^1J_{H(X)H(X')}$ = 1.5, $1/2\lvert{}^1J_{H(X)W} + {}^1J_{H(X')W}\rvert$ = 93)
		isomer B:	
		$C_5\underline{Me}_5$	2.22 (s, 15)
		W-$\underline{H}_A$	6.89 (dd, 2, $^2J_{H(A)H(M)}$ = 5.0, $^2J_{H(A)H(X)}$ = 8.4, $^1J_{H(A)W}$ ≈ 96)
		W-$\underline{H}_M$-W	4.11 (td, 1, $^1J_{H(M)H(X)}$ = 2.3, $^1J_{H(M)W}$ ≈ 90)[h]
		W-$\underline{H}_X$-W	-4.84 (td, 1)
$[Cp^*W(NO)H](\mu\text{-}H)_2[Cp^*W(NO)(CH_2SiMe_3)]$[f]	^1H	$C_5\underline{Me}_{5(A)}$	1.79 (s, 15)
		$C_5\underline{Me}_{5(B)}$	2.04 (s, 15)
		$Si\underline{Me}_3$	0.46 (s, 9)
		W-$\underline{H}_E$	7.21 (dd, 1)

Table 4-II (Cont'd)

	$W\text{-}\underline{H}_D\text{-}W$	5.61 (dd, 1)
	$WCH_C\underline{H}_BSi$	0.01 (d, 1)
	$WCH_C\underline{H}_BSi$	-1.24 (dd, 1)
	$W\text{-}\underline{H}_A\text{-}W$	-6.43 (dm, 1)
^1H in CD_3NO_2	$C_5\underline{Me}_{5(A)}$	1.93 (s, 15)
	$C_5\underline{Me}_{5(B)}$	2.14 (s, 15)
	$Si\underline{Me}_3$	-0.06 (s, 9, $^2J_{HSi}$ = 6.5)
	$W\text{-}\underline{H}_E$	6.57 (dd, 1, $^2J_{H(A)H(E)}$ = 9.0, $^2J_{H(D)H(E)}$ = 5.0, $^1J_{H(E)W(B)}$ = 111.0, $^2J_{H(E)W(A)}$ = 11.5)
	$W\text{-}\underline{H}_D\text{-}W$	5.30 (dd, 1, $^1J_{H(A)H(D)}$ = 2.5, $^1J_{H(D)W(A)}$ = 93.5, $^1J_{H(D)W(B)}$ = 84.0)
	$WCH_C\underline{H}_BSi$	-0.13 (d, 1, $^2J_{H(B)H(C)}$ = 12.5, $^2J_{H(C)W(A)}$ = 6.5)
	$WCH_C\underline{H}_BSi$	-1.39 (dd, 1, $^3J_{H(A)H(B)}$ = 3.0, $^2J_{H(B)W(A)}$ = 7.5)
	$W\text{-}\underline{H}_A\text{-}W$	-6.36 (dm, 1, $^1J_{H(A)W(A)}$ = 78.5, $^1J_{H(A)W(B)}$ = 83.5)
$^{13}C\{^1H\}$ in CD_3NO_2	$\underline{C}_5Me_5$	112.63 (s)
	$\underline{C}_5Me_5$	110.62 (s)
	$C_5\underline{Me}_5$	11.28 (s)
	$C_5\underline{Me}_5$	10.60 (s)
	$Si\underline{Me}_3$	2.79 (s)
	$W\underline{C}H_2Si$	31.74 (s)

Table 4-II (Cont'd)

a All NMR data recorded in C_6D_6 unless otherwise noted.

b ^{183}W satellites obscured by overlap of Cp^* resonance.

c $^1J_{CH}$ data from the gated decoupled spectrum.

d Proton phosphine resonances form an $X_9AAX'_9$ pattern; |N| is the separation of the two most intense peaks.[16]

e $OPMe_3$ was prepared by the method of Steube and co-workers.[17]

f See text for a discussion of this species.

g S/N ratio not high enough to find this resonance.

h $^2J_{HW}$ not resolved.

Results and Discussion

Hydrogenation at relatively low pressures (60-80 psig) of $CpW(NO)(CH_2SiMe_3)_2$ with no Lewis base present, whether done on a preparative scale or NMR tube scale, does not result in $[CpW(NO)H]_2(\mu\text{-}H)_2$ or other readily identifiable novel product, but only in the formation of an intractable tan material. Surprisingly enough, the only compound ever isolated from this reaction was a very low yield of $CpW(O)_2(CH_2SiMe_3)$,[2] with the oxo ligands presumably coming either from the NO ligand of the starting material or from some adventitious O_2.[18]

A. $CpW(NO)(H)(CH_2SiMe_3)L$ ($L=P(OPh)_3$, $PMePh_2$)

Hydrogenolysis of $CpW(NO)(CH_2SiMe_3)_2$ at ~60 psig in the presence of one equivalent of a bulky Lewis base, L, results in the isolation of modest yields of $CpW(NO)(H)(CH_2SiMe_3)L$ (eq. 4-3; step c, Scheme 4-I).

$$CpW(NO)(CH_2SiMe_3)_2 + L \xrightarrow[3\ h,\ 60\ psig\ H_2]{hexanes,\ RT} CpW(NO)(H)(CH_2SiMe_3)L \quad (4\text{-}3)$$

$$-TMS$$

These are bright yellow, crystalline solids that are (for L= $PMePh_2$) stable in air at 0^oC and under N_2 at 20^oC for at least six months (the complex with $L=P(OPh)_3$ very slowly undergoes a thermal decomposition--see section B). They are only slightly

Scheme 4-I

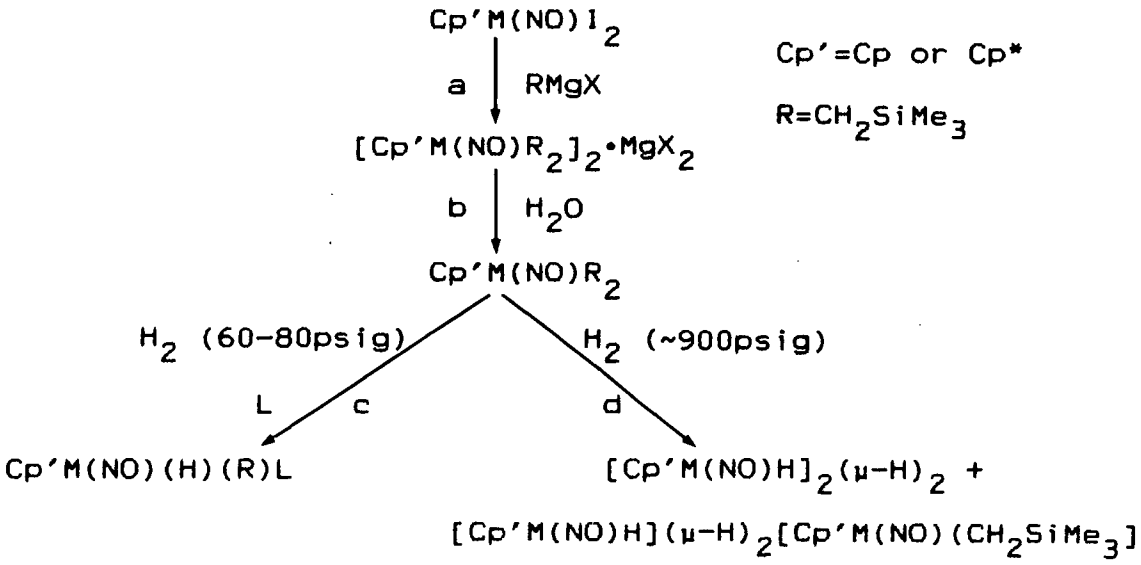

soluble in hexanes and Et_2O, but quite soluble in more polar organic solvents to form somewhat air-sensitive solutions. The IR spectra of these compounds (Table 4-I) show strong, low frequency nitrosyl stretching bands (1550-1600 cm^{-1}) indicative of linear NO groups and suggestive of considerable amounts of W→NO back-donation.[19] Much weaker, terminal W-H stretching bands (1836-1865 cm^{-1}) are also visible. Additionally, in Nujol mull spectra, two medium strength bands at ~1240 and ~1250 cm^{-1} are observed which are characteristic of the CH_2SiMe_3 ligand.[20] The electron-impact mass spectrum of $CpW(NO)(H)(CH_2SiMe_3)(PMePh_2)$ unfortunately does not show any peaks due to a parent ion, but rather a highest-mass pattern with its most intense peak at m/z = 479, which is an overlap of the patterns expected for $(P-CH_2SiMe_3)^+$ and $(P-Me_4Si)^+$.

The ^{1}H NMR spectra of these compounds are particularly informative. In addition to the expected peaks for the Cp, L and $SiMe_3$ protons, an interesting pattern is observed for the W-C$\underline{H}_2$ and metal-hydride peaks--this region is shown in Fig. 4-I for L=$PMePh_2$. The most striking feature is the similarity of the chemical shifts for the methylene and hydride protons. Fortunately, at 400-MHz, the resonances are sufficiently resolved to form an effectively first-order spectrum. Coupling is observed between the two inequivalent methylene protons, the hydride proton, the ^{31}P nucleus of L, and ^{183}W, giving the observed superposition of a 24-line pattern on a 48-line pattern. All the coupling constants (Table 4-II) can therefore be calculated in a straightforward manner. As may be seen, the methylene protons (H_A and H_B) each exhibit markedly different coupling to the hydride proton (H_W) and the phosphorus-31 nucleus. This behaviour for vicinal coupling (H-C-W-H and H-C-W-P) is reminiscent of that observed for organic ethane (H-C-C-H) fragments which are understood in terms of the well-known Karplus equation.[74] Although it is unlikely that the true Karplus equation holds across the H-C-W-H system (and, of course, it cannot across the H-C-W-P fragment), the principle of a larger ^{3}J for a small dihedral angle is well-established and it is possible that a "Karplus-like" relation may hold for organometallic systems. On this basis, a reasonable idea of the relative orientations of H_A, H_B, H_W and P may be obtained and a Newman

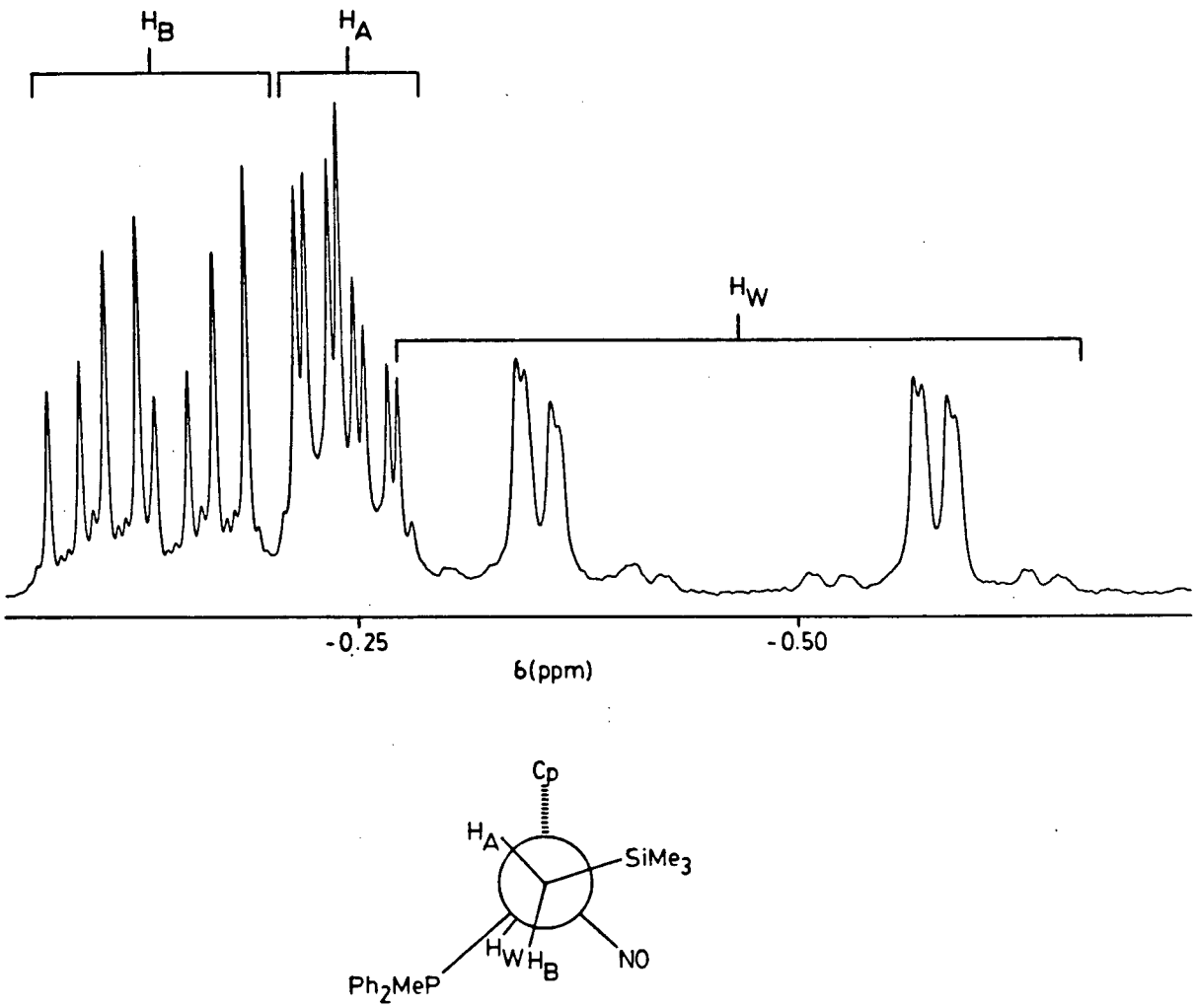

Fig. 4-1. A section of the 400-MHz ^1H NMR spectrum of $CpW(NO)(H)(CH_2SiMe_3)(PMePh_2)$ in C_6D_6 showing the resonances due to the hydride and α-C protons, along with a Newman projection down the α-C-W axis showing the possible orientation of the ligands based on the observed coupling constants.

projection down the C-W bond showing this is also given in Fig. 4-1.

The most obvious probable molecular structures for $CpW(NO)(H)(CH_2SiMe_3)L$ are conventional, four-legged piano-stools. The large two bond coupling between the hydride and phosphorus nuclei (J = 90-117 Hz) is indicative of a cis orientation of the H and L ligands in the base of the piano-stool (see chapter 2). However, neither the NMR spectra nor any other spectroscopic technique indicates whether the H and CH_2SiMe_3 ligands are mutually cis or trans. Our expectation is that they should be trans on the basis that the electron-withdrawing NO and electron-donating L ligands should be trans. Therefore, single crystals of $CpW(NO)(H)(CH_2SiMe_3)(PMePh_2)$ suitable for X-ray analysis were grown and the structural analysis was performed by R.H. Jones and F.W.B. Einstein of Simon Fraser University. (All the X-ray analyses discussed in this chapter were performed by Jones and Einstein and the details of the data collection and refinement will be reported elsewhere.)

Two views of the solid-state molecular structure of $CpW(NO)(H)(CH_2SiMe_3)(PMePh_2)$ are shown in Fig. 4-2 and selected bond angles and bond lengths are given in Table 4-III. As may be seen, this complex does adopt a conventional piano-stool structure. The geometry of the WNO linkage is similar to that of $[CpW(NO)H]_2(\mu\text{-}H)_2$ (chapter 3), again indicating considerable W→NO backbonding.[19] The W-N-O angle is close to linear, although

slightly more bent here than in the dihydride dimer (170.4(9)^{o} vs. 174.3(10)^{o}). The molecule is also quite crowded, as is

Table 4-III Important Interatomic Distances (Å) and Angles (deg) for $CpW(NO)(H)(CH_2SiMe_3)(PMePh_2)$

W-N	1.781(8)	N-O	1.213(11)
W-C(6)	2.246(11)	W-CP	2.023
W-P	2.492(3)		
W-N-O	170.4(9)	N-W-C(6)	94.7(9)
N-W-P	103.3(3)	C(6)-W-P	79.7(5)
N-W-CP	123.8	P-W-CP	129.5
C(6)-W-CP	110.6	W-C(6)-Si	123.2(5)

reflected in the W-C(6)-Si angle of 123.2(5)^{o} which is a marked departure from the expected tetrahedral angle of 109.6^{o}. Unfortunately, the hydride ligand could not be located from the X-ray analysis. However, if a four-legged piano-stool structure is assumed, then there appears to be a "hole" in the metals coordination sphere where the hydride may be located. The molecule has been oriented in Fig. 4-2b so as to place this hole to the right of the W atom (cf. Fig. 4-12). This empty coordination site can be better seen in Fig. 4-3, which shows it to be trans to the CH_2SiMe_3 ligand, thus supporting our expectation. Of course, the compound is chiral and the views shown in Fig. 4-2 and 4-3 are of only one of the enantiomers.

The $CpW(NO)(H)(CH_2SiMe_3)L$ complexes are members of the very small class of isolable transition-metal alkyl hydride compounds and are the first hydridoalkyl nitrosyl compounds known for any

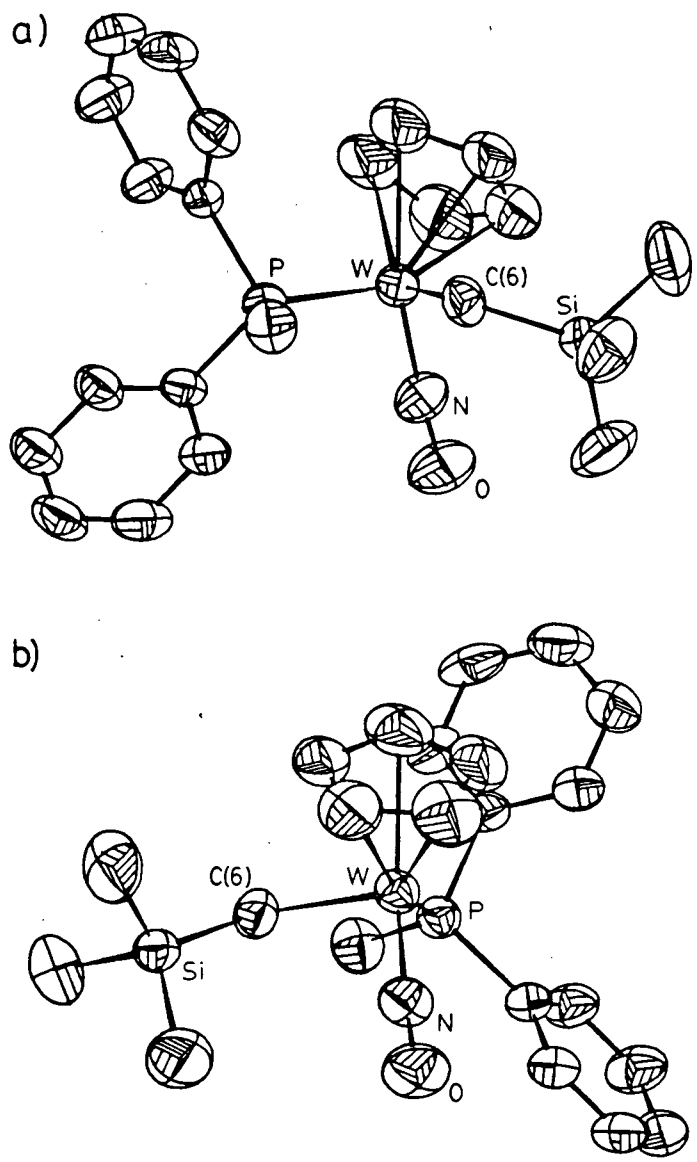

Fig.4-2. SNOOPI diagrams of the molecular structure of $CpW(NO)(H)(CH_2SiMe_3)(PMePh_2)$. a) View showing the NO, CH_2SiMe_3 and $PMePh_2$ ligands spread out. b) View showing the hole where the hydride hydrogen atom is probably located to the right (cf. Fig. 4-12).

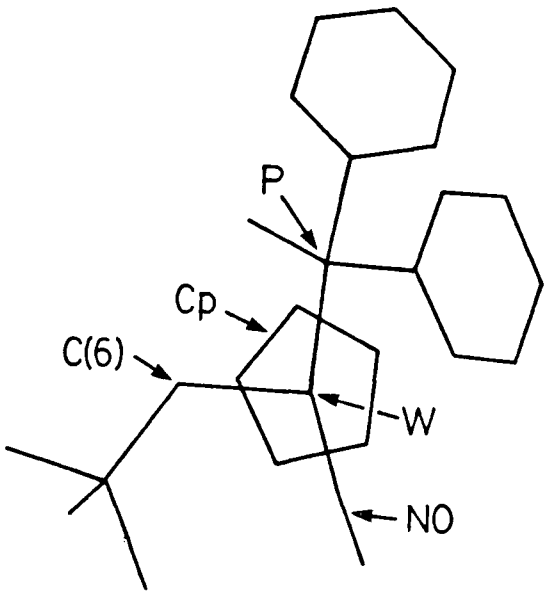

Fig. 4-3. Stick diagram of the structure of $CpW(NO)(H)(CH_2SiMe_3)(PMePh_2)$ as viewed from directly above the plane of the Cp ring showing the hole where the hydride hydrogen atom is probably located to the right of the tungsten atom (cf. Fig. 4-13).

metal. The only other tungsten alkyl hydride complexes in the literature are the tungstenocene derivatives, $Cp_2W(R)H$, whose chemistry was extensively investigated by Green and co-workers in the 1970's.[21] Structurally, the most closely related species are $CpRe(CO)_2(H)(CH_2C_6H_5)$, reported by Fischer and Frank in 1978,[22] and $CpRe(CO)_2(H)(Me)$, mentioned by Yang and Bergman in 1983.[23] Of these Re compounds, only $CpRe(CO)_2(H)(CH_2C_6H_5)$ has

been characterized crystallographically. As with our W compound, the hydride H atom was not located in the structure,[24] however, there is a "hole" in the metals coordination sphere trans (assuming a four-legged, piano-stool geometry) to the benzyl group and the complex is therefore isostructural to the W one. This Re compound is much less sterically crowded than $CpW(NO)(H)(CH_2SiMe_3)(PMePh_2)$, as is evidenced by the Re-C-C angle (across the benzyl group) being much less distorted ($114.8(8)^{o}$) away from the tetrahedral angle. This is not surprising since, in the W compound, a relatively bulky $PMePh_2$ group formally replaces a CO ligand on the Re. Unlike the W complex, unique $^{3}J_{HH}$ coupling is not observed between the hydride nucleus and the individual α-carbon protons for either Re compound. Therefore the extreme crowding in $CpW(NO)(H)(CH_2SiMe_3)(PMePh_2)$ and the "Karplus-like" couplings observed in the ^{1}H spectrum suggest that this alkyl hydride complex is less fluxional in solution than the Re complexes and that it is unlikely that there is substantial rotation about the $W-CH_2SiMe_3$ bond.

As a class, alkyl and the related acyl hydride compounds are very important because they are implicated in a number of homogeneous, catalytic reactions such as olefin hydrogenation and hydroformylation.[25] Usually, however, hydridoalkyl complexes are prone to undergo ready reductive elimination, much more so than related dialkyl or dihydride compounds.[26] Because of the paucity of isolable complexes of this class, little is known

about their chemistry[27] and so further study of these complexes is of considerable interest.

It is worthwhile to speculate as to why these $CpW(NO)(H)(CH_2SiMe_3)L$ compounds are so stable. Thermodynamically, alkyl hydrides are generally believed to be unstable with respect to alkane loss, i.e. $M(R)(H) \rightarrow M + RH$,[26] although this reaction is less favoured for third-row transition metal compounds because of their greater M-C bond strengths than for first- and second-row analogues.[26] Consequently, isolable complexes of this type are considered to be kinetically stable for any of several reasons.[27] Firstly, reductive elimination is not facile if the alkyl and hydride ligands are trans, as in <u>trans</u>-$Ni(H)(Me)[P(C_6H_{11})_3]_2$ (C_6H_{11}= cyclohexyl)[28] and <u>trans</u>-$Pt(H)(R)(PR_3')_2$.[29,30] Related cis compounds undergo reductive elimination readily; for example, <u>cis</u>-$Pt(H)(Me)(PPh_3)_2$ loses methane intramolecularly at -25°C.[31] Secondly, elimination may not occur even from a cis alkyl hydride if the complex is stereochemically rigid. For example, 6-coordinate complexes such as <u>cis</u>-$Ir(H)(CH_2C(O)H)(PMe_3)_3Cl$ are stable even upon extended heating at 100°C.[32] The kinetics of the reductive elimination from the related Rh species showed elimination to only occur after loss of one of the phosphine ligands, forming a nonrigid 5-coordinate intermediate. Thirdly, intramolecular elimination may not occur if the resulting metal-containing product is highly unstable. Norton and co-workers have extensively studied alkane

loss from cis-$Os(H)(R)(CO)_4$ and shown that it goes via an intermolecular pathway,[33] thus not allowing the formation of the unstable $Os(CO)_4$ fragment.

In light of the above results, the stability of the $CpW(NO)(H)(CH_2SiMe_3)L$ complexes can be considered. Although the alkyl and hydride ligands are described as trans across the base of a four-legged piano-stool, they are really not trans in an octahedral sense and there are certainly no intervening ligands between the two to prevent elimination. Therefore the Ni and Pt trans argument above does not hold here. As has been noted earlier, a reasonable case may be made for the $CpW(NO)(H)(CH_2SiMe_3)L$ compounds to be non-fluxional in solution. In spite of the fact that they are formally 7-coordinate, these and the related CpW(NO)IHL complexes discussed in chapter 2, unlike the $CpM(CO)_2LH$ compounds,[34] do not interconvert between cis and trans isomers and appear to prefer to exist in only one form. It may well be, therefore, this rigidity that stabilizes these compounds enough to make them isolable. As for the third possible reason for kinetic stability, at this point there is no way of estimating the potential stability of the CpW(NO)L fragment that would result from intramolecular Me_4Si reductive elimination and so any discussion on this is premature.

B. Thermolysis of $CpW(NO)(H)(CH_2SiMe_3)[P(OPh)_3]$.

When $CpW(NO)(H)(CH_2SiMe_3)[P(OPh)_3]$ is warmed gently in hexanes solution, the mixture gradually lightens in colour and pale yellow, microcrystalline $CpW(NO)(H)[P(OPh)_2(OC_6H_4)]$ precipitates out of solution (eq. 4-4).[34]

$$CpW(NO)(H)(CH_2SiMe_3)[P(OPh)_3] \xrightarrow[12\ h]{50^{\circ}C} CpW(NO)(H)[P(OPh)_2(OC_6H_4)] + Me_4Si \qquad (4\text{-}4)$$

This material has very similar physical properties to those of the hydridoalkyl complexes discussed above, except it is considerably less soluble in common organic solvents. Its IR spectrum shows similar ν_{NO} and ν_{WH} peaks, but, of course, it lacks the bands attributable to the CH_2SiMe_3 ligand. That this compound is an orthometallated species was first suggested by its $^{31}P\{^1H\}$ NMR spectrum (δ_P = 176 ppm) when compared with that of its alkyl hydride precursor (δ_P = 127 ppm)--see Table 4-II. It is generally accepted[36] that, among closely related species, when a monodentate phosphine chelates to form a 5-membered ring, a substantial downfield shift is observed in its phosphorus-31 NMR spectrum. In an attempt to confirm this, a $^{13}C\{^1H\}$ NMR spectrum was run in the hope that this would show direct coupling between ^{183}W and the ring carbon atom attached to it. Unfortunately, the low solubility of this complex in C_6D_6 prevented a useful $^{13}C\{^1H\}$ spectrum from being collected.

Therefore, in order to confirm the structure, a single crystal X-ray analysis was performed on crystals grown from CH_2Cl_2/hexanes at -25°C.

The structural analysis does indeed show that this material is $Cp\overline{W(NO)(H)[P(OPh)_2(OC_6H_4)]}$ and two views of the molecular structure are shown in Fig. 4-4 while selected bond distances and angles are gathered in Table 4-IV. Although these depictions are

Table 4-IV Important Interatomic Distances (Å) and Angles (deg) for $Cp\overline{W(NO)(H)[P(OPh)_2(OC_6H_4)]}$

W-N	1.795(6)	N-O(1)	1.194(8)
W-C(12)	2.221(6)	W-CP	2.024
W-P	2.380(2)	P-O(2)	1.603(4)
P-O(3)	1.583(4)	P-O(4)	1.611(5)
O(2)-C(11)	1.413(7)	O(3)-C(21)	1.420(7)
O(4)-C(31)	1.413(8)		
W-N-O(1)	173.7(5)	N-W-C(12)	92.6(2)
N-W-P	96.0(2)	C(12)-W-P	72.6(2)
N-W-CP	125.6	P-W-CP	136.6
C(12)-W-CP	112.6	W-P-O(2)	112.6(2)
W-P-O(3)	114.9(2)	W-P-O(4)	122.1(2)
P-O(2)-C(11)	112.8(4)	O(2)-C(11)-C(12)	119.3(5)
C(11)-C(12)-W	122.6(4)	P-O(3)-C(21)	128.5(4)
P-O(4)-C(31)	121.2(4)		

the opposite enantiomer to those given for $CpW(NO)(H)(CH_2SiMe_3)(PMePh_2)$, it is apparent that the geometry is remarkably similar. The W-N and N-O distances are the same (within experimental error), while the orthometallated complex has a slightly more linear W-N-O linkage. Inspection of the geometry of the phosphite moiety shows that orthometallation has

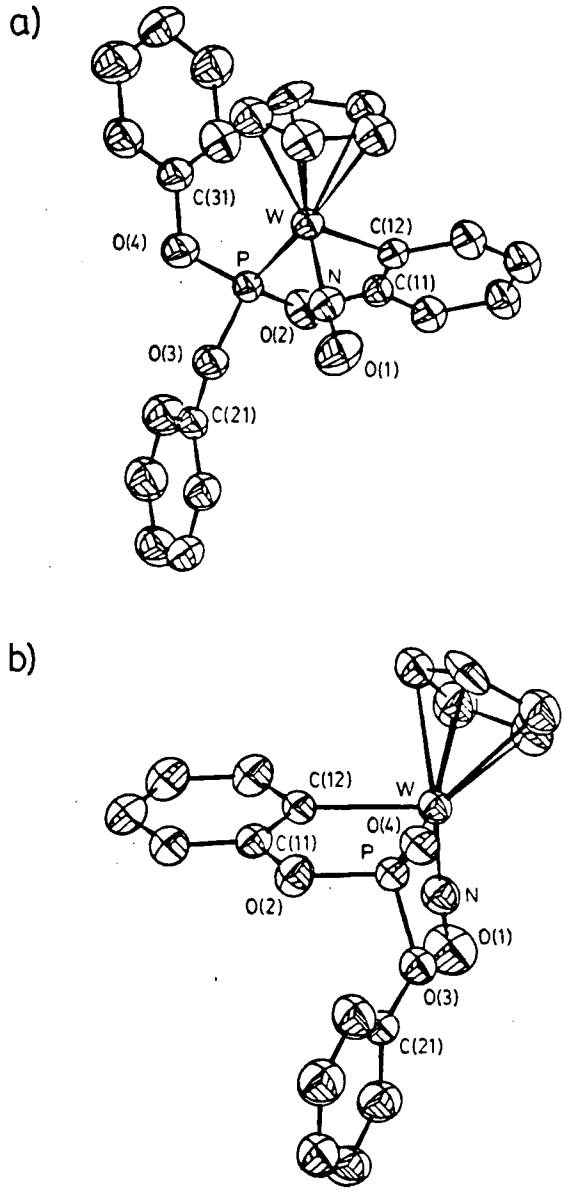

Fig.4-4. SNOOPI diagrams of the molecular structure of $CpW(NO)(H)[P(OPh)_2(OC_6H_4)]$. a) View showing the orthometallated phosphite ligand. b) View showing the hole where the hydride hydrogen atom is probably located to the right (cf. Fig. 4-12). The Ph group attached to O(4) has been omitted for clarity.

not strained this ligand in any well-defined fashion. For example, the W-P-O angles are 112.6(2), 114.9(2) and 122.1(2) for O(2), O(3) and O(4) respectively. Since the O(4) phenoxy group is not the one involved in the chelation, this suggests that these magnitudes of angle differences are not significant. Again, as with $CpW(NO)(H)(CH_2SiMe_3)(PMePh_2)$, the hydride H was not located, however, the orthometallated complex also shows a "hole" in the expected place in the metals coordination sphere and this is shown as before in Fig. 4-4b and Fig. 4-5.

C. Reactions of $CpW(NO)(CH_2SiMe_3)_2$, H_2 and L in NMR Tubes.

The full course of the hydrogenation reaction of $CpW(NO)(CH_2SiMe_3)_2$ leading to $Cp\overline{W(NO)(H)[P(OPh)_2(OC_6H_4)]}$ was followed in a sealed NMR tube by both ^1H and ^{31}P NMR spectroscopy and series' of these spectra are shown in Fig. 4-6 and 4-7. As shown, the reactions were extremely clean and the overall course is summarized in Scheme 4-II. As the reaction proceeded, the resonances due to $CpW(NO)(CH_2SiMe_3)_2$ (marked "A" in Fig. 4-6) were gradually replaced with those due to the hydridoalkyl complex ("B" in the figures) with the concomitant formation of Me_4Si. As the reaction continued, the alkyl hydride resonances were themselves replaced with those due to the final orthometallated product ("C" in Fig. 4-6 and 4-7) as more Me_4Si formed. These spectra illustrate that no other species were produced in significant quantities. Because it is difficult to

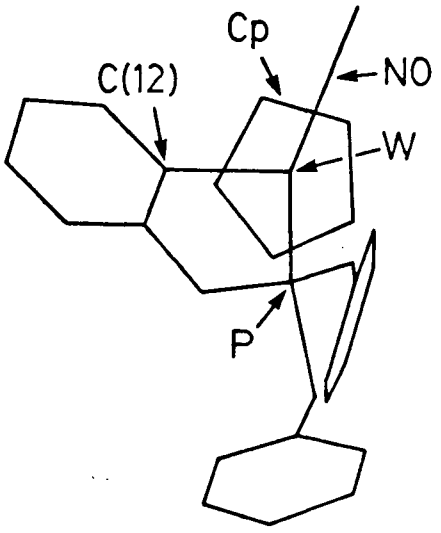

Fig.4-5. Stick diagram of the structure of $CpW(NO)(H)[P(OPh)_2(OC_6H_4)]$ as viewed from directly above the plane of the Cp ring showing the hole where the hydride hydrogen atom is probably located to the right of the tungsten atom (cf. Fig. 4-13).

adequately mix the contents of an NMR tube of the type used,[9] the reaction to produce the alkyl hydride complex was considerably slower (see below) here than on a preparative scale. This resulted in the formation of the orthometallation product being competitive with that of the hydridoalkyl and so resonances due to all three metal-containing species were observed

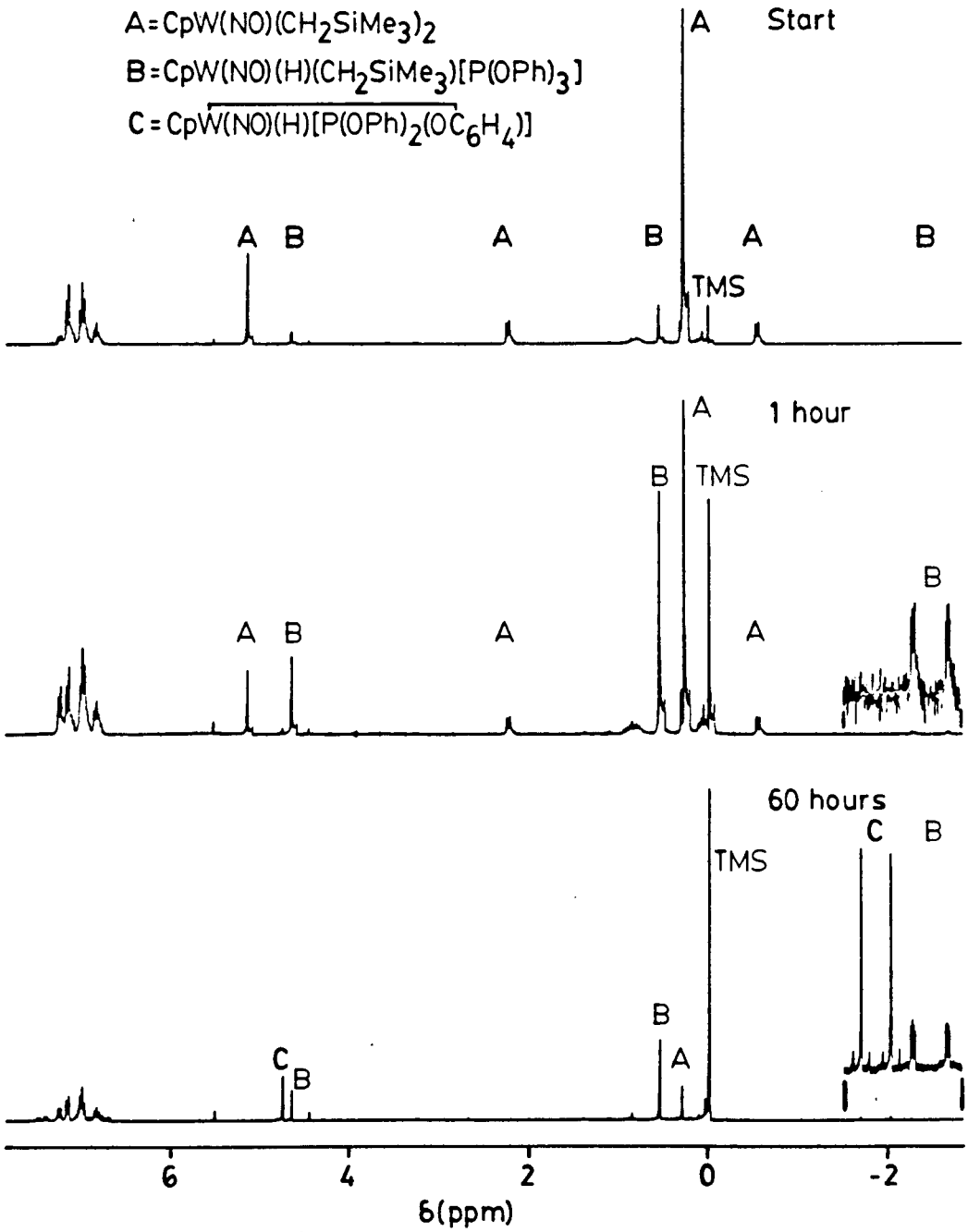

Fig.4-6. The 300-MHz ^1H NMR spectrum of the reaction between $CpW(NO)(CH_2SiMe_3)_2$, $P(OPh)_3$ and H_2 showing the successive formation of $CpW(NO)(H)(CH_2SiMe_3)[P(OPh)_3]$ and $CpW(NO)(H)[P(OPh)_2(OC_6H_4)]$.

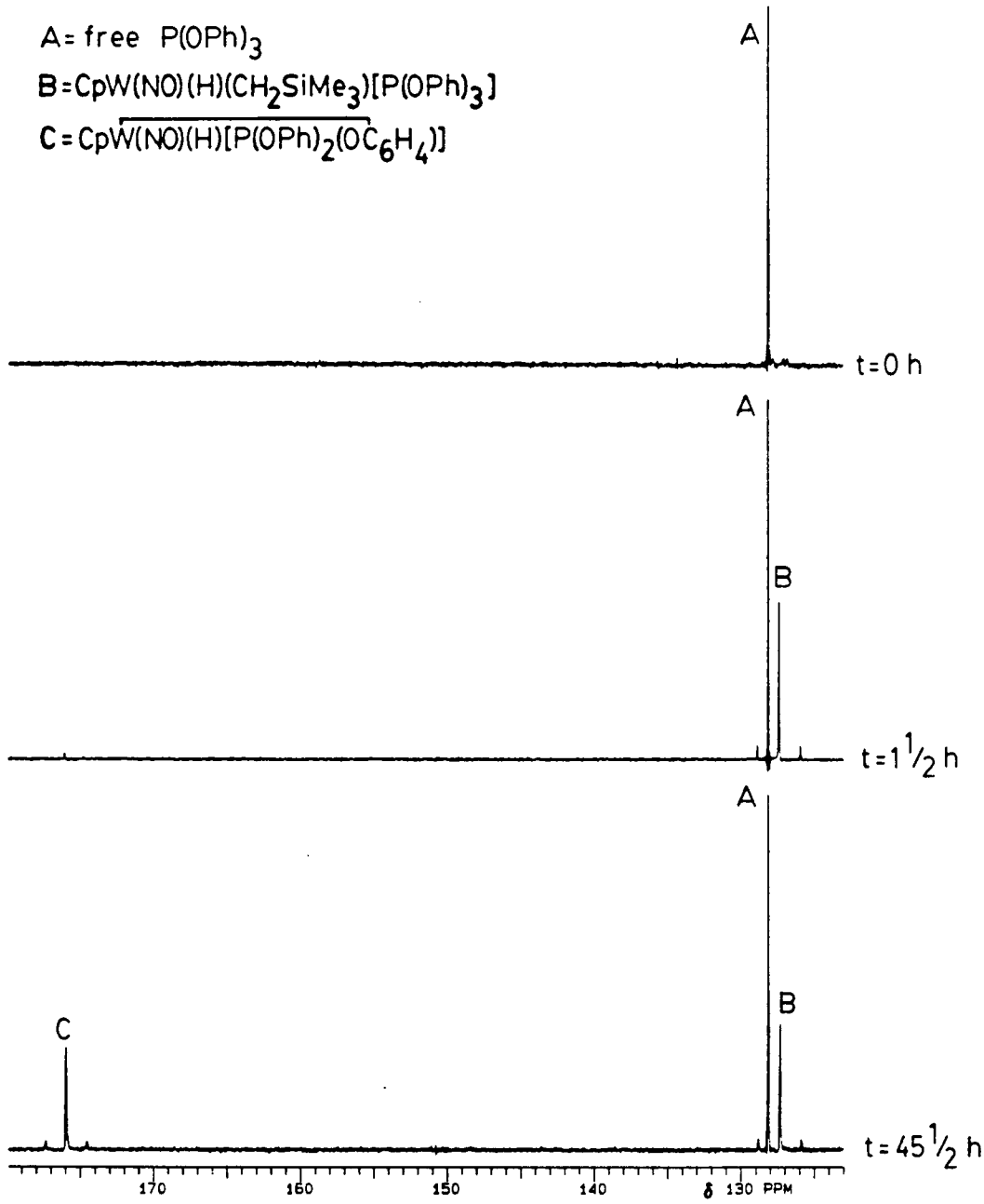

Fig. 4-7. The 121.421-MHz $^{31}P\{^{1}H\}$ NMR spectrum of the reaction between $CpW(NO)(CH_2SiMe_3)_2$, $P(OPh)_3$ and H_2 showing the successive formation of $CpW(NO)(H)(CH_2SiMe_3)[P(OPh)_3]$ and $CpW(NO)(H)[P(OPh)_2(OC_6H_4)]$.

Scheme 4-II

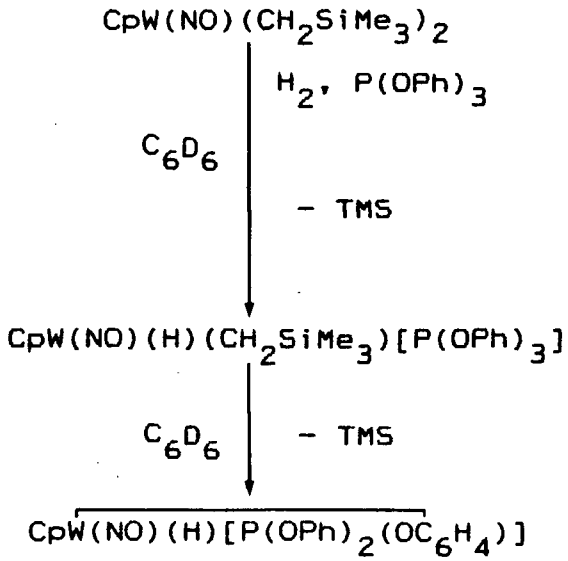

simultaneously in some of the spectra. Preparatively, $CpW(NO)(H)(CH_2SiMe_3)[P(OPh)_3]$ could be isolated without any contamination from the orthometallated complex if the reaction was done on a relatively small scale (see Experimental Section) and if the reaction time was kept short (<3 h).

In light of the NMR study, and with the additional observation that the hydrogenation reaction was substantially slowed when lower pressures of H_2 were used (e.g. 15 psig vs. 60 psig), a reasonable and straightforward mechanism for the reaction can be proposed (Scheme 4-III). This involves first the slow oxidative addition of H_2 to the 16-electron $CpW(NO)(CH_2SiMe_3)_2$ to form a dihydridodialkyl complex that rapidly reductively eliminates Me_4Si to form the $CpW(NO)(H)(CH_2SiMe_3)$ transient. When no L is present, this

material rapidly decomposes (see above), but it may be readily trapped by a suitable Lewis base. Although the alkyl hydride complexes are reasonably stable and isolable, they do apparently slowly reductively eliminate Me_4Si and, when L=$P(OPh)_3$, the resulting $CpW(NO)[P(OPh)_3]$ then undergoes orthometallation to give the observed final product.

When an attempt was made to follow the hydrogenation of the alkyl complex in the presence of $PMePh_2$ in an NMR tube, the reaction was found to be much less clean than when L=$P(OPh)_3$. Signals due to both Me_4Si and $CpW(NO)(H)(CH_2SiMe_3)(PMePh_2)$ did appear in the spectra, along with numerous other peaks in the cyclopentadienyl and silylmethyl regions. Apparently $PMePh_2$ is a much less efficient trapping agent for the $CpW(NO)(H)(CH_2SiMe_3)$ fragment. The observation that this NMR tube reaction was much less clean than in the $P(OPh)_3$ case was in agreement with observations on the preparative scale. In the latter situation, the reaction solution turned from the intense purple colour of the $CpW(NO)(CH_2SiMe_3)_2$ to a deep cherry red when L=$PMePh_2$, rather than the yellow colour observed when L=$P(OPh)_3$. The only way found for obtaining pure alkyl hydride when $PMePh_2$ was used was not to stir the solution and allow $CpW(NO)(H)(CH_2SiMe_3)(PMePh_2)$ to crystallize out of solution as it formed. This crystalline material, which formed a remarkable brick-shaped mass at the bottom of the flask, then had to be picked out manually from the accompanying powdery precipitate

and recrystallized.

Scheme 4-III

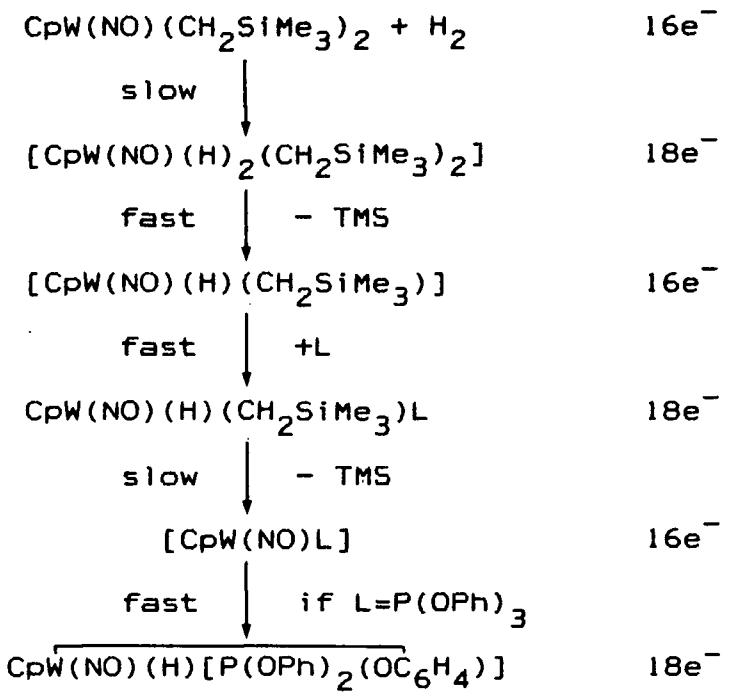

D. The Equilibrium Between $CpW(NO)(CH_2SiMe_3)_2$ and $PMePh_2$.

When the NMR tube containing $CpW(NO)(CH_2SiMe_3)_2$ and $PMePh_2$ was undergoing the freeze-pump-thaw degassing cycles in preparation for the hydrogenation reaction discussed above, it was observed that, at low temperatures, the mixture reversibly changed from the purple of the alkyl complex to a yellow colour reminiscent of $CpW(NO)(CH_2SiMe_3)_2(PMe_3)$.[37] This suggested that the adduct $CpW(NO)(CH_2SiMe_3)_2(PMePh_2)$ is formed at low temperature and so a ^1H and $^{31}P\{^1H\}$ NMR study of this equilibrium

Table 4-V. The Equilibrium Data for the Reaction Between $CpW(NO)(CH_2SiMe_3)_2$ and $PMePh_2$ in toluene-d_8.

T(^oC)	K_1[a] ($Lmol^{-1}$)	K_2[a]	ΔG_1[b] ($kJmol^{-1}$)	ΔG_2[b] ($kJmol^{-1}$)
25	0[c]	-	-	-
0	0[c]	-	-	-
-25	4.4	0[d]	-3.1	-
-50	22	0[d]	-5.7	-
-75	78	0.70	-7.2	0.59
-85	120	1.6	-7.5	-0.74

a see text for definitions of K_1 and K_2

b $\Delta G = -RT\ln K$

c no appreciable adduct A formation

d no appreciable adduct B formation

was undertaken. Sample spectra are given in Fig. 4-8, while the appropriate equilibrium data are listed in Table 4-V. These data show that, in fact, two different low temperature adducts are formed (A and B). This is summarized in eq. 4-5, where R_2= $CpW(NO)(CH_2SiMe_3)_2$, P=free $PMePh_2$, and R_2P_A and R_2P_B are the adducts. These two adducts are indistinguishable in the ^1H NMR spectra. They both give two silyl methyl peaks (labelled X_1 and X_2 in Fig. 4-8) which do not change in intensity relative to each

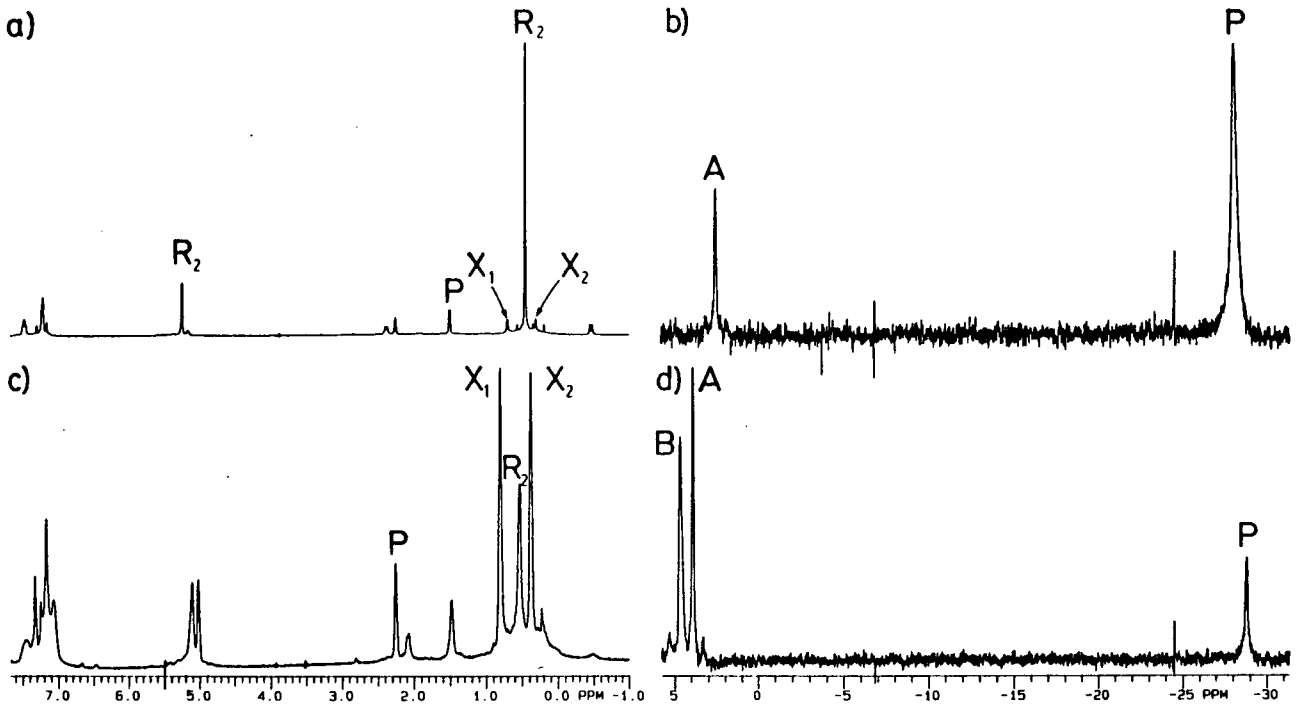

Fig. 4-8. Variable temperature ^{1}H and $^{31}P\{^{1}H\}$ NMR spectra (toluene-d_8) showing the equilibrium between $CpW(NO)(CH_2SiMe_3)_2$ and $PMePh_2$. a) ^{1}H, -25°C; b) $^{31}P\{^{1}H\}$, -25°C; c) ^{1}H, -85°C; d) $^{31}P\{^{1}H\}$, -85°C. R_2 = free $CpW(NO)(CH_2SiMe_3)_2$; P = free $PMePh_2$; X_1, X_2 = coincidental $Si\underline{Me}_3$ peaks (^{1}H spectra) for adducts A and B; A, B = $^{31}P\{^{1}H\}$ peaks corresponding to adducts A and B. Note the slight temperature dependence of the ^{1}H and $^{31}P\{^{1}H\}$ chemical shifts.

$$R_2 + P \xrightarrow{K_1} R_2P_A \xrightarrow{K_2} R_2P_B \qquad (4\text{-}5)$$

$$K_1 = \frac{[R_2P_A]}{[R_2][P]} \quad \text{and} \quad K_2 = \frac{[R_2P_B]}{[R_2P_A]}$$

other as the temperature is lowered. The different adducts manifest themselves in the $^{31}P\{^1H\}$ spectra, where (at -85^oC) δ_A = 3.91, $^1J_{PW}$ = 145 Hz and δ_B = 4.66, $^1J_{PW}$ = 157 Hz (A is the higher temperature adduct and B is the lower).

The most obvious possibilities for A and B are cis and trans isomers. We think this unlikely because a phosphine trans to the strong π-acid NO should exhibit a markedly different ^{31}P chemical shift than if it were trans to a mildly electron-donating alkyl group. We have also seen that, in four-legged piano-stool structures of this type, a trans orientation is preferred and it is likely that both A and B are trans adducts. This molecule is undoubtedly very crowded and the close similarities of the ^1H and $^{31}P\{^1H\}$ spectra of the adducts suggest that they differ only in how the ligands are "locked together" in a rigid structure.

The observation that $CpW(NO)(H)(CH_2SiMe_3)[P(OPh)_3]$ lost Me_4Si and underwent intermolecular C-H bond activation (orthometallation) suggested the possibility that these compounds may be precursors for intermolecular reactivity. Photochemically induced intermolecular activation is currently an area of considerable activity and much has appeared in the

literature.[38] However, thermal activation is a much rarer phenomenon and it was of interest, therefore, to investigate this possibility. Arene C-H bond activation has been observed to be the most facile[39]--in fact, the Cp_2W fragment was found to induce such a reaction both thermally and photochemically.[21] Unfortunately, thermolysis of $CpW(NO)(H)(CH_2SiMe_3)(PMePh_2)$ in C_6H_6 did not result in the identification of any C-H activation product. Nuclear magnetic resonance analysis of the non-volatiles showed only low yields of free $PMePh_2$,[40] $OPMePh_2$,[41] and $CpW(NO)(PMePh_2)_2$[16] in the ^1H and $^{31}P\{^1H\}$ spectra amongst a plethora of decomposition products.

Generally speaking, most known C-H bond activating species contain relatively electron-rich metal centres such as Re, Rh and Ir. Consequently, it was felt that increasing the electron density on the CpW(NO)L fragment would render it more prone to undergo intermolecular oxidative addition once Me_4Si had been lost. The obvious route to try was therefore with a stronger phosphine donor such as PMe_3.[48] However, PMe_3 forms an adduct at room temperature with $CpW(NO)(CH_2SiMe_3)_2$[37] and it thus blocks the site for the initial H_2 reaction. Isolated $CpW(NO)(CH_2SiMe_3)_2(PMe_3)$ does lose some PMe_3 upon dissolution, reforming a small amount of the dialkyl complex. When such a mixture was hydrogenated, some of the desired hydridoalkyl compound could be identified by ^1H NMR spectroscopy, but the reaction was very slow and the desired product could not be

separated. Therefore, this route was abandoned. These experiments did provide support, however, for the initial step in the hydrogenolysis reaction being oxidative addition of H_2 to the 16-electron $CpW(NO)(CH_2SiMe_3)_2$ rather than direct H_2 attack on the metal-carbon bond.

Since changing the phosphine in this system did not offer a promising route to a more electron-rich metal centre, it was decided to turn to the analogous Cp* system. Pentamethylcyclopentadienyl complexes are generally accepted to have more electron-rich metal centres and to enjoy greater thermal stability than their perhydro relatives.[42] The remainder of this chapter discusses this system, including the preparation of the appropriate starting materials.

E. $Cp^*W(NO)I_2$.

Very little Cp* chemistry of the group 6 nitrosyls has been reported. Only the preparation and X-ray crystal structure of $Cp^*W(CO)_2(NO)$ have been published.[10] The synthesis of the desired iodo precursor to the alkyl hydride starting material $Cp^*W(NO)(CH_2SiMe_3)_2$ (steps a and b Scheme 4-1), $Cp^*W(NO)I_2$, has been discussed, along with several of its Lewis base adducts (L= tertiary phosphine or phosphite).[13] During the preparation of this complex for the work described here, a number of interesting features were observed.

The standard preparation of the $CpM(NO)I_2$-type compounds

involves the addition of a stoichiometric amount of I_2 to a CH_2Cl_2 solution of $CpM(CO)_2(NO)$[12] (see p 63). One equivalent of CO is immediately evolved, yielding $CpM(CO)(NO)I_2$, which then loses the second equivalent more slowly as the CH_2Cl_2 solvent is removed under gentle vacuum.[43] The $CpM(CO)(NO)I_2$ complexes have not yet proven isolable. In the case of $Cp^*W(CO)_2(NO)$, the second CO loss is much more difficult and the CH_2Cl_2 is usually completely removed under vacuum before all the CO is released. Consequently, it was decided to use the less-volatile solvent toluene for this reaction. When this is done, shortly after all the I_2 has been added to the orange $Cp^*W(CO)_2(NO)$ solution, a dark red-brown microcrystalline precipitate, presumably $Cp^*W(CO)(NO)I_2$[44] (IR supernatant ν_{CO} = 2052, ν_{NO} = 1676 cm^{-1}), forms out of the deep red-brown solution. As the reaction mixture is further stirred and gently warmed under a slight dynamic vacuum, this material redissolves and eventually $Cp^*W(NO)I_2$ precipitates as the solvent volume is reduced. This complex is isolated by filtration and must be thoroughly washed with Et_2O to remove any residual I_2, otherwise attempts to prepare $Cp^*W(NO)(CH_2SiMe_3)_2$ are futile.

Physically, pure $Cp^*W(NO)I_2$ is a most unusual species. It is thermochromic, being bright green at temperatures at, or below, ~20°C, while it reversibly turns to a dirty-gold colour above ~25°C. This change occurs both in solution in non-coordinating solvents such as toluene and CH_2Cl_2 and in the

solid-phase whether under vacuum or when exposed to air or an N_2 atmosphere. Interestingly, no changes in the positions of the NO-stretching frequencies are observed in the IR spectra of either the Nujol mull or CH_2Cl_2 solution phases as the temperature is altered. As well, variable temperature ^1H NMR spectra in toluene-d_8 show no substantial change in the position of the Cp* resonance, only the usual slight temperature dependence of shift expected for a conventional compound. Indeed, the only physical technique that reflects the observed colour change is, naturally, the UV-visible absorption spectrum (Fig. 4-9). As can be seen, the spectrophotometric difference is not very large; nevertheless it is apparently sufficient for the effect to be startling to the eye.

The most obvious possible explanation for this thermochromism is a monomer-dimer equilibrium. However, recent solution molecular-weight studies (at 23°C)[45] and an X-ray crystallographic analysis[46] indicate that the compound is a monomer both in solution and as a solid. It therefore appears that the colour change is not due to any chemical change, but rather to some subtle electronic factor as yet unexplained. Interestingly, the EI mass spectrum of this compound (Table 4-I) shows a highest mass peak at 952 ($(2P-I_2)^+$), which suggests the complex may undergo agglomeration in the gas phase and that mass spectra of these types of compounds are probably not a useful

guide to their molecularity in the solid state.

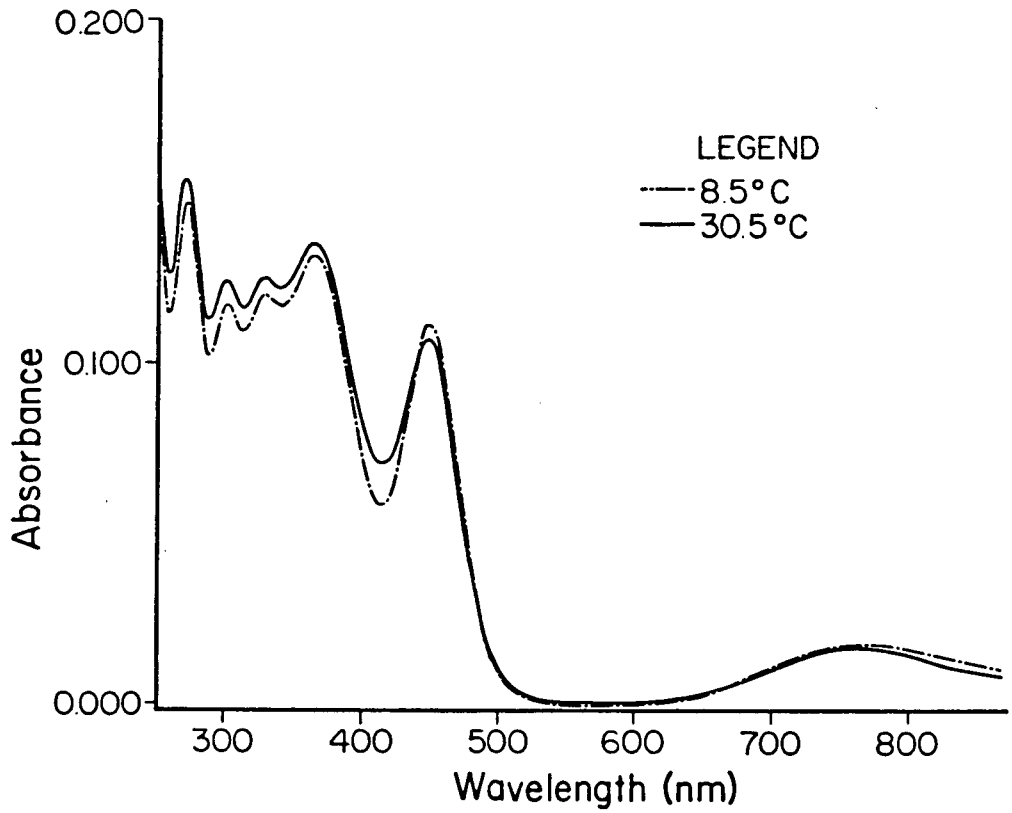

Fig. 4-9. Variable temperature UV-visible spectrum of $Cp^*W(NO)I_2$ in CH_2Cl_2.

Like its perhydro analogue, $Cp^*W(NO)I_2$ is sufficiently air-stable for it to be readily handled in air as a solid. It is somewhat more air-sensitive in solution. Solutions are easily formed in all non-aliphatic common organic solvents to form green or gold coloured mixtures. Coordinating solvents such as acetone do not form thermochromic solutions but instead immediately yield orange solutions, presumably of $Cp^*W(NO)I_2L$ (L=solvent). Unlike

$[CpW(NO)I_2]_2$, $Cp^*W(NO)I_2$ is somewhat thermally sensitive and cannot be stored for extended periods of time. A shelf-life of only 1-2 months at 0^oC is practical--this is decreased somewhat at room temperature. The product of the decomposition is a dark-green, almost black material that has not yet been identified.

F. $Cp^*W(NO)(CH_2SiMe_3)_2$.

The preparation of $Cp^*W(NO)(CH_2SiMe_3)_2$ (eq. 4-6; steps a and b, Scheme 4-I) is analogous to that of the perhydro species.[1,6]

$$Cp^*W(NO)I_2 \xrightarrow{RMgX} 1/2\ [Cp^*W(NO)R_2]_2 \cdot MgX_2 \xrightarrow{H_2O} Cp^*W(NO)R_2 \qquad (4\text{-}6)$$

In this reaction, somewhat more H_2O is needed in the second step to cleave the $[Cp^*W(NO)(CH_2SiMe_3)_2]_2 \cdot MgX_2$ adduct than in the Cp case. Additionally, chromatography of the final reaction mixture must be done with some care, as a small amount of $Cp^*W(O)_2(CH_2SiMe_3)$[2] formation always occurs and the two products have similar chromatographic properties. The $Cp^*W(NO)(CH_2SiMe_3)_2$ product is isolated either by crystallization from pure hexanes at -25^oC, or simply by drying under vacuum the solution containing this complex after it elutes from the column. If the separation from the oxo compound is good, this latter technique is preferred because there is usually considerable yield loss of $Cp^*W(NO)(CH_2SiMe_3)_2$ due to its very high solubility in hexanes. For example, >0.8 g of the dialkyl complex can be

crystallized from <1 mL of hexanes solution.

The $Cp^*W(NO)(CH_2SiMe_3)_2$ compound is an intensely coloured, purple microcrsytalline material that is extremely soluble in all common organic solvents. As a solid, it may be handled rapidly in air, but its solutions are quite air-sensitive. Solution IR spectra show one strong NO stretching band (1543 cm^{-1} in CH_2Cl_2) and the position of the band shows the same dependency on the solvent acceptor number as do the $CpM(NO)L_2$ (L = tertiary phosphine or phosphite) complexes.[16] That is, even though this material is a formally unsaturated, 16-electron compound, it still shows significant Lewis base properties.[47] Nujol mull IR spectra of $Cp^*W(NO)(CH_2SiMe_3)_2$ usually show two ν_{NO} bands at 1549 and 1572 cm^{-1} the latter being due to dissolution of the complex in Nujol, as well as the usual bands for the CH_2SiMe_3 ligand.[20]

The ^1H NMR spectrum of this compound shows the expected Cp^* and silyl methyl peaks, as well as two doublets for the diastereotopic α-C protons (Fig. 4-10). One of these doublets is partially obscured by the Cp^* resonance (in C_6D_6 solution) and may only be seen on a low field (e.g. 80-MHz) spectrometer. In addition to geminal coupling and two-bond coupling to ^{183}W, slight shoulders are observable on the doublets that may be ascribed to four-bond H-H coupling (across the metal)--thus these protons actually form an AA'XX' spin system (exclusive of ^{183}W) but the resonances are not sufficiently resolved for all the coupling constants to be calculable.

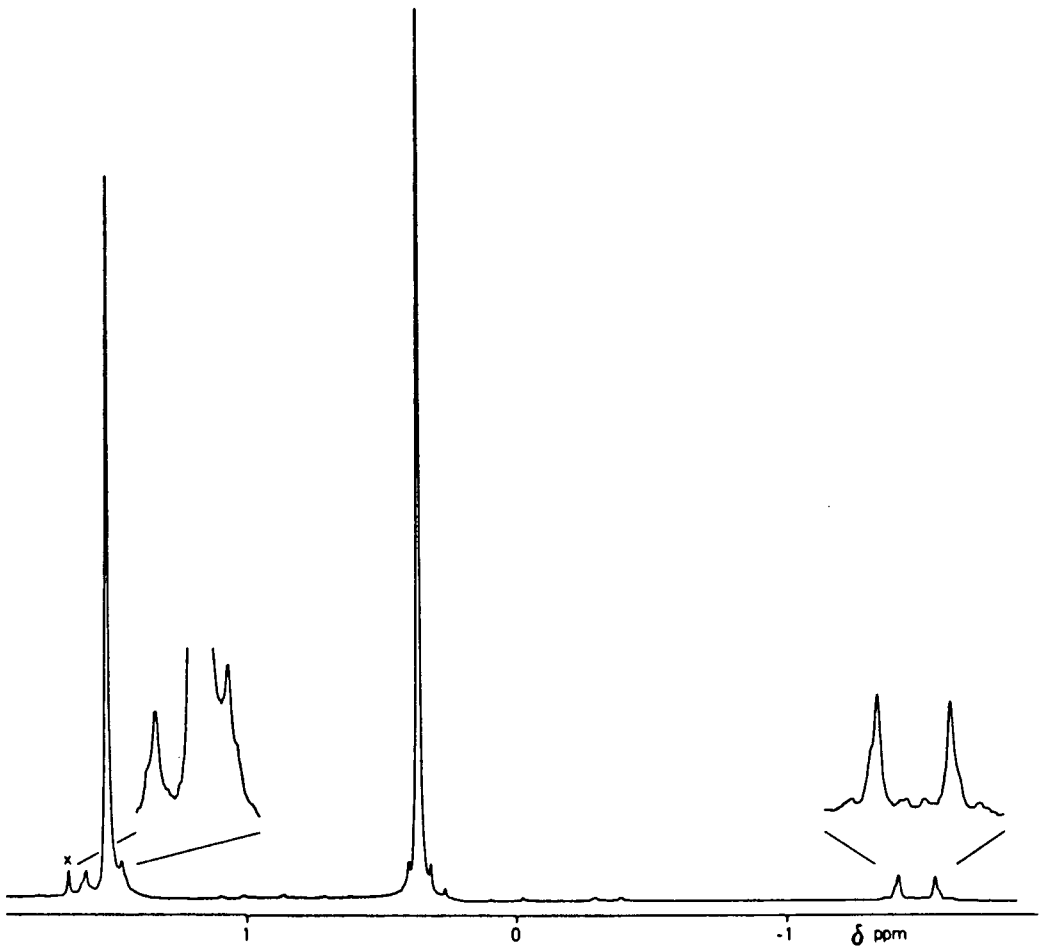

Fig. 4-10. The 80-MHz ^1H NMR spectrum of $Cp^*W(NO)(CH_2SiMe_3)_2$ in C_6D_6.

With $Cp^*W(NO)(CH_2SiMe_3)_2$ in hand, a hydrogenolysis reaction in an NMR tube in the presence of $P(OPh)_3$ (i.e. similar to that in Scheme 4-II) was attempted. Some alkyl hydride formation was observed, but no orthometallation product could be detected in the reaction mixture, as a plethora of products (including Me_4Si) were observed. Inspection of the molecular structure of $Cp\overline{W(NO)(H)[P(OPh)_2(OC_6H_4)]}$ (Fig. 4-4) offers a possible reason

for this. As may be seen, one of the phenyl groups in this structure points up towards the cyclopentadienyl ring--it may be that the Cp* methyls prevent the phosphite from adopting the conformation that would allow orthometallation. Consequently, when $Cp^*W(NO)(H)(CH_2SiMe_3)[P(OPh)_3]$ loses Me_4Si, the resulting fragment cannot trap itself and other reactions occur.

G. $Cp^*W(NO)(H)(CH_2SiMe_3)(PMe_3)$.

As discussed earlier, in the search for an electron-rich metal centre, PMe_3 is a most desirable phosphine for our system.[48] Fortunately, PMe_3 does not coordinate to $Cp^*W(NO)(CH_2SiMe_3)_2$ even at -85^oC in toluene-d_8 and so hydrogenolysis of this dialkyl was carried out in the presence of PMe_3 (eq. 4-7; step c, Scheme 4-I). Using excess PMe_3,[49] this reaction proceeds smoothly to give good (54%) yields of $Cp^*W(NO)(H)(CH_2SiMe_3)(PMe_3)$. Like the other alkyl hydride complexes isolated, this is a yellow, crystalline material that

$$Cp^*W(NO)(CH_2SiMe_3)_2 + \text{xs } PMe_3 \xrightarrow[\text{hexanes, 3 h}]{\text{80 psig } H_2} Cp^*W(NO)(H)(CH_2SiMe_3)(PMe_3) \quad (4\text{-}7)$$

$$\text{- TMS}$$

is air-stable in the solid phase, but somewhat air-sensitive in solution. It is soluble in all conventional organic solvents, with the solubility increasing in the order hexanes < Et_2O

(slight) < benzene < CH_2Cl_2. This compound exhibits a strong nitrosyl stretching absorption in the IR spectrum (Table 4-I) at 1545 cm^{-1} (CH_2Cl_2 solution), some 15 cm^{-1} lower than that observed for Cp*W(NO)(H)(CH_2SiMe_3)($PMePh_2$), suggesting that an increase in metal electron-density has been achieved.[19] The mass spectrum of an analytically pure sample of this complex shows a tungsten-containing highest mass pattern centred at m/z = 603, 90 mass units above the molecular weight. In addition, numerous non-tungsten-containing envelopes of peaks appear up to m/z = 912, indicating that this complex undergoes extensive ion-molecule reactions.

The ^1H NMR spectrum of Cp*W(NO)(H)(CH_2SiMe_3)(PMe_3) (Table 4-II) shows the same features exhibited by the other monomeric alkyl hydride complexes, including the closely bunched pattern for the α-C protons and the hydride resonances. Since the X-ray analysis of the structure of CpW(NO)(H)(CH_2SiMe_3)($PMePh_2$) does not definitively establish the position of the hydride ligand, it was hoped that an NOE difference experiment on Cp*W(NO)(H)(CH_2SiMe_3)(PMe_3) might prove useful in this regard.[50] If the phosphine is cis to both the hydride and alkyl ligands, then the phosphine methyls should be close (in space) to the α-C and hydride protons and so irradiation of the $P\underline{Me}_3$ ^1H signals (δ = 1.09 ppm) should induce a positive nuclear Overhauser effect. As Fig. 4-11 shows, when this irradiation is performed, a positive NOE is observed for the hydride signal, as

well as for <u>one</u> of the α-C protons (H_B in Table 4-II). Not only does this experiment provide further evidence for the trans piano-stool configuration, but it also confirms the assignments of H_A and H_B that were originally based on dihedral angle and coupling constant arguments (see section A) with H_A pointing away from the phosphine ligand and H_B generally pointing towards it (Fig. 4-1).

In order to further confirm the structure, a single-crystal X-ray analysis of $Cp^*W(NO)(H)(CH_2SiMe_3)(PMe_3)$ (at a temperature of ~200 K) was performed. A SNOOPI diagram of the solid-state molecular structure of this material is shown in Fig. 4-12 and important bond distances and angles are given in Table 4-VI. Comparison of the angles and distances for this compound with those of $CpW(NO)(H)(CH_2SiMe_3)(PMePh_2)$ (Fig. 4-2 and Table 4-III) shows these complexes to be remarkably isostructural. The important analogous bond distances (i.e. W-N, N-O, W-P and $W-C_\alpha$) are all the same within experimental error, as are the bond angles (i.e. W-N-O, $N-W-C_\alpha$, N-W-P and $P-W-C_\alpha$). The only important statistically significant bond angle difference is that around the α-carbon atom (W-C(6)-Si = 123.2(5) vs. W-C(11)-Si = 119.8(3) for $CpPMePh_2$ vs. Cp^*PMe_3). This angle is slightly less distorted away from the tetrahedral angle in the $Cp^*W(NO)(H)(CH_2SiMe_3)(PMe_3)$ case than for $CpW(NO)(H)(CH_2SiMe_3)(PMePh_2)$, as might be expected for the less bulky phosphine,[48] although the molecule is still very crowded.

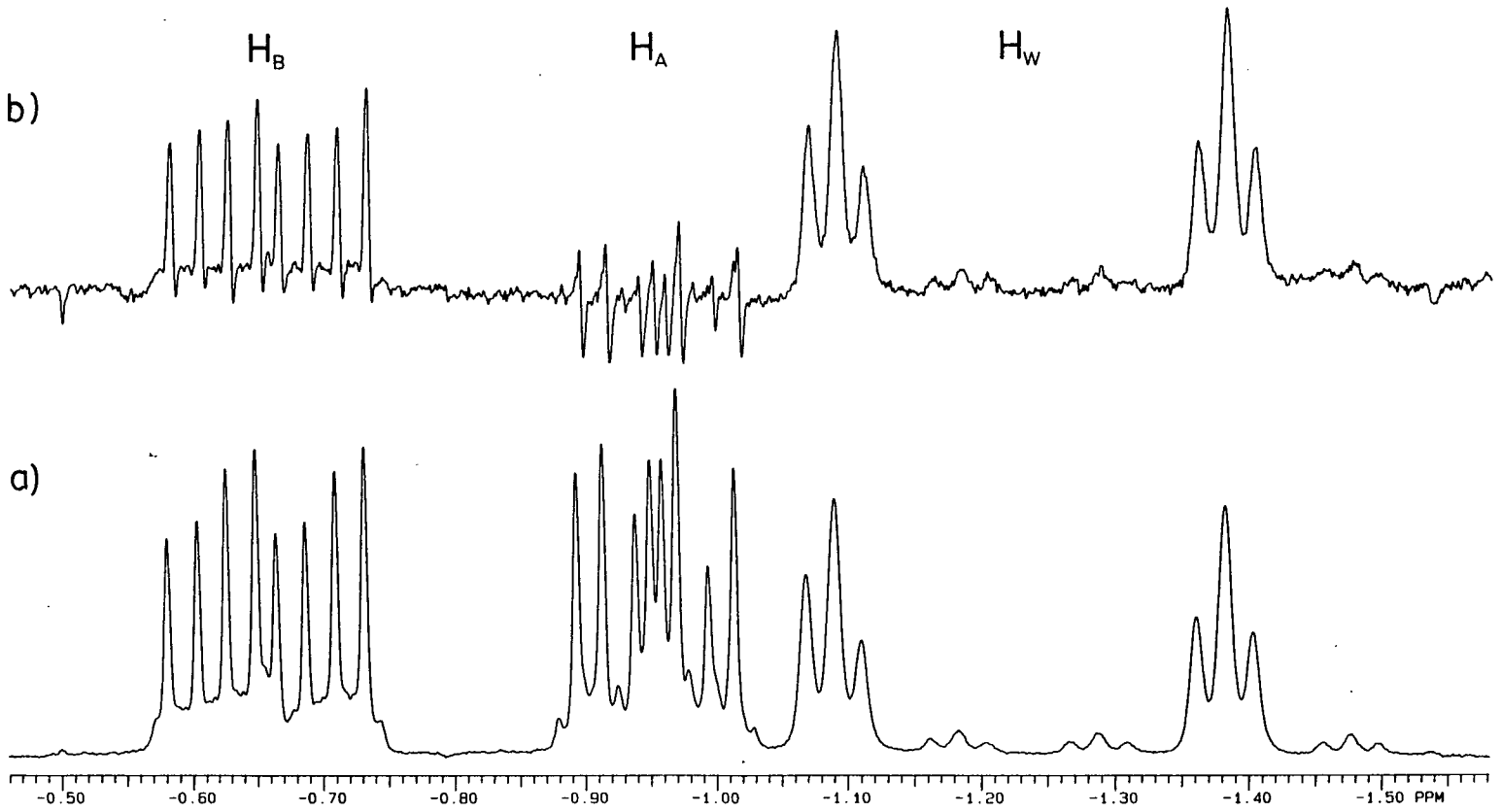

Fig. 4-11. NOE difference experiment on Cp*W(NO)(H)(CH_2SiMe_3)(PMe_3). Only the W-CH_ACH_B-Si and W-H_W region of the ^{1}H NMR spectrum is shown (300-MHz, C_6D_6). a) Normal spectrum; b) NOE difference spectrum upon irradiation of the PMe_3 signal at δ = 1.09 ppm. See text for complete discussion.

Table 4-VI. Important Interatomic Distances (Å) and Angles (deg) for $Cp^*W(NO)(H)(CH_2SiMe_3)(PMe_3)$

W-N	1.771(5)	N-O	1.223(7)
W-C(11)	2.248(6)	W-H(1)	1.75
W-P	2.494(2)	W-CP	2.045
H(1)-C(11)	3.80 (non-bonding)		
W-N-O	169.1(5)	N-W-C(11)	94.0(2)
C(11)-W-P	81.1(2)	P-W-H(1)	61.9
H(1)-W-N	90.1	N-W-P	102.3(2)
H(1)-W-C(11)	142.8	N-W-CP	121.0
C(11)-W-CP	112.0	P-W-CP	132.4
H(1)-W-CP	96.9	W-C(11)-Si	119.8(3)

Fortunately, the hydride hydrogen was located (although not refined) in the structure of $Cp^*W(NO)(H)(CH_2SiMe_3)(PMe_3)$. Fig. 4-12 has been oriented so that this hydrogen is to the right in the picture, and a view from above the molecule is given in Fig. 4-13. These views confirm that the compound does have a trans configuration in a severely distorted four-legged piano- stool. Direct comparisons of Fig. 4-2b and 4-4b with Fig. 4-12 and Fig. 4-3 and 4-5 with Fig. 4-13 show that $CpW(NO)(H)(CH_2SiMe_3)(PMePh_2)$ and $CpW(NO)(H)[P(OPh)_2(OC_6H_4)]$ must also have the same structures.

Examination of Fig. 4-12 shows that the crowding of the basal ligands results in a very interesting situation. In order to relieve the steric strain, the H and CH_2SiMe_3 ligands have been moved away from each other, resulting in an H(1)-C(11) non-bonding distance of 3.80 Å. This is particularly interesting in light of the fact that Me_4Si can be induced to eliminate from the

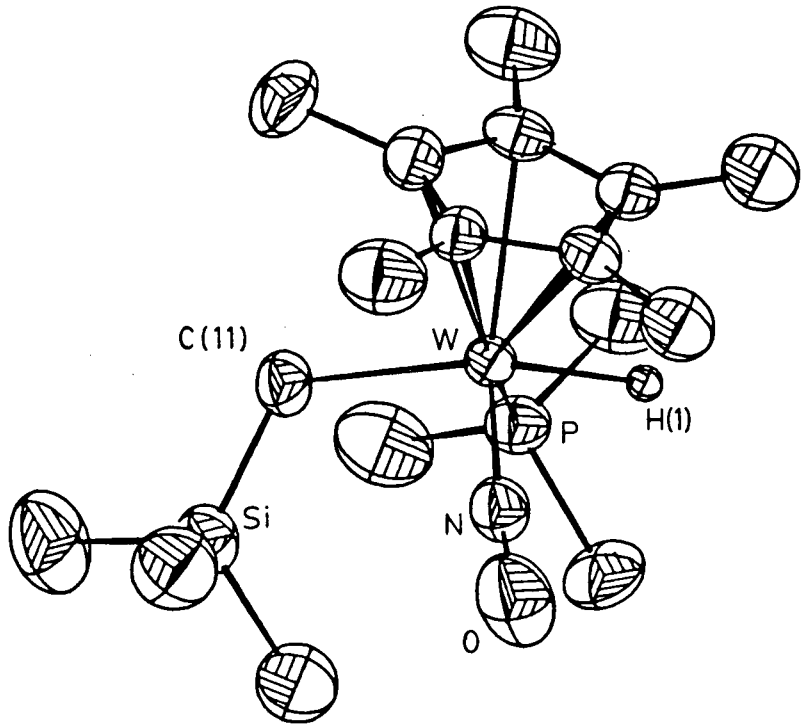

Fig. 4-12. SNOOPI diagram of the molecular structure of $Cp^*W(NO)(H)(CH_2SiMe_3)(PMe_3)$. The molecule is oriented with the hydride hydrogen (H(1)) to the right (cf. Fig. 4-2b and 4-4b).

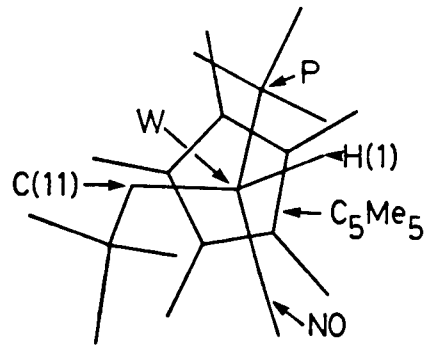

Fig. 4-13. Stick diagram of the structure of $Cp^*W(NO)(H)(CH_2SiMe_3)(PME_3)$ as viewed from directly above the plane of the Cp* ring--note the position of the hydride hydrogen, H(1) (cf. Fig. 4-3 and 4-5).

complex (see p 186). If reductive elimination is intramolecular, the stability of this alkyl hydride may be because the C(11) and H(1) atoms must move a long way before they can bond (see Fig. 4-14). Alternatively, this long C-H distance suggests that perhaps an intermolecular mechanism may be operative (see section A). As a third possibility, there may be a slow equilibrium between the trans form and a cis, with the cis undergoing rapid intramolecular reductive elimination and thus escaping detection. In any event, it would certainly be of interest to investigate the mechanism of the Me_4Si elimination reaction.

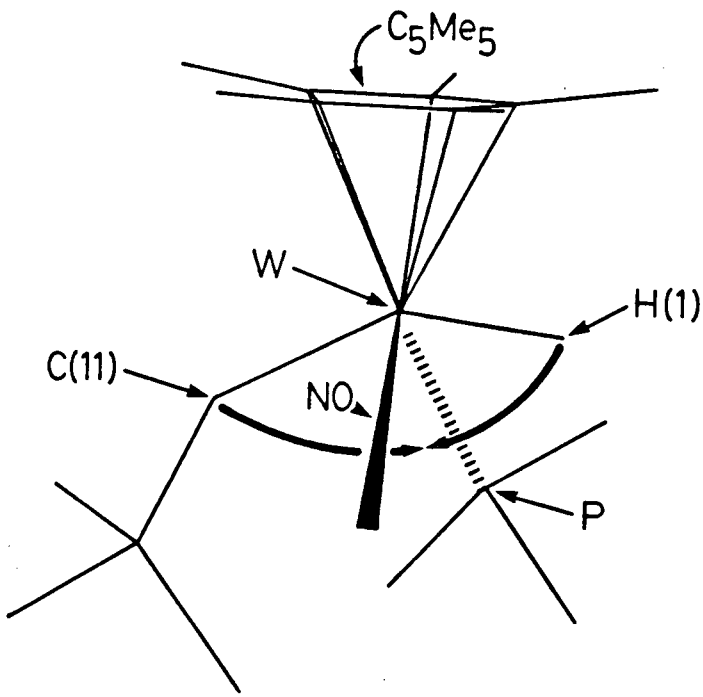

Fig. 4-14. Side view of the structure of $Cp^*W(NO)(H)(CH_2SiMe_3)(PMe_3)$. Note how far H(1) and C(11) must move in order to reductively eliminate.

H. Thermal C-H Activation Involving $Cp^*W(NO)(H)(CH_2SiMe_3)(PMe_3)$.

As we had hoped, thermolysis of $Cp^*W(NO)(H)(CH_2SiMe_3)(PMe_3)$ in C_6H_6 does result in the loss of Me_4Si (by ^1H NMR spectroscopy) and the formation of $Cp^*W(NO)(H)(C_6H_5)(PMe_3)$ (eq. 4-8). Although

$$Cp^*W(NO)(H)(CH_2SiMe_3)(PMe_3) \xrightarrow[40^oC,\ 22\ h]{C_6H_6,\ -\ Me_4Si} Cp^*W(NO)(H)(C_6H_5)(PMe_3) \qquad (4\text{-}8)$$

this reaction is quite clean by ^1H NMR spectroscopy, only a small amount of $Cp^*W(NO)(H)(C_6H_5)(PMe_3)$ was isolated due to the concomitant formation of a very persistent oil and a small amount of $Cp^*W(NO)(PMe_3)_2$.[54,55] The intermolecular activation product has very similar physical properties to the hydridoalkyl complexes already discussed. The Nujol mull IR spectrum lacks the bands attributable to the CH_2SiMe_3 ligand,[20] and strong bands due to the phenyl C-C bond stretches and the ν_{NO} appear at 1560 and 1550 cm^{-1}[51] in CH_2Cl_2 solution, thus making specific assignment of the position of the nitrosyl band impossible (Table 4-1). The ^1H NMR spectrum exhibits the W-H resonance at δ = 5.15 ppm (Fig. 4-15), a substantial downfield shift from the δ = -1.25 ppm of the starting material. When this compound is kept in C_6D_6 at room temperature over the course of several weeks, the phenyl H and hydride peaks disappear and are replaced by a singlet due to C_6H_6. As this occurs, the Cp* and PMe_3 peaks are unaffected,

as is the position of the resonance in the $^{31}P\{^{1}H\}$ NMR spectrum. However, this latter spectrum turns into a 1:1:1 triplet, and therefore these data suggest that the W(D)(C_6D_5) analogue is being formed cleanly after the original compound reductively eliminates benzene. Interestingly, when Cp*W(NO)(H)(CH_2SiMe_3)(PMe_3) is thermolyzed in C_6D_6 instead of C_6H_6, TMS is produced, but the reaction is much less clean and numerous peaks are observed in the Cp* region of the ^{1}H NMR spectrum. This suggests that the oxidative addition of the C-D

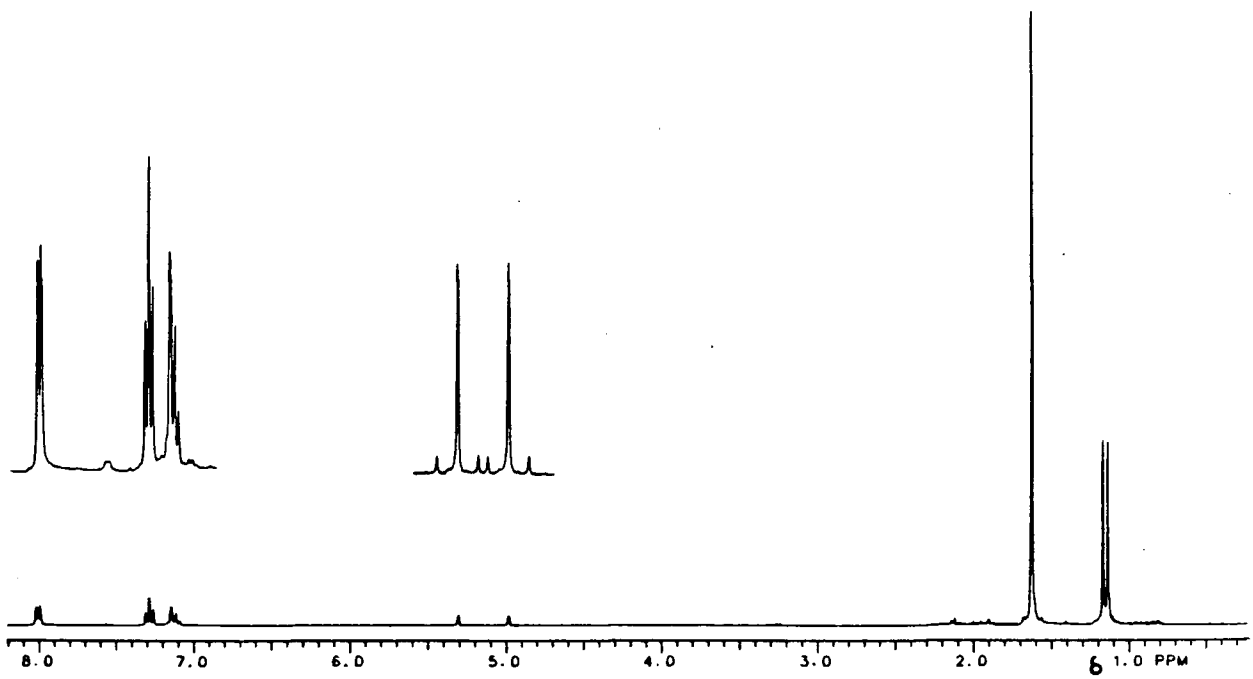

Fig. 4-15. The 300-MHz ^{1}H NMR spectrum of Cp*W(NO)(H)(C_6H_5)(PMe_3) in C_6D_6. The insets show the phenyl (δ = 7 to 8) and hydride (δ = 5.15) resonances.

bond is more difficult than that of the C-H bond, in line with the expected deuterium isotope effect.

The conditions employed in this intermolecular activation are considerably milder than those cited in two recent reports of thermal benzene C-H activation,[52] and so we were encouraged to try other substrates. However, thermolysis of $Cp^*W(NO)(H)(CH_2SiMe_3)(PMe_3)$ in toluene results in a large number of products (by ^1H NMR spectroscopy). Two sets of resonances with the same pattern are observed in a similar region of the spectrum to that of the hydride peak of $Cp^*W(NO)(H)(C_6H_5)(PMe_3)$, indicating that some activation of the aromatic ring of toluene occurs, however, we were unsuccessful at isolating the products.[53] Unfortunately, thermolysis of $Cp^*W(NO)(H)(CH_2SiMe_3)(PMe_3)$ in the presence of n-hexane, cyclohexane or CH_4 in C_6D_{12} does not result in the observation of any C-H activation product. The only identifiable products are $Cp^*W(NO)(PMe_3)_2$,[54,55] free PMe_3 and free $OPMe_3$. Thermolysis was also tried in the presence of PPh_3 to see if arene activation would occur in preference to phosphine binding. The ^1H NMR spectrum shows no evidence for C-H activation and the $^{31}P\{^1H\}$ spectrum indicates a mixture of $Cp^*W(NO)(PMe_3)_2$ (δ_P = -22.56, $^1J_{PW}$ = 454 Hz), $Cp^*W(NO)(PPh_3)_2$ (δ_P = 42.21, $^1J_{PW}$ = 491 Hz) and $Cp^*W(NO)(PMe_3)(PPh_3)$ (δ_{PPh3} = 48.24, $^1J_{PW}$ = 474, $^2J_{PP}$ = 8 Hz, δ_{PMe3} = -23.96, $^1J_{PW}$ = 466 Hz) is formed, with the latter predominating.

Since most successful intermolecular C-H activation is photochemically initiated,[38] the photolysis (Hanovia lamp) of $Cp^*W(NO)(H)(CH_2SiMe_3)(PMe_3)$ was attempted. This resulted only in the loss of all nitrosyl containing species and decomposition into an intractable brown oil. In another effort to induce intermolecular reactivity, sonication was tried in the hope that the transient high-temperatures involved in this process might prove useful.[57] Sonication of $Cp^*W(NO)(H)(CH_2SiMe_3)(PMe_3)$ in C_6H_6 in an ultrasonic cleaning bath (the only sonic source available)[57] did give the activation product, but independent experiments showed that this was merely the result of the warming to ~40°C of the water bath in the cleaner and therefore the conventional thermal reaction.

K. The Redox Chemistry of $Cp^*W(NO)(H)(CH_2SiMe_3)(PMe_3)$.

In a last attempt to invoke C-H activation, the catalytic oxidation of $Cp^*W(NO)(H)(CH_2SiMe_3)(PMe_3)$ with $Ag^+BF_4^-$ in C_6H_6 was tried. It was hoped (Scheme 4-IV) that oxidation of the alkyl hydride to a more reactive 17-electron radical cation (step a) would cause Me_4Si elimination (step b) at a low temperature. The resulting 15-electron species might than be reduced by the starting complex (step c), generating $Cp^*W(NO)PMe_3$, which would then add C_6H_6 (step d), and the 17-electron radical cation, thus forming a catalytic cycle. Unfortunately, this did not work. However, cyclic voltammograms (CV's) run in conjunction with this

attempt suggest that steps a and b of Scheme 4-IV are reasonable and this electrochemistry will now be discussed. George Richter-Addo of our research group ran the CV's in CH_2Cl_2 at a complex concentration of ~5 x 10^{-5} M, using 0.1 M Bu_4NPF_6 support electrolyte with a Pt bead electrode and referenced to the SCE.[58]

When the CV is run over positive potentials at a relatively slow scan speed (Fig. 4-16a), an irreversible oxidation wave is observed at E_{pa} = 0.88 V. This is a considerably lower potential

Scheme 4-IV

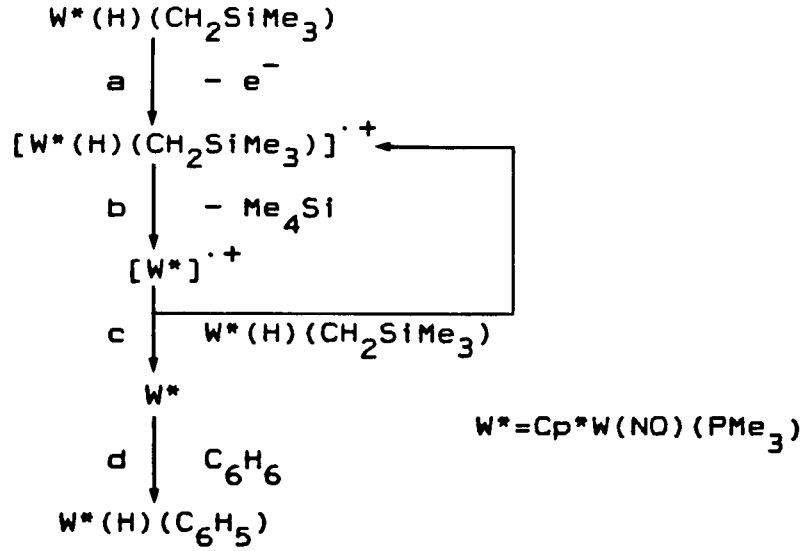

than those observed for the $CpM(NO)_2X$ species[59] (e.g. 1.38 V for $CpW(NO)_2Me$), reflecting the more electron-rich metal centre of the alkyl hydride complex.[60] As the scan rate is increased,

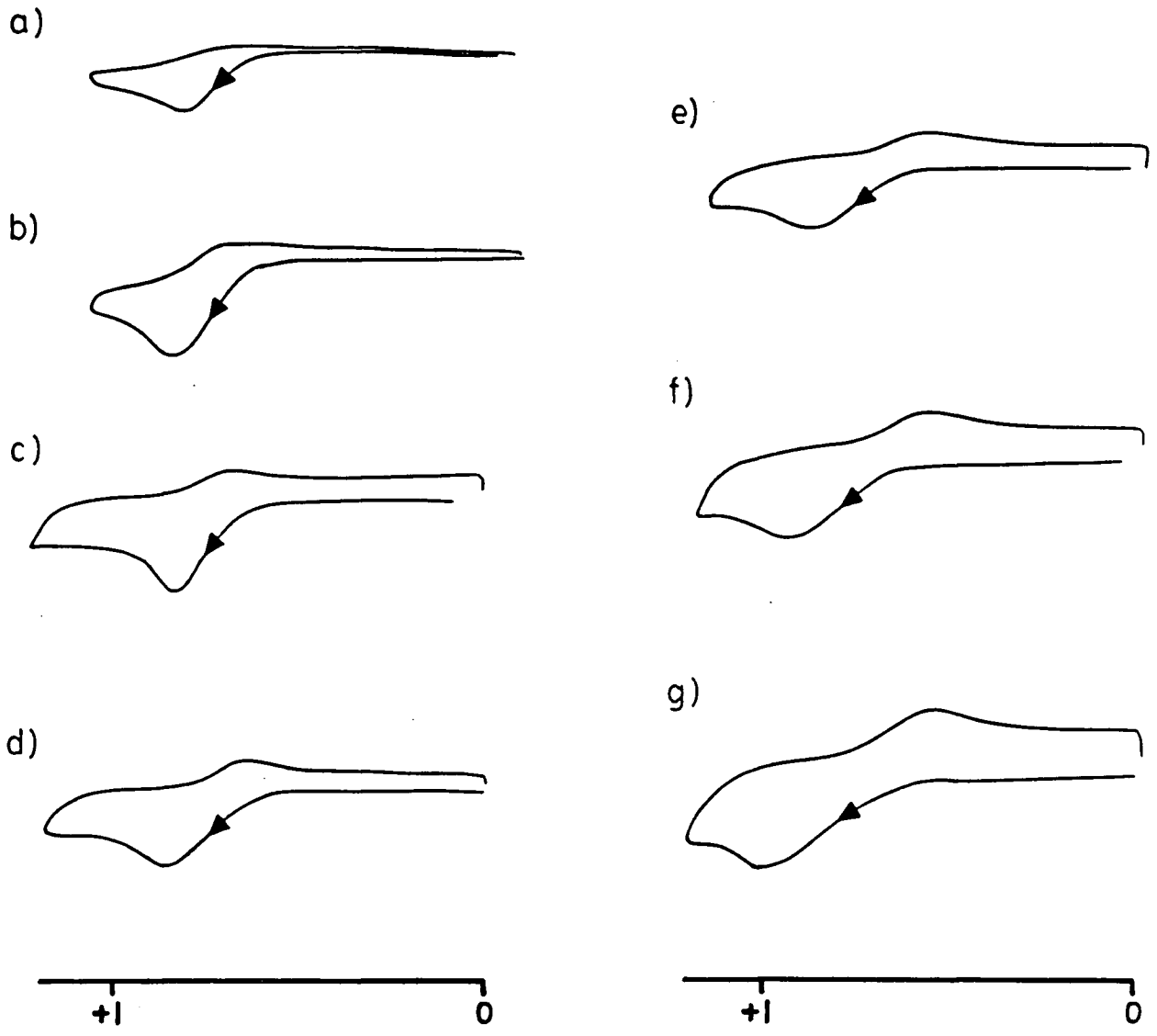

Fig. 4-16. Cyclic voltammograms of the oxidation of $Cp^*W(NO)(H)(CH_2SiMe_3)(PMe_3)$ illustrating the increasingly reversible character as the scan rate is increased. Scan rates (Vs^{-1}): a) 2; b) 10; c) 20; d) 40; e) 80; f) 120; g) 160.

the CV begins to show some reversible character (Fig. 4-16). A plot of the corrected peak cathodic current divided by the corrected peak anodic current (i_{pc}/i_{pa}) versus the scan rate[61] gives a straight line with a positive slop (Fig. 4-17). This indicates[62] that a reversible charge transfer (E_r) followed by an irreversible chemical change (C_i) is occurring (i.e. an E_rC_i mechanism). Treatment of $Cp^*W(NO)(H)(CH_2SiMe_3)(PMe_3)$ with $AgBF_4$ in C_6D_6 results in the immediate deposition of a silver mirror and a colour change in the solution from yellow to red-brown. Proton NMR, GC and GC-MS analyses of the volatiles after vacuum distillation show the primary product to be Me_4Si (a few other, very minor, silyl methyl peaks were observed in the ^1H NMR spectrum). Infrared analysis of the non-volatile residue taken up in CH_2Cl_2 shows only a very small band in the NO region, indicating the presence of no significant tungsten nitrosyl containing species. Taken together, these results suggest that steps a and b in Scheme 4-IV do occur. Such oxidatively induced eliminations are known, but few examples have been studied in detail.[63] In our system, the 15-electron $[CpW(NO)(PMe_3)]^{\cdot+}$ produced unfortunately is not a precursor for C-H bond activation (i.e. steps c and d of Scheme 4-IV do not occur).

Scanning the CV to negative potentials shows a completely featureless voltammogram out to the solvent limit (~-2 V). This indicates that $Cp^*W(NO)(H)(CH_2SiMe_3)(PMe_3)$ is very difficult to reduce. Treatment of the related, and less electron-rich,

$CpW(NO)(H)[P(OPh)_2(OC_6H_4)]$ with Na/Hg in THF for 48 h does not result in any change in the IR spectrum and presumably no reaction.

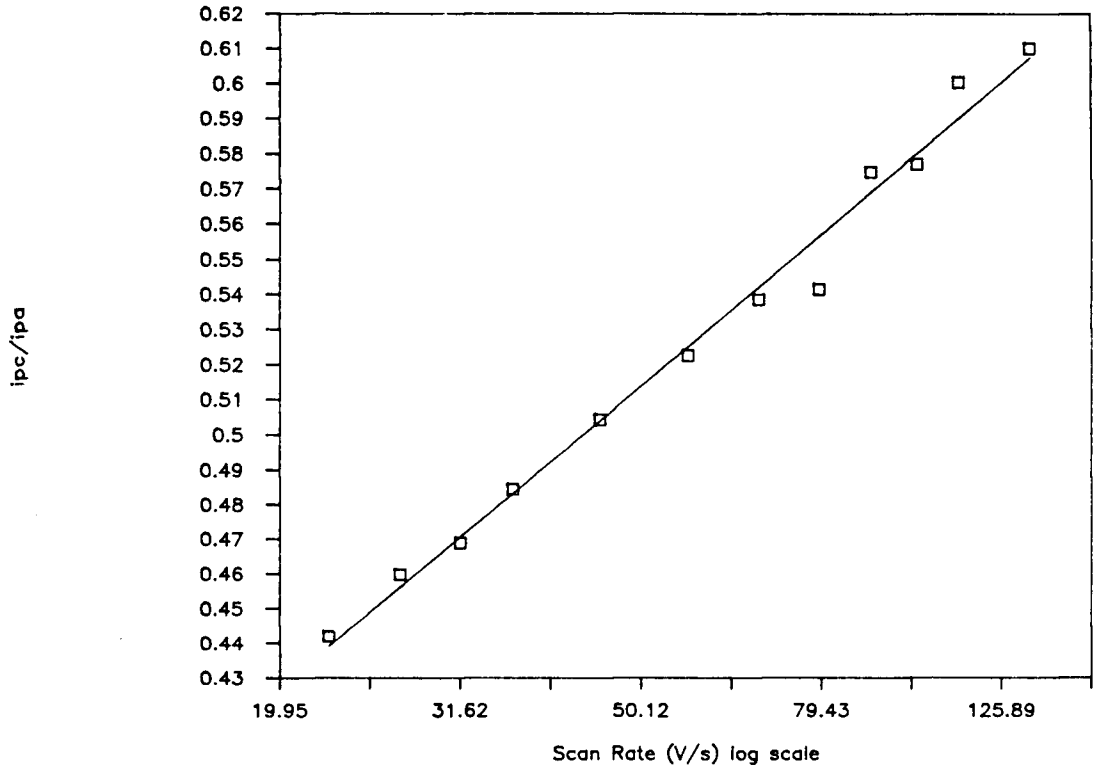

Fig. 4-17. Plot of the corrected cathodic peak current divided by the corrected anodic peak current (i_{pc}/i_{pa}) as a function of the scan rate for the oxidation of $Cp^*W(NO)(H)(CH_2SiMe_3)(PMe_3)$. The positive slope indicates an E_rC_i mechanism.[61,62] (Data points taken from plots similar to Fig. 4-16).

J. Hydrogenolysis of $Cp^*W(NO)(CH_2SiMe_3)_2$ With No L Present.

The work described in this chapter so far stemmed from the attempt to produce $[CpW(NO)H]_2(\mu\text{-}H)_2$ via the hydrogenolysis of $CpW(NO)(CH_2SiMe_3)_2$. Although this was unsuccessful in the unsubstituted cyclopentadienyl system, it was decided to try analogous reactions with the Cp* system. When $C^*pW(NO)(CH_2SiMe_3)_2$ was treated with a low pressure of H_2 (~80 psig--the same pressure used for the alkyl hydride preparations) for ~3 h in hexanes or C_6H_6, complete decomposition was not the result. The ^1H NMR spectrum of the residue in C_6D_6 after removal of the reaction solvent under vacuum showed that a complex mixture of compounds was obtained, along with some decomposition material. Most promisingly, a number of small peaks in the spectrum could be observed that showed $^1H\text{-}^{183}W$ coupling characteristic of metal hydrides. Decoupling experiments indicated that at least 5 hydride containing compounds were present, along with numerous other species. Attempts to chromatograph these reaction mixtures resulted only in trace quantities of non-hydride materials being separated, but in too small quantities and in too impure a form to be identifiable, except for some $Cp^*W(O)_2(CH_2SiMe_3)$. Approximately the same complex mixture was observed when the reaction was done under ~4 atm of H_2 in C_6D_6 in a sealed NMR tube.

However, when the H_2 pressure was increased to ~920 psig (~63 atm), the reaction was complete in under 20 min and a much

less complicated mixture was obtained. When the reaction was done in hexanes, a red-brown precipitate formed along with a very intensely coloured red-brown solution. Removal of the solvent under vacuum and several fractional crystallizations from toluene/hexanes allowed the isolation of two analytically pure compounds in very small quantities. The lower yield and less soluble material was identified as $[Cp^*W(NO)H]_2(\mu\text{-}H)_2$ and the more soluble identified as $[Cp^*W(NO)H](\mu\text{-}H)_2[Cp^*W(NO)(CH_2SiMe_3)]$ (eq. 4-9; step d, Scheme 4-I). These two compounds are very similar in colour and solubility and are difficult to separate. (It should be noted that in the ^1H NMR spectrum (C_6D_6) the $C_5\underline{Me}_5$ resonance of $[Cp^*W(NO)H]_2(\mu\text{-}H)_2$ is coincidental (even at 400-MHz) with one of

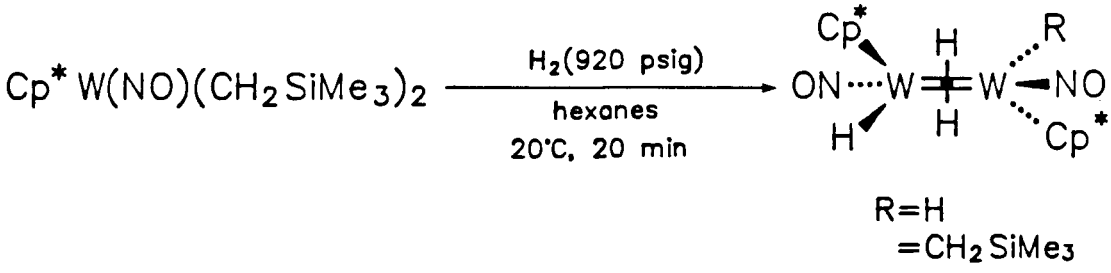

(4-9)

the $C_5\underline{Me}_5$ resonances of $[Cp^*W(NO)H](\mu\text{-}H)_2[Cp^*W(NO)(CH_2SiMe_3)]$, making it difficult to assess when a quality sample of the latter has been obtained.)

K. $[Cp^*W(NO)H]_2(\mu\text{-}H)_2$.

Analytically pure $[Cp^*W(NO)H]_2(\mu\text{-}H)_2$ is a red-brown powder that is slightly soluble in hexanes and Et_2O, somewhat more so in benzene and readily dissolves in more polar solvents such as CH_2Cl_2. The material is easily handled in air as a solid, but forms slightly air-sensitive solutions. It is considerably more soluble in conventional organic solvents than is its perhydro analogue $[CpW(NO)H]_2(\mu\text{-}H)_2$, but complete solubilization in, for example, C_6D_6 is quite slow and the mixture usually must be warmed to obtain a clear solution. Once the solution has become clear, cooling back to room temperature generally does not induce reprecipitation.

The IR spectra of $[Cp^*W(NO)H]_2(\mu\text{-}H)_2$ show some interesting features (Table 4-I). In addition to the expected bands for a terminal hydride ligand, the spectra show two distinct nitrosyl stretching vibrations in both CH_2Cl_2 solution and Nujol mull phases, with this phenomenon being more prominent in the latter. The higher frequency band (1571 cm^{-1} in Nujol mull) is always stronger, but the relative intensities of the bands vary. The reason for these two bands is not clear. Unlike $Cp^*W(NO)(CH_2SiMe_3)_2$, this material is not soluble enough to form a solution in Nujol. Therefore, taken in conjunction with the information gained from the ^1H NMR spectra (see below), the most likely possibility is that the more intense, higher frequency band is due to $[Cp^*W(NO)H]_2(\mu\text{-}H)_2$, while the lower frequency

resonance is due to an isomer with no bridging hydride ligands. The IR spectrum of $[CpW(NO)H]_2(\mu\text{-}H)_2$ shows only one ν_{NO} band at 1599 cm^{-1} (CH_2Cl_2 solution), 33 cm^{-1} above that seen here, reflecting the expected increase in W→NO backbonding upon moving from the Cp to Cp* system.

The ^1H NMR spectrum of $[Cp^*W(NO)H]_2(\mu\text{-}H)_2$ in C_6D_6 (Fig. 4-18) shows that, as for the perhydro compound, two isomers are present. These two isomers show the same AA'XX' (isomer A) and A_2MX (isomer B) hydride patterns as before, but the ratio of A:B is ~9:1 in this case rather than the ~1.4:1 seen for the Cp complexes. The Cp* resonances for the two isomers are coincidental even at 400-MHz, although the hydride peaks are well separated. However, the hydride peaks for isomer B are of such low intensity that the ^{183}W satellites are not discernable and, in fact, the expected high-field hydride signal cannot be found.

Interestingly, unlike in the Cp system, the ratio of isomers A and B changes when a different NMR solvent is used. The ^1H spectrum of $[Cp^*W(NO)H]_2(\mu\text{-}H)_2$ in CD_2Cl_2 shows this ratio to be ~3:1, with A still predominant. The increased proportion of B allowed the observation and integration of the ^{183}W satellites for the two downfield resonances of the A_2MX pattern (i.e. on A_2 and M), as well as permitting the locating of the high-field X part of the spectrum--unfortunately, the signal:noise ratio was not sufficient for the ^{183}W satellites of the latter to be seen. The similarities of the overall patterns and the individual

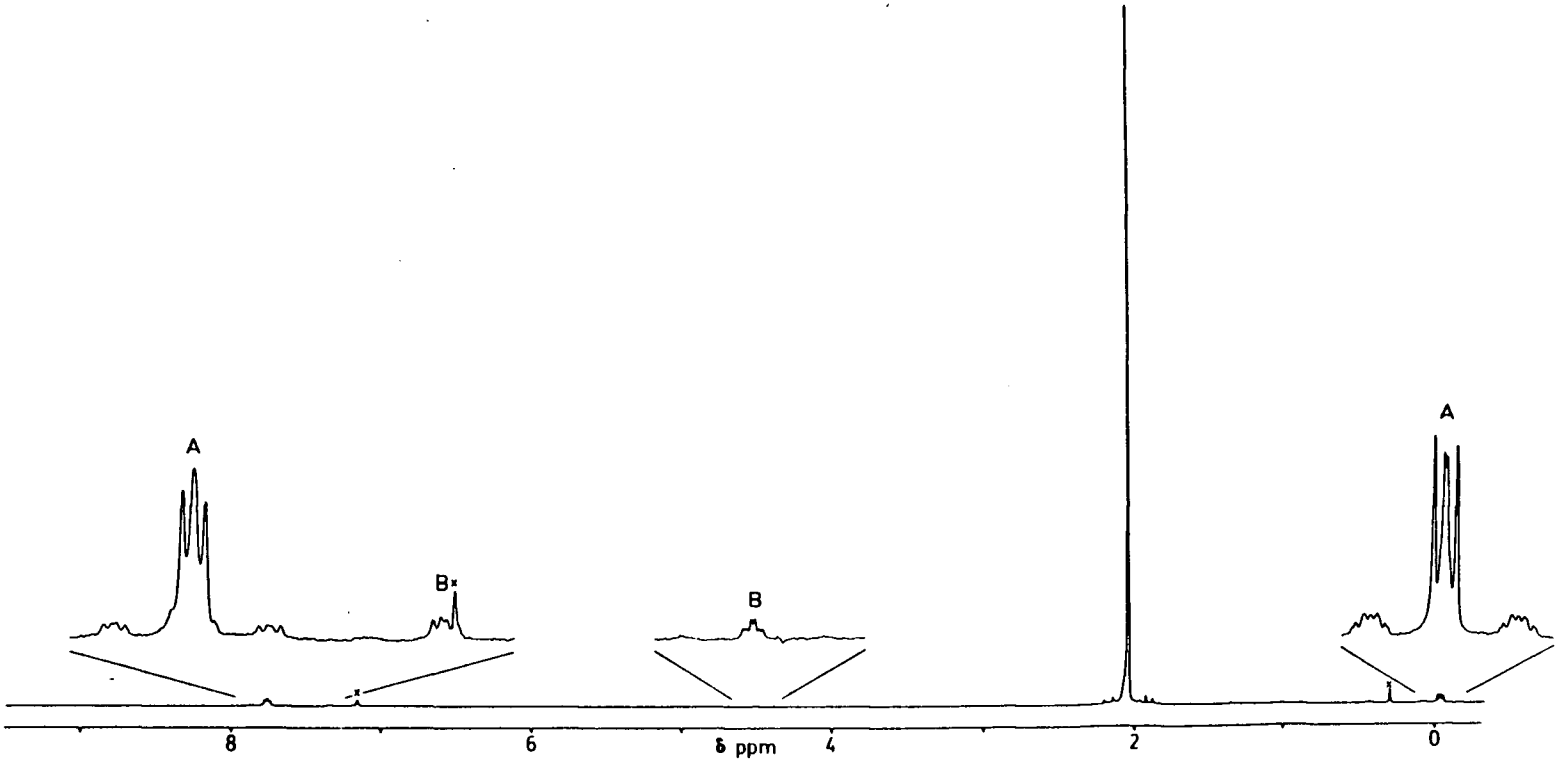

Fig. 4-18. The 400-MHz ^1H NMR of $[Cp^*W(NO)H]_2(\mu\text{-}H)_2$ in C_6D_6. "A" and "B" refer to the hydride resonances for isomers A and B. One of the hydride resonances of isomer B is not visible. See text for complete discussion.

coupling constants in the ^1H NMR spectra of isomers A and B for both the Cp and Cp* systems indicate that these compounds are isostructural (see Fig. 2-4).

The fact that the A:B ratio is solvent dependent for $[Cp^*W(NO)H]_2(\mu\text{-}H)_2$ is suggestive of an equilibrium of the sort given in eq. 4-10. Interconversion between the two isomers must

$$[Cp^*W(NO)H_2]_2 \rightleftharpoons [Cp^*W(NO)H]_2(\mu\text{-}H)_2 \quad \text{isomer A} \qquad [Cp^*W(NO)H]_2(\mu\text{-}H)_2 \quad \text{isomer B} \tag{4-10}$$

be slow on the NMR time scale, however, since fully resolved hydride-hydride coupling is observed, and a minimum lifetime of $\tau \approx 0.2$ s ($J = 1$ Hz--see Table 4-II and chapter 3) may be calculated for one molecule to be in a particular isomeric form. If the interconversion passes through an unbridged $Cp(NO)H_2W{=}WH_2(NO)Cp$ dimer, this must have a transient existence as it is not detectable in the NMR sample. If the isomerization does take place via this complex, then scrambling between bridging and terminal hydrides would be expected. A spin-saturation transfer experiment on the hydride resonances of isomer A in C_6D_6 shows no transfer at all, and, coupled with a T_1 experiment that shows T_1 (H bridging) = 0.98 s, T_1 (H terminal) = 1.42 s and $T_1(Cp^*)$ = 2.49 s for this isomer, suggests that isomerization via an unbridged species is slow and the lifetimes of A and B are at least of the order of seconds. Indeed, this is

what we believe is occurring. The IR spectra, as discussed above, show two nitrosyl stretching bands. However, in CH_2Cl_2 (or CD_2Cl_2) the lower frequency band is of too low an intensity to be due to the less abundant isomer B--it is likely that the ν_{NO} bands for A and B are coincidental. This low frequency NO band is therefore probably due to very short lived $[Cp^*W(NO)H_2]_2$, which can be detected on the fast IR time scale but not on the much slower NMR time scale (see chapter 3).

This hydrogenolysis method of preparing $[Cp^*W(NO)H]_2(\mu\text{-}H)_2$ only produced a very small yield of this material. Therefore, several attempts were made in this Cp* system to try the metathesis method using in chapter 2. Treatment of $Cp^*W(NO)I_2$ with one equivalent of $Na[H_2Al(OCH_2CH_2OCH_3)_2]$ did result in the formation of the intensely green coloured solution expected for $[Cp^*W(NO)I]_2(\mu\text{-}H)_2$ and workup of the mixture in the same manner as described in chapter 2 gave a green microcrystalline product. However, the ^1H NMR spectrum showed this material to contain many products in addition to the iodohydride dimer (δ_{WH} = -0.62 (s), ^{183}W satellites form AA'X pattern, $^1J_{HH'}$ = 4.5, $^1J_{HW}$ = 93.5, $^1J_{H'W}$ = 68.5 Hz--see chapter 2). Attempts to recrystallize this mixture resulted only in decomposition. When the green solution, above, was treated with a second equivalent of $Na[H_2Al(OCH_2CH_2OCH_3)_2]$ in an attempt to prepare $[Cp^*W(NO)H]_2(\mu\text{-}H)_2$, all nitrosyl bands were lost from the IR spectrum and so this route was abandoned.

L. $[Cp^*W(NO)H](\mu\text{-}H)_2[Cp^*W(NO)(CH_2SiMe_3)]$.

The second product obtained from the hydrogenolysis of $Cp^*W(NO)(CH_2SiMe_3)_2$ is the novel dinuclear alkyl hydride complex $[Cp^*W(NO)H](\mu\text{-}H)_2[Cp^*W(NO)(CH_2SiMe_3)]$. This is a bright, red-orange crystalline material that is somewhat more soluble than is $[Cp^*W(NO)H]_2(\mu\text{-}H)_2$. The compound appears to be air-stable as a solid, but forms slightly air-sensitive orange solutions. Its Nujol IR spectrum (Table 4-I) shows a very strong ν_{NO} band at 1559 cm^{-1}, as well as a weak terminal hydride stretch ν_{WH} at 1910 cm^{-1} and weak bands attributable to the CH_2SiMe_3 ligand at 1252 and 1242 cm^{-1}.[20] Unlike the mononuclear species, the electron impact mass spectrum exhibits a $(P\text{-}H)^+$ ion, suggesting that Me_4Si elimination is less favoured.

Single crystals of this dinuclear species suitable for an X-ray crystallograhic analysis were grown from a filtered CD_3NO_2 solution at -25^oC. It is essential that this solution be well-filtered (i.e. through Celite) before crystal growth is attempted, as $[Cp^*W(NO)H](\mu\text{-}H)_2[Cp^*W(NO)(CH_2SiMe_3)]$ shows a great tendency to nucleate about any suspended material.

Two views of the molecular structure of this compound are shown in Fig. 4-19 and selected bond distances, angles and torsion angles are given in Table 4-VIII. As with the other alkyl hydride complexes whose structures have been discussed in this chapter, the WNO linkages in this complex show substantial deviations from linearity, with these being the most bent

(~166°). The two W-N-O angles in the asymmetric molecule do not show any statistically significant difference between them, however. In comparison with the structure of $[CpW(NO)H]_2(\mu\text{-}H)_2$ discussed in chapter 3, these groupings show statistically the same W-N and N-O distances, but the W-N-O angles in the dinuclear alkyl hydride complex are more bent by ~8°, suggesting greater W→NO back donation in the latter compound.[19] This is also reflected in the 42 cm^{-1} (1599 to 1557 cm^{-1} CH_2Cl_2 solution) decrease in the NO stretching frequency. The W-W separation in $[Cp^*W(NO)H](\mu\text{-}H)_2[Cp^*W(NO)(CH_2SiMe_3)]$ is 2.984(1) Å, significantly longer than the 2.9032(8) Å found for

Table 4-VII. Important Interatomic Distances (Å), Angles (deg) and Torsion Angles (deg) for $[Cp^*W(NO)H](\mu\text{-}H)_2[Cp^*W(NO)(CH_2SiMe_3)]$.

W(1)-W(2)	2.984(1)	W(1)-CP(1)	1.997
W(1)-N(1)	1.757(15)	N(1)-O(1)	1.225(17)
W(1)-N(1)-O(1)	165.8(11)	W(2)-W(1)-N(1)	101.7(4)
CP(1)-W(1)-N(1)	101.7	CP(1)-W(1)-W(2)	129.2
W(2)-C(21)	2.227(15)	W(2)-CP(2)	2.057
W(2)-N(2)	1.756(17)	N(2)-O(2)	1.242(19)
W(2)-N(2)-O(2)	166.4(13)	W(1)-W(2)-N(2)	98.2(4)
W(1)-W(2)-C(21)	111.2(6)	N(2)-W(2)-C(21)	93.5(7)
W(2)-C(21)-Si	122.1(9)	CP(2)-W(2)-N(2)	119.0
CP(2)-W(2)-C(21)	108.3	CP(2)-W(2)-W(1)	122.8
CP(1)-W(1)-W(2)-CP(2)	119	CP(1)-W(1)-W(2)-C(21)	111
CP(1)-W(1)-W(2)-N(2)	14	N(1)-W(1)-W(2)-CP(2)	26
N(1)-W(1)-W(2)-C(21)	104	N(1)-W(1)-W(2)-N(2)	159

$[CpW(NO)H]_2(\mu\text{-}H)_2$. In a detailed theoretical study, Sherwood and Hall[64] have shown that the direct metal-metal interaction in the closely related $Os_2(\mu\text{-}H)_2$ bridge of $H_2Os_3(CO)_{10}$ is strengthened by the π-acidity of the carbonyl ligands, which remove metal-metal antibonding electron density. The fact that the W-W distance in the dinuclear alkyl hydride complex is longer than that in $[CpW(NO)H]_2(\mu\text{-}H)_2$ may therefore be the result of the former having more electron density to contribute into metal-metal antibonding orbitals. Like the other alkyl hydride compounds reported in this chapter, this molecule is sterically crowded, particularly around W(2). This is reflected in the distortion of the angle about C(21) from the tetrahedral angle to 122.1(9)°. Unfortunately, the hydride hydrogens could not be located by the X-ray analysis, but the position of the terminal hydride can be approximately assigned by the observation of a "hole" in the coordination sphere of W(1). However, the structure does not give any suggestion whatsoever of further hydride ligands. It is the ^1H NMR spectrum that is definitive as to the existence of the three hydride atoms.

There are extremely few dinuclear hydridoalkyl complexes in the literature. The most extensively studied of these is $(OC)_4(H)OsOs(CH_3)(CO)_4$ by Norton,[33a] but this is not strictly analogous because the alkyl and hydride ligands are on different metal centres. More closely related are the $[Cp_2Zr(R)]_2(\mu\text{-}H)_2$ complexes that appear to be dimers as solids and partially

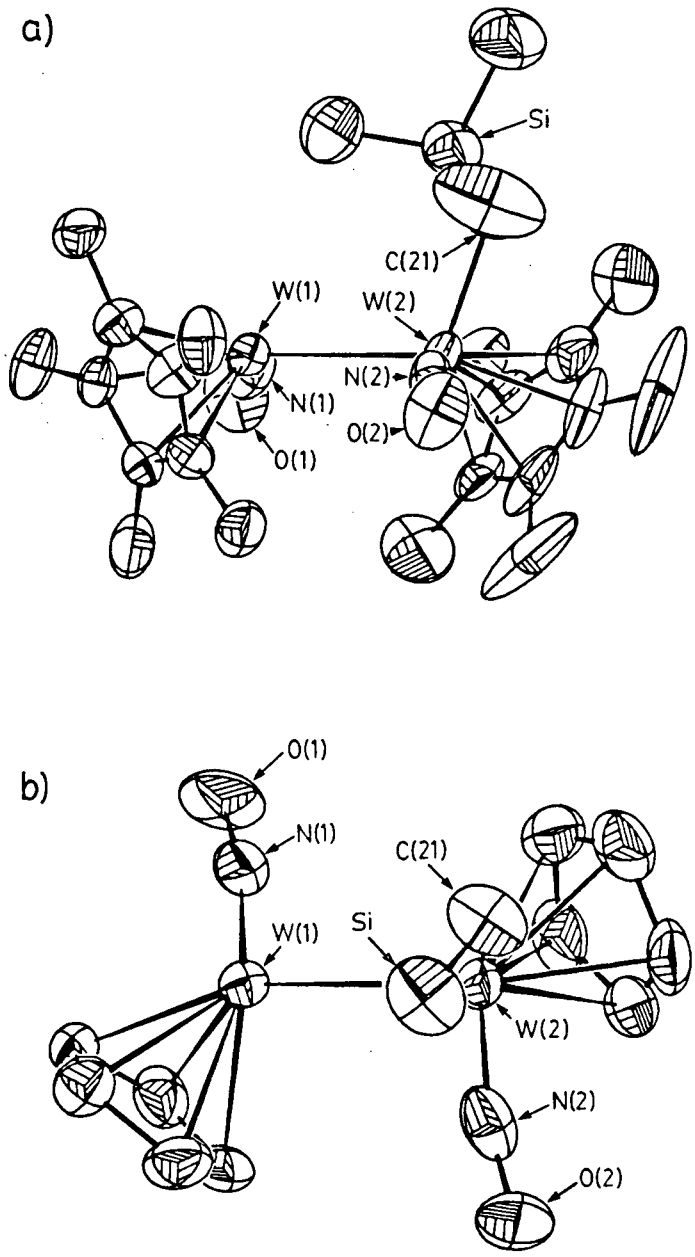

Fig. 4-19. SNOOPI diagrams of the molecular structure of $[Cp^*W(NO)H](\mu\text{-}H)_2[Cp^*W(NO)(CH_2SiMe_3)]$. a) View showing a side view of the molecule; b) View with all Cp^* and $SiMe_3$ methyl groups deleted.

dissociated in solution.[65] The most closely related species[66] reported to date is the structurally characterized $[Cp_2W(\mu\text{-}H)_2Pt(PEt_3)(Ph)]^+$,[67] which was briefly discussed in chapter 3. This seems to be the only other complex known that contains a M$\overset{H}{=\!=}$M-R grouping, although an (R$_3$Si)Pt$\overset{H}{=\!=}$Pt(SiR$_3$) arrangement has been observed.[66d] Very little is known about dinuclear reductive elimination[66a] and so the study of such potential reactivity on $[Cp^*W(NO)H](\mu\text{-}H)_2[Cp^*W(NO)(CH_2SiMe_3)]$, especially in comparison with the related mononuclear compounds, is of great future interest.

M. The ^{1}H NMR Spectrum of $[Cp^*W(NO)H](\mu\text{-}H)_2[Cp^*W(NO)(CH_2SiMe_3)]$.

There is a great deal of information to be gained from a detailed analysis of the ^{1}H NMR spectrum of this complex. This spectrum is definitive as to the constitution of the compound, and provides much information as to its geometry. The full spectrum (in CD_3NO_2) is shown in Fig. 4-20. Nitromethane-d_3 was chosen as the solvent because the residual proton resonances of many of the more common NMR solvents (C_6D_6, $CDCl_3$, CD_2Cl_2, $(CD_3)_2CO$) overlap with peaks due to the complex.[5] Interestingly enough, the compound is much less soluble in CD_3NO_2 than it is in C_6D_6.[68] The first thing that is apparent about the spectrum (both in CD_3NO_2 and C_6D_6), is that there is only one isomer, in contrast to the $[Cp'W(NO)H]_2(\mu\text{-}H)_2$ (Cp'=Cp or Cp*)

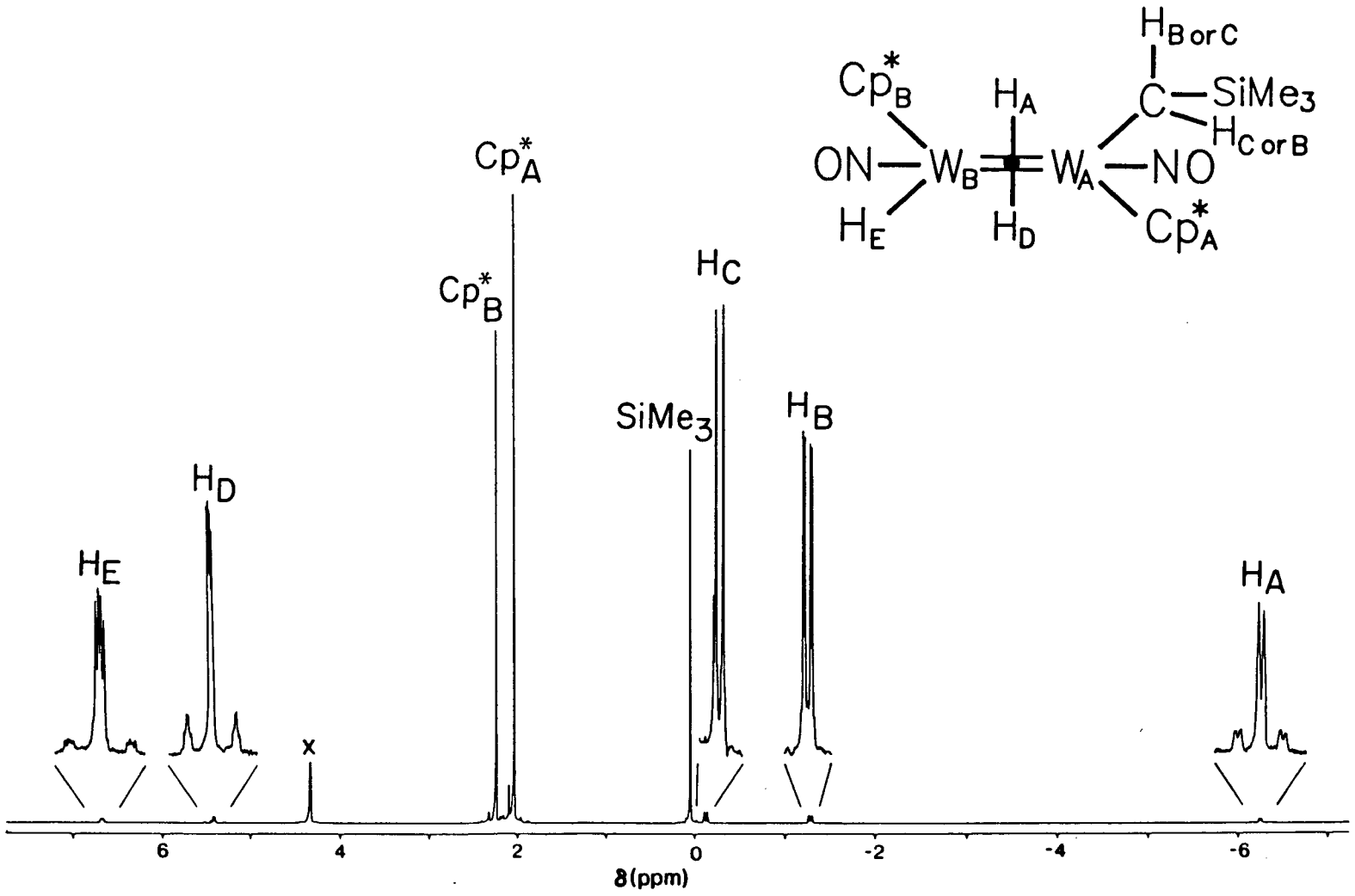

Fig. 4-20. The 400-MHz ^{1}H NMR spectrum of $[Cp^*W(NO)H](\mu\text{-}H)_2[Cp^*W(NO)(CH_2SiMe_3)]$ in CD_3NO_2. See text for a full discussion and assignment.

complexes. Additionally, there is no indication of any fluxionality from the spectrum, as extensive coupling is observed.

Assignment of some aspects of this spectrum are straightforward. Sharp singlets are observed for the two inequivalent Cp* ligands and the $SiMe_3$ group. One of the Cp* resonances (Cp^*_B) is exactly coincident (in C_6D_6) with the analogous peak in the spectrum of $[Cp^*W(NO)H]_2(\mu\text{-}H)_2$ and so is assigned to the ligand on W_B. The two protons on the α-C of the $C\underline{H}_2SiMe_3$ group are assigned (H_B and H_C) on the basis of the geminal coupling constant ($^2J_{BC}$ = 12.5 Hz) and the observation of ^{183}W satellites with small coupling constants similar to those seen for the related mononuclear tungsten compounds.

The assignment of the three remaining sets of resonances is considerably more involved. Protons A through E (Fig. 4-20) form a first-order, five spin system and decoupling at each of their positions established the coupling constants given in Table 4-II. In addition to the geminal coupling noted above, <u>one</u> of the α-C protons (H_B) is coupled to one of the hydride nuclei, H_A, while the three hydride nuclei show full coupling amongst themselves. Expansions of the resonances due to H_A, H_D and H_E are shown in Fig. 4-21, along with their simulations (excluding the ^{183}W satellites).[69] The assignments of H_A, H_D and H_E as hydride ligands are based on the observation of large, one-bond ^{183}W couplings, typical for this class of compound (see chapters 2 and

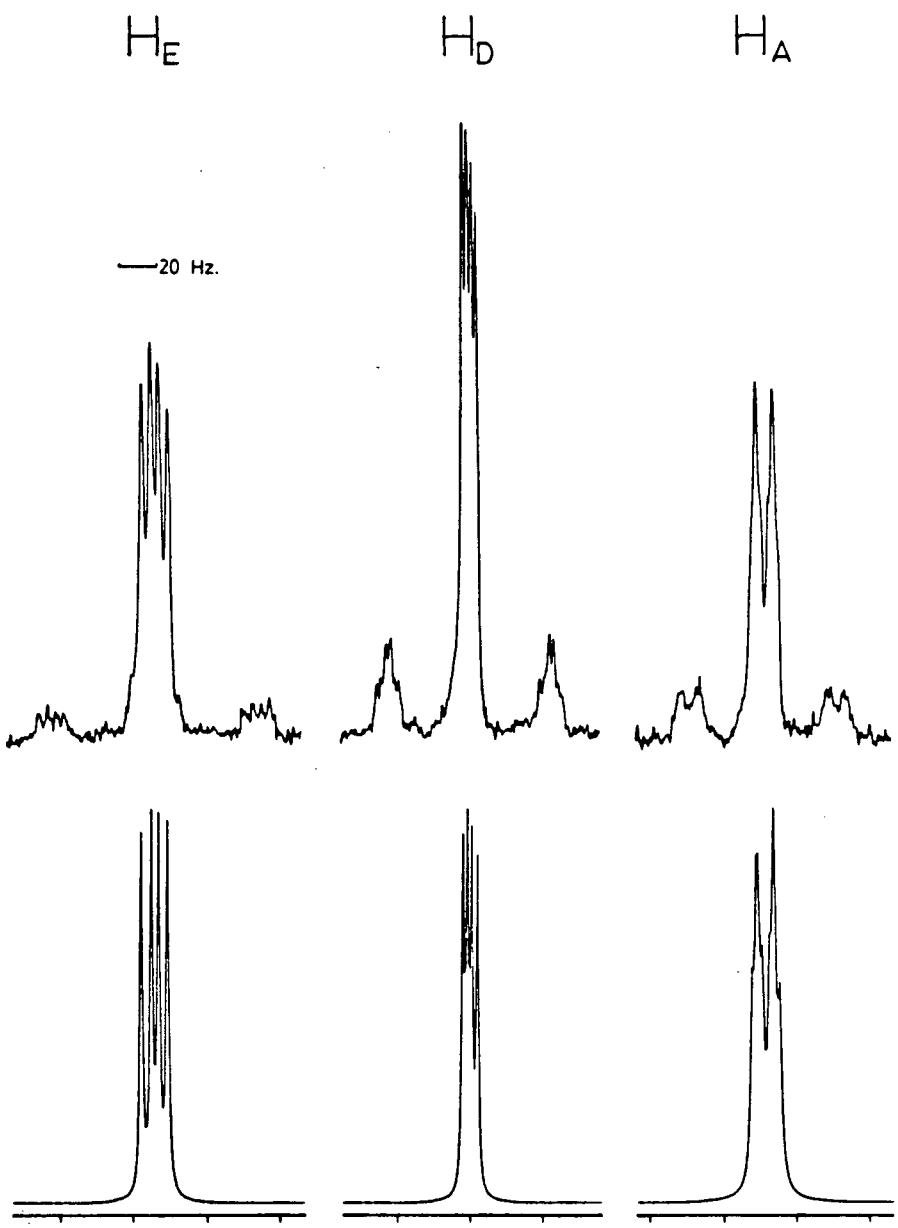

Fig. 4-21. Expansions of the experimental (top) and simulated (bottom) peaks of the hydride regions of the 400-MHz ^1H NMR spectrum of $[Cp^*W(NO)H](\mu\text{-}H)_2[Cp^*W(NO)(CH_2SiMe_3)]$. See Fig. 4-20 for assignment of the resonances.

3). Furthermore, integration of the ^{183}W satellites shows that the H_A and H_D resonances are due to bridging hydride ligands (satellites ~25% of the area), while the H_E peaks are due to a terminal hydride (satellites ~15% of the area). This is given additional support by the detection of shoulders on the main resonance of H_E that can be assigned to two-bond ^{183}W coupling. A particularly noteworthy aspect of these assignments is the relative chemical shifts exhibited by the bridging and terminal hydride ligands (Fig. 4-20). The bridging hydride peaks are far apart, separated by almost 12 ppm, while the terminal hydride resonance is separated from that of a bridging ligand by less than 1.3 ppm. This further illustrates the point made in chapter 3 that the chemical shift of a hydride ligand is not a good indicator of its bridging or terminal nature. Indeed, in this complex, the intermingling of the peaks due to protons A-E would have made assignment impossible without benefit of the ^{183}W satellites.

Assignment of H_A and H_D to the positions shown in Fig. 4-20 can be made on the basis of a series of NOE difference experiments. Enhancements of the peaks due to H_A and H_E were observed upon irradiation of the H_D resonance, while only H_D enhancement occurred when either the H_A or H_E peak was irradiated. This shows that H_D is close (in space) to both H_A and H_E, and is therefore oriented on the side of the W-W axis towards H_E, while H_A and H_E are well separated. Such an

assignment further permits the assignment of "cis" and "trans" $^2J_{HH}$ coupling in an $HW(\mu\text{-}H)_2W$ system. It can be seen that "trans" coupling (~9.0 Hz here) is greater than "cis" coupling (5.0 Hz here) and the assignment given in Tables 2-II and 4-II for the $[Cp'W(NO)H]_2(\mu\text{-}H)_2$ (Cp'=Cp or Cp*) complexes reflect this. It is interesting to note that in all the systems explored in this work, $^2J_{HH}$ couplings are greater than $^1J_{HH}$ couplings across the  interaction--these small $^1J_{HH}$ values are probably manifestations of the H-H antibonding interactions that calculations have shown to be present.[64]

No nuclear Overhauser effect was observed for the peaks due to H_B or H_C when any of the three hydride resonances were irradiated. Consequently, individual assignment of H_B and H_C peaks is not possible.

Because this molecule contains two inequivalent tungsten centres, couplings of the hydride ligands to a ^{183}W nucleus when the latter is situated at one metal centre should be different than when it is at the other. Since ^{183}W satellites due to the isotopomer containing two ^{183}W nuclei cannot be seen, the satellites observed are the result of the superimposition of the spectrum of the isotopomer with ^{183}W at W_A ($^{183}W_A$) on the spectrum of the isotopomer with ^{183}W at W_B ($^{183}W_B$). Inspection of Fig. 4-21 shows that the tungsten-183 satellites for the bridging hydride peaks are not simply smaller versions of the main resonance, but are more complex, indicating that couplings

to $^{183}W_A$ and $^{183}W_B$ are similar, but not identical. Since H_E is a terminal hydride, its one-bond ^{183}W satellites (coupling to $^{183}W_B$) have the same pattern as the main peaks, while the two-bond coupling to $^{183}W_A$ is much smaller and observed as shoulders. Careful analysis of the satellites of the H_A and H_D peaks allow the calculation of individual $^1J_{HW}$ values, but at this stage, they cannot be assigned individually to $^{183}W_A$ and $^{183}W_B$.

The solution to this problem lies with a series of spin tickling experiments.[70] A simplified splitting diagram for three of the spins (H_E, H_A and W_B, where W_B is a ^{183}W nucleus) in the $[Cp^*W(NO)H](\mu\text{-}H)_2[Cp^*W(NO)(CH_2SiMe_3)]$ molecule is shown in Fig. 4-22. Underneath the diagram are denoted the spin states +1/2 or -1/2) of the individual nuclei that give rise to the splittings. The situation is depicted for when all three J's are positive. (The diagram would be the same if all the signs were reversed, with the + and - signs interchanged). This splitting diagram only applies, of course, to the ^{183}W satellites and not to the main resonances of the spectrum. As may be seen, the upfield, or right, half of each set of both the H_E and H_A signals arise from W_B being in the same, +1/2, spin state. Therefore, irradiation of the right half of the H_A spectrum should result in perturbation of the right half of the H_E spectrum, and vice versa. This depends on the sign of $^1J_{H(A)-W(B)}$ being the same as $^1J_{H(E)-W(B)}$ --if these signs were opposite, then irradiation of the right half of the H_A spectrum would give an effect on the

left half of the H_E spectrum. The same result can be obtained from an analysis of the analogous H_D-H_A-W_B splitting diagram, as well, of course, as other possible combinations. This allows us to determine not only the relative signs of the couplings of H_A, H_D and H_E to W_A and W_B but also to determine which $^1J_{HW}$ coupling constant pertains to which tungsten centre. The relevant parts of the spectra from the experiments to make these determinations are shown in Fig. 4-23.

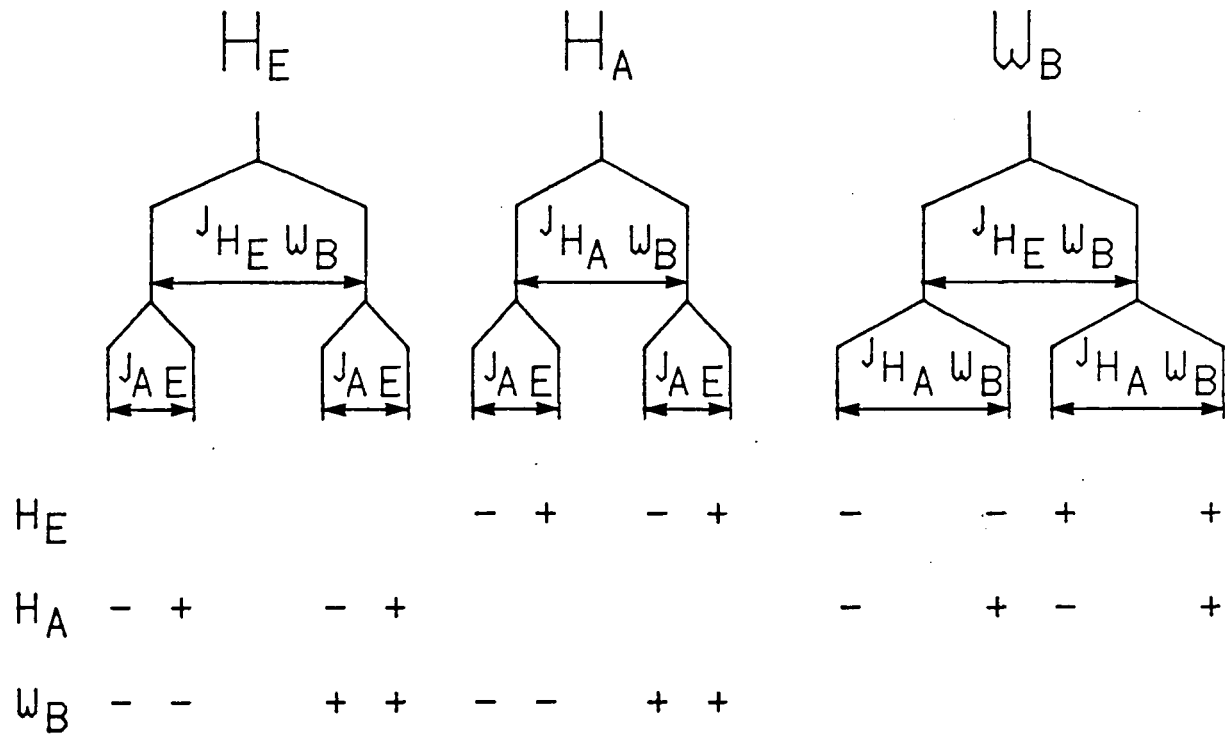

Fig. 4-22. A simplified splitting diagram for couplings exhibited by [Cp*W(NO)H](μ-H)$_2$[Cp*W(NO)(CH_2SiMe_3)]. Spin states (+1/2 or-1/2) are denoted by + or - signs. The situation depicted is that with all three J's positive. See text for a complete discussion.

Figure 4-23a shows expansions of the ^{183}W satellites of the resonances due to H_E, H_D and H_A. The top part of the figure shows the experimental spectra. Directly underneath are shown the superposition of the simulated spectra[69] due to coupling to $^{183}W_A$ (thick line) and $^{183}W_B$ (thin line). (Of course, the assignments shown in Fig. 4-23 are based on the spin tickling experiments about to be described.) The bottom part of Fig. 4-23a shows the simulated spectra after those due to the individual isotopomers have been summed.[71] It is these summed simulations that are to be compared with the experimental spectra and, as can be seen, the agreement is excellent. The other parts of Fig. 4-23 are organized in the same fashion.

Fig.4-23. (next two pages) Spin tickling experiment on $[Cp^*W(NO)H](\mu\text{-}H)_2[Cp^*W(NO)(CH_2SiMe_3)]$. In each section, the top is the experimental spectrum, the middle are the simulations of the individual ^{183}W satellites superimposed upon each other: thick line--coupling to $^{183}W_A$; thin line--coupling to $^{183}W_B$, bottom shows the sum of the simulated tungsten-183 satellites. a) spectrum with no irradiation; b), c) and d) tickling irradiation centred at the arrow. See text for complete discussion.

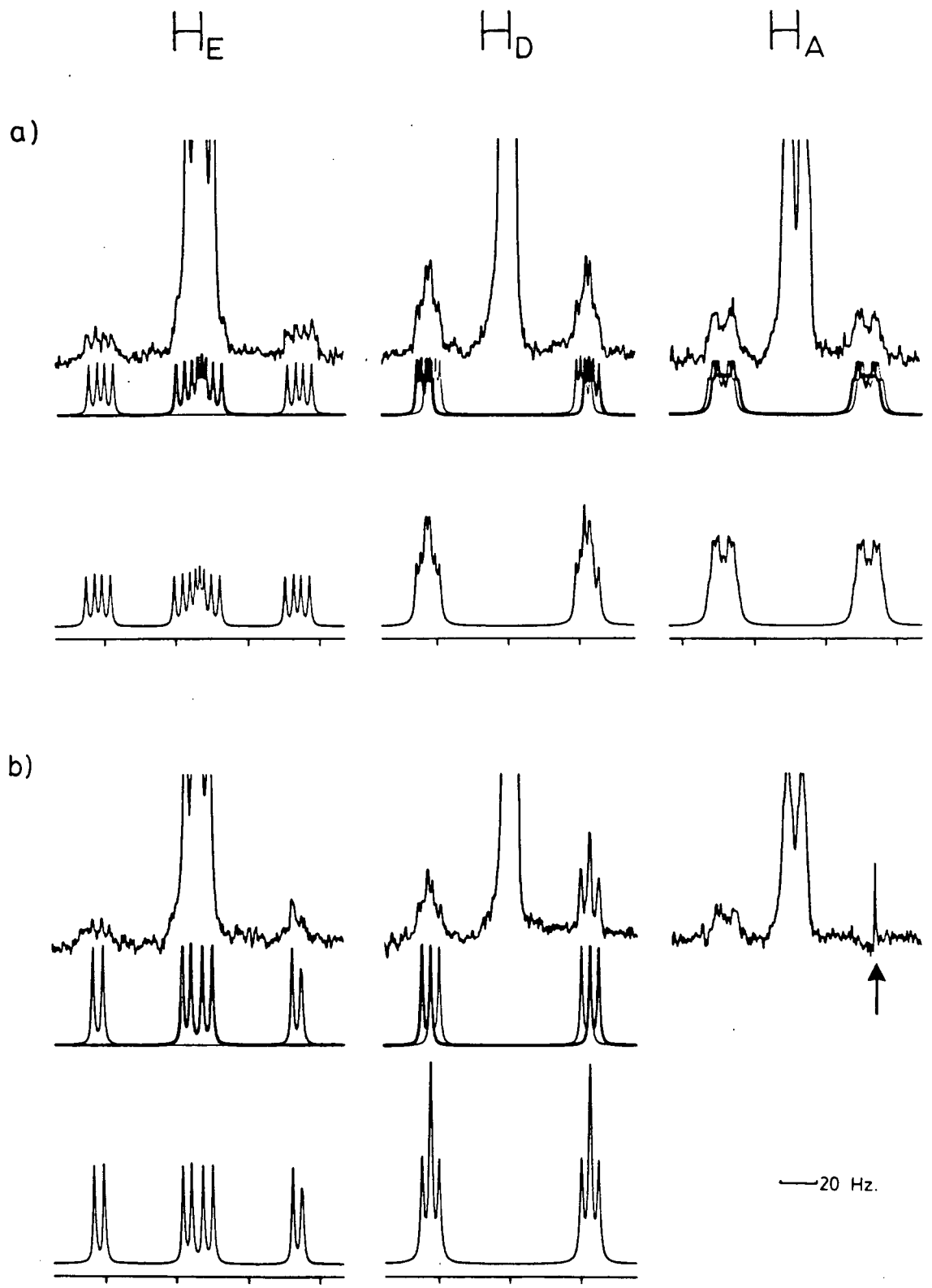
H_E
H_D
H_A
a)
b)
20 Hz.

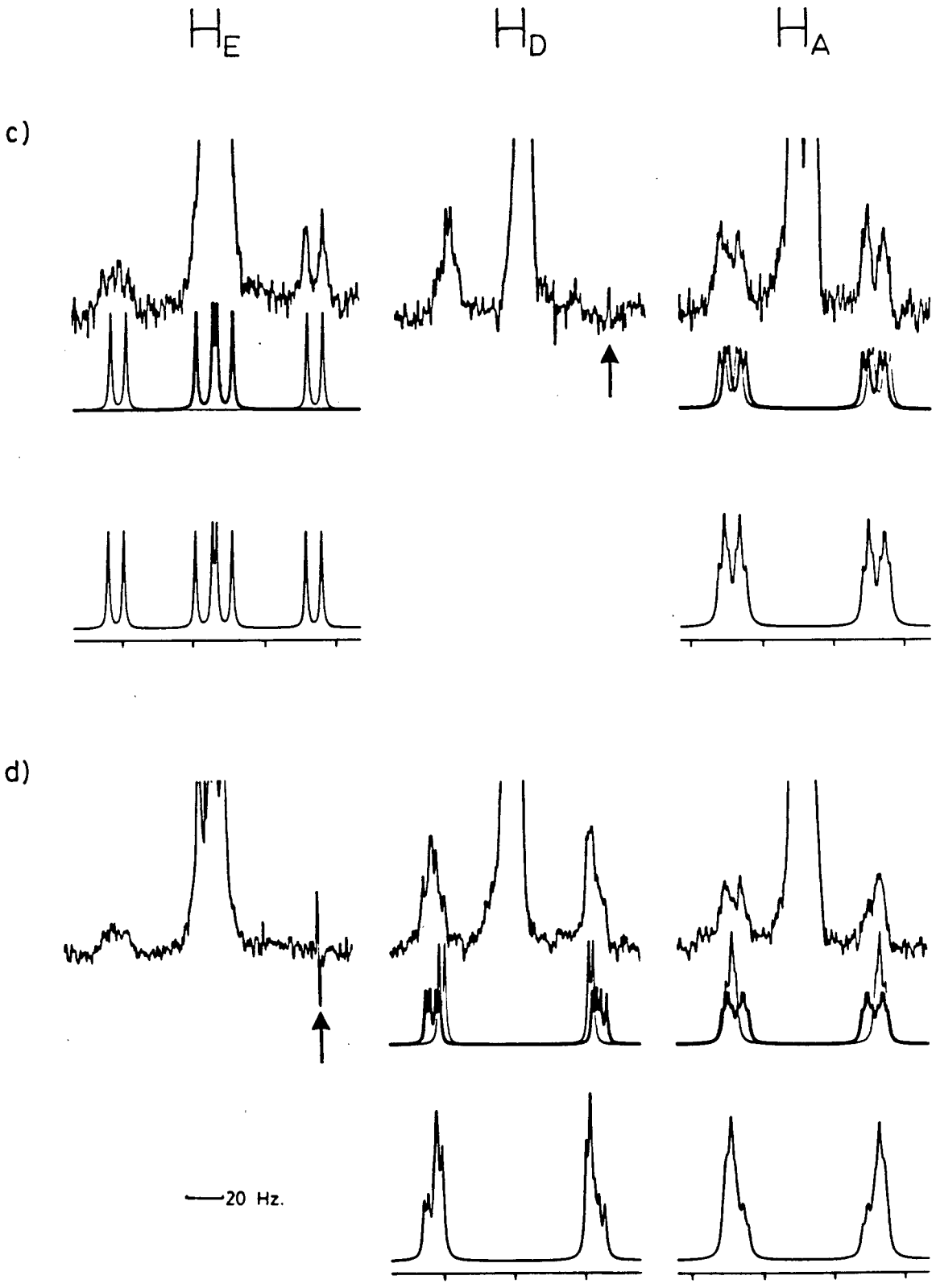
H_E
H_D
H_A
c)
d)
20 Hz.

Normally, when a spin tickling experiment is performed (in a conventional organic, ^{1}H only system), low irradiation powers are used in order to avoid saturating the entire resonance.[70] However, in our system, because the $^{1}J_{HW}$'s are large, the +1/2 spin state of W_B can be irradiated with full, conventional decoupling power without saturating the -1/2 spin state, allowing these tickling experiments to be interpreted similarly to conventional decoupling experiments.

Fig. 4-23b shows the results of the irradiation of the upfield half of the ^{183}W satellites of the H_A spectrum (irradiation centred at the arrow). Because the satellites due to W_A and W_B overlap so much, no differentiation between the couplings to these metal nuclei is possible here. However, as can be seen, this irradiation results in the decoupling of the upfield halves of the satellites for both H_E and H_D. Comparison of these upfield sections with the right half of the simulations given beneath shows excellent agreement. (The simulation computer programme does not allow for decoupling of only half of a doublet and so the left half of the simulations should be ignored.) Fig. 4-23c, showing irradiation of the right half of the H_D spectrum, yields the same result.

It is the irradiation illustrated in Fig. 4-23d that allows the assignment of the one-bond J_{HW} couplings to the individual W_A and W_B centres. Irradiating the upfield half of the one-bond ^{183}W satellites in the H_E spectrum results only in the decoupling

of the part of the tungsten satellites in the H_D and H_E spectra that come from the $^{183}W_B$ isotopomer. Consequently, the observed upfield halves of the H_D and H_E tungsten satellites are the superpositions of the spectra due to the unperturbed $^{183}W_A$ isotopomer and the perturbed $^{183}W_B$ isotopomer, as the simulations illustrate. What is found is that $^{183}W_B$ couples to H_A and H_D with almost the same coupling constant (83.5 and 84.0 Hz respectively), while $^{183}W_A$ exhibit markedly different couplings to these nuclei (78.5 and 93.5 Hz respectively). Why this should be so is not clear.

As noted above, these spin tickling experiments allow the assignments of the relative signs of the hydride-metal coupling constants. In all these experiments, irradiation of the upfield half of a tungsten-183 satellite results in the perturbation of the upfield half of the other satellites. This means that $^1J_{H(A)-W(A)}$, $^1J_{H(A)-W(B)}$, $^1J_{H(D)-W(A)}$, $^1J_{H(D)-W(B)}$ and $^1J_{H(E)-W(B)}$ all have the same sign. In another experiment, the right half of the ^{183}W satellites due to the two-bond coupling of H_E with W_A, which appears as a shoulder on the main resonance (Fig. 4-23a), is irradiated. Because this coupling is small (11.5 Hz), a low irradiation power must be used. Although the results are not as unambiguous as for the other spin ticklings, the spectra appear to again show perturbations of the upfield halves of the H_D and H_E spectra. This means that $^2J_{H(E)-W(A)}$ has the same sign as the other couplings just mentioned. The overall

result of this is that, for this system, the signs of the one-bond bridging and terminal hydride $^{1}H-^{183}W$ couplings and the two-bond terminal hydride $^{1}H-^{183}W$ couplings are the same. This confirms the assumption on this point made for the analyses carried out in chapter 3.

The spin-tickling experiments reported here do not allow assignment of the absolute sign of the hydride-tungsten-183 coupling constants. For this to be done, access to the ^{183}W spectrum of the complex is necessary and appropriate equipment is not available. This is unfortunate, as $[Cp^*W(NO)H](\mu-H)_2[Cp^*W(NO)(CH_2SiMe_3)]$ is uniquely suited to do this. Geminal coupling such as that exhibited by the $W-CH_BH_C-Si$ fragment is always negative[72] and so it would be a relatively simple matter to determine the other absolute signs for the coupled nuclei in this system. Few absolute sign determinations have been made for transition metal-hydride coupling[73] and, as far as we can tell, no such determinations have been made in tungsten systems.

N. The Pathway for the Formation of $[Cp^*W(NO)H]_2(\mu-H)_2$ and $[Cp^*W(NO)H](\mu-H)_2[Cp^*W(NO)(CH_2SiMe_3)]$.

The concurrent formation of these two compounds is intriguing and a likely pathway leading to this occurrence is given in Scheme 4-V. Experiments done in connection with the preparations of the mononuclear alkyl hydride complexes discussed

in section C of this chapter provide support for steps a and b in Scheme 4-V, leading to the formation of the 16-electron W*RH fragment. It is reasonable to expect that this can undergo further hydrogenolysis via steps c and d to form W^*H_2, the other fragment necessary to give the observed compounds. It is expected that step c, like step a, would be relatively slow compared to the rapid reductive eliminations of b and d. These fragments would then undergo the coupling reactions e, f and g to give the dinuclear molecules, $RW^*(\mu\text{-}H)_2W^*R$, $HW^*(\mu\text{-}H)_2W^*R$ and $HW^*(\mu\text{-}H)_2W^*H$, of which the latter two are the isolated products. In the reaction done at 920 psig, the mixed product, $HW^*(\mu\text{-}H)_2W^*R$ is the major product and no $RW^*(\mu\text{-}H)_2W^*R$ compound was observed. This means that there must be a delicate balance between the rate of step c and that of step f in order for some, but not all, of the W*RH to be converted to the W^*H_2 necessary for the formation of both isolatd dinuclear materials. It also means that W^*H_2 is an efficient trap of the W*RH fragment, and that the dinuclear alkyl hydride complex isolated is analogous to the mononuclear species discussed earlier, with the phosphine replaced by the $Cp^*W(NO)H_2$ grouping. It is also interesting to note that the product distribution between $HW^*(\mu\text{-}H)_2W^*R$ and $HW^*(\mu\text{-}H)_2W^*H$ is not noticeably altered when the reaction time (at 920 psig H_2 and in hexanes) is changed from 20 min to 24 h. This suggests that $HW(\mu\text{-}H)_2W^*R$ does not dissociate into mononuclear fragments in solution, nor is it liable to hydrogenation as a dinuclear

species.

Scheme 4-V

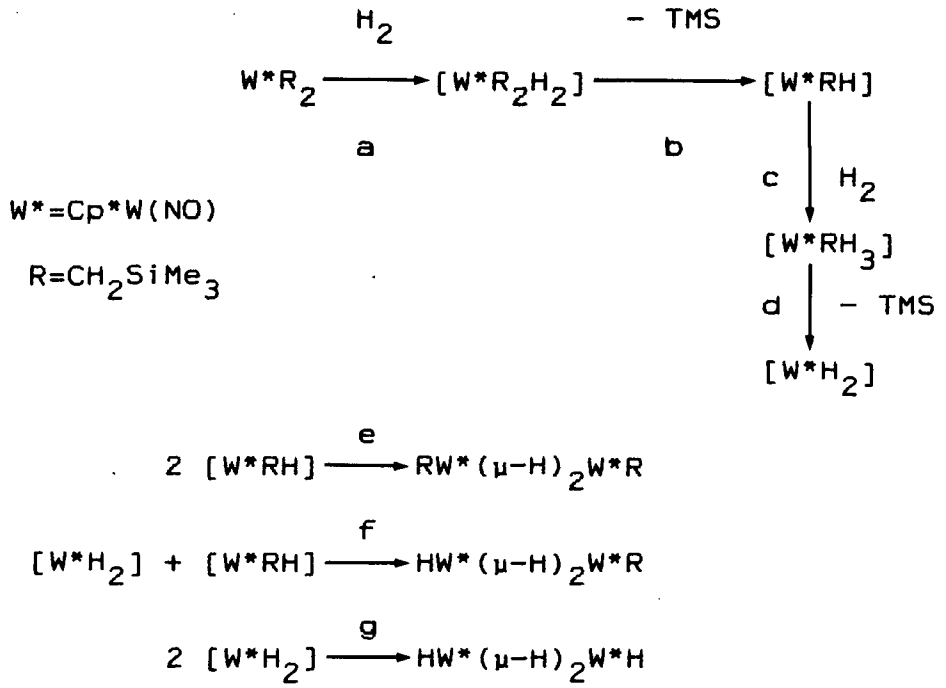

When this hydrogenolysis is done at lower pressures (section J; 80 psig instead of 920 psig), among the numerous peaks present in the ^1H NMR spectrum of the crude reaction mixture are ones attributable to $[Cp^*W(NO)H](\mu\text{-}H)_2[Cp^*W(NO)(CH_2SiMe_3)]$ and $[Cp^*W(NO)H]_2(\mu\text{-}H)_2$. In this system, the proportion of the former to the latter ($HW^*(\mu\text{-}H)_2W^*R$ to $HW^*(\mu\text{-}H)_2W^*H$) appears to be greater than in the higher pressure case. This is as would be expected, since a lower H_2 pressure should not convert as much W*RH to W^*H_2. In addition to the sets of peaks assignable to $HW^*(\mu\text{-}H)_2W^*R$ and $HW^*(\mu\text{-}H)_2W^*H$ is another prominent set similar to

that of $HW^*(\mu\text{-}H)_2W^*R$. Unlike the five spin system (excluding Cp* and $SiMe_3$ resonances) observed for $HW^*(\mu\text{-}H)_2W^*R$ (see section M), this other set consists of a four spin system, lacking a terminal hydride resonance. However, it does include two bridging hydride peaks at $\delta \simeq -7.8$ ($^1J_{HW} \simeq 74$ Hz) and $\simeq 6.0$ ($^1J_{HW} \simeq 96$ Hz) and two geminal $W\text{-}CH_2\text{-}Si$ protons at $\delta \simeq -0.3$ and $\simeq -1.4$ coupled with $^2J_{HH} \simeq 12$ Hz, with the second of these coupled to the first bridging hydride with $^2J_{HH} \simeq 3$ Hz (NMR data in C_6D_6). Comparison of these data with those given in Table 4-II for $[Cp^*W(NO)H](\mu\text{-}H)_2[Cp^*W(NO)(CH_2SiMe_3)]$ in C_6D_6 (the coupling constants are given for the CD_3NO_2 spectrum) shows a remarkable resemblance. In addition, the integrations for the geminal protons in this four spin system is twice that relative to the hydride peaks than is the case for the $HW^*(\mu\text{-}H)_2W^*R$ compound. Taken together, these data strongly suggest the presence of the centrosymmetric dimer

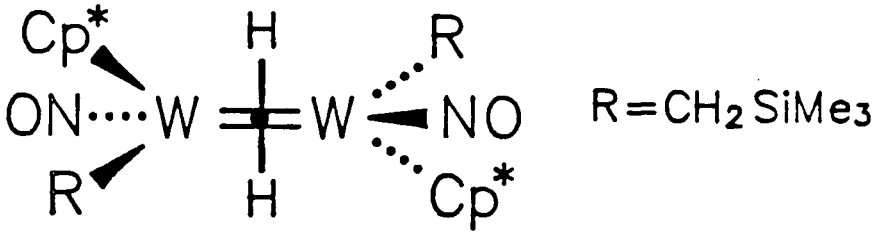

the product of step e in Scheme 4-V. In these lower pressure reactions, this material is present in approximately the same quantity as the $HW^*(\mu\text{-}H)_2W^*R$ complex. Unfortunately, the large number of other products from competing pathways in this reaction mixture has not yet allowed the isolation of this compound.

The fact that $RW^*(\mu\text{-}H)_2W^*R$ production appears to be decreased while formation of $HW^*(\mu\text{-}H)_2WR$ and $HW^*(\mu\text{-}H)_2W^*H$ increases as the H_2 pressure is raised is consistent with the pathway proposed in Scheme 4-V and with step c being somewhat rate determining. Therefore, further increases in H_2 pressure should increase the proportion of $HW^*(\mu\text{-}H)_2W^*H$ formed. However, our apparatus is limited to a pressure of ~1400 psig, and an experiment using 1290 instead of the 920 psig used before did not noticeably alter the ratio of $[Cp^*W(NO)H](\mu\text{-}H)_2$ to $[Cp^*W(NO)H](\mu\text{-}H)_2[Cp^*W(NO)(CH_2SiMe_3)]$. Consequently, it is probable that another, order-of-magnitude, increase in H_2 pressure is necessary to get a substantial improvement in $[Cp^*W(NO)H](\mu\text{-}H)_2$ production, at least in a room temperature, hexanes solvent reaction. It is suggested therefore, that the most promising route to try next to obtain significant amounts of $[Cp'W(NO)H](\mu\text{-}H)_2$ (Cp'=Cp or Cp*), which in some sense has been the motivating force behind most of the work described in this thesis, is to continue high-pressure hydrogenations of the $Cp^*W(NO)R_2$ compounds and investigate the effects of varying the temperature, solvent and R ligand.

O. References and Notes

1. Legzdins, P.; Rettig, S.J.; Sánchez, L.; Bursten, B.E.; Gatter, M.G. J. Am. Chem. Soc. 1985, **107**, 1411-1413.
2. Legzdins, P.; Rettig, S.J.; Sánchez, L. Organometallics 1985, **4**, 1470-1471.
3. Legzdins, P.; Sánchez, L. J. Am. Chem. Soc. 1985, **107**, 5525-5526.
4. Evans, S.V.; Legzdins, P.; Rettig, S.J.; Sánchez, L.; Trotter, J. personal communication.
5. Merck Deuterated Solvents for NMR Catalogue, MSD Isotopes, Montréal, Que, Price List 47C, p 7.
6. Hunter, A.D.; Legzdins, P.; Martin, J.T.; Sánchez, L. Organometallic Syntheses 1986, **3**, 58-69.
7. Threlkel, R.S.; Bercaw, J.E. J. Organometal. Chem. 1977, **136**, 1-5.
8. Osborne, J.H.; Rheingold, A.L.; Trogler, W.C. J. Am. Chem. Soc. 1985, **107**, 6292-6297.
9. Wilmad Cat. #522-PP : 4.97 mm O.D., 2.16 mm I.D.
10. $Cp^*W(CO)_2(NO)$ was first prepared by Malito et al: Malito, J.T.; Shaker R.; Atwood, J.L. J. Chem. Soc., Dalton Trans. 1980, 1253-1258.
11. The preparation of $Cp^*W(CO)_2(NO)$ using C_5Me_5H and $NaNH_2$ is not the optimum route from $W(CO)_6$ and C_5Me_5H. Dryden, N.H.; Phillips, E.C. personal communication.
12. Hoyano, J.K.; Legzdins, P.; Malito, J.T. Inorg. Synth.

1978, **18**, 126-131.

13. $Cp^*W(NO)I_2$ was first prepared by C.R. Nurse of this laboratory (Nurse, C.R. Ph.D. Dissertation, The University of British Columbia, 1983). The preparation described in the present work is superior.

14. Me_3SiCH_2MgCl is sold as a 1.0 M solution in diethyl ether by the Aldrich Chemical Co.

15. Identified by analogy to $CpW(O)_2(CH_2SiMe_3)$.[2]

16. Hunter, A.D.; Legzdins, P. Organometallics 1986, **5**, 1001-1009.

17. Steube, C.; LeSuer, W.M.; Norman, G.R. J. Am. Chem. Soc. 1955, **77**, 3526-3529.

18. Recent results have suggested that the oxo ligand on $CpW(O)_2(CH_2SiMe_3)$ can come from the NO group of the $CpW(NO)(CH_2SiMe_3)_2$ precursor--Phillips, E.C. personal communication.

19. Chisholm, M.H.; Cotton, F.A.; Extine, M.W.; Kelly, R.L. Inorg. Chem. 1979, **18**, 116-119 and references therein.

20. Sánchez, L. personal communication--see also: Pouchert, C.J. "The Aldrich Library of Infrared Spectra", 3rd ed.; Aldrich Chemical Co: Milwaukee, WI, 1981, p 1535.

21. a) Green, M.L.H. Pure Appl. Chem. 1978, **50**, 27-35.

b) Cooper, N.J.; Green, M.L.H.; Mahtab, R. J. Chem. Soc., Dalton Trans. 1979, 1557-1562.

c) Berry, M.; Elmitt, K.; Green, M.L.H. J. Chem. Soc.,

Dalton Trans. 1979, 1950-1958.

22. Fischer, E.O.; Frank, A. Chem. Ber. 1978, 111, 3740-3744.

23. Yang, G.K.; Bergman, R.G. J. Am. Chem. Soc. 1983, **105**, 6500-6501.

24. There was a statistically significant peak in the final difference Fourier map of $CpRe(CO)_2(H)(CH_2C_6H_5)$ that was ascribed to the hydride ligand,[22] but it is not in a chemically reasonable position.

25. Parshall, G.W. "Homogeneous Catalysis"; Wiley: Toronto, 1980.

26. a) Halpern, J. Acc. Chem. Res. 1982, **15**, 238-244.
b) Collman, J.P.; Hegedus, L.S.; Norton, J.R.; Finke, R.G. "Principles and Applications of Organotransition Metal Chemistry"; University Science Books: Mill Valley, CA, 1987, p 100 and references therein.
c) Calhorda, M.J.; Dias, A.R.; Minas de Piedade, M.E.; Salema, M.S.; Martinho Simoes, J.A. Organometallics 1987, **6**, 734-738 and references therein.

27. Halpern, J. Acc. Chem. Res. 1982, **15**, 332-338.

28. Jonas, K.; Wilke, G. Angew. Chem., Int. Ed. Engl. 1969, **8**, 519-520.

29. Michelin, R.A.; Belluco, U.; Ros, R. Inorg. Chim. Acta 1976, **24**, L33-L34.

30. Abis, L.; Santi, R.; Halpern, J. J. Organometal. Chem. 1981, **215**, 263-267.

31. Abis, L.; Sen, A.; Halpern, J. J. Am. Chem. Soc. 1978, **100**, 2915-2916.

32. Milstein, D. Acc. Chem. Res. 1984, **17**, 221-226.

33. a) Norton, J.R. Acc. Chem. Res. 1979, **12**, 139-145.
b) Carter, W.J.; Okrasinski, S.J.; Norton, J.R. Organometallics 1985, **4**, 1376-1386.

34. Orthometallation of aryl phosphine-like ligands was first observed in 1969[55] and is a well-known phenomenon--see Collman, J.P.; Hegedus, L.S.; Norton, J.R.; Finke, R.G. Op. Cit., p 298 and references therein.

35. Bennett, M.A.; Milner, D.L. J. Am. Chem. Soc. 1969, **91**, 6983-6994.

36. Garrou, P.E. Chem. Rev. 1981, **81**, 229-266.

37. Sánchez, L. personal communication.

38. a) Bergman, R.G. Science 1984, **223**, 902-908.
b) Crabtree, R.H. Chem. Rev. 1985, **85**, 245-269.

39. Parshall, G.W. Acc. Chem. Res. 1975, **4**, 113-117.

40. $PMePh_2$: δ_P = -28 ppm (C_6D_6) by comparison with an authentic sample.

41. $OPMePh_2$: δ_H = 1.53 (d, $^2J_{HP}$ = 13.2 Hz), δ_P = 25.0 (C_6D_6) by comparison with an authentic sample; for preparation see ref. 17.

42. Collman, J.P.; Hegedus, L.S.; Norton, J.R.; Finke, R.G. Op. Cit., p 167 and references therein.

43. Legzdins, P.; Martin, D.T.; Nurse, C.R. Inorg. Chem. 1980,

19, 1560-1564 and references therein.

44. C.R. Nurse unsuccessfully attempted to isolate $Cp^*W(CO)(NO)I_2$.[13]

45. Dryden, N.H. personal communication.

46. Jones, R.H.; Einstein, F.W.B. personal communication.

47. $CpW(NO)(CH_2SiMe_3)_2$ also shows Lewis base properties: Brunet, N. personal communication.

48. PMe_3 is one of the most strongly donating of the tertiary phosphines--see Tolman, C.A. Chem. Rev. 1977, **77**, 313-348.

49. A five-fold excess of PMe_3 was used in order to maintain a sufficient concentration of this volatile material in solution--see: Rosenbaum, E.J.; Sandberg, C.R. J. Am. Chem. Soc. 1940, **62**, 1622-1623.

50. Klahn-Oliva, A.H.; Singer, R.D.; Sutton, D. J. Am. Chem. Soc. 1986, **108**, 3107-3108.

51. Aromatic C-C stretching frequencies occur in the 1500-1600 cm^{-1} region of the IR spectrum--see: Morrison, R.T.; Boyd, R.N. "Organic Chemistry", 3rd ed.; Allyn and Bacon: Boston, 1973, p 444.

52. a) Chetcuti, P.E.; Hawthorne, M.F. J. Am. Chem. Soc. 1987, **109**, 942-943.

b) Werner, H.; Höhn, A.; Dziallas, M. Angew. Chem., Int. Ed. Engl. 1986, **25**, 1090-1092.

53. One of the techniques used by investigators of alkane C-H activation to identify and isolate the products of the

reaction has been to treat the resulting alkyl hydride complex with a halogenated hydrocarbon.[38] This usually rapidly results in a much more stable alkyl halocompound that can readily be chromatographed, and thus separated from the original reaction by-products. Unfortunately, this route is unavailable to us, as treatment of the hydridoalkyl complexes described in this chapter with CBr_4 in CH_2Cl_2 gives no significant reaction even after 24 h. As our compounds react with all chromatography media tried (Florisil, Silica gel, Sephadex, Alumina(I) and (III)) except Alumina(V) (which is not useful for effecting significant separations), we have had no success in employing chromatography to isolate small amounts of a desired product from a very dirty reaction.

54. $Cp^*W(NO)(PMe_3)_2$ was identified by its chemical shift and characteristic large $^1J_{PW}$ in the $^{31}P\{^1H\}$ NMR spectrum by comparison with an authentic sample (see Experimental Section).

55. It should be noted that $Cp^*W(NO)(PMe_3)_2$ appears to possess a very electron-rich metal, with $\nu_{NO}(CH_2Cl_2)$ = 1498 cm^{-1}, one of the lowest frequencies known for a (presumably) linear NO group.[56] Like other $CpM(NO)L_2$ compounds,[16] this complex is very air-sensitive and cannot tolerate even brief exposure to air. Interestingly, upon exposure to air, no colour change from its initial orange is observed, however

the elemental analysis then is no longer correct for the bis-L compound and the ν_{NO} disappears in its IR spectrum.

56. Christensen, N.J.; Hunter, A.D.; Legzdins, P.; Sánchez, L. Inorg. Chem. in press.

57. Suslick, K.S. Adv. Organometal. Chem. 1986, **25**, 73-119.

58. Richter-Addo, G.B. personal communication.

59. Richter-Addo, G.B.; Wassink, B. personal communication.

60. Legzdins, P.; Malito, J.T. Inorg. Chem. 1975, **14**, 1875.

61. Mabbott, G.A. J. Chem. Ed. 1983, **60**, 687-702 and references therein.

62. Theoretical curves have been developed for plots of i_{pc}/i_{pa} as a function of scan rate for a number of situations involving various combinations of charge transfer coupled with differing types of chemical reactions. The shape of the plot is characteristic of a particular combination of charge transfer and chemical reaction--see: Nicholson, R.S.; Shain, I. Anal. Chem. 1964, **36**, 706-723.

63. a) Kochi, J.K. "Organometallic Mechanisms and Catalysis"; Academic Press: New York, 1978, pp 282-285, 350-354.
b) Thermally, photolytically and oxidatively induced elimination of benzene has been observed from $Cp_2W(Ph)(H)$. No detailed mechanistic studies have been carried out on the thermal or photochemical reactions.[21] The electrochemically induced reaction has been shown to occur not by simple reductive elimination, but rather to involve

solvent molecules--see: Klingler, R.J.; Huffman, J.C.; Kochi, J.K. J. Am. Chem. Soc. 1980, 102, 208-216.

64. Sherwood, D.E.,Jr.; Hall, M.B. Inorg. Chem. 1982, 21, 3458-3464.

65. a) Gell, K.J.; Schwartz, J. J. Am. Chem. Soc. 1978, 100, 3246-3248.

b) Jordan, R.F.; Bajgur, C.S.; Dasher, W.E.; Rheingold, A.E. Organometallics 1987, 6, 1041-1051.

66. Other known hydridoalkyl complexes with at least one bridging hydride ligand include:

a) $Cp^*(Ph)Ir(\mu\text{-}H)(\mu\text{-}\eta^1\text{-}\eta^3\text{-allyl})IrCp^*$--McGhee, W.D.; Bergman, R.G. J. Am. Chem. Soc. 1986, **108**, 5621-5622.

b) $\{[(Et_3P)_2PtPh](\mu\text{-}H)[PtH(PEt_3)_2]\}^+$--Bracher, G.; Gove, D.M.; Venanzi, L.M.; Bachechi, F.; Mura, P.; Zambonelli, L. Angew. Chem., Int. Ed. Engl. 1978, 17, 778-779.

c) $[Cp_2HW(\mu\text{-}H)(PEt_3)_2(Ph)]^{+(67)}$

d) $\{Pt[P(C_6H_{11})_3](SiEt_3)\}_2(\mu\text{-}H)_2$--Ciriano, M.; Green, M; Howard, J.A.; Proud, J.; Spencer, J.L.; Stone, F.G.A.; Tsipis, C.A. J. Chem. Soc., Dalton Trans. 1978, 801-808.

67. Albinati, A.; Naegeli, R.; Togni, A.; Venanzi, L.M. Organometallics 1983, **2**, 926-928.

68. CH_3NO_2, although a quite polar solvent, is known to have poor donating properties--see: Mayer, U.; Gutmann, V.; Gerger, W. Monatsh. Chem. 1975, **106**, 1235-1257 and references therein.

69. Schatz, P.F. RACOON 2.0; Moore, J.W. director; Project SERAPHIM; Eastern Michigan University: Ypsilanti, MI, 48197, 1984.

70. Becker, E.D. "High Resolution NMR", 2nd ed.; Academic: Toronto, 1980, pp 213-216.

71. The computer program to sum RACOON 2.0 files was written by Neil H. Dryden of our research group.

72. Becker, H.D. Op. Cit., p 95.

73. $^{1}J_{HPt}$ has been found to be positive in trans-[$(Et_3P)_2PtHCl$] --see: McFarlane, W. J. Chem. Soc., Chem. Commun. 1967, 772-773.

74. Becker, E.D. Op Cit., pp 102-104 and references therein.

Spectral Appendix - Selected IR and NMR spectra

[CpW(NO)I]2(μ-H)2 in CH2Cl2 - 0.2 mm cell

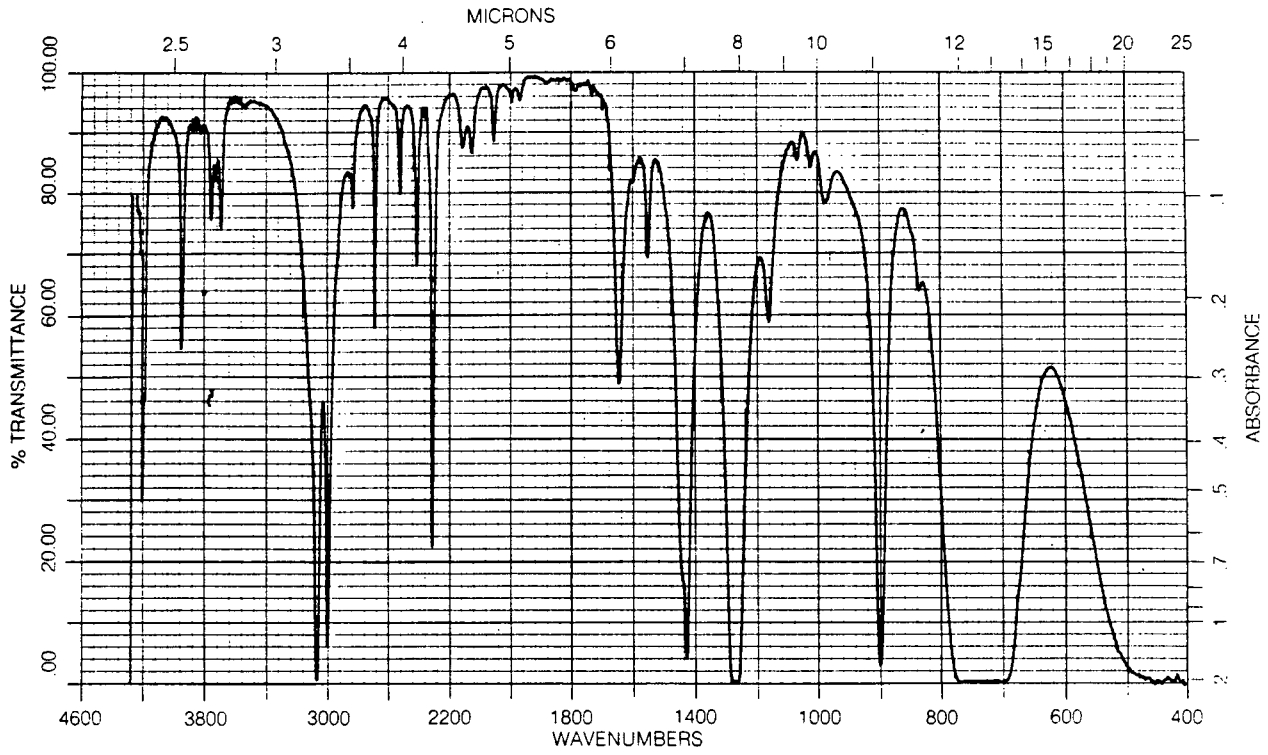

[CpW(NO)H]2(μ-H)2 in CH2Cl2 - 0.2 mm cell

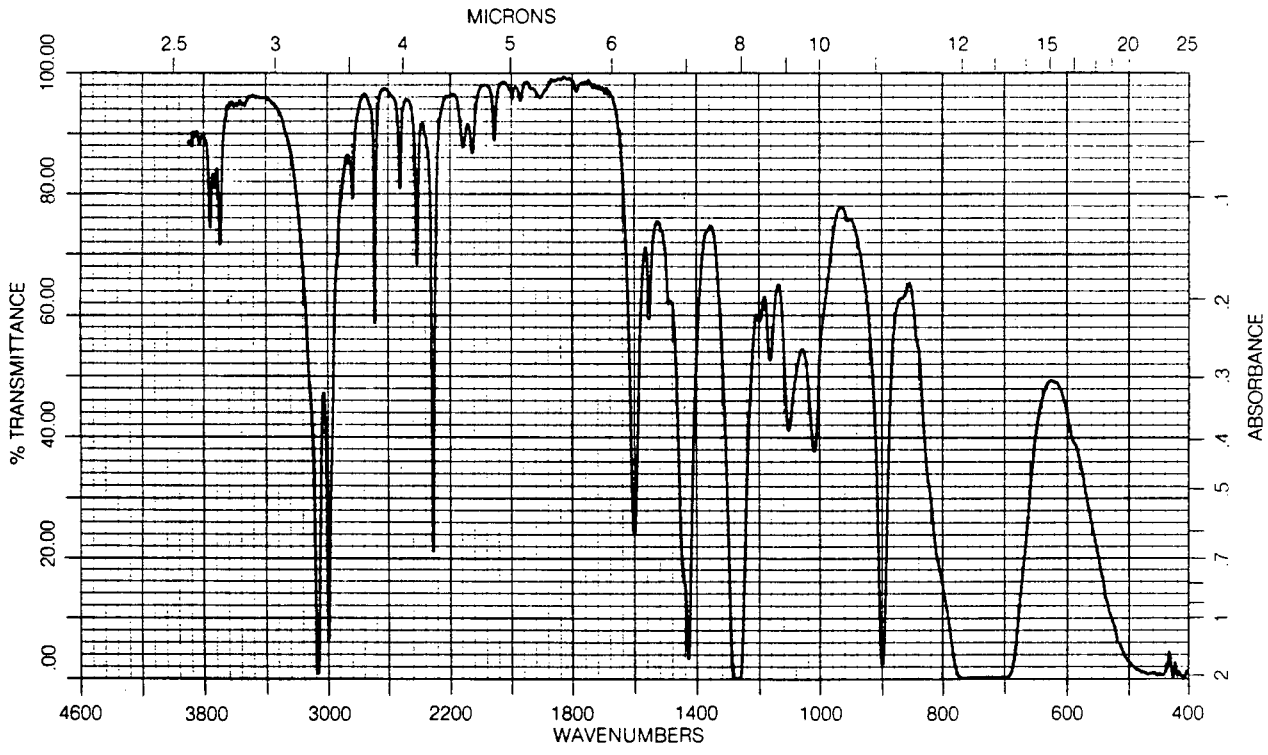

[CpW(NO)(P(OPh)3)]2(μ-H)2 in CH2C12 - 0.2 mm cell

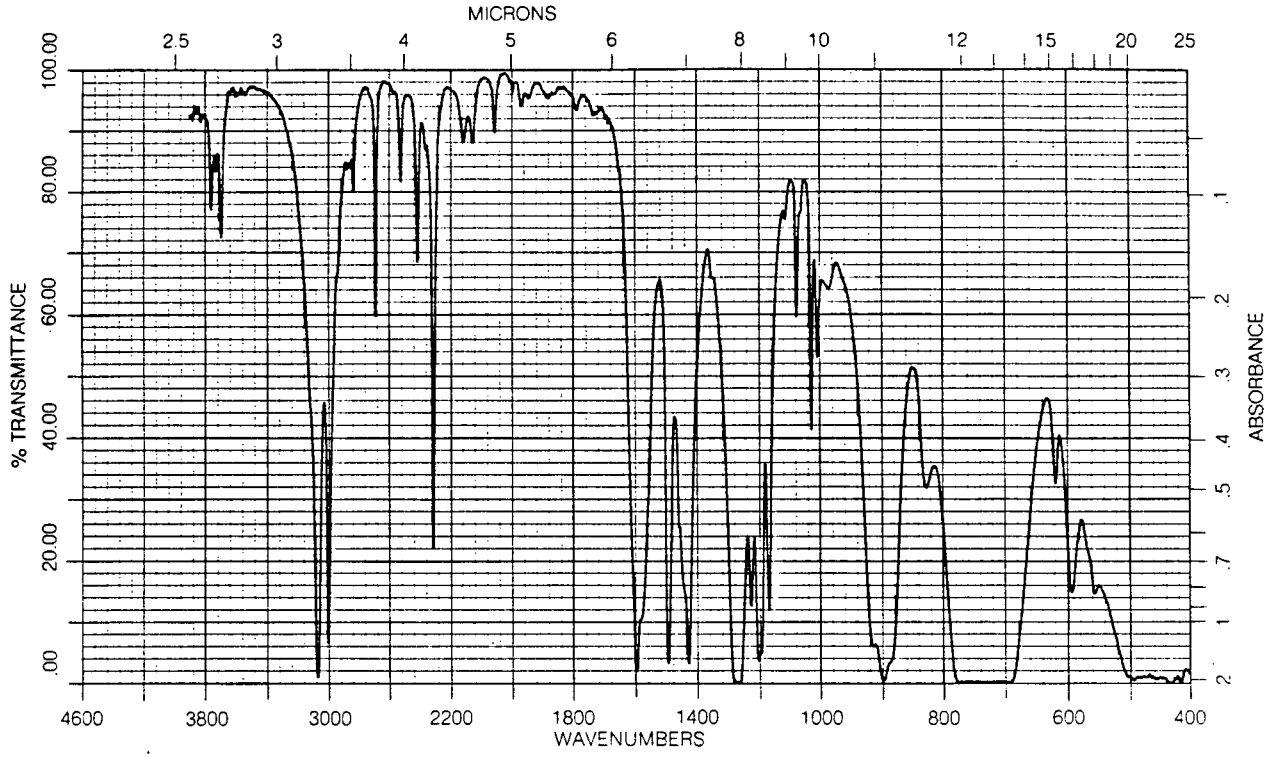

CpW(NO)H2[P(OPh)3] in CH2C12 - 0.2 mm cell

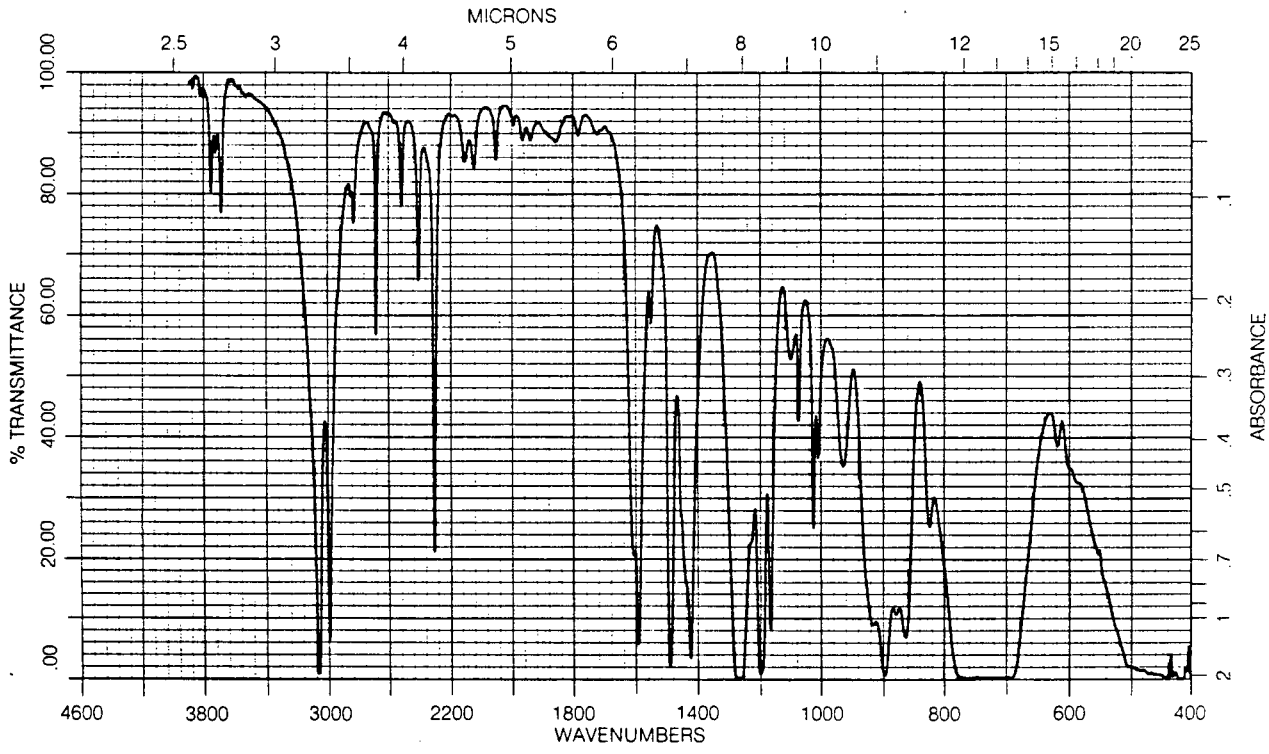

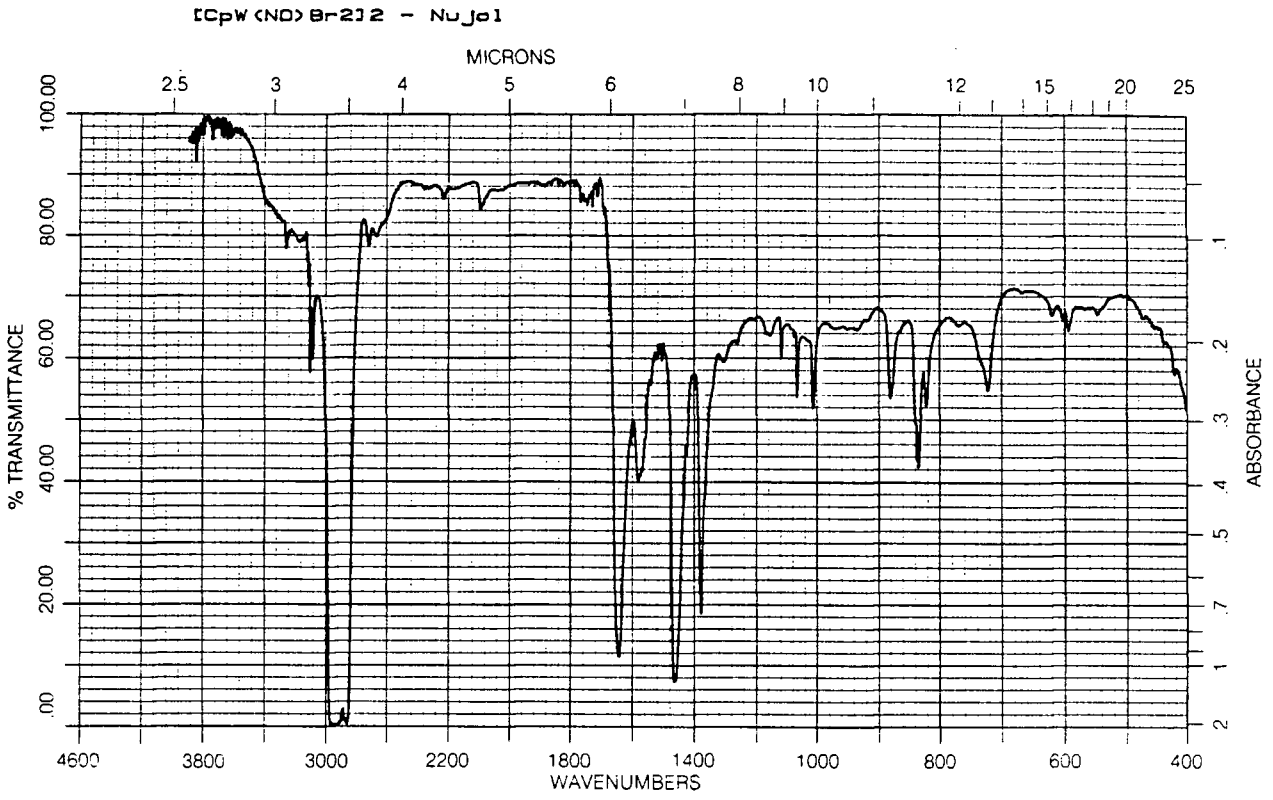
[CpW(NO)Br2]2 - Nujol
MICRONS
2.5
3
4
5
6
8
10
12
15
20
25
100.00
80.00
60.00
40.00
20.00
.00
% TRANSMITTANCE
4600
3800
3000
2200
1800
1400
1000
800
600
400
WAVENUMBERS
.1
.2
.3
.4
.5
.7
1
2
ABSORBANCE

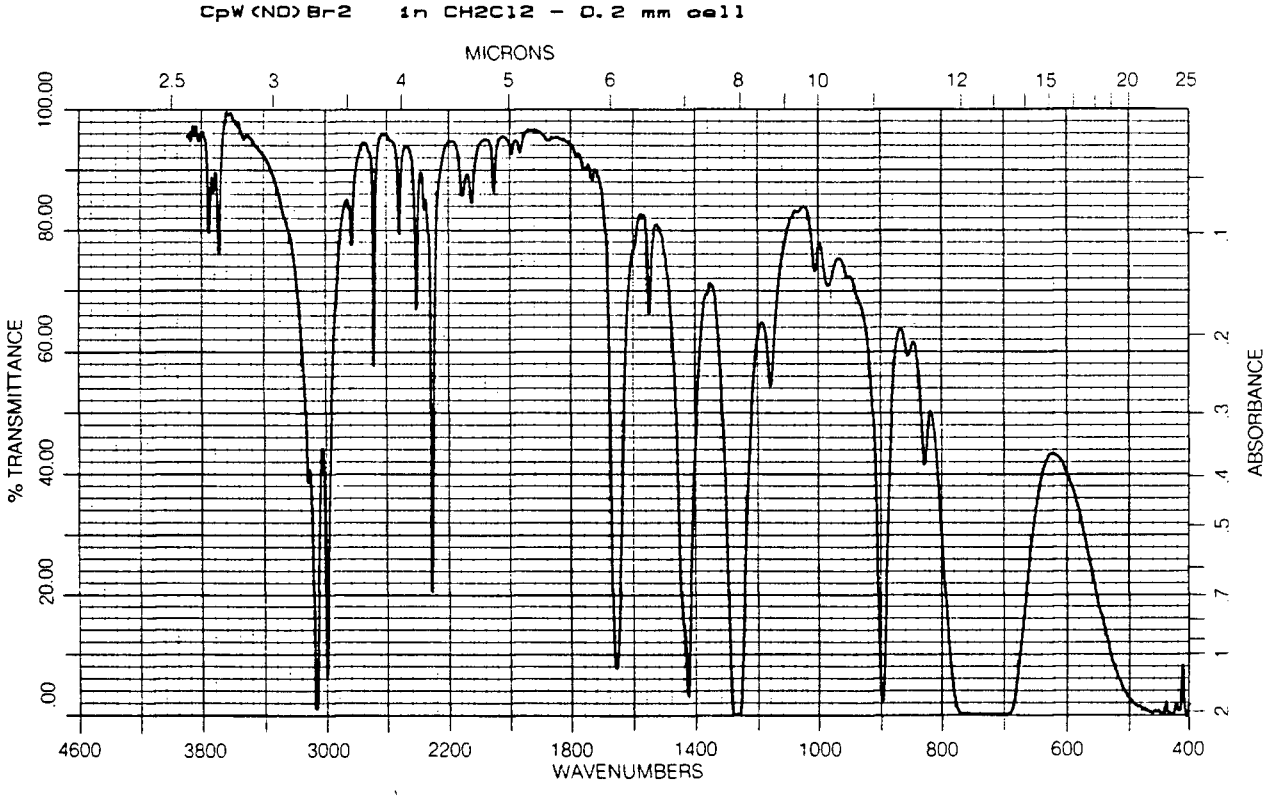
CpW(NO)Br2 in CH2Cl2 - 0.2 mm cell
MICRONS
2.5
3
4
5
6
8
10
12
15
20
25
100.00
80.00
60.00
40.00
20.00
.00
% TRANSMITTANCE
4600
3800
3000
2200
1800
1400
1000
800
600
400
WAVENUMBERS
.1
.2
.3
.4
.5
.7
1
2
ABSORBANCE

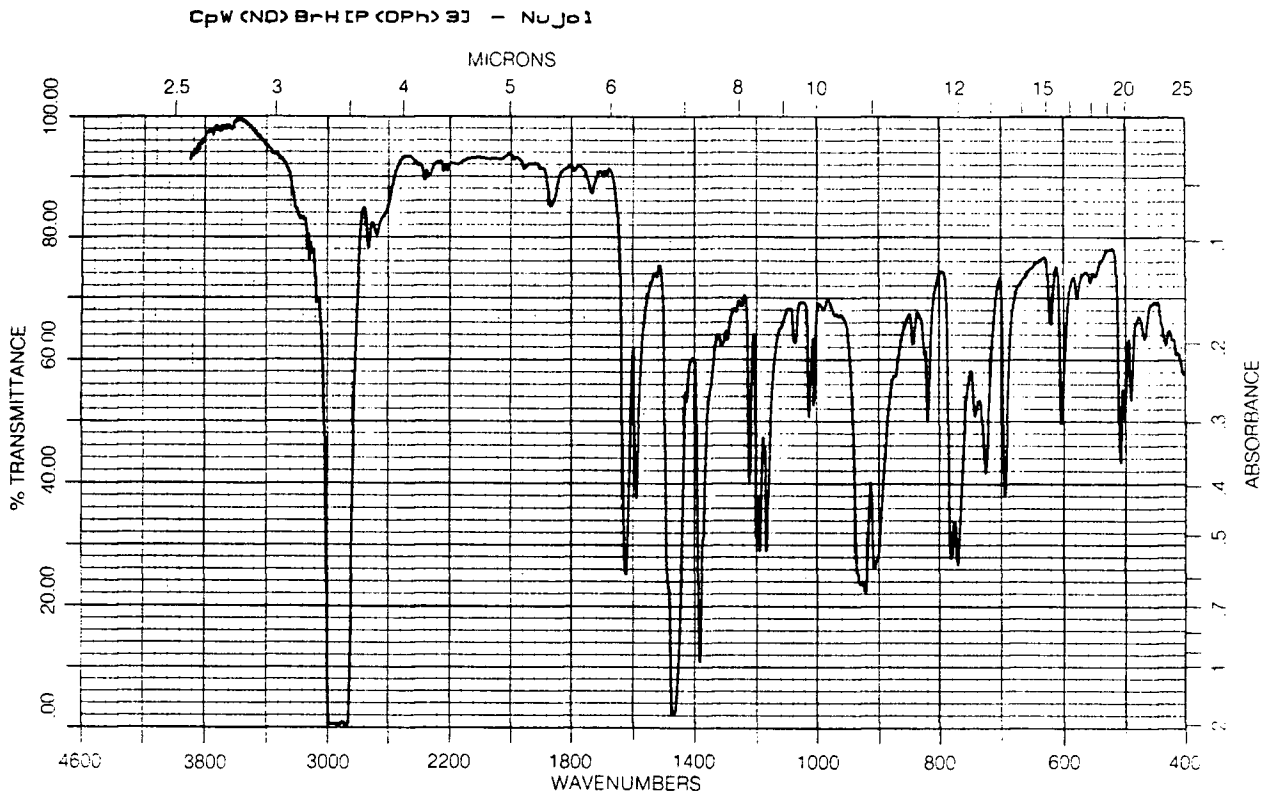
CpW(NO)BrH[P(OPh)3] – Nujol
MICRONS
2.5 3 4 5 6 8 10 12 15 20 25
100.00 80.00 60.00 40.00 20.00 .00
% TRANSMITTANCE
ABSORBANCE
.1 .2 .3 .4 .5 .7 1 2
4600 3800 3000 2200 1800 1400 1000 800 600 400
WAVENUMBERS

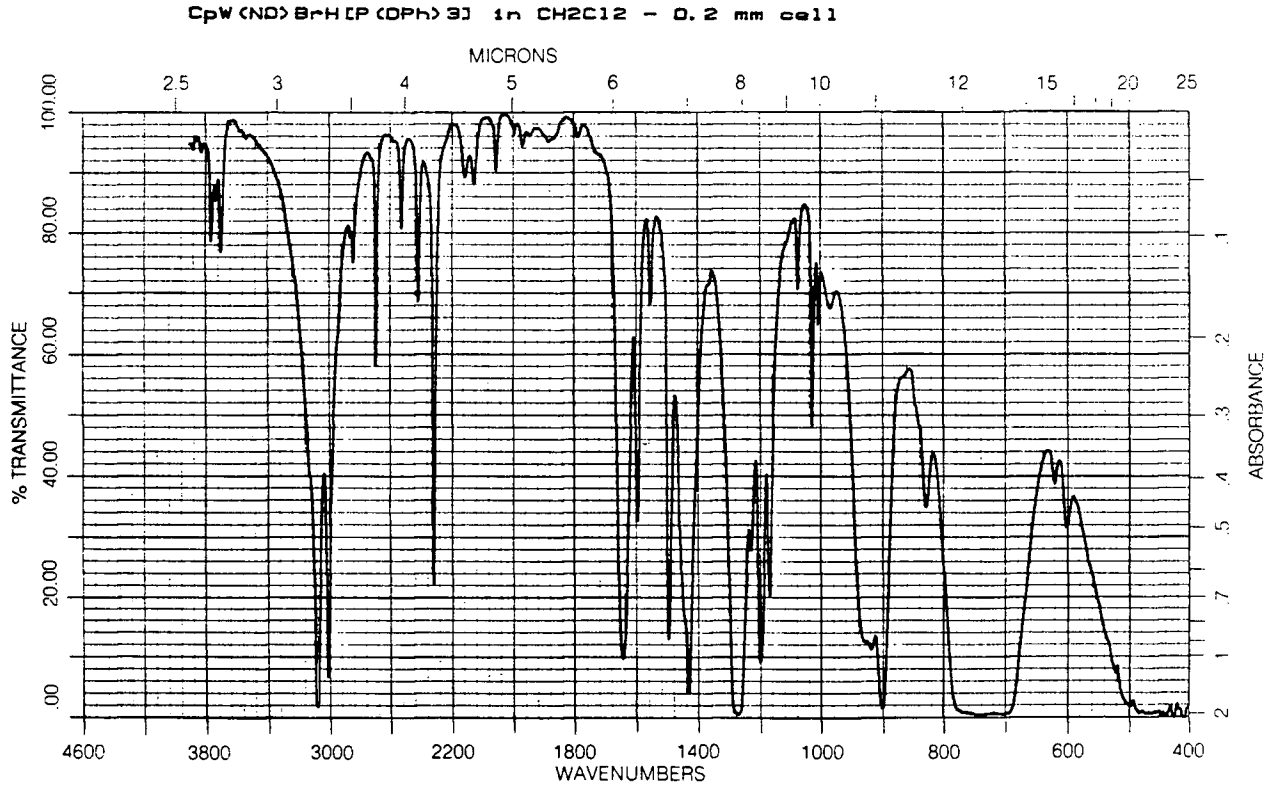
CpW(NO)BrH[P(OPh)3] in CH2Cl2 – 0.2 mm cell
MICRONS
2.5 3 4 5 6 8 10 12 15 20 25
100.00 80.00 60.00 40.00 20.00 .00
% TRANSMITTANCE
ABSORBANCE
.1 .2 .3 .4 .5 .7 1 2
4600 3800 3000 2200 1800 1400 1000 800 600 400
WAVENUMBERS

CpW(NO)BrH[P(OPh)$_3$] NMR in C_6D_6

300-MHz ^1H

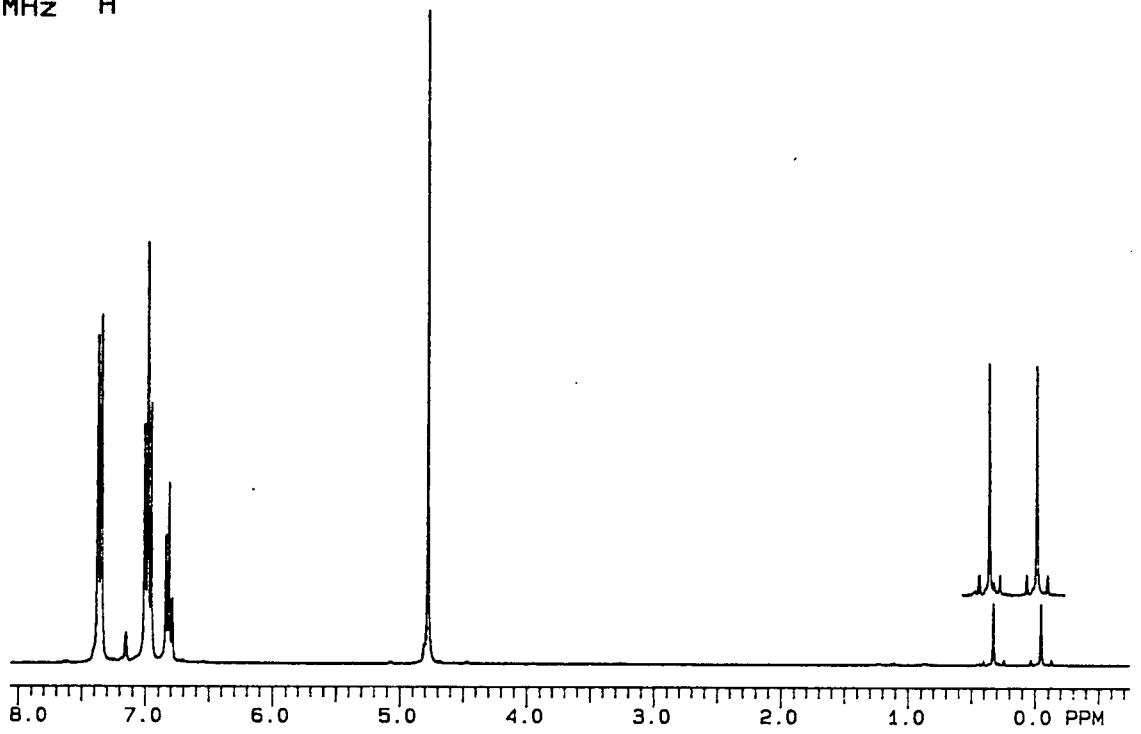

121.421-MHz $^{31}P\{^1H\}$

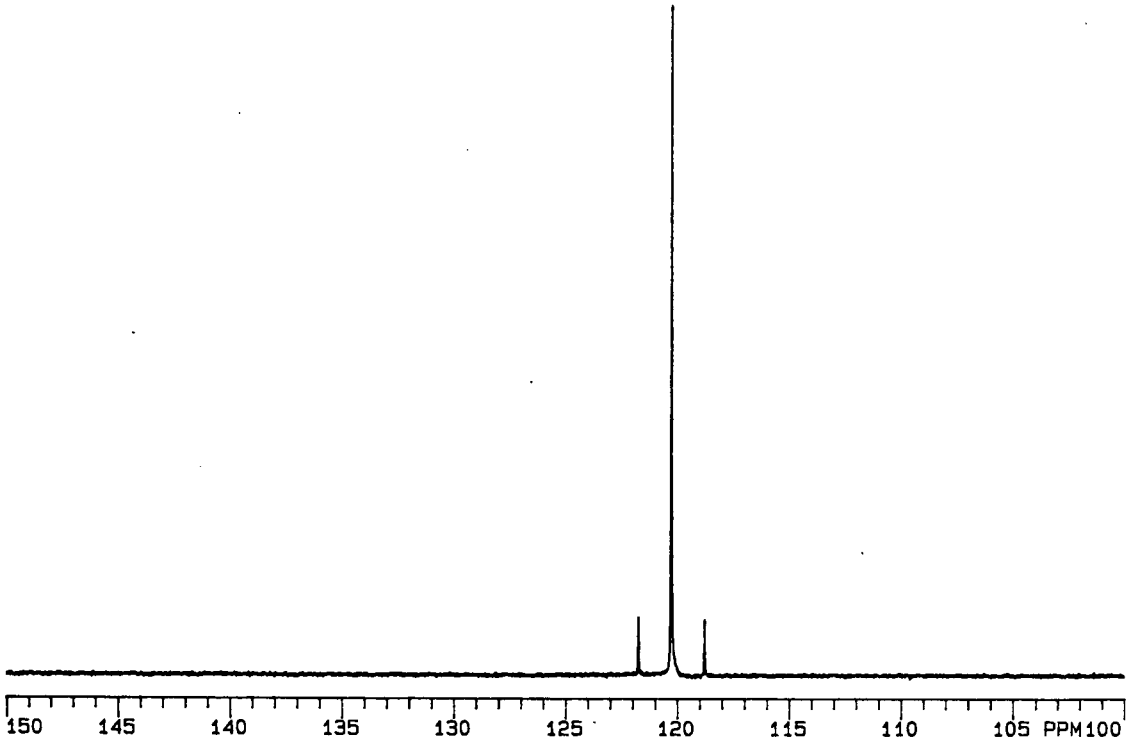

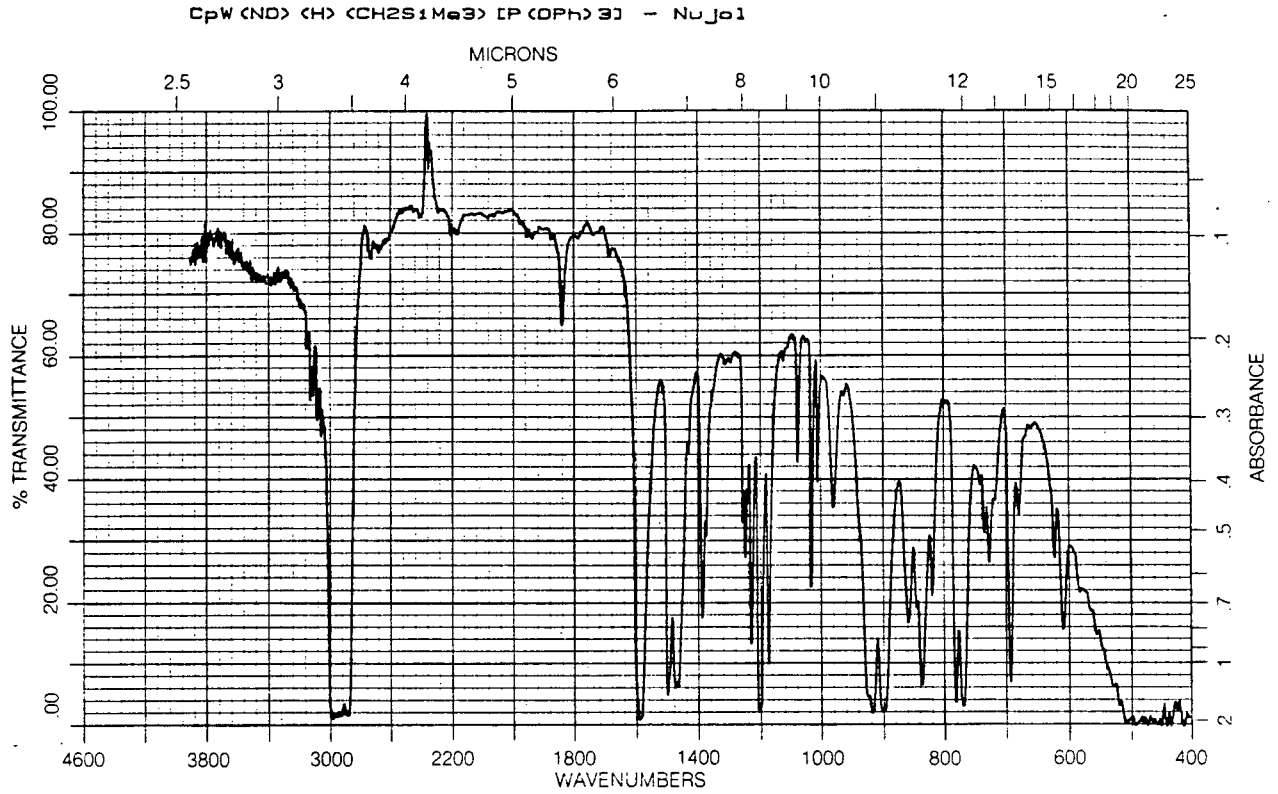
CpW(NO)(H)(CH2SiMe3)[P(OPh)3] – Nujol
MICRONS
2.5
3
4
5
6
8
10
12
15
20
25
100.00
80.00
60.00
40.00
20.00
.00
% TRANSMITTANCE
4600
3800
3000
2200
1800
1400
1000
800
600
400
WAVENUMBERS
.1
.2
.3
.4
.5
.7
1
2
ABSORBANCE

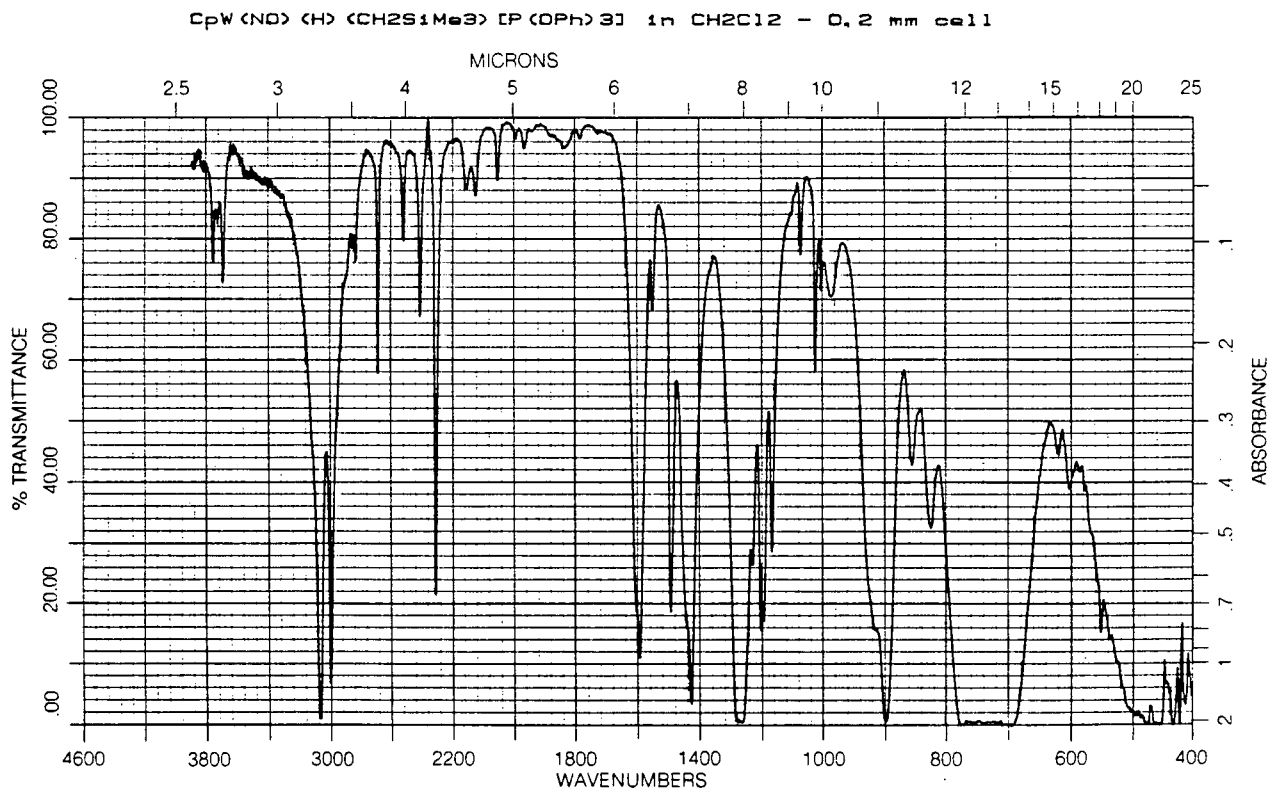
CpW(NO)(H)(CH2SiMe3)[P(OPh)3] in CH2Cl2 – 0.2 mm cell
MICRONS
2.5
3
4
5
6
8
10
12
15
20
25
100.00
80.00
60.00
40.00
20.00
.00
% TRANSMITTANCE
4600
3800
3000
2200
1800
1400
1000
800
600
400
WAVENUMBERS
.1
.2
.3
.4
.5
.7
1
2
ABSORBANCE

$CpW(NO)(H)(CH_2SiMe_3)[P(OPh)_3]$ NMR in C_6D_6

300-MHz ^1H

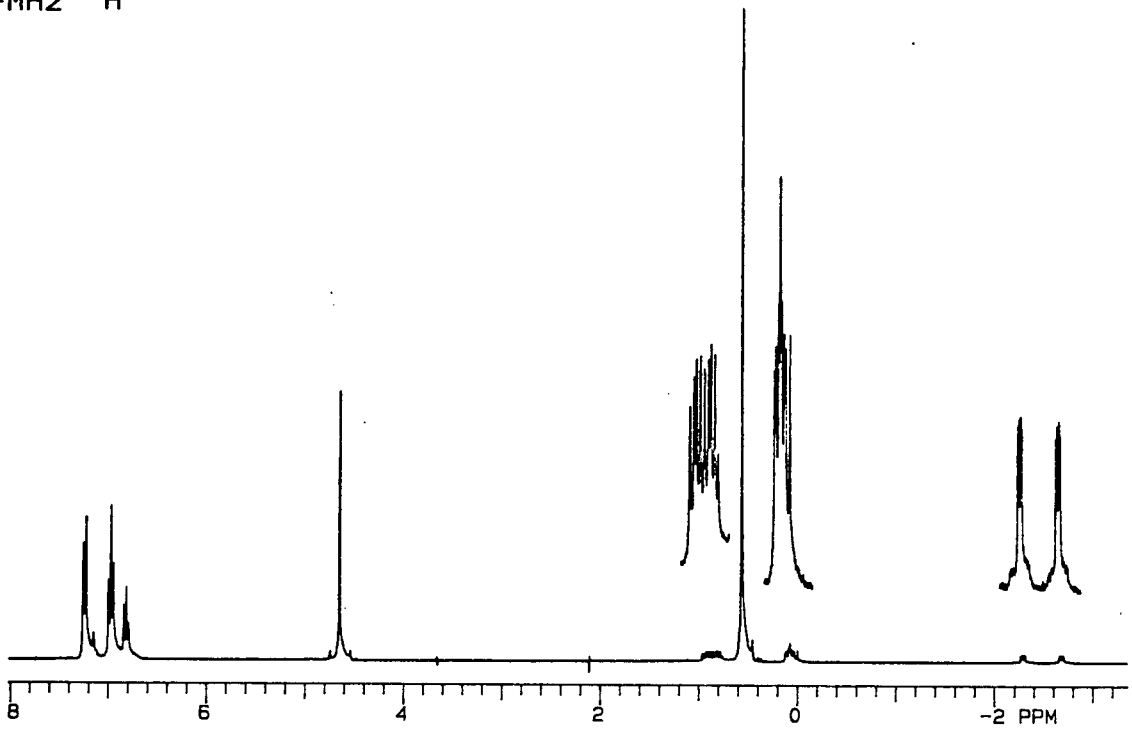

121.421-MHz $^{31}P\{^1H\}$

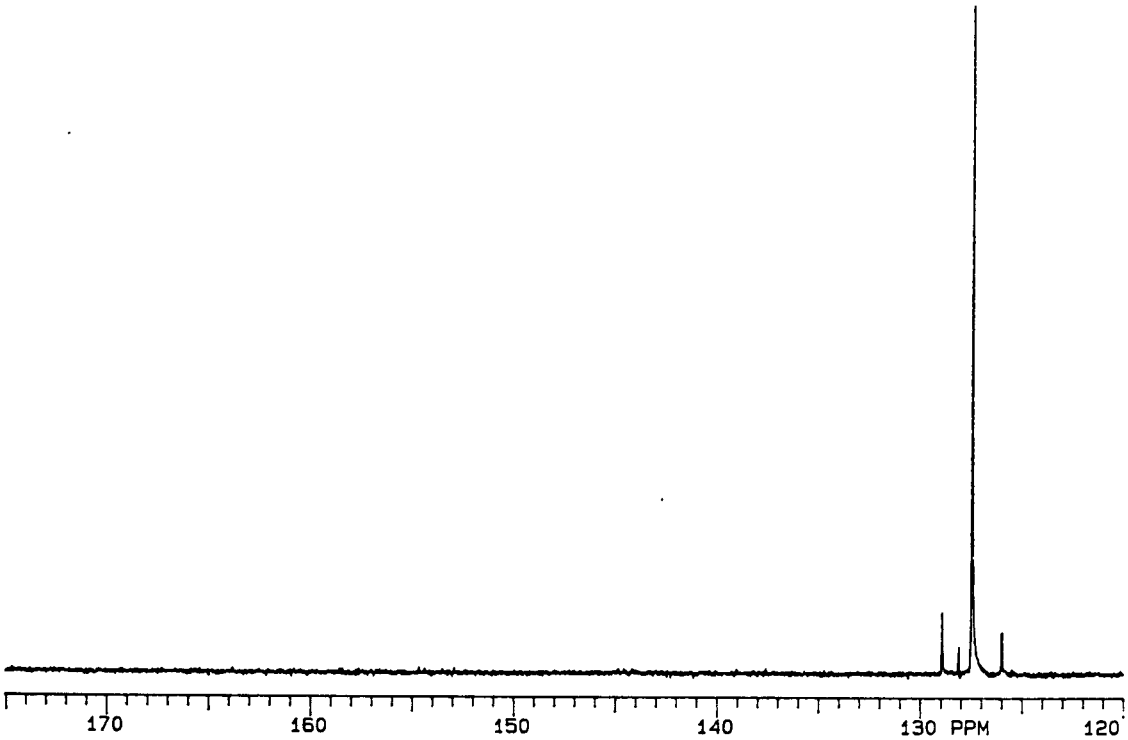

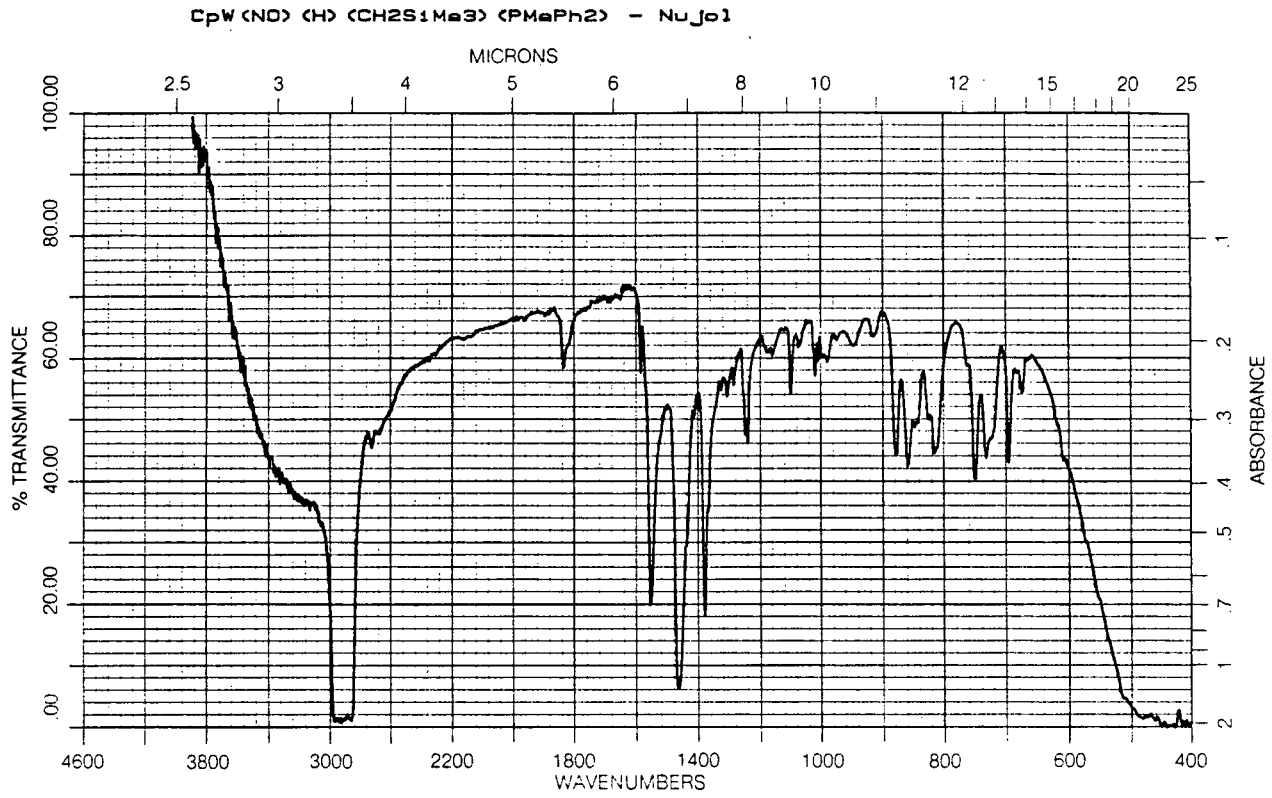
CpW(NO)(H)(CH2SiMe3)(PMePh2) - Nujol
MICRONS
2.5
3
4
5
6
8
10
12
15
20
25
100.00
80.00
60.00
40.00
20.00
.00
% TRANSMITTANCE
ABSORBANCE
.1
.2
.3
.4
.5
.7
1
2
4600
3800
3000
2200
1800
1400
1000
800
600
400
WAVENUMBERS

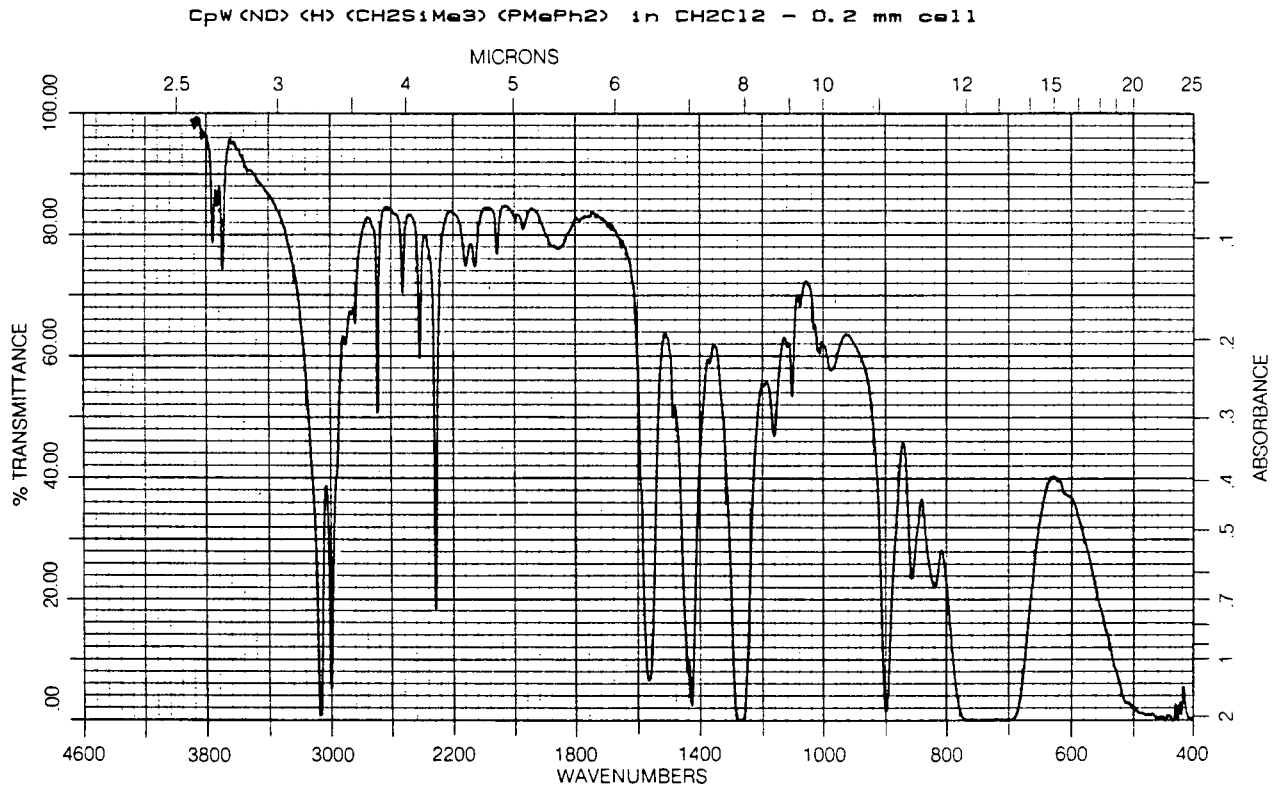
CpW(NO)(H)(CH2SiMe3)(PMePh2) in CH2Cl2 - 0.2 mm cell
MICRONS
2.5
3
4
5
6
8
10
12
15
20
25
100.00
80.00
60.00
40.00
20.00
.00
% TRANSMITTANCE
ABSORBANCE
.1
.2
.3
.4
.5
.7
1
2
4600
3800
3000
2200
1800
1400
1000
800
600
400
WAVENUMBERS

$CpW(NO)(H)(CH_2SiMe_3)(PMePh_2)$ NMR in C_6D_6

400-MHz ^1H

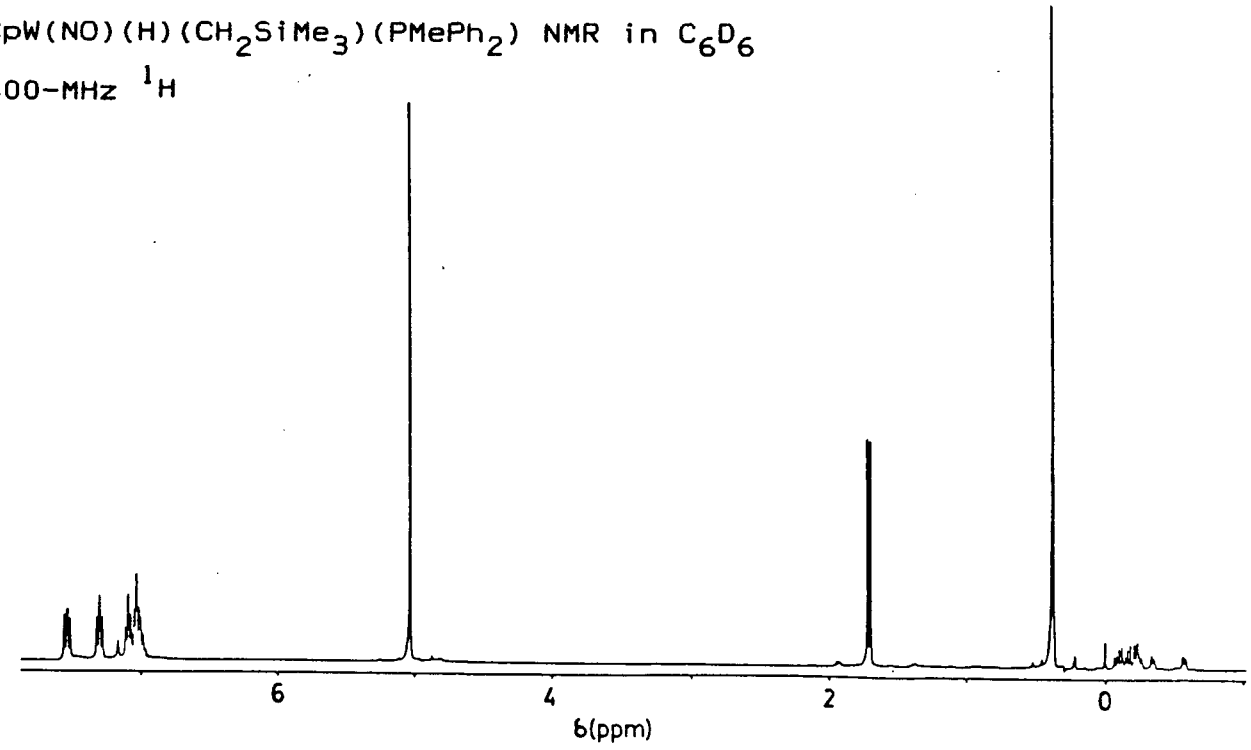

121.421-MHz $^{31}P\{^1H\}$

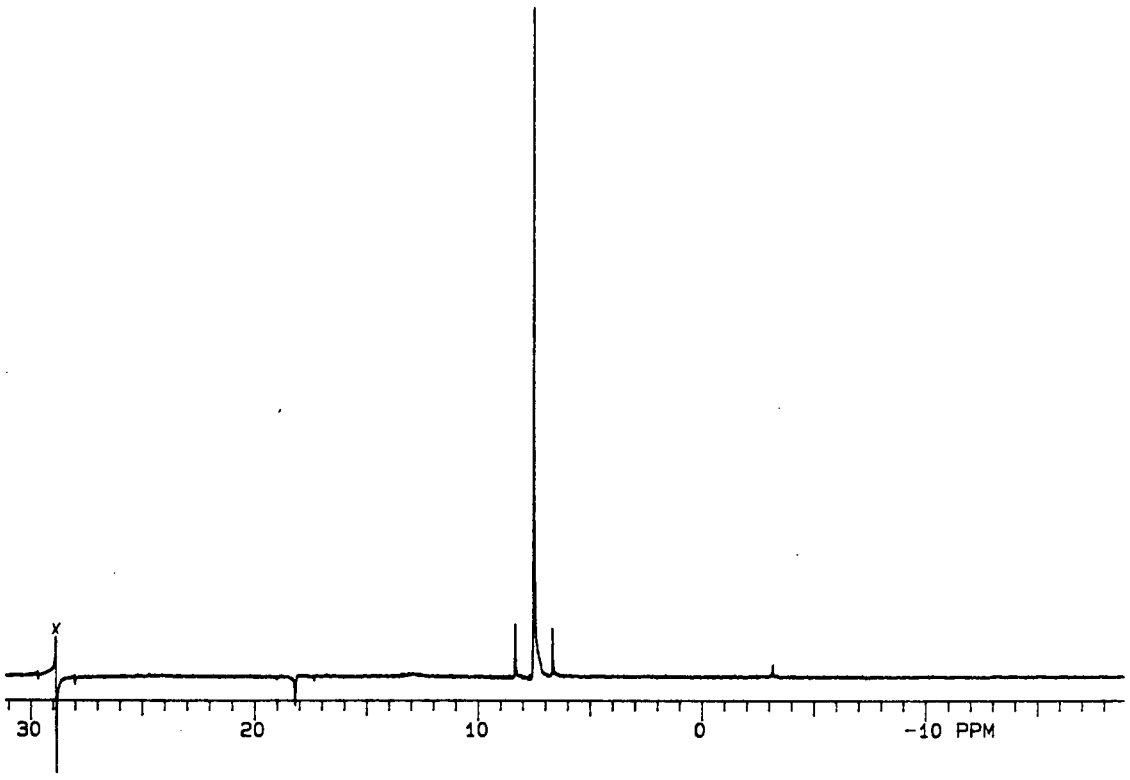

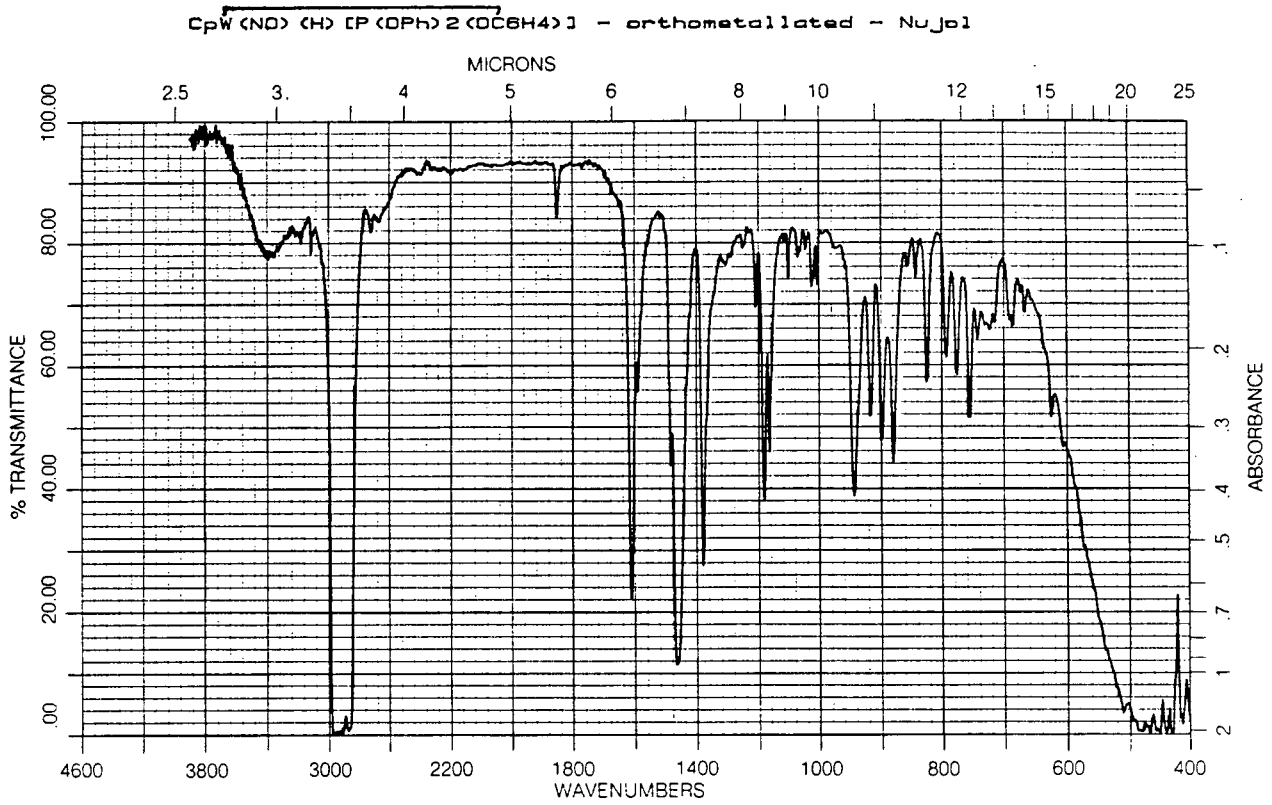
CpW(NO)(H)[P(OPh)2(OC6H4)] - orthometallated - Nujol
MICRONS
2.5
3.
4
5
6
8
10
12
15
20
25
100.00
80.00
60.00
40.00
20.00
.00
% TRANSMITTANCE
.1
.2
.3
.4
.5
.7
1
2
ABSORBANCE
4600
3800
3000
2200
1800
1400
1000
800
600
400
WAVENUMBERS

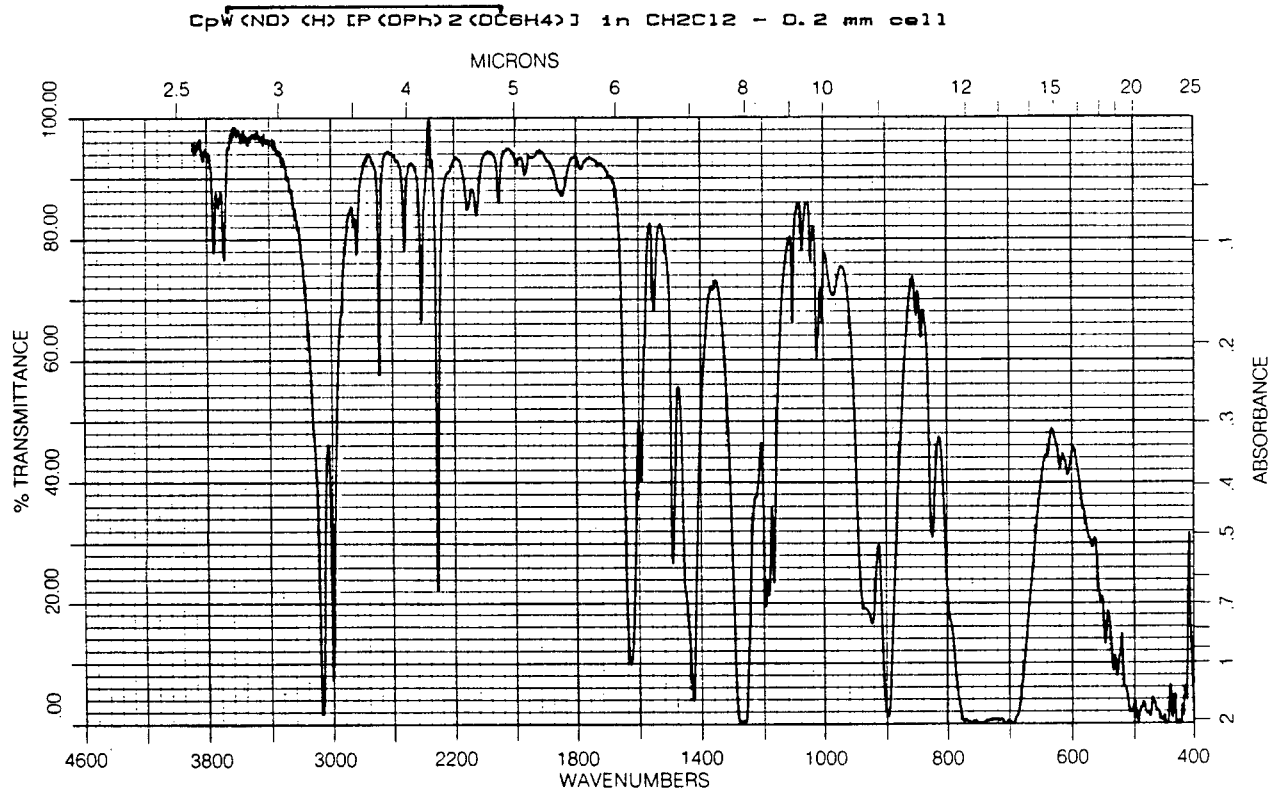
CpW(NO)(H)[P(OPh)2(OC6H4)] in CH2Cl2 - 0.2 mm cell
MICRONS
2.5
3
4
5
6
8
10
12
15
20
25
100.00
80.00
60.00
40.00
20.00
.00
% TRANSMITTANCE
.1
.2
.3
.4
.5
.7
1
2
ABSORBANCE
4600
3800
3000
2200
1800
1400
1000
800
600
400
WAVENUMBERS

$CpW(NO)(H)[P(OPh)_2(OC_6H_4)]$ NMR in C_6D_6

300-MHz ^1H

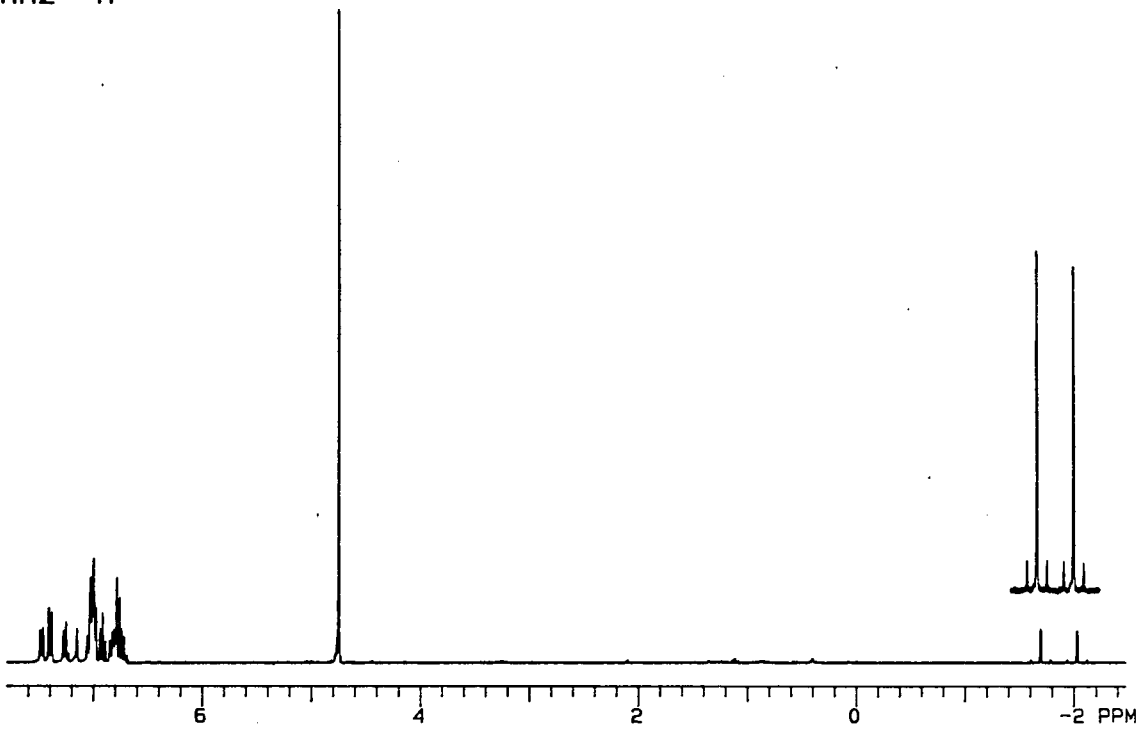

121.421-MHz $^{31}P\{^1H\}$

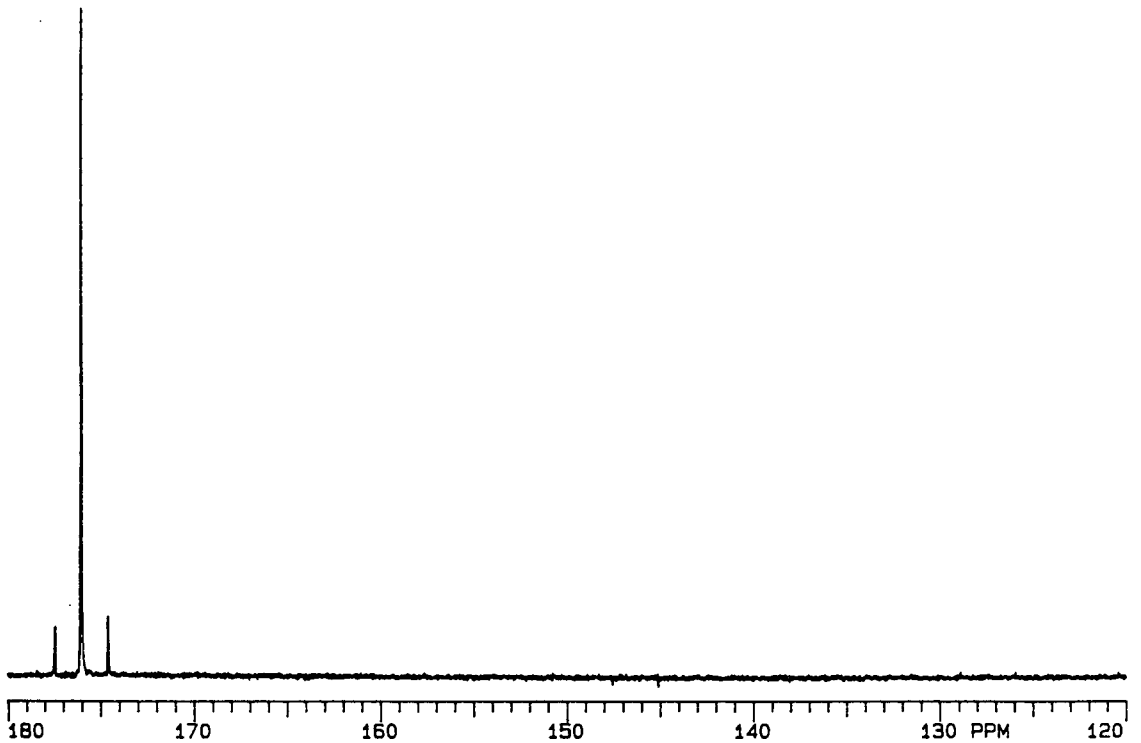

Cp*W(NO)I2 - Nujol

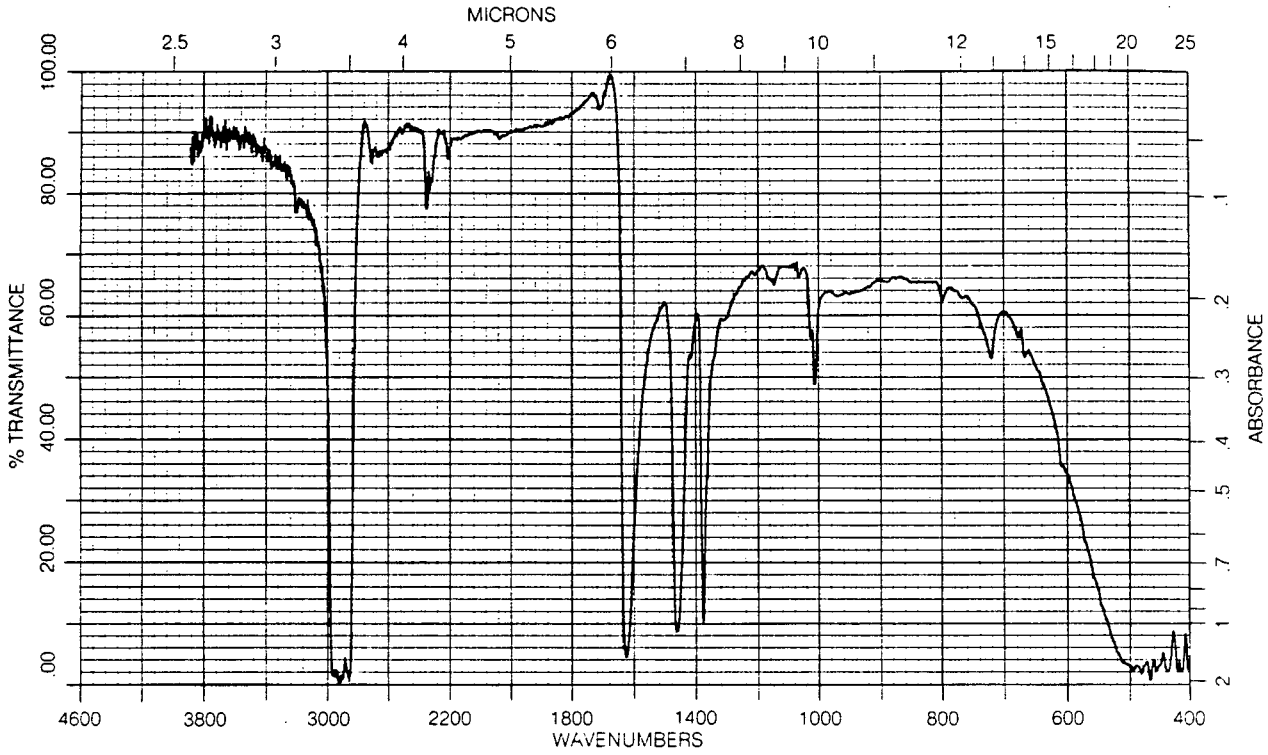

Cp*W(NO)I2 in CH2Cl2 - 0.2 mm cell

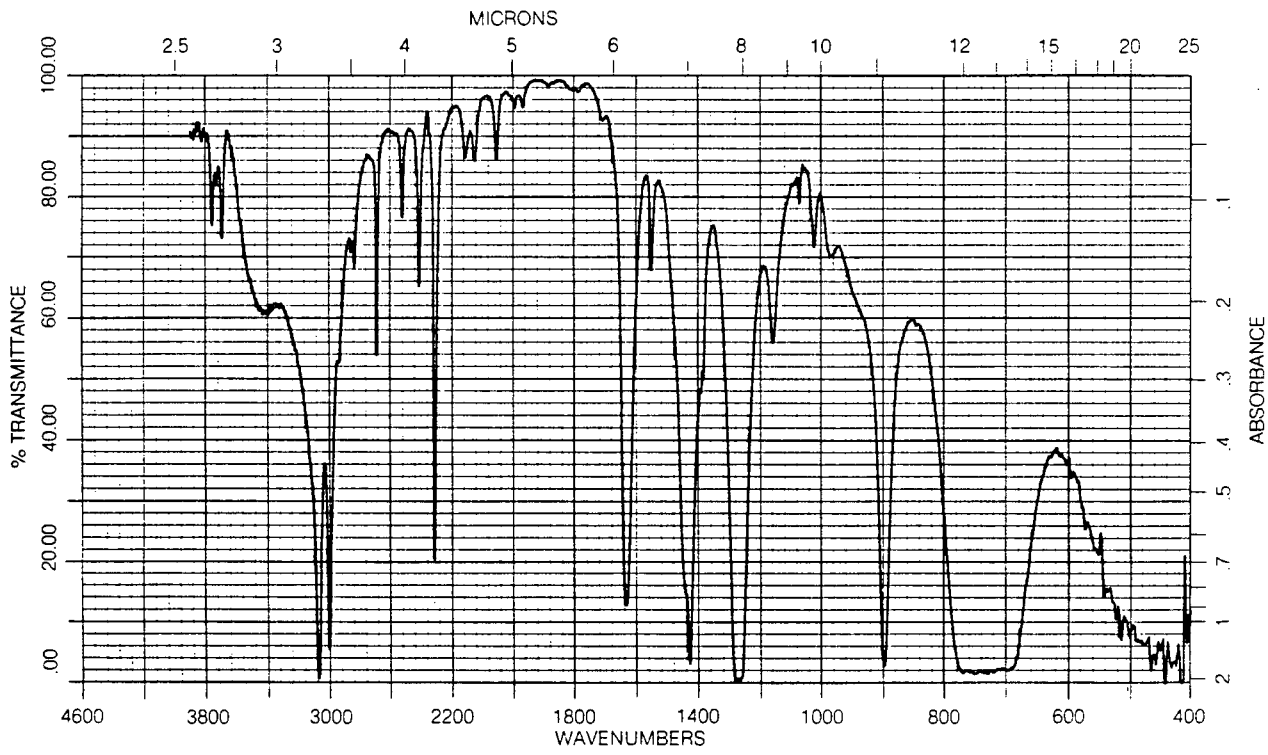

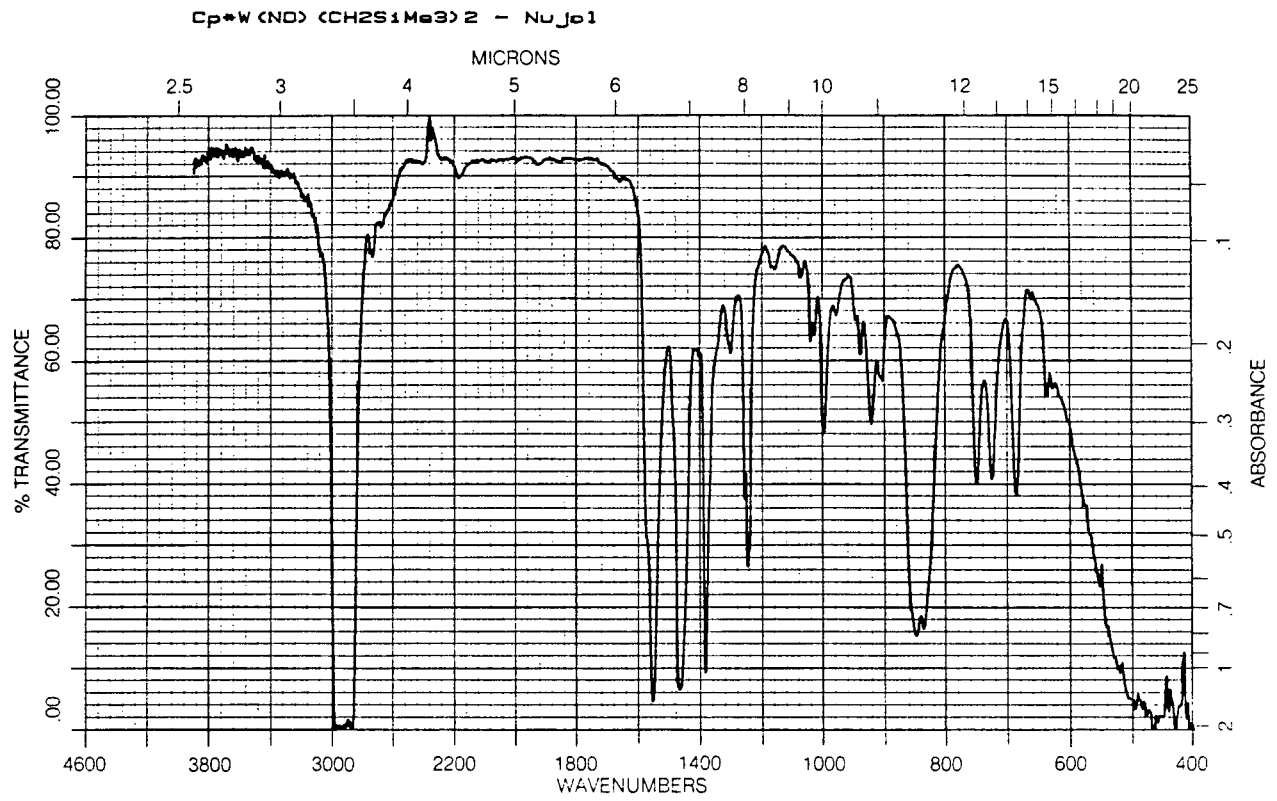
Cp*W(NO)(CH2SiMe3)2 - Nujol
MICRONS
2.5
3
4
5
6
8
10
12
15
20
25
100.00
80.00
60.00
40.00
20.00
.00
% TRANSMITTANCE
.1
.2
.3
.4
.5
.7
1
2
ABSORBANCE
4600
3800
3000
2200
1800
1400
1000
800
600
400
WAVENUMBERS

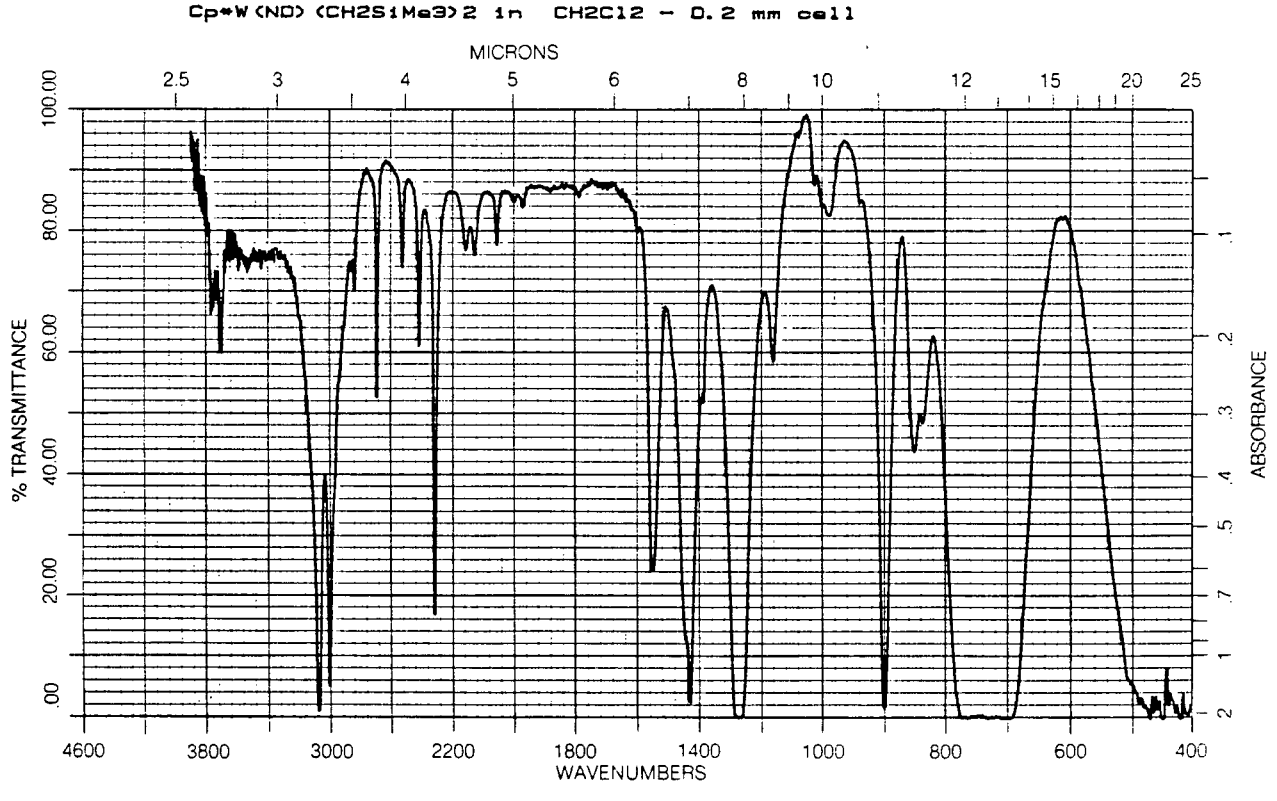
Cp*W(NO)(CH2SiMe3)2 in CH2Cl2 - 0.2 mm cell
MICRONS
2.5
3
4
5
6
8
10
12
15
20
25
100.00
80.00
60.00
40.00
20.00
.00
% TRANSMITTANCE
.1
.2
.3
.4
.5
.7
1
2
ABSORBANCE
4600
3800
3000
2200
1800
1400
1000
800
600
400
WAVENUMBERS

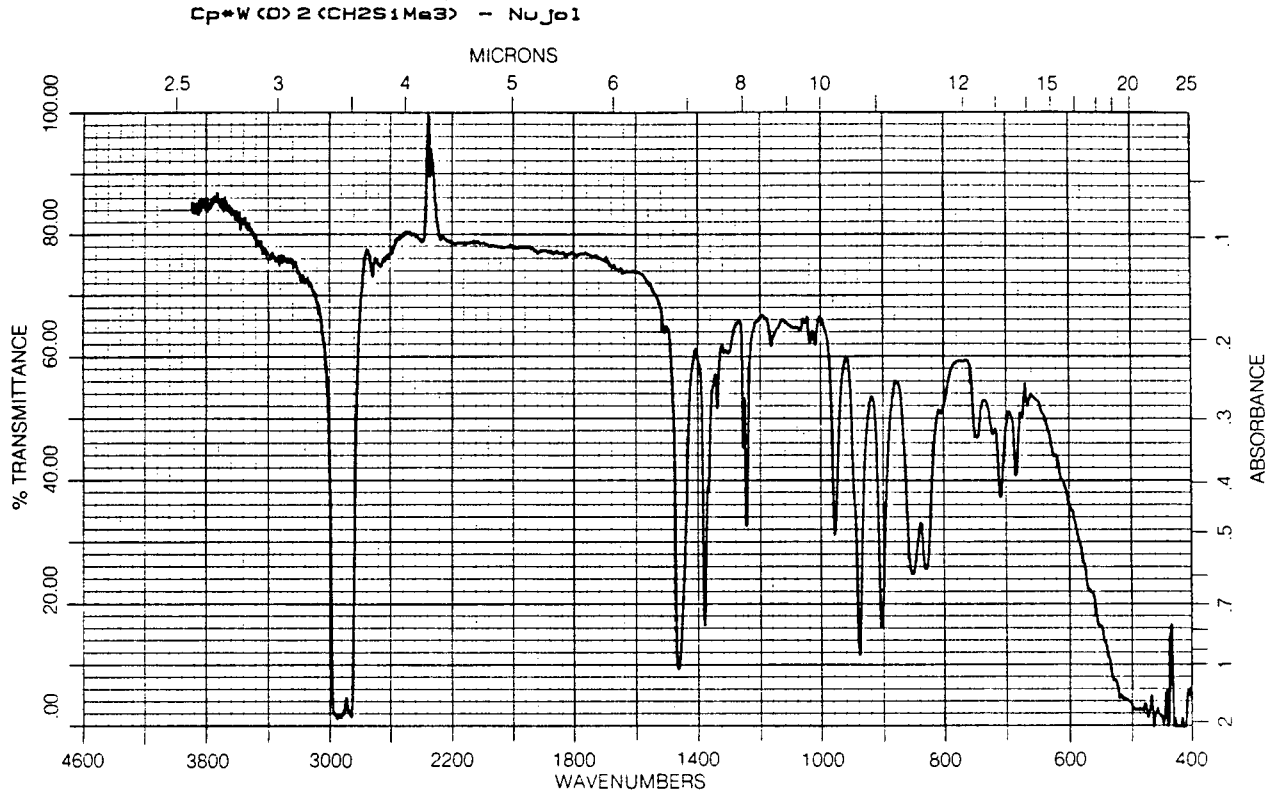
Cp*W(O)2(CH2SiMe3) - Nujol
MICRONS
2.5
3
4
5
6
8
10
12
15
20
25
100.00
80.00
60.00
40.00
20.00
.00
% TRANSMITTANCE
.1
.2
.3
.4
.5
.7
1
2
ABSORBANCE
4600
3800
3000
2200
1800
1400
1000
800
600
400
WAVENUMBERS

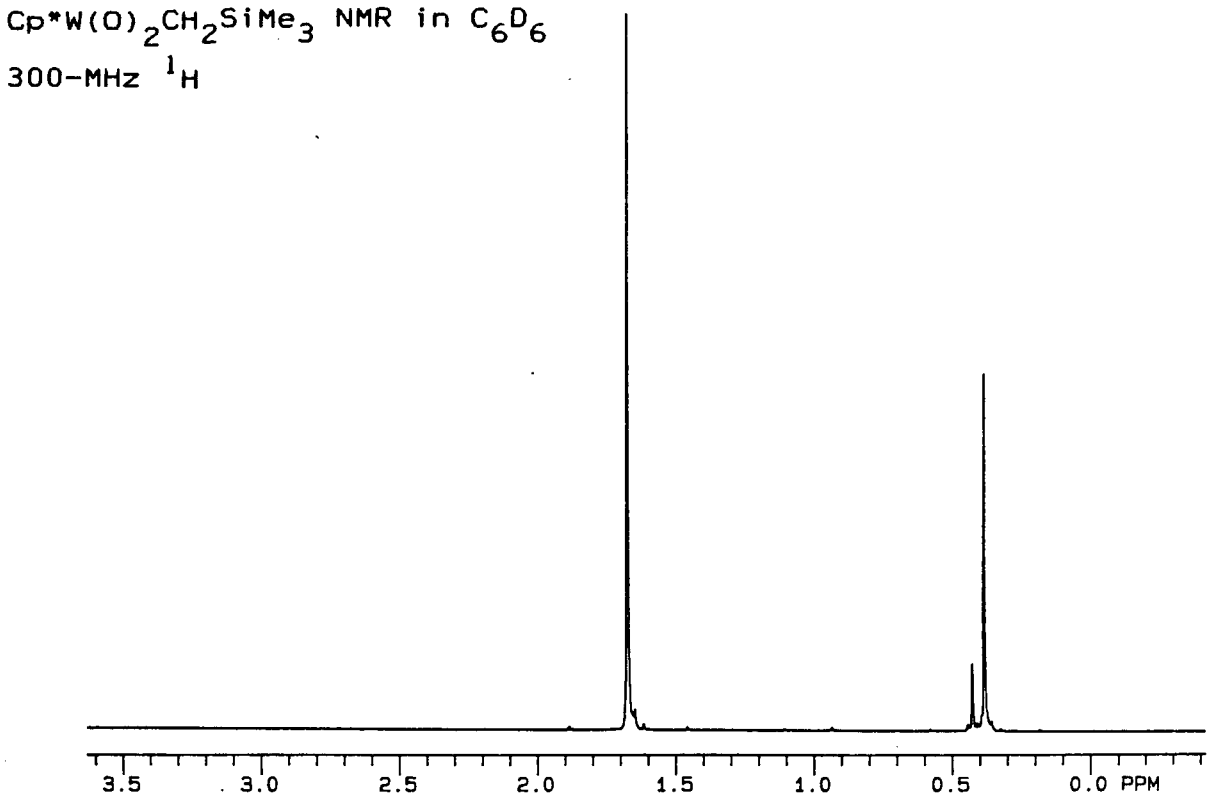
Cp*W(O)2CH2SiMe3 NMR in C6D6
300-MHz 1H
3.5
3.0
2.5
2.0
1.5
1.0
0.5
0.0 PPM

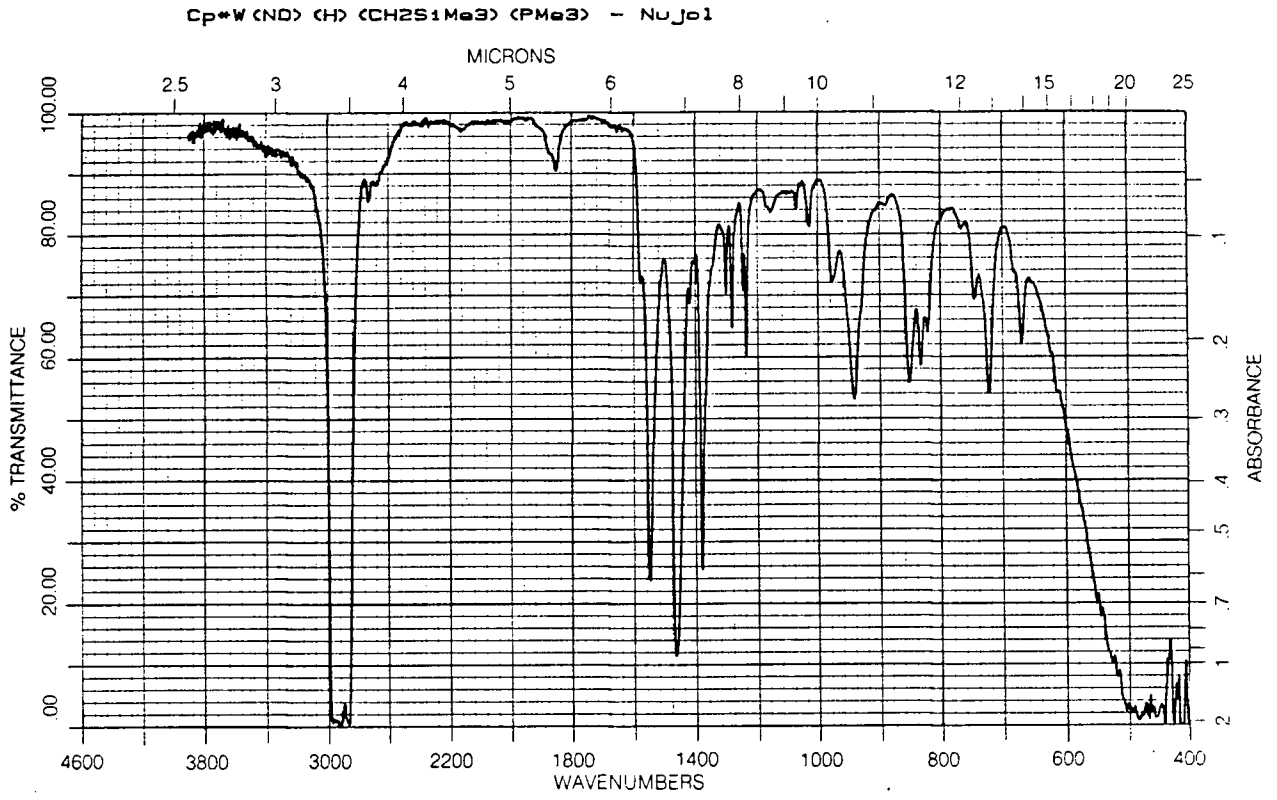
Cp*W(NO)(H)(CH2SiMe3)(PMe3) - Nujol
MICRONS
2.5
3
4
5
6
8
10
12
15
20
25
100.00
80.00
60.00
40.00
20.00
.00
% TRANSMITTANCE
ABSORBANCE
.1
.2
.3
.4
.5
.7
1
2
4600
3800
3000
2200
1800
1400
1000
800
600
400
WAVENUMBERS

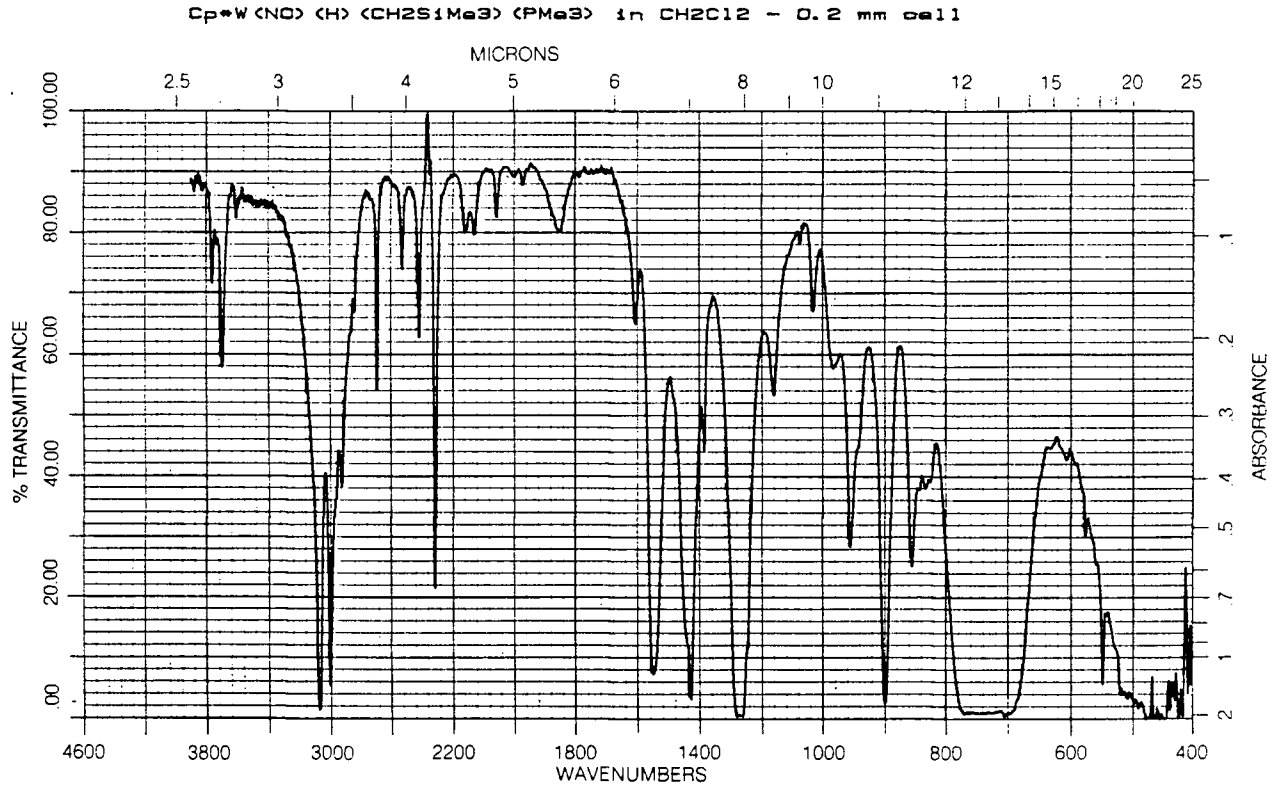
Cp*W(NO)(H)(CH2SiMe3)(PMe3) in CH2Cl2 - 0.2 mm cell
MICRONS
2.5
3
4
5
6
8
10
12
15
20
25
100.00
80.00
60.00
40.00
20.00
.00
% TRANSMITTANCE
ABSORBANCE
.1
.2
.3
.4
.5
.7
1
2
4600
3800
3000
2200
1800
1400
1000
800
600
400
WAVENUMBERS

$Cp^*W(NO)(H)(CH_2SiMe_3)(PMe_3)$ NMR in C_6D_6

300-MHz ^1H

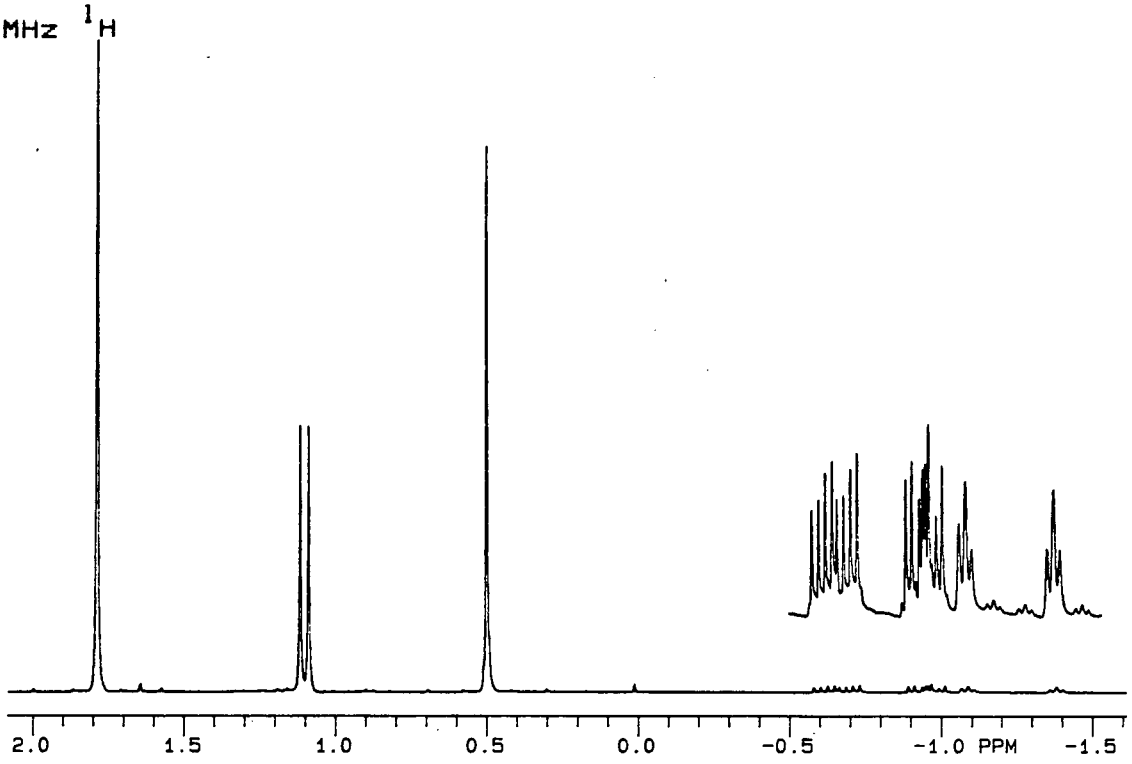

121.421-MHz $^{31}P\{^1H\}$

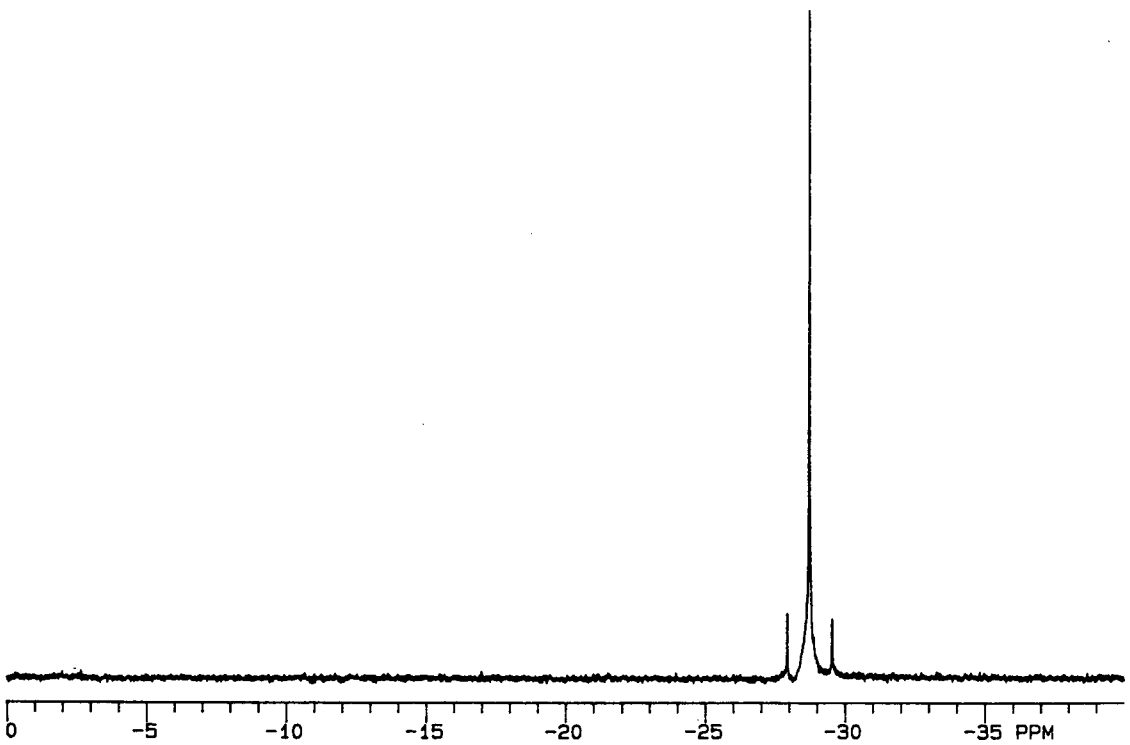

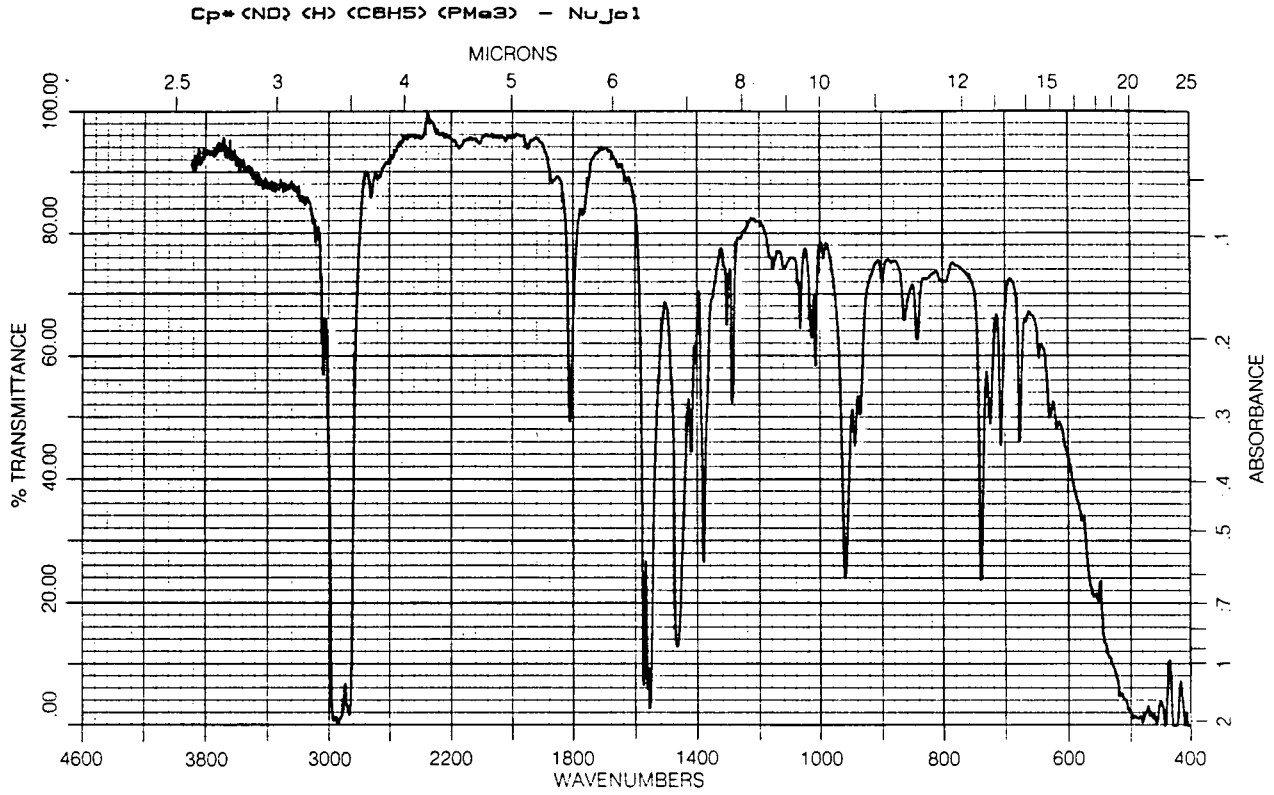
Cp* (NO) (H) (C6H5) (PMe3) – Nujol
MICRONS
2.5 3 4 5 6 8 10 12 15 20 25
100.00 80.00 60.00 40.00 20.00 .00
% TRANSMITTANCE
.1 .2 .3 .4 .5 .7 1 2
ABSORBANCE
4600 3800 3000 2200 1800 1400 1000 800 600 400
WAVENUMBERS

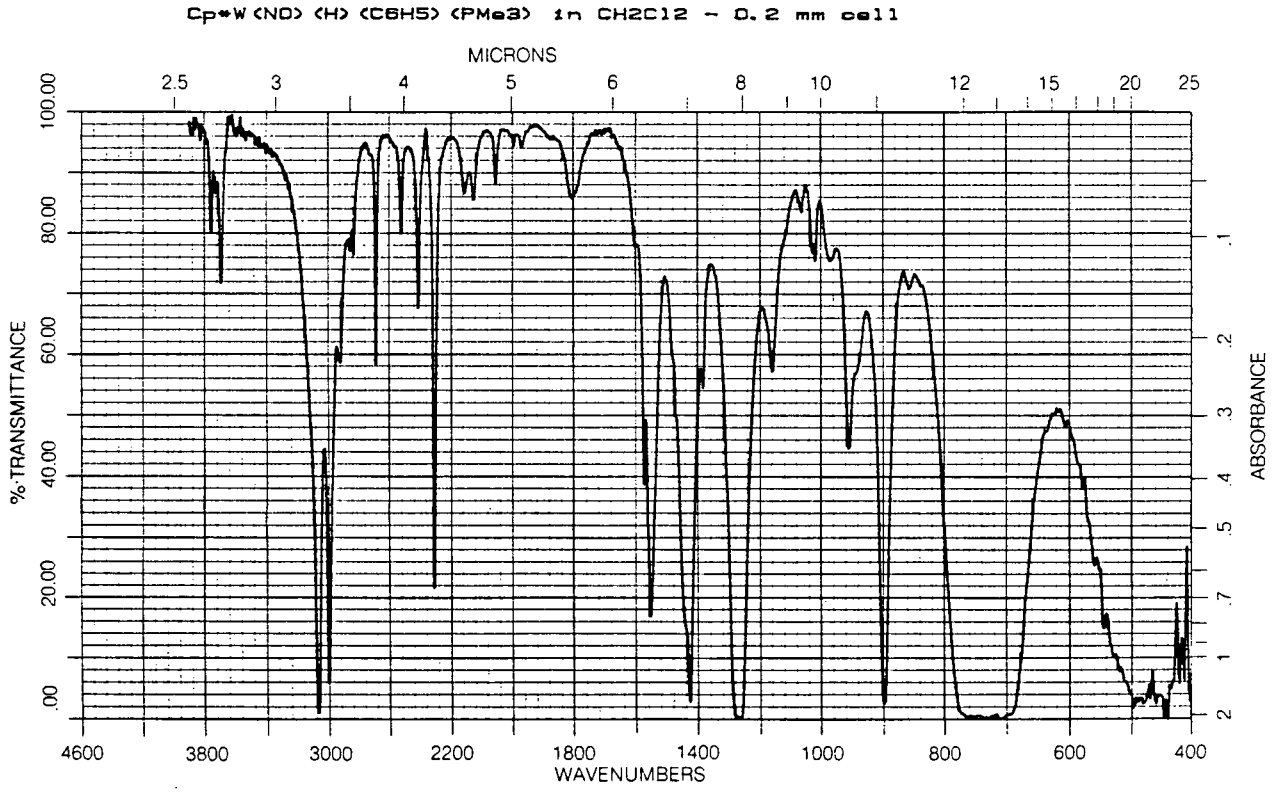
Cp*W (NO) (H) (C6H5) (PMe3) in CH2Cl2 – 0.2 mm cell
MICRONS
2.5 3 4 5 6 8 10 12 15 20 25
100.00 80.00 60.00 40.00 20.00 .00
% TRANSMITTANCE
.1 .2 .3 .4 .5 .7 1 2
ABSORBANCE
4600 3800 3000 2200 1800 1400 1000 800 600 400
WAVENUMBERS

$Cp^*W(NO)(H)(C_6H_5)(PMe_3)$ NMR in C_6D_6

121.421-MHz $^{31}P\{^1H\}$

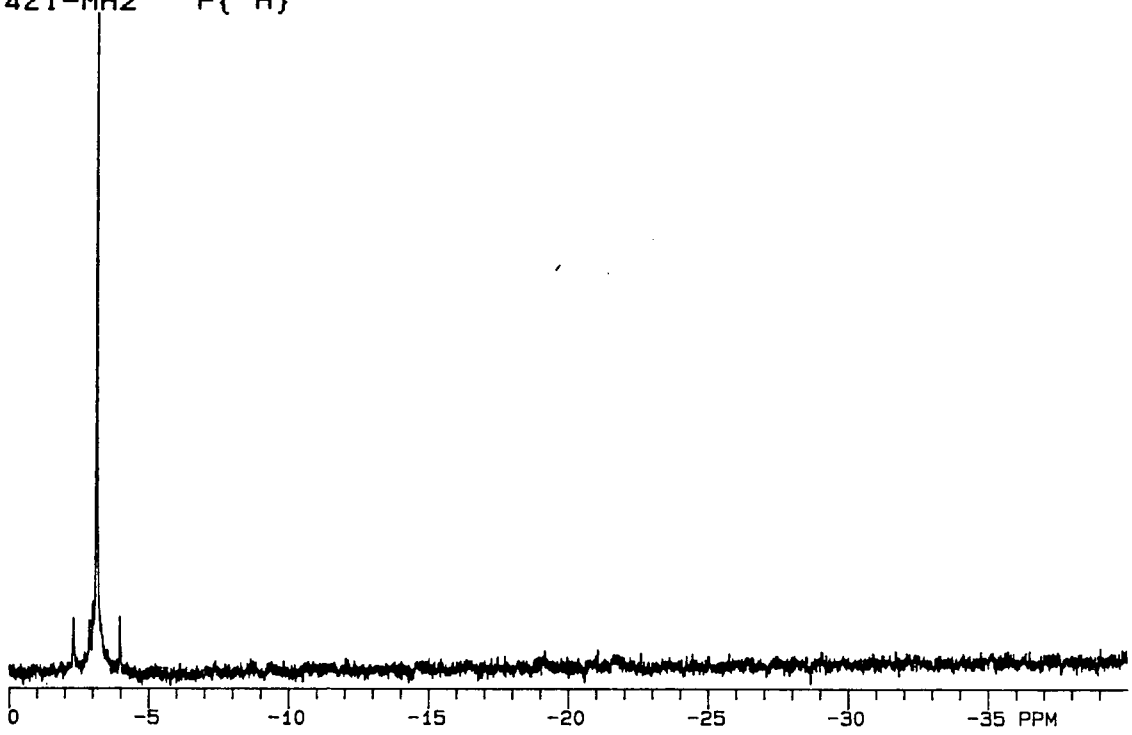

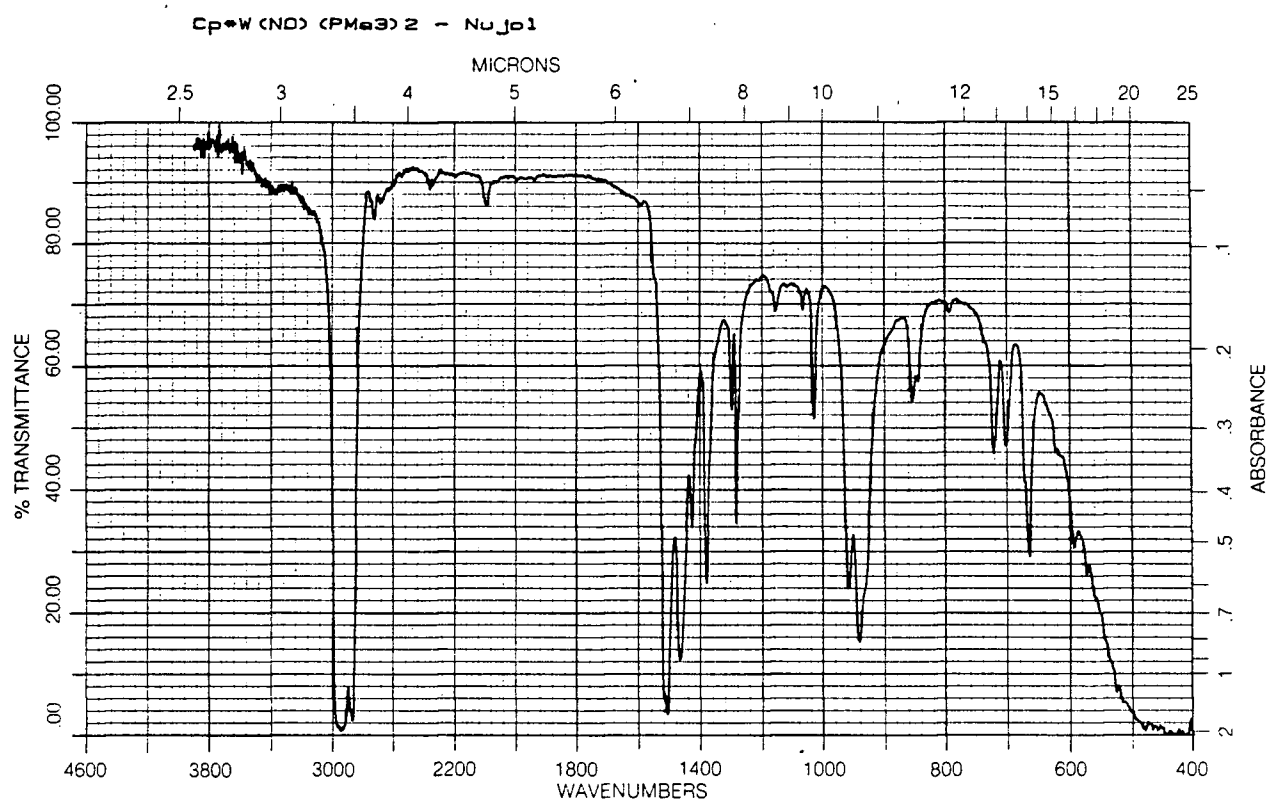
Cp*W(NO)(PMe3)2 - Nujol
MICRONS
2.5 3 4 5 6 8 10 12 15 20 25
100.00 80.00 60.00 40.00 20.00 .00
% TRANSMITTANCE
.1 .2 .3 .4 .5 .7 1 2
ABSORBANCE
4600 3800 3000 2200 1800 1400 1000 800 600 400
WAVENUMBERS

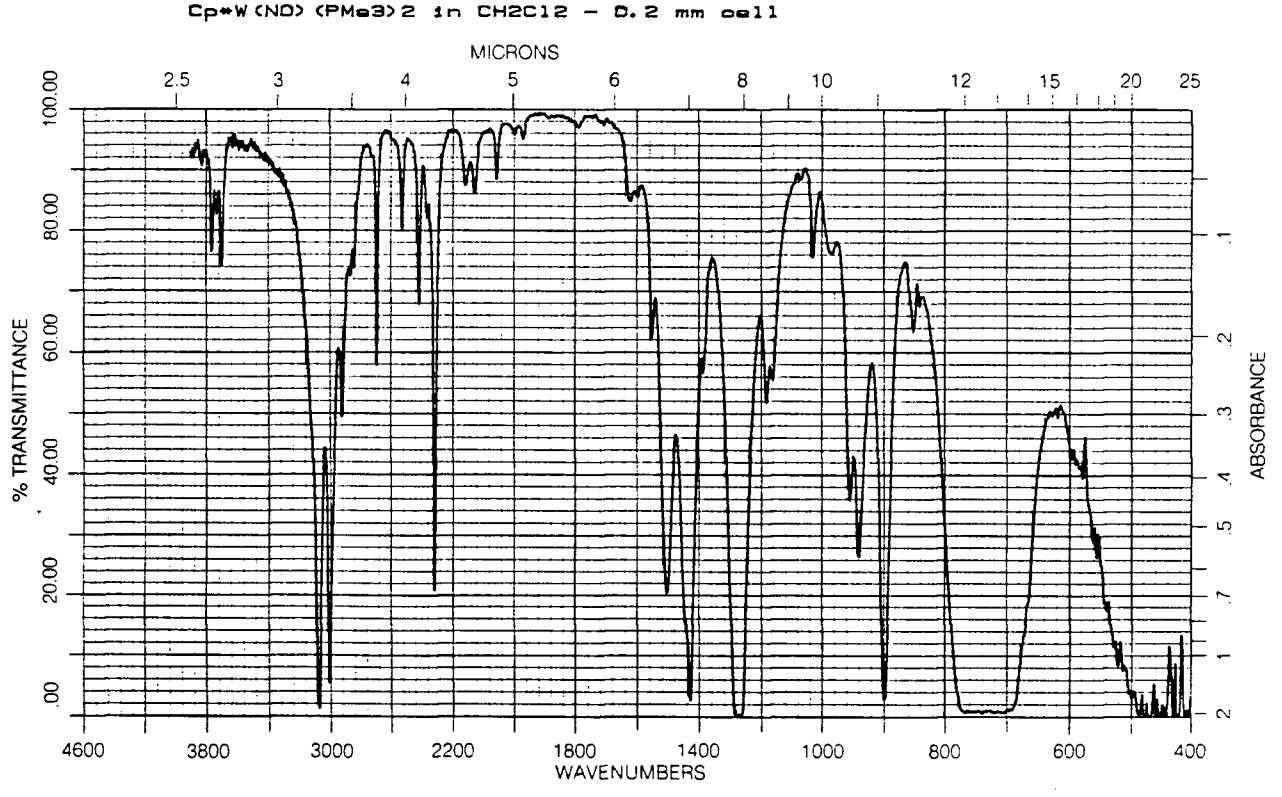
Cp*W(NO)(PMe3)2 in CH2Cl2 - 0.2 mm cell
MICRONS
2.5 3 4 5 6 8 10 12 15 20 25
100.00 80.00 60.00 40.00 20.00 .00
% TRANSMITTANCE
.1 .2 .3 .4 .5 .7 1 2
ABSORBANCE
4600 3800 3000 2200 1800 1400 1000 800 600 400
WAVENUMBERS

$Cp^*W(NO)(PMe_3)_2$ NMR in C_6D_6

300-MHz ^1H

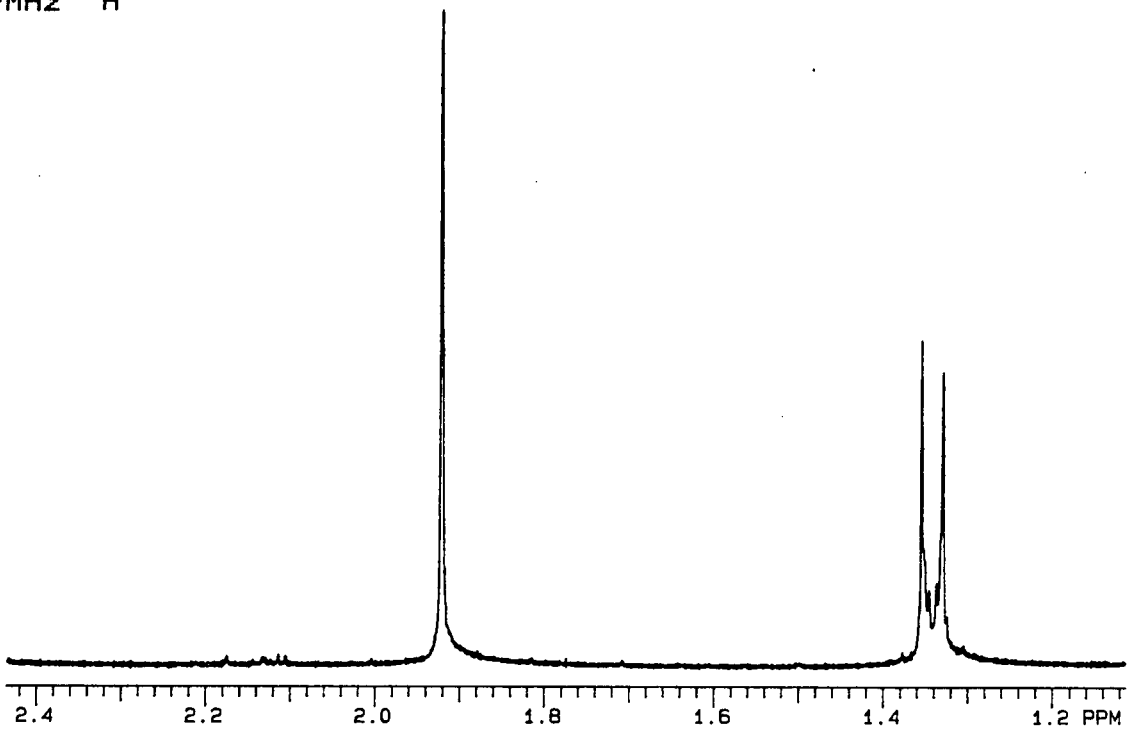

121.421-MHz $^{31}P\{^1H\}$

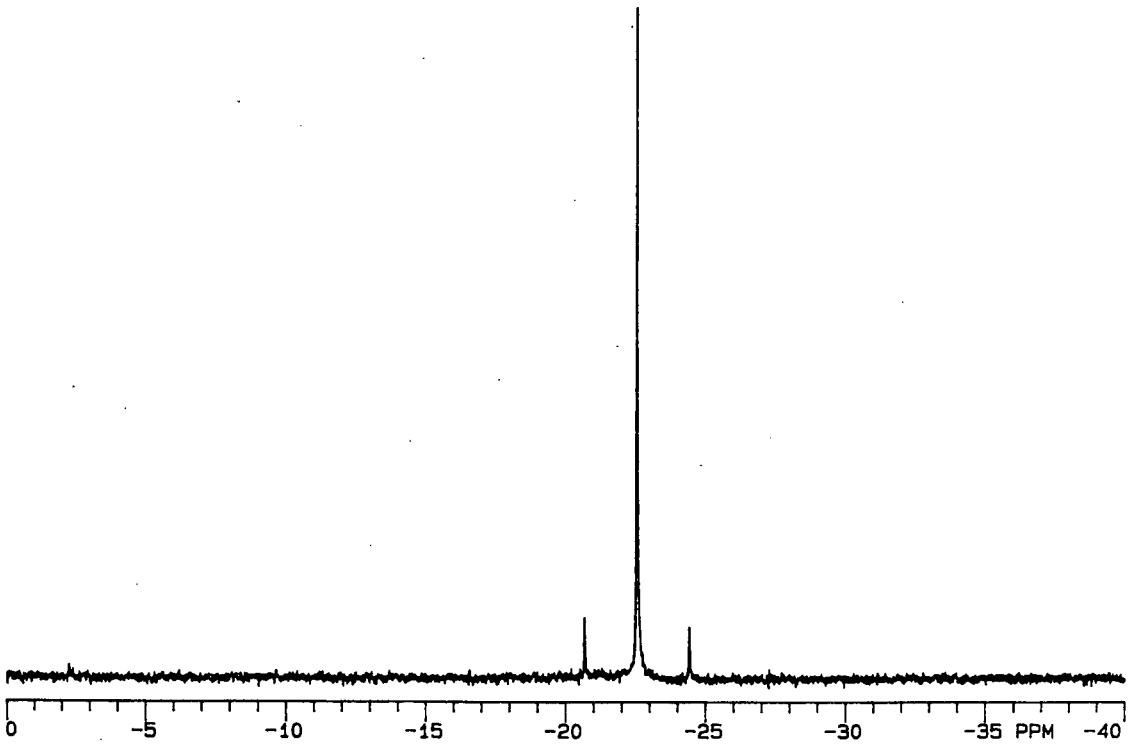

[Cp*W(NO)H]2(μ-H)2 - Nujol

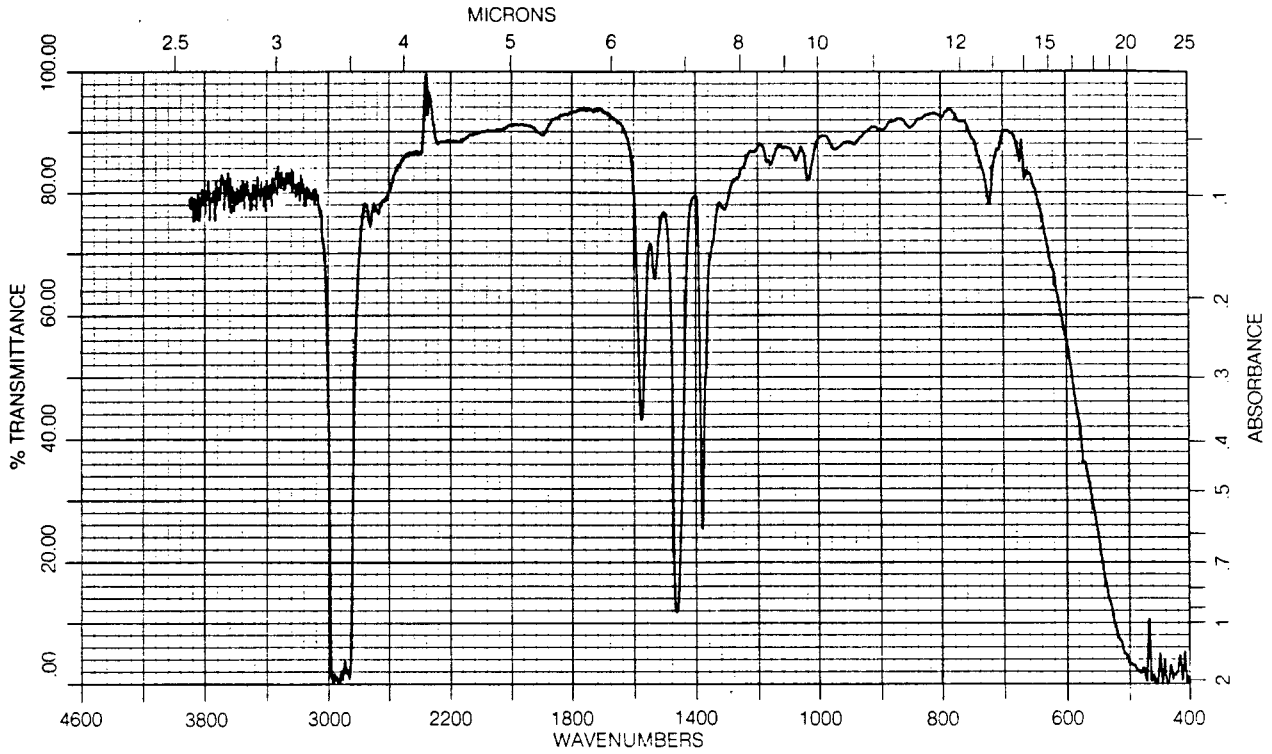

[Cp*W(NO)H]2(μ-H)2 in CH2Cl2 - 0.2 mm cell

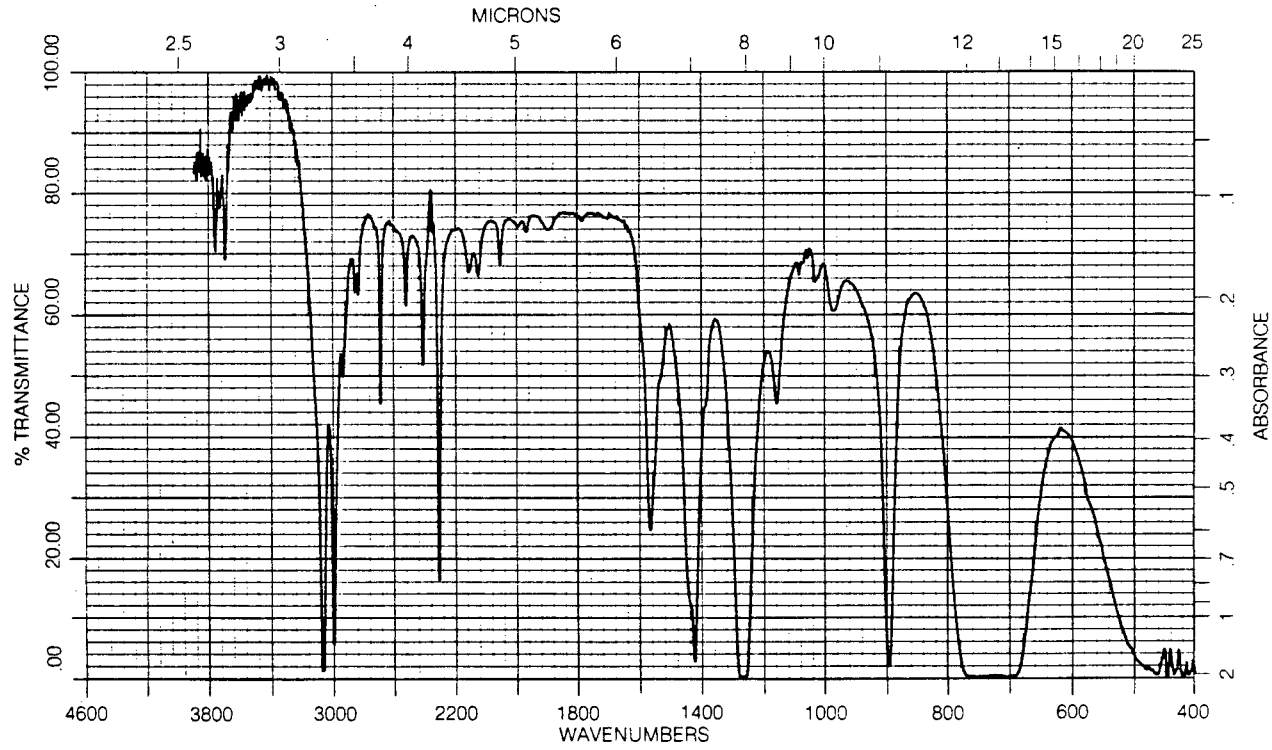

[Cp*W(NO)H](μ-H)2[Cp*W(NO)(CH2SiMe3)] – Nujol

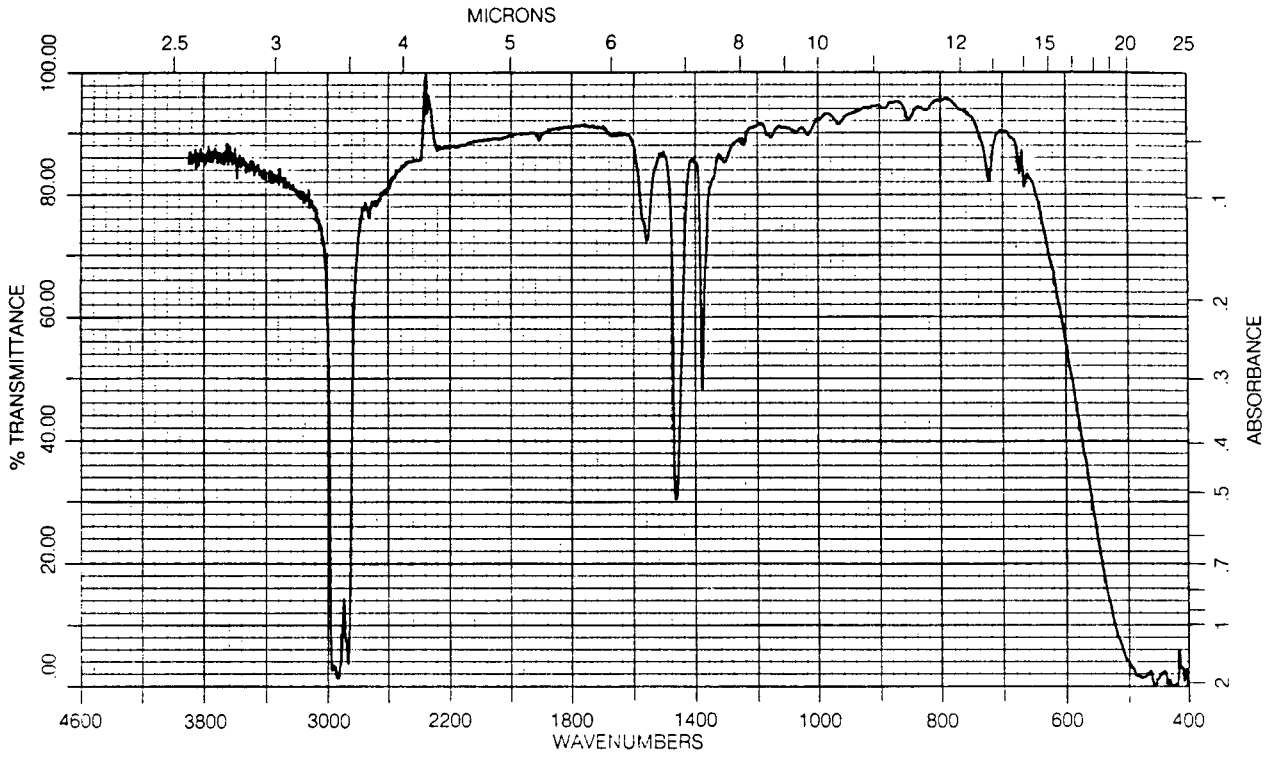

[Cp*W(NO)H](μ-H)2[Cp*W(NO)(CH2SiMe3)] in CH2Cl2 – 0.2 mm cell